UNIVERSITÉ DE STRASBOURG

ÉCOLE DOCTORALE MATHÉMATIQUES, SCIENCES DE L'INFORMATION ET DE L'INGÉNIEUR

Laboratoire des Sciences de l'Ingénieur, de l'Informatique et de l'Imagerie

THÈSE présentée par :

Juan David ARCE VELASQUEZ

soutenue le : **24 Septembre 2020**

pour obtenir le grade de : **Docteur de l'université de Strasbourg**

Discipline/ Spécialité : Energétique et Génie des procédés / Traitement des eaux

---

Modélisation de la stabilisation de l'urine par nitrification au sein d'un bioréacteur à membrane

---

THÈSE dirigée par :
  Mr LAURENT Julien   MCF-HDR, ENGEES/ICUBE-Université de Strasbourg

RAPPORTEURS :
  Mr UDERT Kai   Professeur des universités, EAWAG–Suisse
  Mr HERAN Marc   Professeur des universités, IEM - Université de Montpellier

---

AUTRES MEMBRES DU JURY :
  M. CHOUBERT Jean-Marc   Directeur de recherche-HDR, IRSTEA Lyon Villeurbanne
  M. ESCULIER Fabien   Docteur, LEESU-Université Paris-Est

UNIVERSITY OF STRASBOURG

Abstract

Doctor of Philosophy

Modeling urine stabilization by nitrification in a membrane bioreactor

by Juan David ARCE VELASQUEZ

In this thesis, the conceptualization of an integrated physio-biological model, as well as an experimental analysis of a biological system treating yellow wastewater are presented. The system is a membrane bioreactor designed to treat source separated urine. The main objective is to treat the nitrogen load in the urine by biological nitrification and produce a stable effluent. A laboratory pilot was operated to acclimatize conventional activated sludge to high nitrogen loads. This produced biomass that was used for model calibration by respirometric tests. A pH control driven strategy was applied for the acclimation phase which controlled and fed the system automatically following pH setpoint values. Two protocols were applied for this acclimation. The first used highly diluted urine without strict control of its level of ammonification. The second method employed more concentrated urine with a preliminary storage period favoring ammonification. The second strategy resulted in a better acclimation and less nitrite build-up events. However, the optimal pH range for automatic control was identified empirically. Therefore, following a thorough parametric analysis, the physio-biological model was used to quantitatively assess the respective inhibitions of ammonia and nitrite oxidizing bacteria for various operational scenarios (urine pre-ammonification or not, pH ranges, biokinetic parameters sets). The model was implemented in an ordinary differential equations solver for setting-up the desired on/off control strategy. The results confirmed that pre-ammonified urine yielded shorter acclimation time. The shortest acclimation period was at neutral pH (7-7.05) as observed during the experiments. This numerical implementation should be nevertheless improved in the future by taking into account the response time of the pH probe and associated controller and by incorporating additional physio-chemical processes (fate of phosphorus, precipitation, sulfates...) that could yield a better pH dynamics description. This model paves the way for developing better control algorithms for urine nitrification involving only pH measurement and model predictive control.

Acknowledgements

To the members of my dissertation jury an enormous acknowledgment for the intellectual contribution, the discussion, the advises and your honesty on evaluating my work. This represents a lot to me as a scientist, but also as a person in continuous learning and spiritual growth.

Thanks to my supervisor and mentor Dr. Julien Laurent for giving me opportunity to start this PhD, and for his support over these past four years of my life. Next, to all the wastewater treatment team in the iCube laboratory for their guidance and motivation; Dr. Adrien Wanko and Dr. Paul Bois for the leadership. To my friends and colleges in the lab; Maximillian, Mammad, Milena, Florent, Lee Ahn, Hung, Teddy, Poulcherie, Loïc, Julie, Elena, Eloïse, Paul, Cecile, Querentin. To all the people that contributed to the project "pee for science", thanks for helping me to make science great again.

Je voudrais remercier le personnel technique de l'ENGEES, Marie et Carol du LEE de m'avoir aidé dans l'analyse technique et pour leur précieuse aide et accompagnement. Je remercie également le personnel technique et administrative des installations de l' iCube, Martin, Robert, Yannick et bien d'autres personnes qui m'ont permis de faire fonctionner mon réacteur pilote. Strasbourg me donne après quatre ans des amis extraordinaires et des gens merveilleux autour de moi, à Daniel, Santiago, Elena, Jorge, Ciro, Carlos, Sandra, Marc, Momo, Mehdi, Shunak, Niels, Mathilde, Martin, Lisa, Robin, Dimitri, Jullien, Lesli, pour eux et tous les amis en France et dans le monde entier ; merci pour les mots, le temps, la patience et l'amour.

Enfin à ma famille en Colombie un énorme merci, pour tous les encouragements et l'amour à des milliers de kilomètres, tout l'amour loin de chez soi est précieux, c'est pour vous tous. Mamita linda, este trinfuo es tuyo. À ma deuxième famille en France, Olivier, Isabelle, Anne-Laure et Colette, merci de me faire sentir comme faisant partie d'une nouvelle famille dans ce beau pays.

A celle qui depuis trois est mon support, est là pour me soutenir, me faire rire, me fait pleurer, m'énerve, m'apaise, celle qui malgré les conditions a été toujours là pour essayer de me comprendre et me réconforter. Si je n'ai pas laissé tomber ce projet de thèse c'est en grand partie grâce à toi. Merci infiniment Eloise, je t'aime.

Contents

viii

List of Figures

xiv

List of Tables

Acronyms

NaN_3 Sodium Azide. 124, 128, 132, 144, 189

ALR Ammonium Loading Rate. xi, 94

ANAMMOX Anaerobic AMmonium OXidation. 20, 23

AOB Ammonia Oxidizing Bacteria. xii, xiii, xv, xvi, xxi–xxiii, xxxi, xxxii, xxxiv, 8, 13, 18, 21–23, 27, 28, 39, 47, 48, 51–56, 62, 63, 66, 68, 70, 75, 79–82, 85, 86, 91, 92, 96, 103, 104, 109, 113, 114, 117, 118, 124, 127–129, 131–134, 137, 139, 143–147, 149, 153, 155, 159, 161, 163, 165, 168–170, 172, 176–178, 182–184, 189, 192–195, 197, 198, 201, 203

AS Activated Sludge. v, 21, 22, 25, 28, 31, 34, 39, 47, 81, 84, 87, 109

ASM Activated Sludge Models. vi, xi, xv, xxxii, 34, 37–47, 50, 61, 64, 66, 72–74, 149, 182

ASP Activated Sludge Processes. 83, 85

ATU N-allylthiourea. 124, 128, 131, 134, 137, 139, 192, 194, 195

AUR Ammonium Uptake Rate. 39

BAC Boues activées classiques. xxix

BAP Biomass Associated Products. 43

BNR Biological Nitrogen Removal. 3, 5, 6, 22, 26, 28, 31, 51, 83, 184

BOD Biological Oxygen Demand. 22, 37

BRM Bio-Réacteurs à Membranes. xxxi–xxxiv

CAS Conventional Activated Sludge. 4, 31, 33–35, 37, 39, 43, 44, 61, 83

COD Chemical Oxygen Demand. vi, xxii, xxiii, 6, 11, 15–17, 20, 22, 23, 29, 30, 37, 38, 41, 42, 44, 56, 61–64, 70, 88, 105, 129–131, 150, 164, 189–191

CSTR Completely Stirred Tank Reactors. 24, 25, 38, 152, 177

DCE Directive-cadre sur l'eau. xxix

DO Dissolved Oxygen. xxii, 26, 32, 38, 40, 51, 55, 69, 82, 84, 86, 87, 94, 111, 121–123, 125, 127, 129, 139, 182, 189, 193, 195, 196

DOM Dissolved Organic Matter. 33, 34, 41, 42

DWWT Decentralised Wastewater Treatment. 4, 7

EBA Elimination biologique de l'azote. xxxiv

EC Electrical Condutivity. 57–60

EPS Exo Polymeric Substances. vi, xi, 34–37, 43, 44, 46

Ewag Swiss Federal Institute of Aquatic Science and Technology. xxx, 7

FA Free Ammonia. xiii, xxi, 18, 26–28, 51–55, 57, 68, 69, 74, 75, 78, 79, 81, 82, 85, 128, 132, 133, 138–140, 142, 144–147, 163, 170, 172, 173, 195, 196

FM Fed to micro-organism ratio. 83

FNA Free Nitrous Acid. xiii, xxi, 26–28, 51, 53–55, 69, 74, 81, 82, 85, 87, 103, 128, 133, 138, 163, 172, 195, 196

HRT Hydraulic Residence Time. vii, viii, xi, xii, 25, 31–34, 51, 60, 82, 84, 86, 89–92, 94, 97, 98, 100, 101, 103, 105, 107, 109, 111, 114–118, 178, 182

IAWPRC International Association on Water Pollution Research and Control. 50

IS Ionic Strength. xxi, 18, 19, 56–58, 78

ISS International Space Station. 1, 2

Kla Volumetric Oxygen Mass Transfer Coefficient. xii, 125–127

LCA Life Cycle Analysis. 1

LFS Flowing gas Static liquid Respirometry. viii, xii, 123, 125, 126, 130–133, 137–140, 144–146, 191, 195, 196, 198

LSS Static gas Static liquid Respirometry. viii, 123, 125, 126

MBBR Moving Bed Biofilm Reactor. 24, 25, 83, 84, 87, 103

MBR Membrane Bio Reactor. v–ix, xi, xii, xv, 8, 9, 11, 24, 25, 28, 31–35, 37–39, 41–47, 50, 51, 56, 60–62, 70, 79, 80, 83–87, 89, 94, 100, 101, 103, 105, 109–111, 118, 126, 131–133, 140, 142, 149, 150, 163, 165, 167, 169, 171, 173, 175, 177–179, 181–184, 189, 191, 195

MLSS Mixed Liquor Suspended Solids. xi, xii, 31, 32, 37–40, 42, 44, 60, 88, 94, 104, 109, 125

MLVSS Mixed Liquor Volatile Suspended Solids. xi, xii, 88, 92–94, 104, 109, 124, 126, 142

MNR Maximum Nitrification Rate. 55, 84

NLR Nitrogen Loading Rate. vii, viii, xii, xiii, 24, 25, 27, 28, 47, 55, 83, 84, 87, 89–92, 94, 97, 101, 103–105, 109, 111, 114, 117, 118, 142, 165, 167, 170, 175, 178, 182–184

NOB Nitrite Oxidizing Bacteria. xii, xiii, xv, xvi, xxi–xxiii, xxxi, xxxii, xxxiv, 8, 21–23, 27, 28, 39, 47, 48, 51, 53–56, 62, 63, 66, 69, 70, 75, 79–82, 85, 91, 107, 109, 118, 124, 127–138, 140–144, 146, 147, 149, 153–155, 159, 161, 163–165, 168–170, 172, 173, 175–178, 182, 183, 189, 192–195, 198, 201, 203, 204

WFD Water Framework Directive. 3

WRRF Water Resource Recovery Facility. 1–3, 50

WWTP Wastewater Treatment Plant. xiv, xvi, 1, 3–7, 11, 12, 20, 25, 26, 32, 50, 55, 61, 68–70, 87, 104, 181, 201–203

Nomenclature

$A\mu_{\text{max}_N}$ Arrhenius pre-exponential factor for μ_{max_N}

$A\mu_{\text{max}_N}$ Arrhenius pre-exponential factor for μ_{max_N}

D_i Diffusion coefficient of ion in the solution, m^2/s

Ea_N Activation energy for NOB $44\,\text{kJ}\,\text{mol}^{-1}$

Ea_N Activation energy for NOB $44\,\text{kJ}\,\text{mol}^{-1}$

F Faraday's constant, Coulomb/mol

FA Free ammonia concentration, $\text{g}_{NH_3-N}.\text{m}^{-3}$

I Ionic Strength (IS) of solution, mol/L

K_0 Thermodynamic solubility constant of ion X_i, mol/L/atm

K_La Volumetric oxygen gas/liquid mass transfer coefficient, h^{-1}

$K_{O,A}$ Oxygen half-saturation constant for AOB, $\text{g}_{O_2}.\text{m}^{-3}$

$K_{O,H}$ Oxygen half-saturation constant for heterotrophs, $\text{g}_{O_2}.\text{m}^{-3}$

$K_{O,N}$ Oxygen half-saturation constant for NOB, $\text{g}_{O_2}.\text{m}^{-3}$

$K_{S,FA,A}$ Half-saturation constant of FA for AOB, $\text{g}_{NH_3-N}.\text{m}^{-3}$

$K_{S,FNA,N}$ Half-saturation constant of FNA for NOB, $\text{g}_{HNO_2^--N}.\text{m}^{-3}$

$K_{S,NO_3,H}$ Affinity constant for nitrates of heterotrophs, $\text{g}_N.\text{m}^{-3}$

$K_{S,TNN,H}$ Affinity constant for total nitrites of heterotrophs, $\text{g}_N.\text{m}^{-3}$

K_S Substrate half-saturation constant for heterotrophs, $\text{g}_{COD}.\text{m}^{-3}$

$K_{\text{alk},A}$ Alkalinity half-saturation constant for AOB bacteria, $\text{g}_C.\text{m}^{-3}$

$K_{\text{alk},N}$ Alkalinity half-saturation constant for NOB bacteria, $\text{g}_C.\text{m}^{-3}$

$K_{i,FA,A}$ Inhibition constant of AOB by FA, $\text{g}_{NH_3-N}.\text{m}^{-3}$

$K_{i,FA,N}$ Inhibition constant of NOB by FA, $\text{g}_{NH_3-N}.\text{m}^{-3}$

$K_{i,FNA,A}$ Inhibition constant of AOB by FNA, $\text{g}_{HNO_2^--N}.\text{m}^{-3}$

$K_{i,FNA,N}$ Inhibition constant of NOB by FNA, $\text{g}_{HNO_2^--N}.\text{m}^{-3}$

K_La Oxygen transfer coefficient, d^{-1}

$K_L a_C$ Carbon dioxide transfer coefficient, d^{-1}

$K_L a_N$ Free ammonia transfer coefficient, d^{-1}

OUR_T Total oxygen uptake rate $\text{g}_{O_2}.\text{m}^{-3}\,\text{h}^{-1}$

$O_{2_{sat}}$ Dissolved oxygen at the saturation in the liquid phase, $\text{g}_{O_2}.\text{m}^{-3}$

P_{Total} Total atmospheric pressure , atm

P_α Partial pressure ion i in the gaz phase, atm

Q_{in} Volumetric inlet liquid flow-rate, $\text{m}^3\,\text{s}^{-1}$

Q_{out} Volumetric outlet liquid flow-rate, $\text{m}^3\,\text{s}^{-1}$

R Idel gas constant, mol/L

S_{CO_2} CO_2 concentration, $\text{g}_C.\text{m}^{-3}$

$S^*_{CO_2}$ Carbon dioxide saturation concentration, $\text{g}_C.\text{m}^{-3}$

S_H H concentration, $\text{g}_H.\text{m}^{-3}$

$S^*_{NH_3}$ Free ammonia saturation concentration, $\text{g}_{NH_3-N}.\text{m}^{-3}$

S_O Dissolved Oxygen (DO) concentration, $\text{g}_{O_2}.\text{m}^{-3}$

S_{alk} Alkalinity, $\text{g}_C.\text{m}^{-3}$

S^*_o Dissolved oxygen saturation concentration, $\text{g}_{O_2}.\text{m}^{-3}$

X_A AOB biomass, $\text{g}_{COD}.\text{m}^{-3}$

X_H Heterotrophic biomass, $\text{g}_{COD}.\text{m}^{-3}$

X_N NOB biomass, $\text{g}_{COD}.\text{m}^{-3}$

$Y_{H_{anoxic}}$ Growth yield of heterotrophic biomass in anoxic conditions, $\text{g}_{COD}.\text{m}^{-3}/\text{g}_{COD}.\text{m}^{-3}$

Y_H Growth yield of heterotrophic biomass, $\text{g}_{COD}.\text{m}^{-3}/\text{g}_{COD}.\text{m}^{-3}$

Z_i Ionic charge of ion i, Dimensionless

$[X_i]$ Molar concentration of ion X_i, mol/L

$\Lambda^0_{m,i}$ Molar limiting conductivity, $\text{S/m}/(\text{mol/m}^3)$

α_i Active concentration of ion i, mol/L

λ_i Activity coefficient of ion i, Dimensionless

μ_{max_A} Maximum growth rate of AOB, d^{-1}

μ_{max_H} Maximum growth rate of heterotrophs, d^{-1}

μ_{max_N} Maximum growth rate of NOB, d^{-1}

ρ_j Process Rate Equation

$alphaC_{S_S}$ Carbon mass fraction of S_S (from River Water Quality Model (RWQM)1 COD matrix), $\text{g}_C.\text{m}^{-3}/\text{g}_{COD}.\text{m}^{-3}$

$alphaC_{X_A}$ Carbon mass fraction of AOB bacteria (from RWQM1 COD matrix), $g_C.m^{-3}/g_{COD}.m^{-3}$

$alphaC_{X_H}$ Carbon mass fraction of bacteria (from RWQM1 COD matrix, $g_C.m^{-3}/g_{COD}.m^{-3}$

$alphaC_{X_N}$ Carbon mass fraction of NOB bacteria (from RWQM1 COD matrix), $g_C.m^{-3}/g_{COD}.m^{-3}$

eta_g Correction factor of anoxic growth, $g_{O_2}.m^{-3}$

f_P Fraction of biomass leading to X_p, $g_{COD}.m^{-3}/g_{COD}.m^{-3}$

i_{xb} Nitrogen content in X_H, X_A and X_N, $g_N.m^{-3}/g_C.m^{-3}$

i_{xP} Nitrogen content in X_p, $g_N.m^{-3}/g_C.m^{-3}$

p_i Molar or volumetric ratio of i, v/v

r_A Specific oxygen consumption rate of AOB bacteria $g_{O_2}.m^{-3}/g_{MLVSS}.m^{-3}/h$

r_H Specific oxygen consumption rate of heterotrophic bacteria $g_{O_2}.m^{-3}/g_{MLVSS}.m^{-3}/h$

r_N Specific oxygen rate consumption of NOB bacteria $g_{O_2}.m^{-3}/g_{MLVSS}.m^{-3}/h$

z Charge number, Dimensionless

PSS Practical Salinity Scale, dimensionless

R Universal gas constant $8.31\,J\,mol^{-1}\,K^{-1}$

R Universal gas constant $8.31\,J\,mol^{-1}\,K^{-1}$

Sal Salinity of the liquid phase, PSS

$\alpha_{K_L a}$ Volumetric alpha factor, dimensionless

Para mi Madre…

Modélisation de la stabilisation de l'urine par nitrification au sein d'un bioréacteur à membrane

Dans cette thèse, la conceptualisation d'un modèle physico/biocinétique ainsi qu'une analyse expérimentale d'un système de bioréacteur à membrane traitant des eaux usées jaunes (urine) sont présentées.

Contexte du travail

Beaucoup d'activités humaines génèrent une forte concentration d'ammonium dans les eaux usées, comme par exemple la fabrication et l'utilisation d'engrais, l'industrie pharmaceutique et l'élevage intensif. Cette quantité d'ammonium cause l'une des contaminations les plus courantes dans le sol et les eaux souterraines (Effler et al., 1990). Néanmoins, c'est l'activité humaine elle-même qui génère potentiellement les plus grandes quantités d'ammonium. Les humains consomment dans leur alimentation ordinaire de la matière organique (y compris des protéines) ainsi que des nutriments tels que l'azote, le potassium et le phosphore.

Après la transformation métabolique à l'intérieur du corps, ce qui reste est surtout la forme hydrosoluble de ces nutriments, comme l'urée et le dihydrogénophosphate. Ceux-ci sont les principaux composants de l'urine. En général, les humains produisent environ 1.4 L d'urine et 140 g de matière fécale (en matière humide) par personne par jour (Rose et al., 2015). A titre d'exemple, un cas d'étude pour la Station Spatiale Internationale (SSI) d'après (Clauwaert et al., 2017) a montré qu'un membre d'équipage consomme habituellement 9 à 19 $g_{protein\ -N}\ d^{-1}$ pour un apport en protéines alimentaires de 0.8 à 1.5 $g_{protein}\ kg^{-1}_{massecorporelle}$ avec un poids corporel compris entre 65 et 85 kg. Il excrète la même quantité, principalement sous forme d'urée dans l'urine (7 à 16 $g_N\ d^{-1}$). La plupart de ces nutriments pourraient être récupérés pour produire des aliments dans une approche auto-suffisante. La figure 1 détaille le cycle de l'azote pour ce cas particulier, en tenant compte de certains processus basés sur la nitrification, avec comme objectif de récupérer et réutiliser la plus grande quantité d'azote (stabilisation des flux de déchets pour obtenir une production de composés utiles).

Cette application particulière montre qu'une nouvelle approche orientée vers la récupération/réutilisation est possible, même dans des environnements extrêmes comme le SSI. En effet, l'urine consiste principalement en urée lorsqu'elle quitte le corps. De plus, l'urine produite par l'homme représente 80% de l'azote, 50% du phosphore et 60% de la charge en potassium, tout en ne contribuant qu'à 1% du volume des eaux usées domestiques habituellement traitées dans les Station de traitement des eaux uséess (STEUs) (Judd, 2016; Larsen and Gujer, 1996; Udert et al., 2003a). Au sein des filières conventionnelles de traitement des eaux usées centralisées, l'efficacité de la récupération de ces nutriments (par exemple sous forme de

boues d'épuration ou de biosolides) est vraiment faible. En fait, entre 50 et 100% des déchets perdus sont contenus dans les eaux usées (Puyol et al., 2017).

Dans le contexte actuel, ce nouveau paradigme de traitement des polluants, qui consiste à réutiliser plutôt qu'à simplement dégrader le polluant, rend intéressant de considérer l'urée et son principal dérivé, l'ammonium, comme des nutriments et non plus comme des déchets. Les polluants ont ainsi maintenant le statut de matière première dans une optique d'analyse du cycle de vie. Il s'agit d'un concept d'économie circulaire complet pour le traitement des polluants, un concept qui permet de voir la base d'un développement durable où tout système de production devient autorégénératif, où toutes les matières appelées jusque-là déchets pourraient être reconverties en matières premières. Cela implique un cycle biologique plus technique et efficace, soit pour la modification de la chaîne de production du polluant, soit pour l'exploitation de la STEU. Cela signifie que les processus issus de déchets agricoles et industriels, ainsi que ceux dérivés de la consommation humaine directe, peuvent être considérés comme des cycles autorégénératifs (Pearce, 1995). Ce concept est en fait mieux connu sous le nom de "cradle-to-cradle". Dans ce paradigme, tout déchet n'est pas seulement traité pour être recyclé, mais aussi pour être potentiellement utilisé comme matière première. Ce processus global pourrait être soutenu par les énergies renouvelables (McDonough, W., andBraungart, 2010). Il pourrait s'agir d'une amélioration par rapport au modèle actuel et désuet du triple-R (recyclage, réutilisation, récupération). Cette évolution implique principalement l'évaluation, l'adéquation et la durabilité à long terme des systèmes d'assainissement urbains conventionnels, en termes de performance, des coûts d'infrastructure, de demande élevée en énergie et en eau, de problèmes d'élimination des boues et de recyclage limité de l'azote.

Au fil des ans, différentes techniques ont vu le jour pour stabiliser et récupérer l'azote des différentes sources d'eaux usées. Une nouvelle génération de STEUs (avec des améliorations des capacités de traitement), mais aussi des solutions technologiques alternatives ont été conçues pour parvenir à la récupération de l'azote, de l'énergie, des matières organiques et d'autres ressources potentielles. Ce changement est motivé non seulement par la nécessité de réduire les coûts et la consommation de ressources, en particulier la consommation d'énergie, mais aussi par la nécessité de réduire les effets anthropiques sur les cycles terrestres de l'azote (Batstone et al., 2015). L'une de ces solutions techniques alternatives est la séparation et le contrôle des effluents à la source. Cette séparation à la source et la gestion décentralisée de l'assainissement peuvent offrir de meilleures possibilités de récupération de l'azote, car elles minimisent la dilution et la contamination des excréta humains, la principale source des nutriments azotés (Larsen and Gujer, 1997; Larsen et al., 2009; Wilsenach et al., 2003).

Les STEUs conventionnelles ne sont pas capables de gérer une forte concentration d'azote ammoniacal dans l'eaux résiduelles entrantes. Dans ces procédés de traitement conventionnelles, l'azote provenant initialement de l'alimentation retourne en grande partie dans l'atmosphère sous forme N_2 produit dans les réacteurs anoxiques (par la dénitrification). Dans l'agglomération parisienne, même les unités de traitement intensif arrivent à saturation en termes de capacité de traitement et les niveaux attendus pour les rejets des effluents dans le milieu naturel ne sont plus toujours respectés. L'azote est libéré par la STEUs principalement sous forme de nitrates ou d'azote gazeux inoffensif, ce qui ne contribue pas à des perturbations locales majeures dans la Seine. Par contre l'azote libéré sous forme d'ammonium et de nitrites depuis trois décennies ne cesse toujours pas d'augmenter à des niveaux très élevés par rapport au niveau attendu pour l'atteinte du bon état écologique (Romero

et al., 2016), comme requis par la Directive-cadre sur l'eau (DCE).

Le seuil de la DCE de $0.5\,\text{mg}\,\text{NH}_4^+\,\text{L}^{-1}$ dans la Seine exige donc au moins 98% d'efficacité dans l'élimination de l'azote réduit pour ce cas particulier (Esculier, 2018). Bien que les limites de la faisabilité technique du traitement centralisé des eaux usées semblent avoir été atteintes, les concentrations d'ammonium dans le fleuve devraient être abaissées dans les années à venir. D'autre part, les concentrations de nitrites demeurent un problème. Même avec un traitement avancé des eaux usées, la compatibilité de l'impact environnemental centralisé des rejets d'eau traitée avec la préservation de l'environnement local demeure donc un problème à Paris. En raison du changement climatique, la baisse attendue du débit de la Seine dans les années à venir va encore renforcer cette problématique (Esculier, 2018). Par conséquent, une solution pour le cas présenté de la métropole de Paris ainsi que pour beaucoup d'autres STEU classiques, pourrait être la mise en œuvre complémentaire d'un traitement décentralisé. Celle-ci représente une solution prometteuse pour traiter des eaux usées plus concentrées en ammonium et avec un débit inférieur, ce qui permet de traiter une charge supérieur à celle normalement conçue dans le dimensionnement et la conception des Boues activées classiques (BAC).

Les techniques de Traitement décentralisé des eaux usées (TDEU) représentent ainsi une solution réalisable pour traiter les eaux usées dans de nombreux contextes et scénarios différents : zones géographiques isolées, élimination de polluants spécifiques des eaux industrielles, petites communautés, traitement à l'échelle d'un quartier ou d'une habitation, etc. Il s'agit d'un ensemble de nouvelles approches pour le stockage, le traitement et l'élimination et la réutilisation des eaux usées pour des systèmes de collecte individuels, des installations industrielles ou institutionnelles, et même des communautés entières (Libralato, Ghirardini, and Avezzù, 2011).

Par exemple, dans le cas hypothétique cité par (Larsen and Gujer, 1996), avec une séparation à la source très efficace des nutriments, les nouvelles eaux usées entrantes dans les STEU seraient limitées par l'azote et le phosphore du point de vue du traitement biologique comme le montre le tableau 1. Sans l'excès de phosphore et d'azote provenant de l'urine, le rapport DCO : NTK: TP est assez équilibré pour la croissance biologique. Le phosphore et l'azote disponibles peuvent donc être incorporés par les micro-organismes produits. Une étude de modélisation basée sur un bassin versant réel a montré que cela se produirait à 60 % de séparation urinaire (Wilsenach and Loosdrecht, 2006). Cela signifie que l'élimination des nutriments se ferait simplement par l'incorporation des nutriments dans la biomasse plutôt que par des moyens physico-chimiques et/ou par nitrification/dénitrification conventionnelle nécessitant de l'aération (donc une forte dépense énergétique) et parfois l'ajout de carbone organique exogène (i.e. méthanol). Généralement, en raison de la croissance lente des microorganismes autotrophes et de la variabilité des concentrations en azote et matières organiques, les STEUs sont sur-dimensionnées à cause des différentes concepts de dimensionnement (âge de boues élevé, nécessité de zones/phases aérobies et anoxiques). Avec la séparation à la source, les investissements et les coûts d'exploitation associés seraient considérablement réduits. Le fait de séparer jusqu'à 80% de l'azote des eaux usées en séparant l'urine à la source pourrait déjà concurrencer la plupart des STEUs avec élimination de l'azote global qui ont un rendement d'environ 50% à 60% de l'azote (Wilsenach and Loosdrecht, 2006).

D'autre part, dans ce scénario particulier de séparation, le nouveau traitement biologique au sein de la STEU pourrait fonctionner à des taux de charge beaucoup plus élevés et avec des besoins réduits en oxygène et en énergie (en fonction des besoins de nitrification de l'azote résiduel présent en moindre quantité). Dans ce cas, la production de biomasse pourrait être améliorée directement par l'incorporation

des nutriments dans la biomasse, et cet accroissement de la production de boues pourrait être utilisé pour augmenter la production de biogaz dans les digesteurs, dans un traitement *a-posteriori* des boues. C'est le concept de la redirection du carbone. Cela pourrait conduire à l'autosuffisance des stations d'épuration en termes d'énergie. Encore une fois, pour chaque cas particulier, une étude plus complète et plus réaliste doit être réalisée afin d'avoir le meilleur équilibre entre la consommation d'énergie et les exigences de qualité des effluents. De nombreuses études ont montré que la séparation à la source peut être économe en ressources, mais aussi que ces résultats sont sensibles au choix spécifique de la technologie (Larsen et al., 2009).

Cependant, une critique souvent entendue au sujet des solutions décentralisées est l'absence d'économies d'échelle. En effet, les technologies décentralisées ne sont usuellement considérées que là où il est trop coûteux de construire des réseaux d'assainissement, le principal problème demeurant la robustesse du traitement biologique localement. Le développement technique remet de plus en plus en question cette hypothèse, notamment en raison des progrès techniques réalisés, notamment sur les technologies membranaires (Digiano et al., 2004). Ce progrès n'est pas seulement technique, mais aussi basé sur une "économie de chiffres" : les membranes sont de plus en plus produites en grand nombre, ce qui entraîne une baisse des coûts. Évidemment, ce phénomène est observable pour toute technologie de traitement décentralisée qui devient largement acceptée (et souhaitée par le consommateur). Aujourd'hui déjà, certaines technologies de séparation à la source qui utilisent des membranes sont économiquement compétitives (Oldenburg et al., 2007), surtout grâce à la diminution des coûts fixes et des matériaux de construction des membranes.

Au cours des dernières décennies, de nombreuses études ont été menées sur les technologies TDEU pour les eaux usées jaunes séparées à la source. Au cours des années 1990, plusieurs groupes ont commencé à travailler sur les technologies de séparation à la source pour l'urine (Larsen and Gujer, 1996). Depuis quelques années et avec la prise de conscience du potentiel scientifique et économique de la séparation d'urine à la source et dans un objectif de récupération de nutriments, de nombreux projets ont vu le jour. Citons par exemple le projet Novaquis mené de 2000 à 2006 par l'Swiss Federal Institute of Aquatic Science and Technology (Ewag) qui est un projet interdisciplinaire ayant entre autre travaillé sur les différentes techniques de séparation et sur des sujets plus sociaux comme l'acceptation de cette pratique. Dans le même esprit, le projet Valorisation of Urine Nutrients in Africa (VUNA) a étudié des méthodes de récupération de nutriments grâce à un système couplé de nitrification biologique et de distillation où les nutriments traités sont récupérés de l'urine pure (Etter, Udert, and Gounden, 2014). Un autre objectif pourrait être la stabilisation de l'urine avant un post-traitement pour obtenir un effluent d'eau d'une qualité suffisante pour être réutilisé dans la chasse d'eau des toilettes. Dans les deux cas, le défi important consiste à traiter biologiquement des niveaux d'azote bien au-delà des concentrations habituelles trouvées dans les STEU classiques.

Ojectifs du projet

Le présent travail de thèse s'inscrit quant à lui dans le projet CARBIOSEP qui est un projet R&D financé par le programme FUI 20 ("Fonds Unique Interministériel"). Il vise au développement d'une unité décentralisée et autonome de traitement des

eaux usées jaunes avec pour objectif une minimisation de l'apport de réactifs et consommables, une minimisation de l'instrumentation nécessaire ainsi qu'une fiabilité du système optimisée pour un fonctionnement autonome du système.

Ainsi, cette recherche envisage de traiter biologiquement l'urine séparée à la source sans extraction des boues produites afin d'obtenir un système autonome pendant 2 à 3 mois. Afin d'atteindre les objectifs de traitement des eaux usées, la technique choisie est la nitrification réalisée dans un Bio-Réacteurs à Membranes (BRM) compact, se présentant comme une cartouche amovible. Cela donnerait une autonomie très intéressante et un avantage logistique sur les solutions actuelles pour ce type de systèmes décentralisés. Les contraintes et les différents défis auxquels est confronté ce projet sont divisés en trois points principaux :

- La rétention élevée des solides (âge des boues élevé),

- Les affluents avec une forte concentration d'urée (donc une forte charge d'azote),

- La présence de composants minéraux dans l'urine (en particulier des sels).

Dans ce contexte, l'objectif de cette thèse est de développer et de valider un modèle biocinétique plus précis qui représentera le comportement du BRM en grandeur réelle. Ce modèle permettra de simuler différentes conditions de fonctionnement, notamment de prévoir des défaillances, et de coupler ensemble des processus physicochimique et biologiques tout en acquérant une compréhension des mécanismes et des vois d'assimilation et d'inhibition des bactéries. Potentiellement, toutes ces connaissances permettront d'éviter un mauvais dimensionnement du procédé et d'en améliorer la conception et le fonctionnement. En termes de performance, le niveau visé correspond à un effluent contenant au moins autant de NH_4^+ et NO_3^-.

Problématique scientifique

La stabilité du procédé biologique constitue un verrou car elle exige une interaction bien maîtrisée des bactéries AOB et NOB. La nitrification biologique nécessite en effet une gestion optimisée des interactions entre ces deux types de bactéries autotrophes impliquées dans le processus de nitrification. Cet aspect est particulièrement critique pour les effluents à forte teneur en azote tels que l'urine (Udert et al., 2003a; Udert and Wächter, 2012).

L'un des objectifs est ainsi d'obtenir une biomasse acclimatée à de hautes teneurs en azote dans le réacteur biologique. La nitrification, en relation avec les phénomènes de stripping CO_2 et NH_3, est à l'origine d'importantes variations du pH des eaux usées à forte teneur en azote. A son tour, le pH affecte l'équilibre acido-basique des composés présents dans les eaux usées (ammoniac / ammonium, nitrites / acide nitreux...) qui peuvent agir soit comme substrats soit comme inhibiteurs de la croissance bactérienne (Anthonisen et al., 1976a). Par conséquent, le pH apparaît comme un paramètre crucial pour le contrôle et la stabilité du processus. Le contrôle du débit de l'affluent par des mesures de pH peut être une bonne stratégie pour maintenir une valeur de pH intéressante pour un taux de nitrification approprié et aussi pour mettre en œuvre l'augmentation progressive du Taux de charge d'azote (TCA) pendant la période d'acclimatation.

Le problème est de comprendre et maîtriser les meilleures conditions pour traiter l'urine (fraîche ou stockée), notamment les effets de l'alcalinité que d'autres auteurs ont déjà mis en évidence. Il est souhaitable *in fine* d'obtenir un système auto-contrôlé

pour acclimater la biomasse aux affluents riches en azote, ce sans utiliser de produit chimique pour stabiliser le pH. Dans ces conditions, sans ajustement "chimique" du pH, seulement 50% environ du $NH_4^+ - N$ de l'urine peut être converti en nitrate (Feng, Wu, and Xu, 2008). Chen (2009) conclut la même chose: l'alcalinité présente dans l'urine ne fournit que 41% de l'alcalinité nécessaire à la nitrification complète de l'urine. Comprendre la relation entre le pH et les bactéries nitrifiantes aidera à comprendre et à optimiser le démarrage du réacteur ainsi que d'évaluer les capacités maximales atteignables avec la technologie BRM. Par conséquent, le modèle biocinétique développé se doit de représenter la dynamique du pH sur l'acclimatation et le fonctionnement du bioréacteur.

Travail réalisé

Afin d'atteindre ces objectifs, **la méthodologie suivante a été mise en place** :

1. Après une analyse documentaire approfondie (chapitre 1, un modèle biocinétique représentant tous les processus pertinents a été conceptualisé (chapitre 2) ;

2. Une étude pilote a été menée (chapitre 3) : un système de nitrification dans un BRM a été mis en œuvre. Une stratégie d'acclimatation basée sur le contrôle du pH a permis de démarrer et piloter le système ;

3. Des tests respirométriques ont été effectués afin de caractériser l'activité de la biomasse et d'estimer les paramètres cinétiques des bactéries nitrifiantes (chapitre 4) ;

4. le modèle a été évalué sur la base d'une analyse de sensibilité des paramètres biocinétiques. Il a ensuite été utilisé pour l'analyse de différents scénarios d'acclimatation (chapitre 5).

Conceptualisation d'un modèle biocinétique

Pour une meilleure compréhension et une amélioration éventuelle du système CAR-BIOSEP, un modèle physico-chimique et biologique intégré a été conceptualisé. Dans ce modèle, la qualité et les propriétés de l'affluent ont été mises en évidence et les principaux paramètres opérationnels et environnementaux qui influent sur cette qualité et sur le rendement du système ont été intégrés. Cette conceptualisation aide non seulement à mieux comprendre la dynamique du système, mais aussi à faire avancer les défis scientifiques et les outils technologiques dans le développement de modèles physico/chimiques intégrés. Cet exercice d'analyse théorique donne un modèle dérivé de ASM qui prend principalement en compte :

- Impact de l'ammonification sur le devenir du carbone minéral et le pH,

- Deux étapes de nitrification pour identifier séparément la nitritation et la nitratation, et donc les activités des AOB et NOB,

- Description des conditions de limitation/inhibition pour les bactéries nitrifiantes,

- Inclusion des paramètres physiques comme la température, la rétention totale des solides par la membrane, l'échange liquide-gaz et l'impact de l'alcalinité sur la biomasse,

- Contribution de l'activité de la biomasse à la dynamique de la consommation/génération des protons à l'intérieur du réacteur (prédiction de l'impact de l'activité bactérienne sur le pH),

- Dégradation à long terme des résidus "non biodégradables" sur le fonctionnement à âge des boues infini du BRM.

La construction de ce modèle a été réalisée selon les objectifs opérationnels du projet CARBIOSEP et chaque procédé inclus a été analysé en fonction de cette application particulière (eaux usées fortement chargées en ammoniac). Toutes ces connaissances permettront enfin d'éviter un mauvais dimensionnement du procédé, d'améliorer la conception, le fonctionnement et l'optimisation du système à l'échelle réelle.

L'équilibre entre l'impact du pH sur la biomasse et la production de protons issue de l'activité biologique a été conceptualisé avec succès. L'effet du pH sur la croissance de la biomasse autotrophe est pris en compte en considérant les équilibres HNO_2/NO_2 et NH_3/NH_4^+ comme substrats/inhibiteurs des bactéries. Le pH est modélisé par la consommation ou la production de composés acide/base et de protons au cours de processus biologiques, associés au calcul de l'équilibre chimique pour les espèces azotées, ainsi que pour le carbone inorganique.

Essais pilotes d'acclimatation de la biomasse

Des boues activées classiques ont été acclimatées pour traiter des affluents en haute teneur en azote. Un pilote de laboratoire a été adapté pour traiter l'urine séparée à la source, comme le fait le réacteur CARBIOSEP à échelle réelle, et ainsi obtenir les boues acclimatées qui seront représentées par le modèle conçu. L'objectif opérationnel était d'obtenir une qualité d'effluent stable pendant la période d'acclimatation. L'absence d'ajout externe d'alcalinité conduit à la nitrification de la moitié de l'azote entrant dans le système, ce qui est un bon moyen de stabiliser et de valoriser l'effluent du réacteur.

Les bactéries autotrophes sont des organismes à croissance lente par rapport aux bactéries hétérotrophes, surtout en raison de leur faible efficacité dans le rendement de croissance et du fait qu'elles sont plus sensibles à l'inhibition par les substrats ou par les produits. Ces problèmes provenaient des différences d'activité bactérienne dûs soit à des conditions de croissance défavorables, soit à la concentration de certains composés inhibiteurs (comme pourrait l'être l'excès de substrat). C'est pourquoi le démarrage constitue l'étape la plus difficile lors de l'exploitation du BRM pour traiter l'urine séparée à la source. L'objectif était de réduire le temps nécessaire pour obtenir une biomasse nitrifiante stable, tout en maintenant la qualité de l'effluent.

Deux stratégies experimentales d'acclimatation consecutives ont été testées et comparées afin d'acclimater la biomasse sans utiliser de produits chimiques externes. Une acclimatation automatique utilisant les variations "naturelles" du pH comme paramètre de contrôle a été implémentée. Cette stratégie de contrôle est basée sur la mesure du pH à l'intérieur du réacteur: un seuil haut de pH aide à déclencher l'alimentation en urine alors qu'un seuil bas stoppe cette alimentation. Ainsi, la dynamique des eaux usées jaunes d'entrée (en termes de teneur en azote et d'alcalinité) et l'effet direct de l'élimination biologique de l'azote sont en équilibre et contrôlent la variation du pH dans le BRM. Cette stratégie permet d'utiliser le pH non seulement comme indicateur de fonctionnement, mais aussi comme variable

de contrôle dans le processus d'acclimatation. Les mesures du pH ont été utilisées comme indicateur de l'état des réactions biologiques dans le réacteur.

Dans la première stratégie, l'urine a été diluée 20 fois avec de l'eau du robinet et son stockage préalble n'a pas été contrôlé, d'où des variations importantes du fractionnement de l'azote de l'alcanité à l'entrée. Cette stratégie entraîne des instabilités récurrentes dans l'exploitation du BRM, et donne aussi une longue période d'acclimatation pour obtenir une concentration de biomasse relativement intéressante pour le fonctionnement réel ultérieur du système.

Deux leçons ont été tirées de cette première campagne expérimentale. Premièrement, l'hydrolyse préalable de l'urée n'ayant pas été maîtrisée, les variations de pH observées sont liées de manière concomitante à l'ammonification dans le réacteur générant de l'alcalinité et de l'azote ammoniacal, aux réactions de nitrification, etc. Dans ces conditions, le contrôle de l'alimentation par des seuils de pH ne semble pas être en corrélation avec l'activité biologique des AOB et NOB.

Pour la deuxième campagne expérimentale, l'urine administrée a été maintenue concentrée sur deux facteurs de dilution (3 et 5 fois). L'hydrolyse au maximum de l'urine dans le réservoir de stockage permet de mieux stabiliser et contrôler la qualité de l'entrée en termes de NH_4, Azote Kjeldahl total (NTK) et d'alcalinité. Dans ces conditions, l'acclimatation paraît mieux maîtrisée avec la stratégie de pilote de l'alimentation par seuils de pH.

Au cours de ces deux campagnes expérimentales, il a été nécessaire à plusieurs reprises de modifier les valeurs des seuils de pH pour l'alimentation du réacteur. La fourchette la plus efficiente a été 7-7.05 lors de la deuxième campagne. Cependant, une meilleure compréhension et évaluation quantitative de la relation entre le pH et les bactéries nitrifiantes permettrait de mieux analyser et optimiser l'étape d'acclimatation des boues, le démarrage du réacteur et les conditions Elimination biologique de l'azote (EBA) obtenues avec la technologie proposée. Ainsi, l'utilisation du modèle biocinétique développé prend ici tout son sens afin de mener à bien cette analyse. Au préalable, il est important de bien identifier les paramètres bioncinétiques d'intérêt et de calibrer ceux qui se révèlent les plus sensibles et identifiables expérimentalement.

Tests respirométriques

La biomasse acclimatée a été caractérisée par des tests respirométriques, pour déterminer certains parmètres de l'activité bactérienne et calibrer principalement les constantes de demi-saturation et d'inhibition pour les différentes populations nitrifiantes décrites dans le modèle. Comme le réacteur effectuait une nitrification à 50% d'azote réduit, un protocole d'essai respirométrique dans des boues fortement acclimatées a été conçu. Il consiste en un lavage préalable de la biomasse par concentration/dilution avec une solution saline. Ce protocole a permis d'identifier expérimentalement des paramètres biocinétiques clés à partir des boues acclimatées dans différentes conditions. Les résultats ont été obtenus principalement pour la souche bactérienne NOB, la plus sensible à l'accumulation du substrat et celle dont le taux de croissance est le plus lent parmi les bactéries nitrifiantes. Il est à noter que le modèle a permis de prédire de manière satisfaisante la dynamique de l'oxygène dissous et du pH lors des essais respirométriques.

Evaluation du modèle

Le modèle construit contient un grand nombre de paramètres. L'identification de certains paramètres clés peut donc se révéler complexe. Par conséquent, le modèle a été évalué par le biais d'une analyse de sensibilité locale prenant en compte également les éventuelles corrélations entre paramètres. Cette analyse a révélé que les paramètres sensibles et identifiables pour la prédiction du pH et des concentrations des espèces azotées sont notamment les constantes de demi-saturation et d'inhibition de la biomasse nitrifiante. Cela confirme l'identification réalisée au chapitre précédent via les tests respirométriques.

Par conséquent, après une analyse approfondie de l'identifiabilité des paramètres, le modèle biocinétique a été utilisé pour évaluer quantitativement les inhibitions respectives des bactéries oxydatives de l'ammoniac et des nitrites pour divers scénarios opérationnels (pré-ammonification ou non de l'urine, plages de pH, jeux de paramètres biocinétiques). Le modèle a été implémenté dans un solveur d'équations différentielles ordinaires permettant d'integrer la stratégie de contrôle marche/arrêt souhaitée. Les résultats ont confirmé que l'urine pré-ammonifiée permettait un temps d'acclimatation plus court. La période d'acclimatation la plus courte a été observée à un pH neutre (7-7,05) comme lors des expériences. Cette implémentation numérique devrait néanmoins être améliorée à l'avenir en tenant compte du temps de réponse de la sonde de pH et du contrôleur associé et en incorporant des processus physico-chimiques supplémentaires (devenir du phosphore, précipitation, sulfates...) qui pourraient déboucher sur une meilleure description de la dynamique du pH. Ce modèle offre des perspectives pour le développement d'un meilleur algorithme de contrôle de la nitrification de l'urine impliquant uniquement la mesure du pH et le contrôle prédictif en ligne.

Context of the project

Introduction

Excess of ammonium is one of the most common forms of contamination in soil and ground-water (Effler et al., 1990). Lots of production activities generate a high-strength ammonium wastewater: fertilizer manufacturing and use, pharmaceutical industry, and livestock. Nevertheless, human daily activity itself releases the higher load of ammonium.

Indeed, in their ordinary diet humans consume organic materials, including proteins and nutrients such as nitrogen, potassium, phosphorus. After the metabolic transformation inside the body, what remains is mostly the water-soluble form of those nutrients, presented in the form of urea and phosphate which are the main components of urine. In general, humans produce about $1.4\,\text{L}$ of urine and $140\,\text{g}$ of feces (wet weight) per person per day (Rose et al., 2015). As an example, one study applied to the International Space Station (ISS) (Clauwaert et al., 2017) showed that a crew member usually consumes between $9\,\text{g}_{\text{proteinN}}\,\text{d}^{-1}$ to $19\,\text{g}_{\text{proteinN}}\,\text{d}^{-1}$ for a dietary protein intake of $0.8\,\text{g}_{\text{protein}}\,\text{kg}^{-1}_{\text{body weight}}$ to $1.5\,\text{g}_{\text{protein}}\,\text{kg}^{-1}_{\text{body weight}}$ with a body weight between $65\,\text{kg}$ to $85\,\text{kg}$, and excretes the equivalent amount, mainly in the form of urea in urine ($7\,\text{g}_{\text{N}}\,\text{d}^{-1}$ to $16\,\text{g}_{\text{N}}\,\text{d}^{-1}$). Most of the nutrients could be potentially recovered to produce food in a self-sustainable approach. Figure 1 details the nitrogen cycle for this particular case, taking into account some nitrification-based processes to recover and reuse the highest quantity of nitrogen (via stabilisation of waste streams to achieve production of useful compounds).

This particular application shows that a nutrient recovery/re-use approach is possible, even in extreme environments such as the ISS. When urine leaves the body, it is almost sterile (even if some bacteria is present in the urinary tract) and consists mainly of the substance urea. In fact, as presented in Figure 2, the urine produced by humans accounts for 80 % of the nitrogen, 50 % of the phosphorus and 60 % of the potassium loading in domestic wastewater, while contributing to no more than 1% of the volumetric ratio of domestic wastewater usually treated in the WWTPs (Judd, 2016; Larsen and Gujer, 1996; Udert et al., 2003a). However, the efficiency of conventional WWTP in recovering those nutrients (for example within sewage sludge or bio-solids) is very low. In these conditions, most of the wastewater resources are lost and generate pollution when they could be used as resources. Between 50 and 100% of lost waste resources (in terms of nutrients) are contained in wastewater (Puyol et al., 2017). Thus, the conventional wastewater system is often criticised since it leads to an inefficient and linear flux of nutrients (left Figure 3).

The new approach in terms of sanitation solutions is the implementation of Water Resource Recovery Facilitys (WRRFs) as a part of a Life Cycle Analysis (LCA) for every single nutrient present in wastewater, and particularly in urine. The new pollutant treatment paradigm of reuse over removal, makes it interesting to consider urea, and its principal derivative ammonium, as nutrients, thus as a raw material in a LCA. This represents a complete circular economy concept for pollutants treatment, a concept that is the base of a sustainable development where any production system
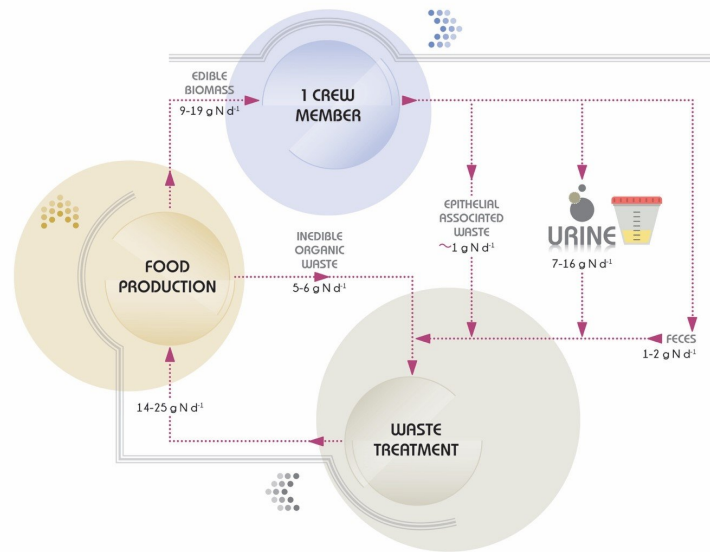
FIGURE 1: Schematic diagram of the theoretically calculated nitrogen balance for one ISS crew member.
(Clauwaert et al., 2017)
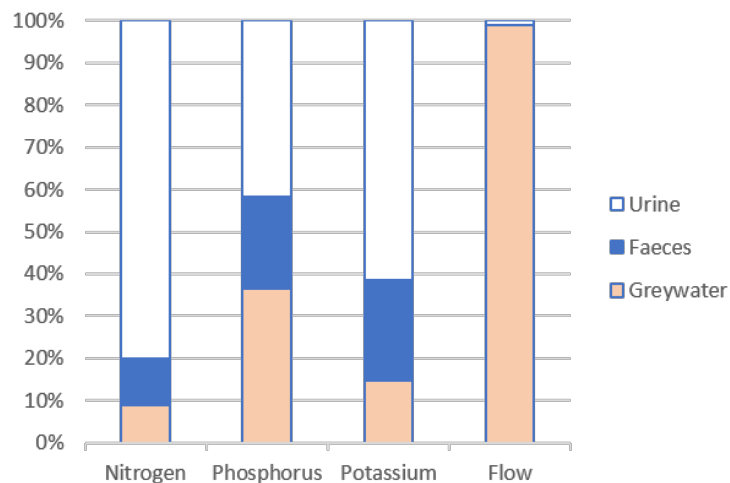
FIGURE 2: Release of nutrients from urine into the wastewater stream.
(Wilsenach, 2002)

becomes auto-regenerative. The aforementioned material considered "waste", could be reconverted into raw material in a more efficient cycle, namely for a production chain as for the WRRF conception. This approach encourages a system change as illustrated in Figure 3.

It means that waste from agricultural and industrial processes, as well as those derived from direct human consumption, could be considered as auto-regenerative cycles (Pearce, 1995). This concept is better known as cradle-to-cradle. The idea is to shift the paradigm from waste being treated and then recycled, to one where it is used as raw material for providing renewable energy (McDonough, W., andBraun-gart, 2010). This could be an improvement over the current and outdated triple-R
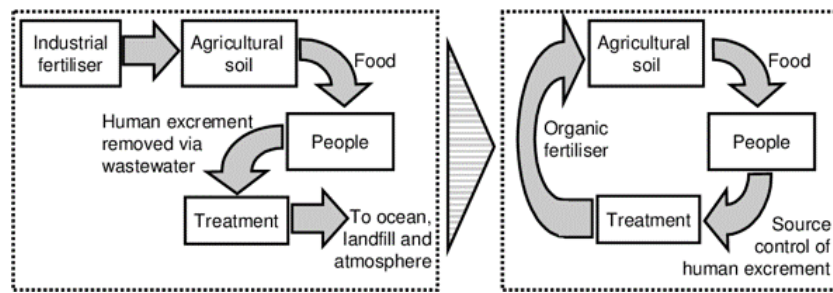
FIGURE 3: Linear flux of nutrients (left) while WRRF systems are aiming at a closed nutrient cycle (right).
(Wilsenach, 2006)

model (recycle, reuse, recovery). This evolution involves the evaluation, the adequacy and the long-term sustainability of conventional urban water and sanitation systems. Performance, infrastructure costs, high energy and water demand, sludge disposal problems, and limited nitrogen recycling must be considered.

Over the last few years, alternatives have been developed to stabilise and recover nitrogen from different wastewater sources. A new generation of WRRFs and of alternative technological solutions have been conceived to achieve nitrogen recovery, where energy, organics, and other resources are recovered as valuable byproducts instead of being wastefully dissipated or destroyed. Technological advancement is being driven not only by a need for reduced cost and resources, particularly energy consumption, but also by the need to reduce anthropogenic effects on terrestrial and aquatic nitrogen cycles (Batstone et al., 2015). One of these alternative technical solutions is source separation and control. Source separation can provide better opportunities for nitrogen recovery, as it minimizes dilution and concentrates contamination of human excreta, one of the main source of nitrogen nutrients in domestic wastewater (Larsen and Gujer, 1997; Larsen et al., 2009; Wilsenach et al., 2003).

The issue is the inability of classical WWTPs technologies to handle a high concentration of ammonium-nitrogen in the influents. This is particularly true for locations such as Paris, where the local footprint (calculated from the discharge of nitrogen and phosphorus through the Paris Megacity area) is minimized by intensive treatment units using conventional Biological Nitrogen Removal (BNR) through nitrification and denitrification. Ultimately, food waste nitrogen mainly goes back to the atmosphere as harmless N_2 in the anoxic reactors (denitrification). Taking Paris as an example, even intensive treatment units reach a saturation point in terms of treatment capacity. The expected levels required for discharge into the natural environment are difficult to achieve. The nitrogen is released from the WWTPs either in the form of nitrate or harmless nitrogen gas, which does not contribute to major local disruptions in the Seine river inside the Paris Megacity. However, the amount of nitrogen released as ammonium and nitrites is still high relative to the expected level for a safe ecological state (Romero et al., 2016), as required by the Water Framework Directive (WFD).

For this particular case, the WFD threshold of $0.5\,\text{mg}\,NH_4^+\,L^{-1}$ in the Seine river thus requires at least a 98% removal efficiency of TKN nitrogen (Esculier, 2018). Despite reaching the limits of the technical feasibility of centralized wastewater treatment, ammonium concentrations in the river should be lowered in the coming years to values compatible with the WFD. With that said, the nitrite concentration levels
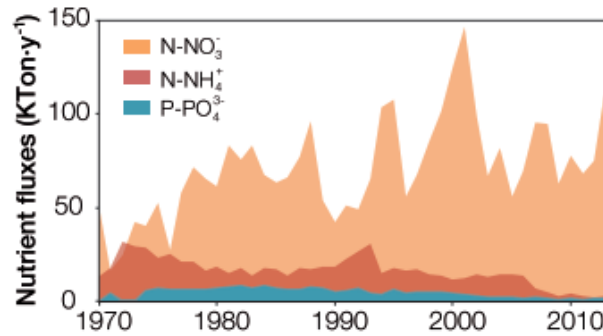
FIGURE 4: Release of nutrient's excess to the Seine river.
(Romero et al., 2016)

remain a concern. Even with advanced wastewater treatment technologies, the compatibility of the centralized approach's environmental impact with the preservation of the local environment remains a problem in Paris. The expected decrease of the Seine river flow in the coming years will enhance this affair even more (Esculier, 2018). As presented in Figure 4, the situation has been getting worse since the late 1990s. Therefore, a promising solution for the Paris Megacity case and for many others classical WWTP, could be the implementation of decentralized techniques treating more concentrated ammonium wastewaters in a lower flow-rate, which means a higher loading rate than the normal one used in the design of Conventional Activated Sludge (CAS) processes.

Decentralized treatment

Decentralised Wastewater Treatment (DWWT) could support wastewater treatment and resources recovery in many different scenarios: isolated geographical zones, specific wastewater pollutant removal, small communities, developing countries and rural areas (owing to the lower investment in infrastructure such as sewer network). It consists of a variety of new approaches for storage, treatment, and disposal/reuse of wastewater for individual collector systems, industrial or institutional facilities and even entire communities (Libralato, Ghirardini, and Avezzù, 2011). Their advantages are related to short time installation, the compactness of the system, and autonomy. Disadvantages and problems are related to weak or unsuitable organizational models as well as institutional setups that can hinder the correct operation of these systems (Larsen et al., 2016).

Decentralized systems and source-separation present an opportunity to rethink the urban water and nutrient cycle.

Reducing potable water consumption

A single household uses a tremendous quantity of potable water which will most often finish as gray-water that will be mixed with black-water from the toilets. Figure 5 shows the proportions of water used for different ends in France by 2010. Average consumption is 148 liters per person per day and the percentages show that one-quarter of domestic water uses (including toilet flushing and car washing) do not require a drinking water quality. In other words, a great deal of household

potable water that is used will be found in the sewer that transports wastewater to the WWTP.
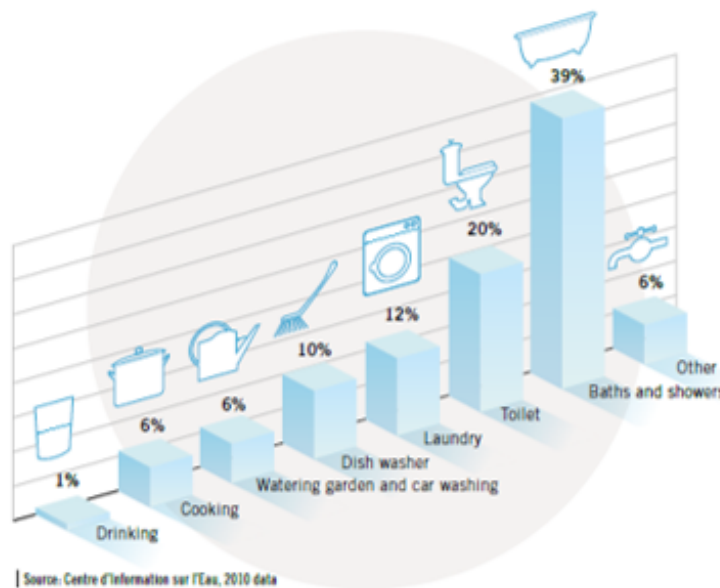
FIGURE 5: Breakdown of domestic water consumption by use in France by 2010.
(Da Costa et all, 2015)

Decreasing and optimizing water consumption poses an interesting challenge. The Federation of French Water Companies sees this as an opportunity to reduce withdrawals for domestic use. By combining one strategy of 16% to 20% reduction of distribution system leakage and a strategy of 40% reduction of per-household use, this should decrease the amount of drinking water resources required in Metropolitan France in the long term.

Optimizing the design of centralized WWTPs

The hypothetical case cited by Larsen and Gujer, 1996 considers a highly efficient source separation of nutrients: the new incoming wastewater to the WWTP is now limited by nitrogen and phosphorus from a biological treatment point of view as shown in Table 1. Without the excess of phosphorus and nitrogen coming from urine, the COD : TKN : TP ratio is fairly balanced for biological growth and the available phosphorus and nitrogen can thus be incorporated by the produced microorganisms. As nitrogen in this case limits growth, any addition of this nutrient will result in a direct increase of biomass.

A modeling study based on a real catchment showed that decentralized systems offer advantages when urine separation reaches 60% (Wilsenach and Loosdrecht, 2006). It means that nutrient removal would be achieved simply by the incorporation of the nutrients into the biomass rather than by BNR and/or physico-chemical means. Generally, classical WWTPs are oversized due to the slow growth of autotrophic microorganisms. Also, oversized due to the presence of the common "morning peak" and "afternoon peak" of nitrogen/organic matter (human urine and faeces are more concentrated in the morning and in the afternoon) that feeds the treatment plants. In fact, these systems are built several times larger because excess

nitrogen elimination is necessary. The oversize is due essentially because of the requirement of higher sludge age for nitrification and anoxic conditions required for denitrification. The large investments and operation costs for these systems would no longer be necessary if the BNR and denitrification stage could be avoided. Separating up to 80% of wastewater nitrogen at the source by collecting urine can compete with most denitrification treatment plants which typically achieve 50-60% nitrogen removal.

TABLE 1: Change in wastewater composition with separation of urine
(theoretical approach) (Larsen and Gujer, 1996)

Type of Wastewater	COD : TKN : TP ratio
Classical wastewater	100 : 10 : 1.25
Wastewater without urine	100 : 1.4 : 0.6
Mainly urine wastewater	100 : 67 : 5.3
Redfield nutrient ratio	100 : 16 : 1

In Table 1, the theoretical case of 100% source-separated urine reveals that urine accounts for 86% of the nitrogen and 52% of the phosphorus loading in domestic wastewater, which is in concordance with Figure 2. This shows that nitrogen is the limiting nutrient in the treatment of classical wastewater. Even if the table does not show a difference in the COD content, it is important to remark that COD contribution from urine is not negligible for the total value in classical wastewater. In the same table, the Redfield ratio (*e.g.* the average elemental ratio composition carbon to nitrogen to phosphorus of marine phytoplankton biomass throughout the world's oceans (Eddy, 2003)) is used to compare nitrogen to phosphorus ratios. It can roughly be seen as the optimal ratio for biomass growth and thus biological wastewater treatment. It dictates the biogeochemical impacts of phytoplankton growth (the impacts of carbon and nutrients extraction by organisms from the surrounding seawater (Wilt et al., 2016)) and decay. The Redfield ratio helps to put in evidence the nutrients excess potential of total urine separation (leading to a ratio **C/N/P**=19/13/1). Source-separated urine has an atomic ratio of 13:1 that increases after urine hydrolysis because an important amount of phosphate precipitates as struvite or hydroxyapatite (Udert et al., 2003b). These nitrogen and phosphorus nutrients could be for example assimilated into valuable algal biomass using photosynthesis. As nitrogen in this case limits growth, any addition of this nutrient will result in a direct increase of biomass.

Energy saving and production

On the other hand, in this particular scenario of efficient separation, the new WWTP biological treatment could be operated at much higher loading rates and at reduced oxygen and energy requirements (depending on the requirements for nitrification of residual nitrogen present in less quantity). Thus, techniques such as enhanced primary treatment (settling, sieving...) and/or processes such as High Rate Activated Sludge can be applied to increase biogas production in anaerobic digesters (Sancho et al., 2019), without issues related to organic substrate limitation for denitrification. This is the concept of carbon redirection. This could lead to self-sufficient treatment plants in terms of mechanical energy. Once again, for each particular case, a more complete and realistic study must be performed in order to have the best balance between energy consumption and effluent quality requirements. Many studies

showed that source separation can be resource efficient, but also that these results are sensitive to the specific choice of technology (Larsen et al., 2009).

Development of urine treatment/stabilisation technologies

An often heard criticism about decentralized solutions is that there are no economies of scale. Decentralized technologies are usually considered where it is too expensive to build sewers, but the main problem still remains the robustness of on-site biological wastewater treatment. Technical development increasingly challenges this assumption, particularly because of the progress in membrane technology (Digiano et al., 2004). This progress is not only technical, but also based on an "economy of numbers": membranes are increasingly produced in large numbers, resulting in decreasing prices. Obviously, this is valid for any decentralized treatment technology that becomes broadly accepted (and consumer desired). Some source separation technologies are already economically competitive (Oldenburg et al., 2007).

Many investigations have been conducted over the past decades on DWWT technologies for source-separated yellow wastewater/urine. Since the 1990s, several groups have worked on source separation technologies for urine (Etter, Udert, and Gounden, 2014; Harder et al., 2019; Hellström, 1999; Larsen and Gujer, 1996; Mackey et al., 2014; McConville et al., 2017; Oldenburg et al., 2007; Sun et al., 2012; Wilsenach, 2002).

Nowadays, source separation techniques projects have gained relevant importance and a notable scientific development for many objectives. Nutrient recovery is one of them and was explored by the Novaquatis project held between 2000 and 2006 by the Ewag. It was an interdisciplinary project on urine source separation technology, and also on related social topics such as consumer acceptance. From this background, they carried out the VUNA project for nutrient recovery from source-separated urine (Etter, Udert, and Gounden, 2014): the technology is based on a biological nitrification and distillation coupled system. Another objective could be the stabilisation of urine prior to a post-treatment to obtain an effluent water with sufficient quality for reuse in the flush of toilets. In both cases, the challenge is to deal with nitrogen levels exceeding the usual concentrations found in the classical WWTP facilities.

CarbioSep project

The CARBIOSEP Project is an R&D program funded by the FUI 20 ("Fonds Unique Interministériel") program. It aims to develop a decentralized and autonomous yellow wastewater treatment unit, conceived as a technical and sustainable solution being cost-effective and economical, while maintaining a good outlet water quality.

The high nitrogen content present in this yellow wastewater represents a challenge for choosing the most effective and low-cost technique for each particular application, and for determining whether or not complete nitrification is expected (Udert et al., 2003a). A decentralized system must be autonomous for a considerable period of time and must ensure a stable and permanent quality of the outlet water, in order to be outperform conventional sanitation systems. The principal treatment objective is to obtain a stabilized effluent 1:1 ratio ammonium nitrate by nitrification of the yellow wastewater. This would stabilise and valorize the effluent for a potential tertiary treatment.

This research envisages to treat source separated urine without excess sludge wastage in order to get an autonomous system for 2-3 months. In order to achieve the wastewater treatment goals, the chosen technique is nitrification carried out in a compact MBR, presented as a removable cartridge, to stabilise mainly urine as a source of nitrogen. This means that the system will treat mainly yellow wastewater and that there is no sludge wastage for approximately two or three months, which will give an interesting autonomy and a logistical advantage over the current solutions for this type of decentralized system. The constraints and different challenges that are encountered in this project can be divided into three main categories:

- the high retention of solids (high sludge age),

- the high concentration of urea (thus a high nitrogen load),

- the presence of mineral components in the urine (in particular salts).

In this context, the objective of this thesis work is to develop and validate a more accurate biokinetic model that will represent the behaviour of the full-scale MBR. This model will lead to the simulation of different operating conditions (prevention of failures) and also to the integration of physio-chemical/biological processes together. This will allow for a better understanding of the mechanisms of assimilation/inhibition by bacteria. Furthermore, this knowledge will potentially be useful for avoiding poor dimensioning of the process and to improve the design, operation and optimization of the real scale system. The performance target of the project is to treat urine by nitrification and to obtain an effluent of at least equal parts of NH_4^+ and NO_3^-.

The stability of the biological process is particularly challenging, as it requires the well-tuned interplay of AOB and NOB. Biological nitrification requires optimized management of interactions between those two types of autotrophic bacteria that are involved in the nitrification process. This aspect is particularly critical for effluents with a high nitrogen content such as urine (Udert et al., 2003a; Udert and Wächter, 2012). One of the the goals is to obtain acclimated biomass containing a high nitrogen content within the biological reactor. Nitrification, in connection with the phenomena of CO_2 and NH_3 stripping, is at the origin of important variations of the pH in high nitrogen content wastewaters. In turn, the pH affects the acid-base equilibrium of the compounds present in the wastewater (ammonia / ammonium, nitrites / nitrous acid ...) which can act either as substrates or inhibitors of the bacterial growth (Anthonisen et al., 1976a).

In order to reach the objectives of the project, the following methodology has been set up:

| 1 | Literature review on urine nitrification challenges MBR modeling and operational issues of the biomass acclimation (chapter 1). |

| 2 | Conceptualization and development of a biokinetic model representing all the relevant processes (chapter 2). |

| 3 | Pilot-scale study (chapter 3): a nitrifying system within a MBR was implemented. An acclimation strategy based on pH control allowed to start-up the system and acclimate the biomass. |

| 4 | Implementation of respirometric tests in order to characterize biomass activity and estimate kinetic parameters of nitrifying bacteria (chapter 4). |

| 5 | Model validation over the experimental data of pilot reactor start-up and operation. Different case scenarios were also tested to evaluate the predictive potential of the model (chapter 5). |

Chapter 1

Literature review

Urine is the excrement fraction containing the majority of nutrients. Thus, source separation could simplify the wastewater treatment process and improve effluent quality (Wilsenach et al., 2003). In order to achieve this objective, it is important to understand the dynamics and the technical issues of working with urine. Therefore, an analysis of urine characteristics and of its variability over time must be achieved. In the present chapter three issues are discussed:

1. a review of urine properties and main stabilisation techniques (handling issues),

2. MBRs highlights and their use on source-separated treatment,

3. modeling approach to better understand both urine dynamics and MBR performance related to the specific treatment goals.

1.1 Urine characterization and challenges

Source separated systems to treat urine are faced to urine handling constraints. As presented before, human urine is highly concentrated in nutrient content (see Figure 2). Also, urine is highly unstable in presence of different kinds of bacteria. Urine leaving the human body could be contaminated with bacteria and bacterial urease hydrolyzes urea present in the urine to ammonia after a short-term storage. This leads to a significant increase of pH and alkalinity (Udert et al., 2003a). This phenomena is called urea hydrolysis (see Figure 1.1).

To better understand these particular problems, the first step is to analyse the urine in terms of origin and composition. This will impact the different interactions that may occur during storage and/or transportation inside a process scheme to stabilise it. It will allow to identify the best technical solutions to stabilise source separated urine. For example, when considering the conventional coupled nitrification/denitrification scheme (like in a classical WWTP), urine has a unfavorable COD to nitrogen ratio for the denitrification phase and not enough alkalinity for full nitrification by biological ways (Sun et al., 2012). For our particular project objective, an analysis of the different technical solutions to stabilise source separated urine has been carried out. It is presented in this chapter (see Section 1.2).

1.1.1 Fresh urine composition

The composition of human urine can vary according to many factors as: socials, economic, geographical, hygienic, habits, drinking water access, specific physical activities, body size, or environmental factors.
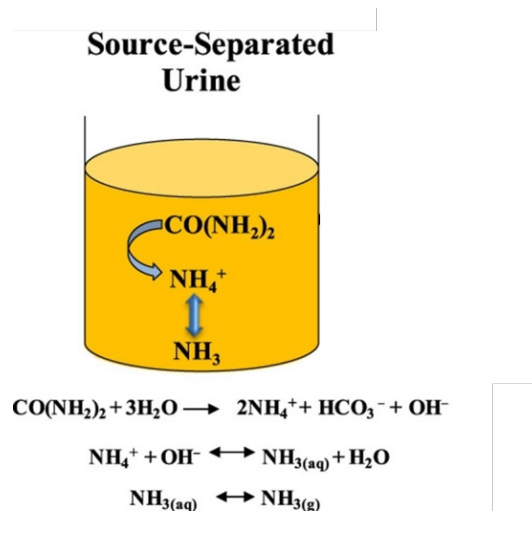
Figure 1.1: Urea hydrolysis in stored urine (modified from Tun et al., 2016)

TAN concentration of source-separated human urine varies depending on all of these factors. The TAN concentrations reported for source-separated human urine from households, schools and workplaces ranged from 1.80 to 2.61 g N L^{-1} (Maurer, Pronk, and Larsen, 2006; Udert et al., 2003a). In fresh urine according to Visek (1972), about 85% of nitrogen is fixed as urea (0.4 to 0.5 M urea (Mobley and Hausinger, 1989)) and about 5% as total ammonia, which results in an annual release of 10 kg of urea per adult (Visek, 1972). Besides organic nitrogen (5–8 g N L^{-1})(mainly creatinine, amino acids and uric acid) and inorganic nitrogen (0.4 g N L^{-1}) (mainly ammonia) (Udert, Larsen, and Gujer, 2006), fresh urine contains 3.5% organics (9 g COD L^{-1}) and 1.5% inorganic salts (21 mS cm^{-1}) sodium, potassium, chloride, magnesium, calcium, ammonium, sulfates, phosphates, etc..., but it is highly diluted with approximately 95% water (Zhao et al., 2016) coming from the urine itself. For an average daily consumption of 150 Liters per person in France, it represents an initial 99.15% times dilution that will be increased even more by the mixing with all the households that feds and contribute to the normal WWTP influent.

Humans typically excrete between 1.27 kg PE d^{-1} to 1.36 kg PE d^{-1} of urine, with a water content of 95% by assuming that each person uses the toilet around five times a day and flushes it after use (Wilsenach, 2002) and with a variable composition as shown in tables 1.1 and 1.2. This table represents the variability in the urine components from the fresh separated urine, but also the effect of the storage, which means the influence of time, temperature and other process variables that must be taken into account for the correct sizing, operation and control of the chosen treatment process.

1.1.2 Effects of storage

Urea hydrolysis - UREOLYSIS

The enzyme urease (urea amidohydrolase) hydrolyses urea to ammonia and carbamate. The latter decomposes spontaneously to carbonic acid and a second molecule of ammonia (Mobley and Hausinger, 1989) (figure 1.2).

$$H_2N-\overset{\overset{\displaystyle O}{\|}}{C}-NH_2 \; + \; H_2O \; \xrightarrow{\text{urease}} \; NH_3 \; + \; H_2N-\overset{\overset{\displaystyle O}{\|}}{C}-OH$$

$$H_2N-\overset{\overset{\displaystyle O}{\|}}{C}-OH \; + \; H_2O \; \longrightarrow \; NH_3 \; + \; H_2CO_3$$

$$H_2CO_3 \rightarrow H^+ \; + \; HCO_3^-$$

$$2NH_3 \; + \; 2H_2O \rightarrow 2NH_4^+ \; + \; 2OH$$
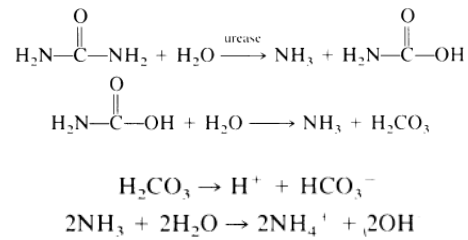
FIGURE 1.2: Urea hydrolysis (Mobley and Hausinger, 1989)

The catalyst, urease, is produced by a variety of eukaryotic and prokaryotic organisms but bacteria are the most abundant (Mobley and Hausinger, 1989) including many but not all AOB (Koper et al., 2004). The overall reaction can be written as follows:

$$NH_2CONH_2 + 2H_2O \Longrightarrow NH_3 + NH_4^+ + HCO_3^- \qquad (1.1)$$
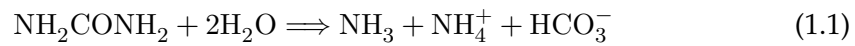
There are several mechanisms for the regulation of urease synthesis. Environmental conditions such as the availability of nitrogen sources, the urea concentration or the pH can regulate the urease synthesis. However, many bacteria synthesise urease consecutively. In addition to urease, a second enzyme is known to hydrolyse urea, urea amidolyase, which is produced by several yeasts and algae (Mobley and Hausinger, 1989).

Evolutions of urine composition following storage

The table 1.3 presents an example of the variation of urine composition due to storage. From this characterisation of fresh and stored urine, it could be concluded that this change over the time is a result of bacteria contamination and environmental factors (e.g temperature). This causes ureolysis that degrades urea to produce ammonia and increase pH.

Urine composition (unit)	Fresh	Stored
pH	5.8	9.4
Conductivity (mS cm^{-1})	9.1	25.9
DOC (g L^{-1})	7.29	2.81
$NH_4^+ + NH_3$ -N (g L^{-1})	0.57	8.67
Urea (g L^{-1})	4.95	1.05
Anions		
NO_3^- (g L^{-1})	0.16	n.d.
SO_4^{2-} (g L^{-1})	1.61	1.28
PO_4^{2-} (g L^{-1})	2.86	1.18
F^- (mg L^{-1})	91.6	55.8
Cl^- (g L^{-1})	2.67	2.40
Cations		
Na (g L^{-1})	0.83	1.01
K (g L^{-1})	0.52	1.17
Mg (mg L^{-1})	76.0	n.d.
Ca (mg L^{-1})	88.0	3.1

Note: n.d. = not detected.

FIGURE 1.3: Example for the variation of urine composition during storage.
(Jaatinen et al., 2016)

TABLE 1.1: Concentration of compounds in fresh and stored urine.

Component	Fresh urine				
	(Rose et al., 2015)	(Liu et al., 2016)	(Udert, Larsen, and Gujer 2006)	(Larsen, 2013).	(Flanagan and Randall, 2018)
	Data from different studies	Urine from laboratory members		Some values based on literature	Stabilized source separated urine with $Ca_{(OH)_2}$
pH	5.5–7.0	6.0 ± 0.3	6.2	6.2	12.32 ± 0.1
Ammonia-N (mg L-1)	125–600	1125 ± 147	480	463	356 ±34.5
Urea (mg L-1)	9300–23300		7700	8367	12800 ± 987
N-tot (mg N L-1)	4000–13900	7523 ± 1097	9200	8830	
P-tot (mg P L-1)	350–2500	448 ± 56		800-2000	6.17 ± 0.124
Total phosphate-P (mg L-1)	205–760		740		
TOC (mg L-1)		5298 ± 792	22 (mM)		
COD (mg O2 L-1)	6270–17500		10000		
Dissolved COD (mg O2 L-1)					
Conductivity (mS cm-1)	160–270	14.95 ± 1.87	3800 (mg/L)	4970 (mg/L)	
Calcium (mg L-1)	32–230		190	233	995 ± 72.3
Magnesium (mg L-1)	70–120		100	119	15.3 ± 2.5
Potassium (mg L-1)	750–2610		2200	2737	621 ± 91.5
N/P/K Ratio	5.3/0.46/1 -5.3/0.96/1		4.2/0.3/1	3.2/0.5/1	21.2/0.0093/1

TABLE 1.2: Concentration of compounds in fresh and stored urine.

Component	Stored urine				
	(Fumasoli et al., 2016)	(Udert, Larsen, and Gujer, 2003)	(Udert and Wächter, 2012)	Jacquin et al., 2018	(Jagtap and Boyer, 2020)
	Urine from men, only	Simulated values during storage	Urine from men, only	Mixed and stored urine at 4 °C	Urine from men and women stored for 9 months
pH	9.0 ± 0.1	9.1	8.69 ± 0.11	7.9 ± 0.6	9.1
Ammonia-N (mg L-1)	4140 ± 870	8100	$2{,}390 \pm 250$		3400
Urea (mg L-1)		0			1100
N-tot (mg N L-1)		9200		6682 ± 1488	4500
P-tot (mg P L-1)					140
Total phosphate-P (mg L-1)	242 ± 23		208 ± 49	937 ± 192	
TOC (mg L-1)		490(mM)		5160 ± 1130	2100
COD (mg O2 L-1)				7003 ± 2062	
Dissolved COD (mg O2 L-1)	$3{,}860 \pm 870$		4500 ± 910		
Conductivity (mS cm-1)		3800 (mg/L)		17.4 ± 5.0	0.32
Calcium (mg L-1)			16 ± 3	155 ± 36	
Magnesium (mg L-1)			< 5	25 ± 24	
Potassium (mg L-1)	1470 ± 130		1410 ± 320	2377 ± 374	1500
N/P/K Ratio	2.82/0.16/1		1.7/0.15/1	2.8/0.4/1	3/0.093/1

The initial cause of changes in the fresh urine composition is the contamination with microorganisms, which can hardly be avoided in urine-collecting systems. Fresh urine hardly contains any microorganisms; there are evidences that urine of healthy people may contain bacteria, but it is still uncertain whether these are viable or connected with bacterial infection (Wolfe et al., 2012). Faecal sterols measured in source-separated urine indicate cross-contamination with transmissible pathogens and other bacteria from faeces (Larsen, 2013). The organic load of yellow water is relatively low, with a specific contribution of $13\,\mathrm{g\,COD\,p^{-1}\,d^{-1}}$. Nevertheless, COD levels in source separated urine are high $(10\,\mathrm{g\,L^{-1}})$. This organic matter (measured as COD) is composed of organic acids, creatinine, amino acids and carbohydrates, which can be degraded by anaerobic bacteria such as fermenters during storage. The main dissolved compound in urine, urea $(9.3\,\mathrm{g\,L^{-1}}$ to $23.2\,\mathrm{g\,L^{-1}}$ (Rose et al., 2015)) is also organic, but does not present any COD (Udert, Larsen, and Gujer, 2006).

According to Udert, Larsen, and Gujer (2006) microbial urea hydrolysis, mineral precipitation and ammonia volatilisation are the most important transformation processes that must be taken into account in urine storage. This is clear because storage is not only important in terms of space, but also because when the fresh urine is exposed to microbial contamination already present in the waste, it causes degradation of organic matter and hydrolysis of urea. The hydrolysis converts urea to NH_3 and NH_4^+. During this process, pH increases to approximately 9.2. Bacteria in the collection system produce the enzyme urease which decomposes urea into ammonia and bicarbonate, thereby raising the pHvalue. More important even is the fact that at these pH, the precipitation of various secondary compounds (primarily phosphate compounds as struvite $(MgNH_4PO_4.6H_2O)$, hydroxyapatite $(Ca_5(PO_4)_3(OH))$ and calcite $(CaCO_3)$ occur, that can cause fouling of pipes and potentially damage many other equipment.

The consequence of organic matter degradation is bad odour caused by ammonia striping at high pH. Following urea hydrolysis 90% of the nitrogen is in the form of TAN $(NH_3 + NH_4)$, as opposed to fresh urine where 85% of the nitrogen is fixed as urea. Due to the pH increase (from 6.2 to 9.1), the ammonia fraction (NH_3) of TAN becomes high. Ammonia is very volatile (Henry's constant: $62\,\mathrm{mol\,L^{-1}\,atm^{-1}}$ at $25\,°C$ (Bates and Pinching, 1949)). Therefore, it can be lost through volatilization during storage and transport of urine. Ammonia volatilization is not only a loss of a valuable nutrient, but it also can cause health and odour issues. Urea hydrolysis also strongly increases the alkalinity (Udert, Larsen, and Gujer, 2006). Those three phenomena; urea hydrolysis, ammonia volatilisation and the potential metal precipitation caused by pH change, remain the most important ones for analysing the dynamics around urine storage, treatment and stabilisation.

To overcome these issues, stabilisation of urine is made necessary. This stabilisation could be easily achieved in function of the main objective and the overall goal of the treatment process:

1. Physical techniques for hygienisation, volume reduction and stabilisation (Boyer et al., 2014; Ishii and Boyer, 2015), storage, evaporation, freeze-thaw, reverse osmosis, ammonia stripping, nanofiltration (Maurer, Pronk, and Larsen, 2006).

2. Physicochemical techniques as acidification, struvite formation, isobutylaldehyde-diurea (IBDU) precipitation, electrodialysis, ozonation (Maurer, Pronk, and Larsen, 2006) and ion-exchange (Boyer et al., 2014).

3. Biological ways (nitrification, anammox, etc...) (Kartal, Kuenen, and Van Loosdrecht, 2010; Udert and Wächter, 2012; WEF, 2011)

4. Non conventional techniques such as microalgae (Batstone et al., 2015; Puyol et al., 2017; Wilt et al., 2016)

1.1.3 Urea dynamics and ammonium equilibrium

It has been shown in the previous section that the storage condition generates changes in the urine composition (see Figure 1.1). This lead to complex dynamics involving the rate of urea hydrolysis, the subsequent production of bicarbonate ions that increases the pH and the potential striping phenomena enhanced by this increase. This could result in bad odours but also to dangerous environments with overcharged ammonia vapours. Urea ($CO(NH_2)_2$) becomes hydrolyzed to ammonia and bicarbonate by the enzyme urease or by urea amidolyase (Hunik, Meijer, and Tramper, 1992). Udert, Larsen, and Gujer (2006)) demonstrated that after complete urea hydrolysis, total ammonia became 90% of the nitrogen in stored urine. All the organic nitrogen waste present in the urine could be stabilised by transforming all the component via ammonification, it means "all proteins and peptides are converted into amino acids by proteases produced by living organisms, while amino acids and other amide containing molecules can be hydrolyzed by amidases to form ammonia" (Clauwaert et al., 2017).

This quantity of ammonia produced is in chemical equilibrium with its acid form, ammonium which is also dissolved in the liquid phase (equation 1.2). This equilibrium depends on the pH of the solution as shown in figure 1.4. It yields two problems for urine stabilisation: ammonia stripping at high pH for stored urine that will create bad odours, but also the true quantity of FA (the real substrate for AOB bacteria) available for the nitrification performance.

$$NH_4^+ + OH^- \leftrightharpoons NH_3 + H_2O \qquad (1.2)$$
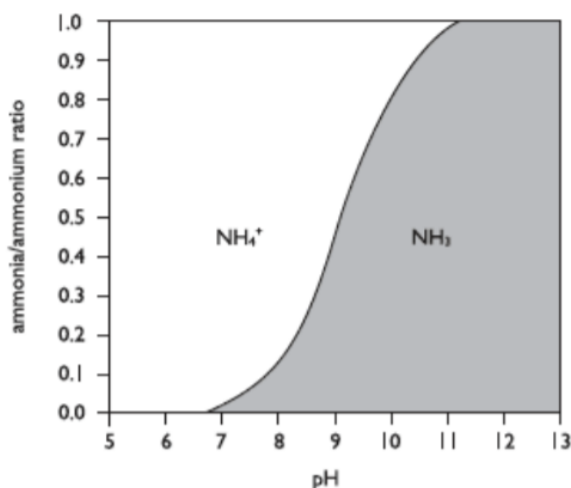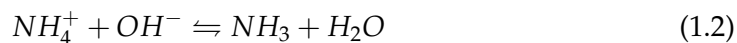
FIGURE 1.4: Ammonium equilibrium with pHat IS I= $0.7225\,\mathrm{mol\,kg^{-}1}$
(Clegg and Whitfield, 1995)

The thermodynamic equilibria of species involved is used to calculate the speciation and the particular pKa taking in to account the IS influence. It means that deviations from the ideal behaviour must be taken into account. Indeed, interaction of ions in a concentrated solution like urine causes a deviation from ideal behaviour.

The activity of the ions in equilibrium reactions is less than expected from simplest calculation with the molar concentrations. To account for this behaviour, the molar concentration is corrected by a factor known as the activity coefficient. The modified ionic concentration is called the active concentration, as determined in the following expression:

$$\alpha_i = \lambda_i.[X_i] \tag{1.3}$$

where

α_i = active concentration of Xi
$[X_i]$ = molar concentration of ion Xi
λ_i = activity coefficient of ion Xi

Activity coefficients are estimated in the general pH model using the Davies equation, which is a simplification of the extended Debye-Hückel law. The activity coefficient λ_i for each ion i in solution is determined as follows (Curl, 1979):

$$log\lambda_i = -0.5Z_i^2.\left(\frac{\sqrt{I}}{1+\sqrt{I}} - 0.2.I \right) \tag{1.4}$$

where,

Z_i = ionic charge of ion Xi
I = IS of solution

The expression for IS is as follows:

$$I = 0.5\sum [X_i]Z_i^2 \tag{1.5}$$

where,

n = the number of ionic species in solution

With these considerations, as an example the equilibria for the ammonium species could be written as:

$$\frac{\alpha_{H^+}\alpha_{NH_3}}{\alpha_{NH_4^+}} = K_{NH_3} = 3.966\exp^{-10} \tag{1.6}$$

This physical equilibrium will affect the fate of substrate and its speciation in the liquid phase that can be assimilated to the available substrate for biomass. In addition, pH variations could affect system behaviour. In the case of urine, salt accumulation leads to a high influence of the IS and these deviations from the ideal behaviour must be considered in a modeling approach.

1.2 Overview of urine stabilisation techniques and involved biochemical reactions

The main techniques to stabilise human urine and foster enhancement of nutriments are based in volume reduction, in order to concentrate nutrients. Several processes (e.g. evaporation, reverse osmosis, partial distillation etc..) have been considered in finding an effective method to reduce the water content of human urine (see Maurer, Pronk, and Larsen, 2006 for a detailed discussion). Significant water reduction was achieved by evaporation (> 96%) and the freeze–thaw process (75%), although these

processes required unacceptably intensive energy. Furthermore, the dissolved ammonia contained in source-separated human urine can be easily evaporated to the atmosphere during the process (Tun et al., 2016).

Storage is also a predominant mode of disinfection considered for source separated urine. Here, following the urea hydrolysis process that takes place in stored urine, the stabilisation principle is based only on the the production of NH_3, taking advantage of its biocide properties (Ishii and Boyer, 2015). However, the storage time required for adequate disinfection is difficult to determine, as it depends on the pathogen content (type and concentration), NH_3 content, pH and temperature of the stored urine mixture, which are often highly uncertain and variable over time (Hellström, Johansson, and Grennberg, 1999; Ishii and Boyer, 2015; Jaatinen et al., 2016; Muys, 2014).

Maurer, Pronk, and Larsen (2006) reviewed the possible biological and physical techniques for treating separated urine. Because biological treatment is more effective and relatively inexpensive, it has been widely adopted in contrast to physicochemical technologies. In this study, we will only focus on biological treatment. These strategies are based on the reactions described on figure 1.5.

This figure presents the possible biologically mediated reactions that occur in the environment and lead to nitrogen transformation. Most of WWTPs rely on aerobic nitrification followed by anoxic denitrification for nitrogen removal. Several strategies have been developed for the treatment of wastewater containing high-strength nitrogen and a generally low content in biodegradable COD. For instance:

- old well-known physico-chemical processes: stripping (Teichgräber and Stein, 1994);

- biological processes such as conventional biological nutrient removal, short-cut nitrogen removal combined or not with Anaerobic AMmonium OXidation (ANAMMOX) (Kartal, Kuenen, and Van Loosdrecht, 2010).
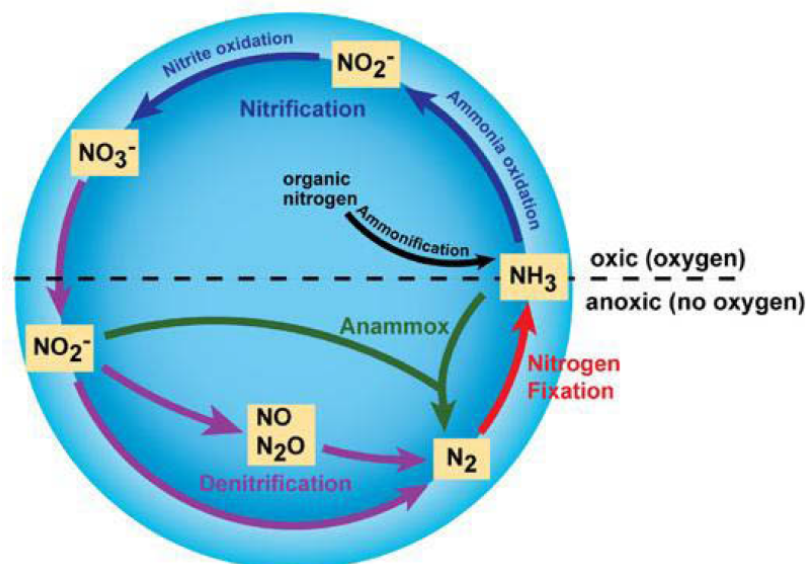
FIGURE 1.5: Biological cycle of nitrogen. Source: (Bernhard, 2010)

1.2.1 Nitrification

Nitrification is the sequential biological oxidation of ammonia to nitrate. The process occurs in the natural environment and is applied in the AS process for TAN removal. The nitrification reaction consists of two sequential oxidation steps (figure 1.6).
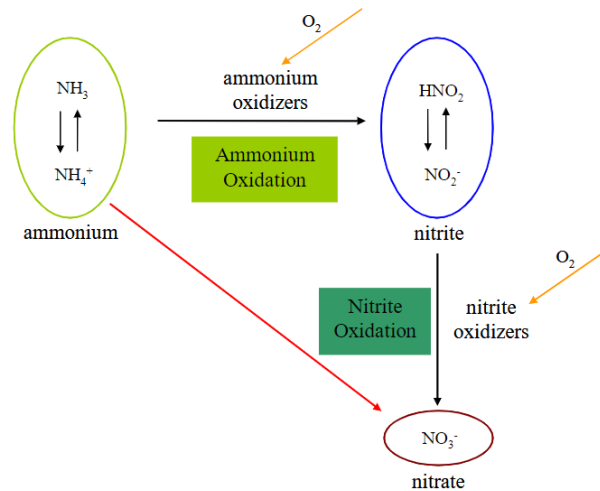
FIGURE 1.6: Two steps nitrification scheme. Source: (Chen, 2009)

First, ammonia (NH_3) is oxidized to hydroxylamine (NH_2OH) with the enzyme ammonia monooxygenase (AMO). The second step involves the oxidation of hydroxylamine to nitrite (NO_2^-) with the enzyme hydroxylamine oxidoreductase (HAO) (Kowalchuk and Stephen, 2001). During the oxidation of ammonia to nitrite, hydrogen ions are released and thus decrease the pH if no sufficient alkalinity is present. This step converting ammonia to nitrite is normally performed by AOB. This reaction is called nitritation as shown in figure 1.5.

The second step, the nitratation, is the conversion of nitrite to nitrate by NOB.

Nitrification is mediated by nitrifying bacteria AOB and NOB. Some heterotrophic bacteria can also oxidize ammonia to nitrate, but this is only a very small contribution to the overall ammonia oxidation (Van Hulle et al., 2010). The nitrifying bacteria obtain carbon from dissolved CO_2 and energy for growth from oxidizing ammonia and nitrite. One mole of carbon dioxide to be assimilated into nitrifying bacteria requires approximately 30 moles of ammonium ions or 100 moles of nitrite ions to be oxidized (Chen, 2009). AOB, which are responsible for the ammonia oxidation, have 25 cultured species, among which *Nitrosomonas* is the most extensively studied genus (Egli et al., 2003). NOB which are responsible for the nitrite oxidation have many cultured species of which numerous described in the last decade (Chen, 2009). They differ in ecophysiological requirements. *Nitrospira* were found to be the dominant nitrite oxidizers in both enriched and full scale nitrifying systems. The pH range of the 2 reactions is usually of 5.5 to 8.3, which makes bicarbonate the main alkali species according to the equilibrium (Muys, 2014):

$$CO_2 + H_2O \rightarrow HCO_3^- + H^+ \tag{1.7}$$
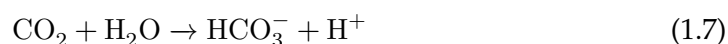
The equilibrium of the carbonate system in water plays an important role in nitrification and depends strongly on the pH. This carbonate system is usually the pH buffer available in wastewater and neutralizes the production of protons.

Urine nitrification for stabilization has been extensively studied in literature (Table 1.3). Different configurations with different concentrations of synthetic and real human urine have been reported. Overall, nitrification is a difficult process because of the possible free ammonia inhibition, the unstable pH and high salt concentration. The adaptation of the culture after the start-up phase can help to prevent these problems.

1.2.2 Denitrification

Nitrogen compounds can either be removed in the AS processes by assimilation or by denitrification following nitrification. In nitrification ammonia is first oxidized to nitrite and nitrite is then oxidized to nitrate. Commonly, after the last step in the nitrification scheme (Figure 1.5), nitrate is removed by anaerobic denitrifying bacteria. According to certain authors, total BNR through aerobic nitrification and possibly anoxic denitrification is the most common methodology for BNR of high nitrogen concentration wastewater (Carrera et al., 2003). Performing denitrification would hamper nitrogen recovery through N_2 losses in the atmosphere and would require biodegradable COD, which is limiting in pure urine (table 1).

1.2.3 Partial nitrification/denitrification: shortcut nitrogen removal

These procedures depend on the inhibition or the wash-out of nitrite-oxidizing bacteria (NOB), by which nitrification stops at nitrite without being oxidized to nitrate. Then, these nitrites can be reduced to nitrate by denitrification or by reaction with remaining ammonia.

The nitrate shunt is based on the inhibition of the second stage of nitrification (nitration). Thus, the oxygen requirement (aeration) is theoretically reduced by 25% because the nitrogen is then oxidized only up to the nitrite stage and not nitrate. In a second step, denitrification takes place in anoxic conditions in a similar way to the conventional treatment, but the organic carbon requirement is theoretically reduced by 40%. Thus, this option is attractive for its substantial energy savings as well as for its applicability to relatively carbon-deficient effluents (minimum Biological Oxygen Demand (BOD)5/NTK of about 2 as opposed to values close to 4 for conventional treatment). In addition, the denitrification rate from nitrites is 1.5 to 2 times higher than from nitrates.

The objective here is to inhibit NOB. This can be achieved by playing on several parameters:

- Dissolved oxygen: the oxygen affinity of NOB is lower than that of AOB. Thus, by working at low oxygen concentrations (between 0.3 and 1.2 mg/L), it is possible to wash out NOB.

- pH: the NH_3 and HNO_2 forms of ammoniacal nitrogen and in the form of nitrites respectively inhibit the AOB and NOB populations at different concentrations. By playing on these inhibition phenomena by controlling the pH, it is also possible to select only AOBs.

- Temperature: at temperatures above about 30 °C, the growth rate of AOBs becomes higher than that of NOBs. By setting a suitable sludge age at these temperatures, the leaching of NOB is achieved. This is the principle of the SHARON process (single reactor high-activity ammonia removal over nitrite) which operates between 30 °C to 40 °C for a sludge age of 1 to 1.5 days.

The SHARON process (single reactor system for high ammonia removal over nitrite) presented by Volcke, Vanrolleghem, and Loosdrecht, 2006 partly nitrified ammonium to nitrite with less aeration than full nitrification (Hellinga et al., 1998). In short-cut nitrogen removal, this nitrites ions can then be denitrified in anoxic conditions by heterotrophic bacteria, requiring less biodegradable COD than denitrification over nitrates. This makes this attractive for wastewater with low C:N ratio.

1.2.4 Shortcut nitrogen removal and Anammox

An upcoming way for nitrogen removal is to use an anaerobic AOB (ANAMMOX bacteria), which uses ammonium and nitrite to produce nitrogen gas and water (Kartal, Kuenen, and Van Loosdrecht, 2010). The process uses that kind of bacteria that does not require any addition of organic compound. These procedures depend on the inhibition or the wash-out of nitrite-oxidizing bacteria (NOB), by which nitrification stops at nitrite without being oxidized to nitrate (see previous paragraph). Then, these nitrites can be reduced by reaction with remaining ammonia. In a biofilm system based on nitritation and ANAMMOX, aerobic nitrifying bacteria deplete oxygen in the outer layers of the biofilm, creating anaerobic conditions in the inner layers for the ANAMMOX bacteria.

ANAMMOX uses a nitrite/ammonium mix to produce dinitrogen gas and some nitrate under anaerobic conditions (Ahn et al., 2006). The CANON (complete autotrophic nitrogen removal over nitrite) process is the combination of SHARON and ANAMMOX in one aerated reactor (Ahn et al., 2006).

In contrast to conventional denitrification, the ANAMMOX does not require additional organic carbon source, which makes it competitive on the market. Eventually, this process promises less investment funds for both oxygen and carbon sources (Vadivelu et al., 2006). Nonetheless, these approaches seem not feasible yet for the decentralized purpose since the operation could be costly and complex. However, full-scale applications have been increasing (Chatterjee, Ghangrekar, and Rao, 2016; Du et al., 2014; Kartal, Kuenen, and Van Loosdrecht, 2010; Lackner et al., 2014) and the understanding of the principal mechanisms are encountered to major advances (Schielke-Jenni et al., 2015; Vavilin and Rytov, 2015).

1.2.5 Conclusion

Denitrifying source-separated urine is not interesting for the stabilisation and nutrients recover. Techniques as ANAMMOX or SHARON process does not have a particular impact on the oxygen consumption for total or even partial nitrification of ammonium in order to stabilise the influent. Instead, they are interesting for the denitrification stage starting from the formed nitrite, where the effluent with low COD/Total Nitrogen (TN) ratio could be completely denitrified with lower energy requirements. When dealing with urine (ratio **C/N**=1), denitrification will be way more expensive, As one of the main goals of the project is to stabilize the influent and reduce its potentially harmful effects on the ecosystem, it was chosen to completely nitrify ammonium until nitrate in order to optimize a potential recover of nitrogen in the process effluent.

1.3   Urine nitrification

1.3.1   Technologies for urine nitrification

Nitrification has been used to stabilize source separated urine using different types of reactors e.g. Completely Stirred Tank Reactors (CSTR), Sequencing Batch Reactor (SBR), Moving Bed Biofilm Reactor (MBBR) (Edefell, 2017; Fumasoli et al., 2016; Jubany et al., 2008; Olofsson, 2016; Udert, Larsen, and Gujer, 2003; Udert and Wächter, 2012). Different conclusions could be drawn from these studies.

Fumasoli et al. (2016) operated a MBBR nitrification reactor for 3.5 years and reached maximum nitrification rates of $930\,g_N.m^{-3}\,d^{-1}$. These rates were obtained at temperature of $27\,°C$ and influent TAN concentration below $1790\,g_N.m^{-3}$. At influent TAN concentration of $4100\,g_N.m^{-3}$ it was possible to nitrify urine at a rate of $120\,g_N.m^{-3}\,d^{-1}$ at $22.5\,°C$. Edefell (2017) managed to increase the urine concentration also in a MBBR reactor to $4680\,g_N.m^{-3}$ with a corresponding nitrification rate of $60\,g_N.m^{-3}\,d^{-1}$. This was possible when the influent pump was exchanged from fixed flow to pH-regulation at a pH of 6.2. The maximum nitrification rate during the experiment was $160\,g_N.m^{-3}\,d^{-1}$ when the concentration in the reactor was $2230\,g_N.m^{-3}$.

Due to the potential inhibition of autotrophic biomass at high nitrogen concentrations, nitrification process control and biomass acclimation should be carried out by slightly increasing the NLR. An example of this procedure is the study from Jacquin et al., 2018: an excellent nitrification performance was obtained within a MBR treating source-separated urine (for a NLR as high as $1.6\,kgN/m^3/d$, the nitrification efficiency remained over 98%). Some MBR specific features can explain these results: high molecular compound retention, free and attached biomass retained in the bulk and infinite SRT. The particularities of this MBR sludge were studied in the framework on the project (Appendix B).

However, this implies a very intensive measurement effort as source-separated urine is highly variable in composition: in order to adjust for example the NLR, one has to know the exact concentration of organic and ammonia nitrogen in the feed urine. Furthermore, in order to obtain nearly 100% nitrification obtained by Jacquin et al. (2018), it was necessary to control the pH with a base solution.

The table 1.3 summarizes technologies using either suspended biomass (as the classical CSTR or attached biomass (as the MBBR) in order to analyse effluent quality and nitrification rates, to the particular operative conditions implemented. This will help us to better understand those results and better guide our experimental approach.

TABLE 1.3: Comparison of different technologies for urine nitrification.

	Suspended Biomass				Attached biomass			
Author	(Chen, 2009)	(Sun et al., 2012)	(Udert et al., 2003a)	(Udert et al., 2003a)	(Sun et al., 2012)	(Udert et al., 2003a)	(Feng, Wu, and Xu, 2008)	(Jacquin et al., 2018)
Reactor technology	SBR	SBR	SBR	CSTR	MBR	MBBR	Packed Bed Bioreactor	MBR
Dilution % artificial urine	-	15 (no organics)	-	-	19 (no organics)	-	12.5	-
Dilution % real human urine	10-29	28-47	13-42	137	28	16-87	10	16.4-3
N oxidation rate (gN L -1 d -1)	1.05	0.4-0.75	0.3-1.3	0.8	0.25	0.38	0.044	1.6
pH	7.6	6.4-6.5	6.0-8.8	6.9	6.3	7.0-7.8	6.65-8	7
T (°C)	25	25-35	24.5	30	35	25.3	27	19.9
DO (mg O2 L -1)	1.5	2	2.0-4.5	2.0-4.5	3	3.0-5.2	4.29	
Innoculum			AS WWTP	(Fux et al., 2002)		(Fux et al., 2004)		AS WWTP (8.000 P.E)
SRT (days)	40-50	20-450	>30	4.8	20-450			Infinite
pH control	External chemicals	Uncontrolled	Uncontrolled	Uncontrolled	Uncontrolled	Inflow rate	Uncontrolled/External chemical	External chemicals
Feeding	Semi-continuous HRT = 1.5d	Level controller			Level controller		Batch	Fixed HRT = 40h
Inhibition handeling	Feeding cycles	Free			Free		Controlling pH via the inflow	Progressive increase in NLR
Effluent quality	100% NO_3^-	50% NO_2^- 50% NH_4^+	50% NO_2^- 50% NH_4^+	50% NO_2^- 50% NH_4^+	50% NO_2^- 50% NH_4^+	50% NO_3^- 50% NH_4^+	95% NO_3^- 5% NH_4^+	100% NO_3^-

From the table 1.3 it is possible to analyse that:

- all experimental campaigns used aerobic and non limiting oxygen conditions (DO over $1.5\,\mathrm{g_{O_2}.m^{-3}}$),

- most of the studies presented used an important urine dilution rate,

- the only way to obtain 100% nitrification of ammonium to nitrate is the external chemical control of the pH,

- the uncontrolled systems or the control of pH by the inlet flow always leads to a partial nitrification of ammonium (around 50%): the inlet feed control of pH allows to not stop nitrification at the first stage and to obtain a constant ratio ammonium/nitrate in the effluent.

Even if the majority of the experimental campaigns in table 1.3 did not control pH or simply used external chemicals to do so, it is clear that the understanding of pH dynamics is critical for the correct comprehension of whatever BNR technology is used to treat source-separated urine. Furthermore, in the framework of our treatment goals and specific constraints of the CarbioSep project, controlling pH with external chemicals was not desirable. Thus, a major scientific interest is found in understanding pH influence on the process.

In this study, the experimental campaigns aim therefore at implementing an automatic acclimation using the "natural" pH variations as a control parameter without external alkalinity addition. This is why the review of the different nitrification technologies is oriented to the self-oriented control systems to treat source-separated urine. Next, it is necessary to analyse the impact of different operational conditions over the performance of the nitrification.

1.3.2   Biomass acclimation, start-up and control strategy

As presented briefly in the Introduction, biomass inhibition kinetics are not yet fully understood. For practical purposes, it is important to monitor the nitrification process carefully. One solution that has been proposed in the framework of VUNA project is feeding the system in such a way that the pH does not get too high or too low (Etter, Udert, and Gounden, 2014). The product of these efforts is a stable solution without the typical urine smell and with no easily degradable substances.

Urine has high concentrations of nutrients and salt that can cause inhibition and/or malfunction in conventional nitrifying biomass. The start-up of system treating yellow wastewater is not as flexible as nitrification processes in the classical WWTP. The microbial communities from domestic WWTP often have lower autotrophic biomass fraction than required for urine treatment. During the start-up phase the biomass is likely to adapt this composition to enhance nitrifying organisms growth (Egli et al., 2003). Various approaches have been reported (Chen, 2009; Fumasoli et al., 2016; Olofsson, 2016; Udert, Larsen, and Gujer, 2003). Udert, Larsen, and Gujer (2003) increased the influent ammonia concentration from $1700\,\mathrm{g_N.m^{-3}}$ to $7100\,\mathrm{g_N.m^{-3}}$ successfully over the course of 70 days. The urine was enriched with ammonia to reach high nitrogen concentrations. Gradual increase of nitrogen concentration and load allows the biomass to slowly acclimate to the compounds presents in urine (Gòdia et al., 2002; Hunik, Tramper, and Wijffels, 1994; Muys, 2014).

FA and FNA concentration in the system are dependent on temperature and pH. Thus in order to control and/or suppress these inhibitory effects, at least one if these two variables must be surveyed carefully (Kim, Lee, and Keller, 2006). There is no

way to control the temperature in the reactor,thus the best way to control nitrification in the reactor will be optimizing pH dynamics.

Fluctuations in pH and nitrogen load

Uncontrolled increase of pH or nitrogen load lead to an intensification of AOB activity due to more available substrate. The NOB have slower response to the changes and nitrite could be therefore accumulated (Udert and Wächter, 2012). Fluctuations in nitrogen load can be slightly controlled by having sufficiently large storage tanks (Etter, Hug, and Udert, 2013). Yet, this creates a problem of space for certain applications. More importantly, minimizing the risk of pH variations is crucial since it could affect rapidly system stability via the influence the FA and FNA concentrations following chemical equilibria (see Section 2.3). High pH increases the FA concentration while the FNA decrease. Apparently, elevated pH is more critical to the nitrification process than pH drop (Udert and Wächter, 2012).

Ammonia oxidation generally declines or stops when pH falls under 6 (even if authors like Udert, Larsen, and Gujer (2005) found AOB activity at acid pH values). When the pH raise again the nitrifying activity is recovered (Udert, Larsen, and Gujer, 2003). Several strategies to decrease pH can be implemented: reducing nitrogen load, enhancing carbon dioxide aeration to promote stripping or adding chemicals (Udert and Wächter, 2012). This pH dynamic is potentially present when urine load and bacterial activity are slightly unbalanced. Variations can be reduced by regulating the process with pH controlled influent as proposed by Udert, Larsen, and Gujer (2003) and Udert and Wächter (2012). Notwithstanding, Uhlmann (2014) reported contradictory results. This of course highlights the complex microbial dynamics in urine nitrification processes.

Nitrite accumulation

Some authors have reported nitrite accumulation after elevated pH or nitrogen load (Etter, Hug, and Udert, 2013; Udert and Wächter, 2012; Uhlmann, 2014). Loading rate increase of 10% can result in serious nitrite accumulation as presented by Udert et al. (2015). Continuous operation at higher pH (6.2 compared to 5.8) also increased the risk of nitrite accumulation as found by Fumasoli et al. (2016). Nitrite concentrations around $50\,g_{NO_2^- - N}.m^{-3}$ or higher, demand instant action to prevent further increase and inhibition of the bacteria (Udert et al., 2015). By reducing the NLR the AOB activity can be reduced and may allow the NOB to oxidise the accumulated nitrite. It seems like the best solution to avoid nitrite accumulation is maintaining favourable operating conditions for NOB to minimise the risk of microbial imbalances with AOB activity.

External chemical control of pH

Due to shortage of alkalinity in urine, about half of the total nitrogen can be oxidised. Indeed, the oxidation to nitrate requires 2 moles of alkalinity for 1 mole ammonia. However, in hydrolysed urine the ratio is approximately 1:1. As a consequence about half of the total nitrogen is nitrate after treatment (Udert, Larsen, and Gujer, 2003). Therefore, to achieve entire nitrification of the inlet FA, external chemicals must be added to supply the additional alkalinity needs and also to stabilise the pH in the reactor. Thus, the process stability might increase due to lower

risk of FA inhibition. Some lab-scale experiments have used potassium bicarbonate $KHCO_3$ (Fumasoli et al., 2016), sodium carbonate Na_2CO_3 (Feng, Wu, and Xu, 2008), sodium bicarbonate $NaHCO_3$ (Hellström, Johansson, and Grennberg, 1999) and $NaOH$ (Jacquin et al., 2018). Nevertheless, these chemicals are rather expensive, decreasing the economic profitability of the system and requiring more equipment and maintenance.

Intermediary conclusions

It is important to notice that AOB activity is the one that mostly lowers the pH and not NOB activity. If instabilities in the microbial community appears and AOB activity becomes more important, pH regulated NLR can enhance nitrite accumulation by increasing the load to maintain the operational pH set-point. The pH could on the other hand decrease and inhibit NOB with increasing FNA concentrations. This is why selecting the correct operational pH set-point is thus important for the start-up and the normal operation of the urine nitrifying system.

Therefore, pH appears as a crucial parameter for control and stability of the process. Controlling influent flow-rate by pH measures can be a good strategy to maintain an interesting pH value for an appropriate nitrification rate and also to implement the progressive rise of NLR for the acclimation period. The problem is to understand the better conditions firstly to feed the urine (fresh or stored), secondly the alkalinity effects that other authors already highlighted and thirdly obtain a self controlled system to acclimate biomass to high nitrogen influents without using chemical to stabilise pH. Eventually, without pH adjustment only about 50 % of the NH_4^+-N in urine can be converted to nitrate (Feng, Wu, and Xu, 2008). Chen (2009) gives the same conclusion; the alkalinity additional needs to be added is around 50% to achieve full urine nitrification. Understanding the relation between pH and nitrifying bacteria will help to understand and optimise the reactor start-up and the maximum BNR that we can achieve with the MBR technology. Therefore, the biokinetic model should successfully represent pH dynamics over the acclimation and the normal operation of the pilot.

1.3.3   Urine nitrification modelling

All the operational parameters analysed in the previous subsection reflect the need to interconnect and better understand the link between them as well as the impact on the treatment goals. A powerful tool to perform some of these analyses is biokinetic modeling. This section will present a review of some biological models used to interpret and predict biological nitrification of high-strength nitrogen influent and source-separated urine particularly.

Nitrification and denitrification process have been traditionally modelled as one-stage processes (Henze, 2007). This is of course particularly important and valid for the main application of classical AS. Indeed, since the late eighties, domestic wastewater remains the main field of application of BNR solutions. For these kind of applications, nitrite accumulation rarely takes place, because in classical wastewater treatment systems urine is strongly diluted in the inlet (see Section 1.1.1). However, the recent development and use of new processes including decentralized technologies treating urine reveals the needs to include nitrite inside complete metabolic pathways into the biological models of these systems. As presented before in this section, nitrite accumulation is mainly the origin of inhibition phenomena that results in systems malfunctioning problems and uncompleted treatment goals.

Nowadays, there are various different biological models describing nitrite build-up, as reviewed by Sin et al. (2008) and Haandel (2012). Few of these models focus on side-stream processes (as could be the reject stream from membranes, supernatant liquid from sludge digesters and the centrate/filtrate return stream from sewage sludge dewatering processes, among others according to EPA (2009)). Others deal with the treatment of highly nitrogen loaded wastewater (Hellinga, Loosdrecht, and Heijnen, 2010; Volcke et al., 2001; Wett and Rauch, 2003; among others) Most of them are more suitable to conventional wastewater systems (e.g. Kaelin et al., 2009; Sin and Vanrolleghem, 2006).

Concerning the fate of organic matter, a huge quantity of the side-stream models cited by Sin et al. (2008) have been developed for applications without significant amounts of biodegradable organic matter in the system. These side-stream models focused mainly in detailed modelling of heterotrophic conversions or organic matter availability and transformations.

Finally, different models also differ in terms of pH inclusion, more precisely in terms of his influence in biological activity and also the impact of biological activity in the pH contribution. pH plays an important role in highly nitrogen loaded streams and therefore, modeling for this kind of application must take it into account. The main biokinetic models focusing on high nitrogen strength streams and evidencing nitrite build-up and pH prediction are summarised in Table 1.4.

By a global analyse of the models the most important points to retain are:

- Influence of alkalinity or particularly of inorganic carbon could be represented in the biological model via a Monod or an exponential logistic type term (Guisasola et al., 2007).

- Most of the pH contribution and description is made by a global charge balance that takes into account negative ions and assumes a global quantity of positive ones. The pH is the not a state variable as itself so variation in dynamic modeling may not be accurate enough.

- Concerning heterotrophic activity, in general denitrifying growth on nitrite has been studied in less details than autotrophic growth. COD removal is modeled as usual.

- Some models, particularly the ones that represents SHARON process consider ammonium (NH_4) rather than ammonia (NH_3) as a substrate. This is preferred because biomass actually can only transport the uncharged NH_3 over its membrane (Hellinga et al., 1998). For our particular conditions this assumption is not valid.

TABLE 1.4: Summary of biological models taking into account nitrite formation.

Model reference	High TN strength streams	2-step nitrification	pH	Complex organic matter	COD/TN ratio
Hellinga, Loosdrecht, and Heijnen, 2010	+	+	+	X	Low
Volcke et al., 2001	+	+	+	X	Low
Hao, Heijnen, and Van Loosdrecht, 2001	+	+	X	X	Low
Wett and Rauch, 2003	+	+	+	+	Low
Moussa et al., 2005	+	+	X	X	Low
Van Hulle et al., 2005	+	+	+	+	Low
Pambrun, Paul, and Spérandio, 2006	+	+	X	X	Low
Sin and Vanrolleghem, 2006	X	+	X	+	High
Jones et al., 2012b	+	+	+	+	Low
Magri et al., 2007	+	+	+	+	Low
Kampschreur et al., 2007	X	+	X	X	High
Kaelin et al., 2009	X	+	X	+	High
Jubany, Baeza, and Carrera, 2007	+	+	X	X	High
Fumasoli, Morgenroth, and Udert, 2015	+	+	X	X	High
Ganigué et al., 2010	+	+	+	X	High

Following a thorough literature review of the available modeling frameworks and given the objectives of the present project, a biokinetic model has been conceptualized. The detailed presentation of the processes, stoechiometry and kinetics is provided in chapter 2.

Now that the different possibilities of biological modeling of urine nitrification are analysed, the focus is the use of a MBR as a treatment technique and the implication on the physical and biological aspects of this technology over the nitrification objectives.

1.4 MBR to treat source-separated urine

The advantages of MBR over CAS processes are well known; including more optimized reactor volume, high and constant effluent quality leaving the membrane, efficient rejection of pathogenic bacteria, stability over high load operation and load peaks in the influent, independent control of solids SRT from the HRT, higher volumetric load of treatment and finally a reduction in sludge production (Patsios and Karabelas, 2010). But from all of them, the main advantage of MBR processes over other wastewater treatment facilities is their ability to process a significant organic load with excellent results. Indeed, the effluent is free of solid particles (most of them retained by the membranes), only the dissolved compounds including inert carbon pollution (non-biodegradable by AS bacteria) remain. Its purification results on nitrogen and phosphorus pollutants are also excellent subject to good sizing and operation of the treatment technology.

MBR are also particularly suitable in wastewater treatment when dealing with large incoming load variations due to the possibility of increasing the concentration of sludge inside the reactor. Indeed, the MBRs can operate at higher MLSS concentrations due to the decoupling between the SRT and the HRT. Thus, this can reduce the amount of sludge produced and their subsequent treatment becomes less expensive. Likewise, high concentrations of MLSS and the presence of the membrane as a physical separation mechanism, make MBRs more compact in space than CAS.

MBRs have not been widely used specifically for source-separated urine nitrification. Nevertheless, they could be highly interesting for several reasons such as retention of slow-growing bacteria as the nitrifiers, removal of pathogens and increased performances regarding micro-pollutants such as pharmaceuticals.

Although MBR technology offers several advantages for the quality of the treated water, certain operating parameters make its implementation slightly more complex. Membrane fouling remains the main handicap of the system, although it is unavoidable. This factor contributes significantly to the operational cost and hampers the widespread application of MBR technologies. Precisely, the problem of fouling remains the main obstacle to the development of MBR. The advantages and disadvantages of membrane bioreactors are summarized in the table 1.5 with the main potential uses for source-separated streams as described by Delrue (2008).

In order to have a complete overview of the different types and technologies that are used and also the modelling tools developed for the stabilisation of urine, we can analyse first the bidirectional influence of MBRs and BNRs (in fact physical separation over biological activity en vice-versa) and their consequences in terms of modelling.

TABLE 1.5: Summary of Advantages, disadvantages and main uses
of the membrane bioreactor process.

Advantages	Disadvantage	Potential use
Pollutant removal efficiency	Operating and investment costs	Rejection in sensitive environment
Load variation management Decoupling SRT/HRT	Membrane fouling management Oxygen transfer compromised	Large load variations treatment process
Compactness, flexibility	Complex management of the process	Retrofitting of existing WWTP

1.4.1 The interrelation between biological treatment and membrane separation

In MBR technology, the biological treatment and membrane separation processes cannot be considered as independent sequential unit operations, as they are in direct and indirect co-relation (Fenu et al., 2010a). Also, the specific hydrodynamic constraints of the system are completely interconnected with the first two. All of these three factors mentioned above (namely physical membrane separation, biological nitrification and hydrodynamics) are influenced by the inputs of the system and interact with each other as shown in figure 1.7.
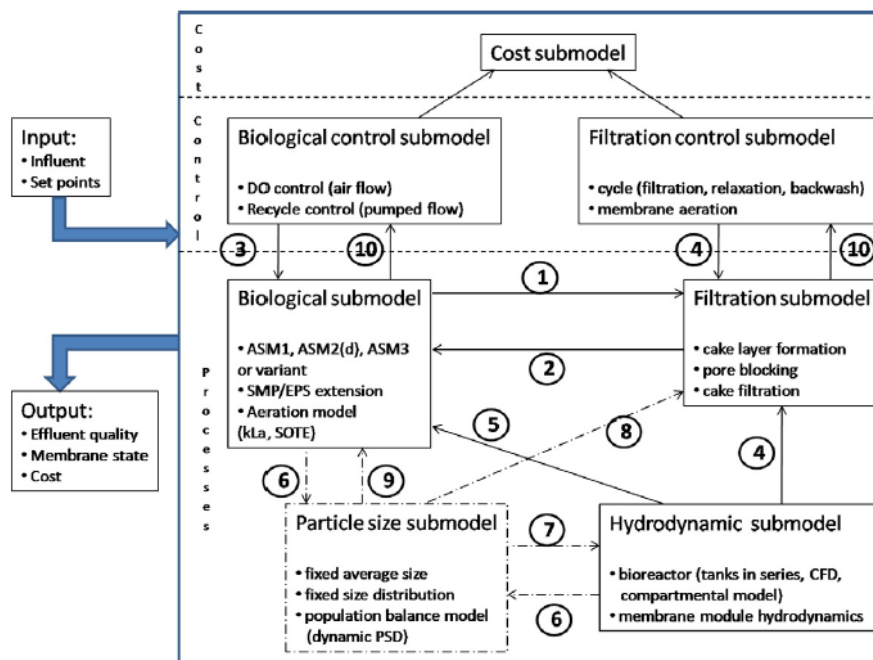
FIGURE 1.7: Influences of multiple physico-chemical phenomena in a numerical model adapted from (Naessens, Maere, and Nopens, 2012a).

Biological compounds are produced, disrupting the filtration process (**arrow 1**). Then, the membrane retains compounds depending on the pore size of the membrane (either from the inlet or produced by the biomass), leading to ascending concentration, influencing aeration and biological processes (**arrow 2**). Aeration provides DO for aerobic reactions and recirculation flows affect suspended solids concentrations of the mixture (MLSS) and gradients affecting conversion bio-kinetics

(**arrow 3**). Aeration and flow are applied to reduce fouling (**arrow 4**). Hydrodynamics (mixing) affect the homogeneity of the bioreactor (dead zones, recirculation, short circuit) (**arrow 5**). The particle size distribution is affected by aeration (both for biological needs and membrane scouring) and mixing, both causing shear-induced deflocculation (**arrows 6**). Particle size affects hydrodynamics (by rheology) (**arrow 7**), filtration behaviour (**arrow 8**) and bio-kinetic conversion rates (**arrow 9**). Process variables are passed to the control area that returns a set of control actions (**arrows 10**). The latter influences the operational cost of the entire system. This shows first that a thorough understanding of MBR systems is not straightforward. Secondly, a conventional approach of performing only experimental measurements to identify the specific interactions would be very time-consuming and expensive to handle.

In particular, strong process interactions hinder simple analysis, since a change in a parameter can affect multiple processes, which can mask influences on separate processes.

1.4.2 Influence of biological processes on membrane separation

The mixed liquor can be conveniently subdivided into three components: suspended solids, colloids and solutes. Although, the contribution to fouling of each component is still unclear, the contribution of the mixed liquor supernatant (*i.e.* soluble material and colloids) appears to be relatively higher than that of suspended solids. Indeed, in terms of fouling mechanisms, it is considered that the biomass supernatant is mainly responsible for the irreversible shrinkage and blockage (very difficult to treat) of the pores of the membrane, whereas the suspended solids tend to form an essentially reversible cake layer (Judd, 2008; Le-Clech, Chen, and Fane, 2006; Meng et al., 2009).

1.4.3 Influence of Membrane Separation on Biological Processes

Membrane separation has a significant influence on biological processes in MBR wastewater treatment plants, which can be attributed to two different mechanisms, acting directly and indirectly:

1. membrane filtration directly affects the biological treatment by the complete retention of all components of the mixed liquor that are larger than the pores of the membrane. This contrasts with CAS processes where biomass components with poor settling characteristics are washed out with the effluent from the sedimentation tank. In CAS, non-flocculent microorganisms are not retained in the system whereas in a MBR, the microorganisms forming flakes and dispersed ones are retained. For that (Massé, Spérandio, and Cabassud, 2006) showed significant differences in sludge morphology. At a similar SRT, the number of non-flocculent bacteria was significantly higher in the MBR. In addition, it was concluded that in MBR systems, a significant proportion of Dissolved Organic Matter (DOM) is released from the membranes and, therefore, retained in the bioreactor, unlike the CAS where it is washed out.

2. membrane filtration may also indirectly influence biological processes and some particular biomass kinetics. Since the separation of biomass from treated wastewater in MBR plants is independent of the sedimentation characteristics of suspended solids, it is possible to independently control HRT and SRT in order to obtain optimal biological treatment without constraints due to sludge settling.

1.4.4   Importance of an AS model for MBR technology

When using a biokinetic model for MBRs, significantly different properties of the system compared to CAS processes have to be considered. There is a high probability that a rather different set of model parameters and/or various modifications and adaptations of the models are necessary (see Figure 1.9). The resulting model must be able to adequately describe the complex biological processes that take place in the bioreactor as well as to consider biomass characteristics that greatly affect the membrane filtration performance as previously explained.

When a model needs to be built from scratch for a new or unexplored technology, or for different operating conditions than usual, the goal of the modelling process is to analyse the system (build knowledge about process or new operating constraints) for each specific application. For example if the objective is to analyse the irreversible fouling phenomena in the membrane, a basic model of the biomass kinetics in the MBRs should at least be able to provide estimates of the concentration of EPS in AS flocs and the concentration of DOM in the bioreactor supernatant considering the existence of SMP. Knowledge of the variation of these substances in response to changes in operating parameter values (SRT, HRT, aeration rate, etc.) is of paramount importance to adjust MBR design and operation for the purpose of minimizing irreversible fouling of the membrane.

In order to clarify the available modeling tools as a function of the objectives of the system, the next section present the MBR existing modeling tools highlighting the importance, the challenges and the interest of each approach, keeping in mind the goals of the system.

1.5   MBR modelling

As highlighted in the previous section, filtration modeling in combination with biokinetic modeling is an important feature to consider when modelling a MBR. This section reviews the available modelling frameworks for both components.

For the correct description of all the biological reactions that occur within a MBR as well as the interaction with the filtration mechanisms, three approaches can usually be applied depending on the modeling objectives:

1. direct application of ASM type models,

2. modification of these models by including the fate of EPS/SMP substances,

3. coupling physico-chemical phenomena to classical ASMs.

1.5.1   Brief summary of physical Models for MBR operation

Influence of the physical separation in the model

The phenomenon of membrane fouling remains the main obstacle to universal and large-scale applications of MBRs. Membrane fouling would reduce the productivity of the system, increase the energy requirement for the gas wash and the cleaning frequency, which could shorten the life of the membrane and lead to higher replacement costs. There is therefore great interest in studying the causes, characteristics, mechanisms and possible control of membrane fouling in MBRs when the phenomena is verified experimentally.

Membrane fouling in MBR is the result of interactions between the slurry suspension and the membrane unit (Le-Clech, Chen, and Fane, 2006). For a given membrane and operating conditions, membrane fouling is directly affected by the sludge suspension. This consists of a very complex system composed of various salts, organic substances, colloids, cells and sludge flocs. All these substances have a fouling potential affecting the integrity of the membranes. Meanwhile, on the basis of the relative contributions of the fouling components to the total fouling of the membrane, several mechanisms for fouling membrane description had been proposed, in particular;

- pores fouling by colloidal particles,

- adherence of the solids,

- gel and cake layers formation,

- consolidation of the cake layer.

.

Spatial and temporal changes in the composition during the long-term operation and their osmotic pressure effect have been also proposed (Lin et al., 2014).

The complete retention of flocs but also free bacteria, biopolymers and organic colloids among other substances is the main difference of MBR compared to CAS processes. All these products are likely to be converted (become substrate and be metabolized by microorganisms, especially polysaccharides more than proteins) (Böhm et al., 2012).

Two classes of organic compounds originating from the microbial metabolisms can be defined:

1. EPS can be bound, floc or soluble hooks and free to move between flocs and mixed liquor. There is no scientific consensus or standard procedure for EPS analysis and interpretation of results from different methods becomes quite complex (Laspidou and Rittmann, 2002a).

2. SMP bring together all of the soluble cell products that are either released during cell lysis, diffused across the cell membrane, excreted or lost during bacterial metabolism. Substrate utilization, cell lysis and hydrolysis of EPS are the processes that mostly contribute to SMP formation. From an operational point of view, they can be defined as the soluble products that come out in the effluent of a biological treatment system and that were not present in the inlet (Noguera, Araki, and Rittmann, 1994).

EPS have been shown to be key substances, which have complex interactions or relationships with all these membrane impurities and fouling mechanisms in MBRs (Figure 1.8). Understanding these interactions or relationships seems to be a fundamental way to understand membrane fouling and develop strategies for controlling membrane fouling in MBRs.

Despite many efforts to improve this understanding, the roles of EPS in membrane fouling are still not well understood or regularly reported. This situation can be attributed to the complex nature of membrane fouling by EPS and SMP in MBRs. In the meantime, studies have generally been limited to the single treatment system. It is therefore necessary to summarize and analyse the progress of past research in order to analyse if including fouling prediction in the model predictions is necessary,
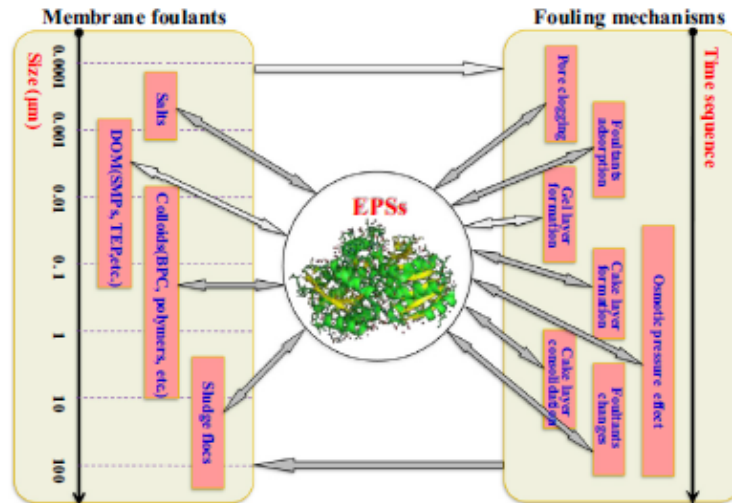
FIGURE 1.8: Influences of EPS on membrane fouling (Sheng, Yu, and
Li, 2010).

relevant and feasible. Nevertheless, no up-to-date review of this subject is yet available, although several review papers have been devoted to summarizing the effects of EPS on the properties of sludge (Fenu et al., 2010a; Sheng, Yu, and Li, 2010).

Filtration modelling can be greatly simplified by considering the membrane as a point-settler or an ideal separation step (complete solids retention). However, it is important not to neglect the fouling process, especially when considering modelling for operational optimization, in systems where fouling could not be avoided or controlled. When it is necessary to include it, the modelling of the filtration process is carried out mainly mechanically, using Darcy's law and the concept of RIS to describe the influence of different fouling mechanisms on the permeability of the membrane.

RIS models for fouling

Virtually all mechanical filtration models use Darcy's law of filtration as a theoretical starting point for the model equations. This directly links the membrane flux to the measured Trans-membrane Pressure (TMP). This is made mainly using a constant for the sludge viscosity or in the best cases a parameter related to temperature and/or total solids. Darcy's law allows to calculate the membrane resistance R, which is generally considered to be the combined effect of the membrane-specific resistance R_m and a number of fouling mechanisms deteriorating the filtration process.

$$R = R_m + R_b + R_c + R_p \tag{1.8}$$

Where;
R_m membrane resistance (calculated using Darcy's law on ultra pure water filtration), cake layer resistance R_c and pore blocking resistance R_p. Filtration is hampered by low temperature, EPS contributes significantly to resistance to R_b. Biofouling and high solids concentrations contribute to R_p and R_c. Aiming to subdivide the membrane surface to account for the unequal distribution of shear intensity by aeration of the membrane and deposition of impurities.

It should be emphasized that modelling of this kind of phenomena becomes necessary only when the influence of membrane fouling is empirically remarkable and could not be neglected for the correct description of the system performances.

1.5.2 Applying ASM models without modifications

The application of the ASM1 model as it is designed for CAS processes could be envisaged for the modelling of a MBR. The following specificities have to be considered (Fenu et al., 2010a);

- Higher SRT,

- Higher concentration of biomass and yet viscosity,

- Accumulation of SMP and EPS due to retention of the membrane,

- Higher aeration rates related to oxygen supply and membrane scouring,

- Improvement of nitrification.

The figure 1.9 represents the conventional ASM models used over the years to describe and understand operation of different MBRs for a variety of applications.

The diagram in figure 1.9 helps to track the simplified evolution of MBR modeling based on ASMs, but also to understand the limits and better identify the needs in terms of modelling approaches and process identifiable variables. The most important factors and the principal variations added when choosing a classical ASM for describing MBR performances are described bellow:

Fractionation of organic pollution This characterization of COD can be conducted by two approaches: physicochemical methods or trial/error test methods in order to calibrate the experimental results to model predictions on the MLSS (Choubert et al., 2010; Spérandio, Heran, and Gillot, 2007).

1. Physical and biological separations of respirometry or BOD measurement combined to evaluate each component of the total COD present in the inlet. This detailed characterization allows to know the degree of biodegradability and the physical state of the substrate.

2. Prediction and calibration of the steady state MLSS among a test / error procedure for a long period campaign data.

The choice of the fractionation method is related to the sludge retention, because at high SRT values the hydrolysis of the "inert" fraction becomes much more important. Thus the classical ASM type models which do not take into account this hydrolysis, can give an overestimation of the amount of sludge inside the reactor. In this case, the test trial/error method is recommended, since a high sludge retention time implies seasonal variations in the organic load of the inlet.

Stoichiometry and biokinetics

The possible differences in the standard set of model parameters for MBR applications may be related to the specificity of the biomass retained, the concentration of this biomass, the hydrodynamic constraints of the system and especially of the

Unmodified ASM

Jiang et al. (2005) - ASM 1
- Laboratory scale MBR.
- Sensitivity analysis at steady state.
- Strong influence of parameters Y_H Y_A b_H b_A μ_{mmaxH} and μ_{mmaxA} over the MLSS effluent COD and OUR.
- Higher b_A value.
- Inlet fractionation is critical (COD X_i S_s X_s and S_{NH}).

Delrue et al. (2010) ASM1
- First approach at full-scale.

Jimenez et al. (2010) - ASM1
- Laboratory scale MBR.
- Impact of primary sedimentation and primary filters for the inlet wastewater on MBR performance.
- At high SRT a biological phenomenon appears that current biological models do not consider.

Fenu et al. (2010c) -ASM2
- Full-scale MBR.
- Energy forecast rather than effluent quality forecast.

Verrecht et al. (2010) -ASM2
- Full-scale MBR.

Lobos, Heran, and Grasmick (2009) - ASM3
- Simulation-based approach.

Saroj et al. (2008) - ASM3
- Simulation-based approach

Kaelin et al. (2009) - ASM3
- Simulation-real scale CSTR based approach

FIGURE 1.9: Unmodified ASM models applied to MBR modelling

aeration (for both biological needs and scouring) over the membrane. The most important parameters are MLSS, oxygen transfer (α_{Kla} factor dynamics), nitrogen species (S_{NH}, S_{NO}), phosphorus concentration (S_{PO_4}) and oxygen consumption rate description (OUR and DO) (Di Bella, Mannina, and Viviani, 2008; Hulle, Decaan, and Promotor, 2005; Naessens, Maere, and Nopens, 2012b).

Nitrification improvement

It is necessary to emphasis where in the ASM the nitrification improvement by using a MBR is present. The latest research results (see Fenu et al., 2010a) showed that the nitrification parameters were the most affected by the differences between the CAS and MBR processes, depending of the hydrodynamic and operational conditions. In conclusion it was recommended to determine the kinetics and physical parameters of the model as a coherent set for each new application case in the MBR.

The apparent improvement in nitrification for MBR may be related to several factors: selectivity of microorganisms, increase in the bioavailability of substrates due to the smaller size of the flocs, growth of nitrifying bacteria clusters at the surface of low density flocs (Manser, Gujer, and Siegrist, 2005).

From the review of modeling approaches performed by Fenu et al. (2010a), it was highlighted that it is necessary to have more specific experimental information with respect to the specific growth rate of autotrophs μ_A (among excess/substrate deficiency tests for example), as well as a differentiated analysis of the microbial autotrophic species resent (mainly AOB and NOB).

These growth-rate differences can be partly explained by the reduction of K_{NH} and K_{OA} half-saturation constants in the model:

- K_{NH}: the values are always lower or in the same order of magnitude for MBR compared to conventional CAS processes (Manser, Gujer, and Siegrist, 2005). The influence of the high biomass concentration was evidenced: in these conditions, ammonium diffusion limitations may occur. This causes an increase of the apparent value of K_{NH}, yielding a decrease of both Ammonium Uptake Rate (AUR) and autotrophic specific growth rate (μ_A) (Parco, Wentzel, and Ekama, 2006).

- K_{OA}: the smaller size of the flocs assists in the decrease of the oxygen transfer resistance, but at the same time this size of the flocs is also dependent on the hydrodynamic constraints and the type of aeration of the system as well as SRT, with deflocculation directly proportional to the increase in SRT (Manser, Gujer, and Siegrist, 2005). It is thus produced by the increase of the aeration, or by the reduction of the mass load (ratio F / M), phenomena which lead to the reduction of the active fraction in the sludge (Massé, Spérandio, and Cabassud, 2006).

In summary, the K_{NH} and K_{OA} half-saturation constants depend on the operating conditions (SRT, MLSS concentration, viscosity, oxygen concentration, floc size distribution). Thus, the particularities of the MBRs processes must be integrated somehow in the model to clarify the direct effect on real process conditions like the nitrification or oxygen transfer.

In AS systems nitrite is an intermediate of nitrification and denitrification. It is important to highlight finally that ASM family of models (Henze, 2007) and ASM 3 in particular (Gujer et al., 1999) do not originally consider nitrite (NO_2^-) as a state variable mainly for simplicity reason and because the exact fate of nitrite during denitrification process was not sufficiently known at the time. This will be an important consideration for the modeling choices made for the present thesis work.

Fate of dissolved oxygen

In a MBR process, due to the very low operating load (higher SRT), oxygen consumption will vary according to the flow of biodegradable Organic Matter (OM) in

the inlet rather than as a function of the particular kinetics parameters (S. Krause, M. Wagner, and P. Cornel, 2003). The gas/liquid mass transfer is related to the concentration of biomass and the effects of this concentration on the viscosity of the medium.

The effect of dissolved oxygen in the reactor on the performance of the biological treatment is high. As part of the ASM biological model, (Fenu et al., 2010a) and (Delrue et al., 2010) used specific protocols to measure standard aeration efficiency for coarse and fine bubble aeration. However, they did not convincingly demonstrate good model performance for validation of dynamic oxygen concentrations. Some other authors as for example Verrecht et al. (2010) used a mechanistic approach. The model proposed by these authors incorporates differences in the type of diffuser (coarse and fine bubble) and the negative effects of high MLSS aeration efficiency by relating the α_{kla} factor to the MLSS. The values of the parameters were chosen from the literature and the model was confronted with the measured airflows and the DO concentration. The dynamic aeration controller (as it is present in reality) was added after the biokinetic calibration and was fitted to adjust the measurements, thus that deviations and simulated control actions of the actual system would influence the calibration results.

Sludge production

At high SRT, the MLSS is composed mainly by particulate materials from the inlet and bacterial lysis. In this condition, the cell maintenance becomes more important than the growth. The high sludge concentration in the reactor can lead to a decrease in the specific oxygen consumption due to the accumulation of refractory materials and the reduction of the active fraction of biomass (Tan, Ng, and Ong, 2008). This fraction, considered as inert in the ASM model, always leads to an overestimation of the amount of sludge by the model. The most important parameters for the prediction of MLSS are Y_H, b_H and f_p: their modifications play a very important role in other processes. This is the case for Y_H which is also related to the consumption of electrons acceptors (oxygen consumption or nitrates elimination). This is therefore rather preferred for model calibration to set values of particulate inert fraction X_I according to the characteristics of the influent (Spérandio and Espinosa, 2008). Perspectives and points of attention for future research include the influent characterization and fate of inorganic compounds, especially for systems operating at high SRT.

Influence of inlet fractionation

Here, the challenge is the correct determination of the inert fractions (S_i, X_i), considering the possible contribution of inert substances resulting from the bacterial metabolism.

Knowing that at high sludge retention time (decrease of active biomass in the mixed liquor), the biomass entering by the inlet becomes less negligible, the correct evaluation of the heterotrophic biomass X_h in the inlet becomes more important (Fall et al., 2014; Fallah et al., 2010). This contribution is related to the characteristics of the treatment system (pre-treatments, hydraulic residence time, presence of toxic industrial agents in the influent, etc...).

Equally important is the fate of inorganic compounds present in the influent: high SRT can indeed result in a possible solubilization of these particulate compounds (Villain and Marrot, 2013). This particular effect has already been demonstrated several times experimentally. This solubilization mechanism must be correctly integrated into the mathematical matrix of the chosen ASM model (Di Bella et al., 2015).

In addition, ASM1 does not provide the information necessary to accurately determine the concentration of supernatant DOM in MBR systems. It is unclear whether the slowly biodegradable (COD) needs to be treated as a soluble or particulate fraction. The ASM1 model does not take into account the influence of the operating conditions on the DOM concentration. SMP production is not modelled as it is assumed that the DOM concentration depends entirely on the inlet characteristics (Lu et al., 2001).

A comparison between ASM1 and ASM3 application for MBR modeling is presented in table 1.6. The conclusion of this table is that the main points to be treated for the use of the unmodified models are the correct characterization of the inlet (fractionation) and the estimation of the stoichiometric and biokinetic parameters to model the processes. This is a prerequisite for any modeling exercise and must be considered before adding more than the already existing default variables and parameters.

ASM 1		ASM 3	
For	**Against**	**For**	**Against**
Model used by preference for modeling biological processes	No nitrogen or alkalinity limitation for Xh.	Fix ASM1 defects	No elimination of incorporated organic P
More experimental data expanded	Undifferentiated nitrifiers rate of disintegration of under aerobic and anoxic conditions	Nitrifiers rate of disintegration can be connected as assistant modules	No incorporated chemical precipitation
A more important database set for stoichiometric and biokinetic parameters	Intra-cellular storage of PHAs has not been addressed.	Two-step nitrification–denitrification process	No growth of embedded filamentous organisms.
More used for big scale treatment systems	Fate of supernatant DOM is not described	Accuracy in dynamics of the activated sludge	No pH calculation.
Commercial and open-source tools more base on this model	Inert degradation of the COD for high SRT operations	Strong physiological and biochemical basis	Calculation costly
Model easy to access/modify, thus to be adapted	Over estimation of MLSS for high SRT operation	Ideal tool for process understanding and design	Difficult to estimate
Fractionation and calibration protocols well established	More experimental information on autotrophic growth to explain nitrification improvement	Quantification of energy storage	No able to predict nitrite and nitrate over time
Easy to manipulate and adaptable to different process control strategies	No pH calculation.	Describe better ready biodegradable substrate and OUR	No adapted to model-based control

TABLE 1.6: Comparative of unmodified ASM 1 and ASM 3 for MBR modelling

After analysing the advantages and disadvantages of using either ASM1 or ASM3, the following aspects should be highlighted:

- Nitrification of high nitrogen loaded influents is not well represented by the classical ASM models

- Biomass over-estimation is one essential difference when using classical ASM models in the MBR operative description compared to the CAS system.

- Specific biokinetic parameters as the ammonium half saturation constant K_{NH_4} and the oxygen saturation constant K_{O_2} are critically different for the nitrification of high nitrogen content streams in a MBR due to the particularities of the membrane separation and the aeration system influence in the transfer and in the flocs properties.

1.5.3 Interest of including the fate EPS / SMP in the biokinetic model

Generally in ASM framework, the production of EPS is not taken into account and Biomass Associated Products (BAP)s are not produced by the hydrolysis of EPS: they come either from cell lysis or hydrolysis of biodegradable organic compounds (Jiang et al., 2008; Lu et al., 2001). Including the formation and degradation of EPS/ SMP may be considered for certain defined cases.

Figures 1.10 and 1.11 summarizes the evolution of the stand alone models for the quantification and interpretation of EPS and SMP in biological process.
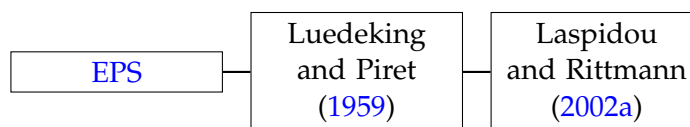
FIGURE 1.10: Evolution of EPS stand-alone models
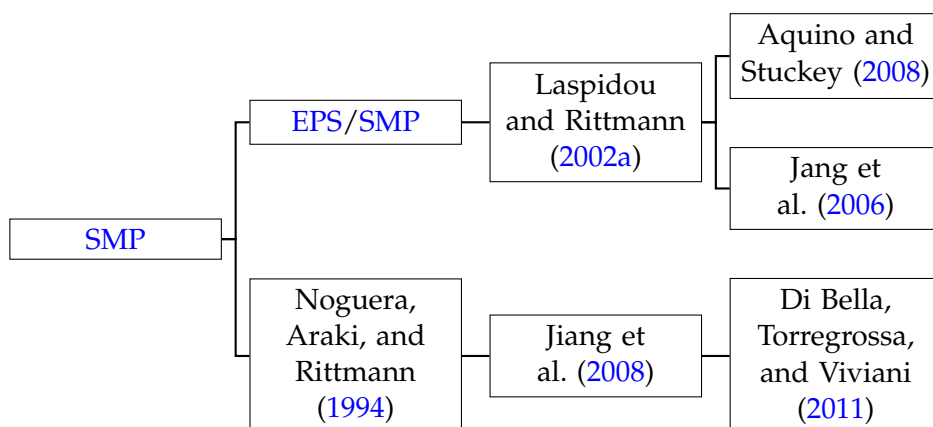
FIGURE 1.11: Evolution of SMP stand-alone models

The two main problems with modified ASM models are the difficulty in determining new parameters experimentally and also the over-parameterization of the model. This difficulty in clearly identifying the new parameters added to the model must be taken into account and strategies to reduce them are also possible; couple the Utilization Associated Products (UAP) / BAP as soluble SMP, neglect the modeling of EPS or model them with equations different to the ASM model.

The application of the modified ASM models with the EPS / SMP concepts is justified according to the modeling objectives (Di Bella, Torregrossa, and Viviani, 2011; Jiang et al., 2008). If it is not necessary, these concepts creates difficulties in the calibration of the new parameters introduced, thus the application of the modified models may be advisable for describing very precisely some particularities of the process when it is absolutely necessary:

Influence on physical separation and membrane fouling

The influence of EPS / SMP on membrane fouling or their use as indicators of this phenomena has been known and evaluated in several investigations. Their presence could be important for the modeling of the physical separation process and they should thus be included in the biological model to correctly explain and predict the behavior of the system.

For the prediction of soluble COD leaving in the effluent

In the MBR, the mixed liquor supernatant is composed of living cells and SMP mainly. These values are generally low and stable, but it is essential to know them for predicting accurately effluent quality. If the content is too high, it can represent a threat for a tertiary treatment technique for example.

For modeling high SRT processes

The operation of high-sludge MBRs is related to the corresponding influence on specific sludge production and the biological characteristics of autotrophs (Massé, Spérandio, and Cabassud, 2006). Interactions between different bacterial species in the biological reactor at high sludge age have been studied for CAS processes since the nineties (Laspidou and Rittmann, 2002b). In particular, the interactions between the nitrifying bacteria and the heterotrophic bacteria has been a topic of interest. In this case the SMP from autotrophic bacteria serves as a substrate (by decreasing the minimum concentration necessary) for the growth of heterotrophic bacteria, even at very low organic loads in the inlet (i.e. a low F / M ratio).

In high-sludge and low-organic load (F/M of 0.01 $g_{O_2}.m^{-3}/g_{MLVSS}.m^{-3}/d$) MBR processes, more interactions between nitrifying and heterotrophic bacteria can be found: the SMP produced by the former will reduce the minimum substrate concentration for heterotrophs (apparent K_S) and therefore encourage their growth. Therefore, the modeling of EPS and SMP becomes important for the prediction of fouling but also for the prediction of MLSS.

These results show that the particular conditions of MBRs contribute to increase the effect of high SRTs for biological treatment. On the one hand, the high selectivity of the membrane allows the retention of colloidal materials of size between 0.04 - 0.45 mm, which contains a refractory fraction composed of polysaccharides bound to proteins that accumulate in the membrane body (Lubello et al., 2009). On the other hand, the high concentration of MLSS has a direct influence on the bacterial interactions within the reactor. Thus, the importance of SRT for MBR processes is fundamental for the understanding of biokinetic phenomena.

1.6 Summary modified **ASM** models to treat urine in a **MBR**

TABLE 1.7: Summary of Modified ASM Models.

Model	Bioprocesses simulation					Provision of key variables for fouling predictions		Application to MBR	Model evaluation	Model ease-of-use	
	Carbon oxidation	Nitrification	Denitrification	Hydrolysis	Phosphorus removal	SMP	EPS			Processes	State variables
ASM1 Spérandio and Espinosa, 2008	+	+	+	+	x	x	x	+	+	8	13
ASM2/2d Fenu et al., 2010a; Henze, 2007	+	+	+	+	+	x	x	+	+	19/21	19/20
ASM3 Janus and Ulanicki, 2010	+	+	+	+	x	x	x	+	+	12	13
De Silva and Rittmann, 2000	+	+	+	x	x	+	x	+	+	?	10
Lu et al., 2001	+	+	+	+	x	+	x	+	+	10	12
Lu et al., 2010	+	+	+	+	x	+	x	+	x	17	12
Lee et al., 2002	+	+	+	+	x	+	x	+	x	12	13
Ahn et al., 2006	+	+	+	+	x	+	+	+	x	15	16
Oliveira-Esquerre et al., 2006	+	+	+	+	x	+	x	+	+	14	14
Jiang et al., 2005	+	+	+	+	+	+	x	+	+	27	22

1.7 Scientific scope of the research

After making a complete literature review about urine treatment and stabilisation technologies, biological modelling of urine nitrification, modelling challenges of MBR technologies and the use of MBR modelling for urine treatment, the next are the main scientific questions and hypothesis that will guide and define the present research.

The present study (as mentioned in the Introduction) faces the problem of urine stabilization and nitrification in a MBR process. It focuses on operational and modelling aspects. This kind of process is definitely interesting to investigate, especially in the case of streams rich in nitrogen (e.g. yellow wastewater, leachate).

From the modelling point of view, the main challenge is how to manage to correctly predict the potential nitrite accumulation during biomass acclimation as well as during the normal operation of the reactor. Nitrite presence in the effluent definitely reduces the environmental value of our application project. Most importantly, it can lead to inhibition of the nitrirication process. That is why it is a non desired component. Nitrite build up in the reactor could be presented as a result of unbalanced activity between AOB and NOB activities. As seen in section 1.3.2, nitrite accumulation could be reduced in the effluent in case of sufficient AS plus a low-organic load (F/M). A lot of questions arise on the modelling capacity of the ASM framework presented in this section. Even including some extensions and linking with other modelling approaches, using ASMs for urine treatment is still highly related to each particular application.

The choice made in this study was to model our system modifying an existing ASM according to the specific technical and scientific constraints of the application.

The following were the global scientific questions to be answered that guided this thesis.

- How to represent in the model and to understand the interactions between biokinetics/chemical equilibrium/ gas-liquid transfer?.

- Is it possible to link in a reliable way the pH variations to the acclimation degree of the biomass? Is it related to the applied NLR?.

- Are biomass biokinetic parameters they different in function of the acclimation protocol applied to obtain it?

- Are there differences between biomass acclimated via chemical control of pH or via the inlet urine flow control?

- Is it possible to identify the best conditions for biomass acclimation and ultimately control it thanks to the biokinetic model?

To answer these questions and develop the process technology which is the goal of the Carbiosep project, the following methodology was applied:

- a biokinetic model was developed by selecting the relevant processes and represent them in accordance with the specific objectives of the project (treatment of urine, importance of pH, use of a MBR with complete sludge retention...) (chapter 2

- an acclimation protocol based on pH control by the inlet feed was applied at lab-scale in order to produce data for model calibration/validation (chapter 3

- respirometric characterization of the acclimated biomass was carried out to identify the saturation and inhibition constants of AOB and NOB strains (chapter 4).

- the model was evaluated by a sensitivity analysis to highlight the most significant biokinetic parameters. Then, a scenario analysis was conducted to evaluate different acclimation procedures (chapter 5).

Chapter 2

Conceptualization of the biokinetic model

This chapter will present in details the main characteristics of the biokinetic model that was specifically developed to meet this project's objectives. First, each biological or physical process included in the model is discussed in a comprehensive way: choice of the limiting/inhibiting variables, stoichiometry...

The organic matter in the raw wastewater is often divided into a number of categories as shown in figure 2.1. For each category there can be a direct contribution from the raw wastewater, as indicated by the dotted arrows, but also a contribution due to the internal biomass cycle. In order to better characterize these categories, the most widely used fractionation protocol is based on biodegradability. While the slowly or readily biodegradable substrate is utilized for biochemical processes and therefore changes its form, inert material leave the biological nutrient removal system in the same form as it enters. Dissolved inert material is of little interest for the operation of a biological process, unless it is toxic or it potentially could be degraded over the time to produce more available substrate (as could be the case on a very high SRT process). Particulate inert material can contribute to sludge accumulation thereby influence the aeration efficiency and other operational parameters. The readily biodegradable substrate is used for growth of biomass and supply of energy and the slowly biodegradable substrate is hydrolyzed to readily biodegradable substrate.

Bacteria need energy permanently in order to grow and to support essential life activities. Growing cells utilize exogenous substrate, located outside the cell membrane and exogenous nutrients for growth and energy storage (mainly in a stable form as ATP molecules). The major part of bacteria in the activated sludge called heterotrophic bacteria use organic carbon in the form of small organic molecules as substrate and some bacteria called autotrophic bacteria which are essential to biological nutrient removal, use inorganic carbon as substrate. When the bacteria decay the organic carbon of the bacteria is partly reused. The life cycle of biomass is illustrated in figure 2.1 which is a very simplified illustration of the biochemical processes in the activated sludge. Substrates and nutrients are absorbed within the biomass faster than they are utilized, but the bacteria cannot accumulate large amounts of such products. Instead, the substrates and nutrients are chemically modified into a few types of large molecules, typically polysaccharides, lipids and polyphosphates which can be stored for a long period of time without significant energetic expenses.

$$\text{Substrate} + \text{Nutrients} + \text{Oxygen} \rightarrow \text{Biomass} + \text{Energy} \qquad (2.1)$$
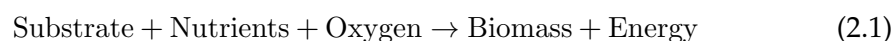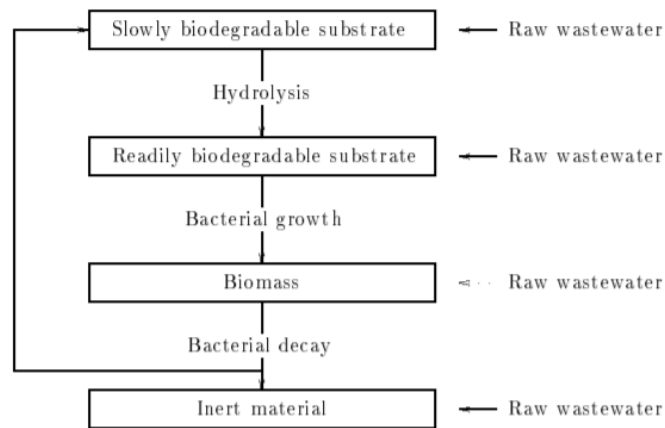
FIGURE 2.1: The regeneration and production of biomass in the activated sludge (Carstensen, 1996)

Over the last decades, for modelling of wastewater processes most effort has been placed in detailed and complex deterministic models. The theory of the activated sludge processes has been developed steadily. A major step towards combining the theory of the different processes and unifying the terminology used to describe the processes is the International Association on Water Pollution Research and Control (IAWPRC) ASM1 (Henze et al., 1986), that has gained the place as the most important one for describing WWTP operation and also for design and process optimisation objectives. This model has been extended and updated (e.g. ASM2 and ASM3) in order to include additional processes like enhanced biological phosphorus removal. Recently, coupling biological models with physico-chemical modelling frameworks has been the subject of many research projects with the context of the shift of paradigm towards WRRFs (e.g. Flores-Alsina et al. (2015)). These model expresses a very detailed theoretical relationship between all the processes in activated sludge using Monod kinetic expressions. However, higher model complexity yields a huge number of parameters which implies that an identification of all the parameters by numerical methods could be challenging and that the model could be unsuitable for control or predictive objectives.

Even more important is the fact that the application of this model to different types of raw wastewater has some restrictions. A literature review of the available models found in literature to describe yellow wastewater treatment within a MBR has been carried out. Some particularities of our MBR treatment system as the infinite SRT and the accumulation of solids, pH based control of the feed, etc. has to be taken into account. The result of this analysis are presented in this chapter that present each particular component of the developed model and also its direct effect on the system operation and process stability. It has been quickly concluded that the most challenging issues were linked to the properties of urine (high nitrogen concentration, alkalinity, stability...). Aspects related to membrane filtration and interaction with the biomass activity were nevertheless reviewed and are presented in Chapter 1

The biokinetic model proposed is a modified ASM1 model including two nitrification steps and pH prediction to describe system performances. The biokinetics,

physical oxygen transfer phenomena and pH dynamics are represented. Model includes biokinetics (nitrification in two stages, inhibition of nitrifying bacteria, endogenous respiration and hydrolysis of refractory materials at high SRT) physico-chemical processes (influence of pH, gas liquid transfer), production and consumption of alkalinity, in 20 equations and 24 components as shown in Table 2.1. The significant biological processes essential to our particular biological nutrient removal system are presented and detailed below. The presentation of the processes given here is general but it is sufficient to understand their importance in each practical application.

2.1 Main operational and environmental parameters to consider

There are a number of environmental factors influencing nitrifying bacteria activities and the rates of the processes presented in this second part of this chapter. These factors include temperature, effect of pH value, DO concentration, presence of toxic and inhibiting materials, salt concentration, rate limiting concentrations of nutrients and substrates (inhibition and limitation), product inhibition, intermediate inhibition and growth limitation by inorganic carbon or phosphate (Udert et al., 2003a), microorganism concentration (including the proportion of heterotrophs to autotrophs), ammonium nitrogen loading, SRT and HRT (Wiesmann, Choi, and Dombrowski, 2006), organic load, TAN, Total Nitrite Nitrogen (TNN), alkalinity and of course the particular dynamics behaviour of the bio-system (S. Krause, M. Wagner, and P. Cornel, 2003).

Some of these factors are related to the nature of the raw wastewater and some are connected to the process variables and the chosen technology for the BNR. On one hand during the nitrification (NH_3 oxidation) alkalinity is consumed, on the other hand for every ammonium molecule oxidized, two protons are released, leading to a pH decrease that will eventually affect the process. Of all these factors, FA and FNA (highly depending on pH), alkalinity and temperature are the most critical, which will be explained in detail in the next sections. Also, the influence of the MBR over the performance of the nitrification is considered, even if a more detailed analysis is presented in the Chapter 1.

Taking a closer look to the nitrification process itself, for a stable conversion of a urine solution it is required that NO_2^- is oxidised at the same rate than NH_3 (Udert et al., 2003a). During storage, the organic matter is degraded through microbial activity and the urea is hydrolysed. This ammonification process is a well-known process. The hydrolysis releases NH_3 and causes the pH to increase up to values close to 9.0. In an ideal solution, as explained in chapter 1, the pH will reach pKa value of 9.2, when no other buffering substances are in solution : at this point, the activity of the species NH_4^+/NH_3 are really close. However, the real solution also contains carbonate species and phosphate species. The NH_3 is very volatile and the exchange between liquid and gas phase is really important, thus the nitrogen loss could be significant (Udert and Wächter, 2012) and potentially harmful.

The biological activity of NOBs and AOBs strongly depends on the pH value: indeed, the concentrations of their substrates (NH_3 for AOB (Koops et al., 2006) and HNO_2 for NOB (Rosenberg et al., 2013)) are dependent on acid-base equilibrium with their form NH_4^+ acid or basic NO_2^-. Moreover, NH_3 and HNO_2 are not only limiting but also inhibitory (Anthonisen et al., 1976b). AOBs may be inhibited by their HNO_2 product (Hunik, Meijer, and Tramper, 1992), whereas inhibition of NOB by

nitrates is usually negligible (Hunik et al., 1993). This interdependence between the nitrifying activity and the pH is particularly pronounced for effluents such as urine, in connection with the high concentrations of substrate and the large pH variations between the inlet water and the outlet water (Udert and Wächter, 2012).

2.1.1   pH and Alkalinity

All knowledge of biochemical processes shows that the nitrification of highly loaded ammonia nitrogen influents requires - among others:

1. sufficient alkalinity to buffer the acidification of the medium;

2. bicarbonate ions as a substrate for autotrophic biomass.

One of the most important parameters in the nitrification process is pH which determines the acid-base equilibrium of NH_3, NO_2^- and hydroxylamine (NH_2OH) (Udert et al., 2003a).

The fate of alkalinity (here not only determined by bicarbonates but also by free ammonia as a very important contributor in urine) is therefore necessary to be described in the model, all this in relation to the pH. Influence and prediction of pH for nitrification, in connection with the phenomenon of stripping of CO_2, is at the origin of important variations of the pH. In turn, the pH affects the acid-base equilibrium of the compounds present in the waste water (ammonia / ammonium, nitrites / nitrous acid ...) which can play the role of substrates or inhibitor of the bacterial growth. It is therefore necessary to take the pH into account as a model variable. However, in the more recent modified model, its value should be calculated from the balance of the ionic species present in solution (Ganigué et al., 2010). Few are the models that treat pH as a state variable, so it can not be derived from a simple mass balance resulting in a differential equation. That is an important improvement present in this thesis work. pH in the present model became a state variable and all the contributions and the particular consumption from the different biological processes are linked to the inter-phase gas/liquid exchange and the liquid chemical equilibrium of the different components, to better predict pH dynamics in the system and his direct impact on the biological process.

The acid/base chemical equilibrium between ammonium and ammonia i the liquid phase is written as follows (Anthonisen et al., 1976a):

$$NH_4^+ + OH^- \rightleftharpoons NH_3 + H_2O \tag{2.2}$$
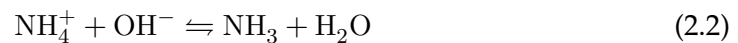
The equilibrium constant of this reaction (pKa) is 9.25. Higher the pH is, higher FA concentration is. The main substrate for AOB is NH_3 as they have affinity for NH_3 rather than NH_4^+ (Anthonisen et al., 1976b; Suzuki, Dular, and Kwok, 1974). By increasing the pH more NH_3 becomes available for the AOB (Suzuki, Dular, and Kwok, 1974). A sudden increase in pH can therefore causes instability in the process since NO_2^- oxidisers are unable to increase in growth rate as fast as the NH_3 oxidisers. The best nitrification rates can be achieved when the pH lies in the range of 6.8 and 8.0 (EPA, 2009). The optimum pH range is 7.9 to 8.2 for *Nitrosomonas* and 7.2 to 7.6 for *Nitrobacter* (Alleman, 1985; Holloway and Lyberatos, 1990). These optimal pH ranges also depend on the free ammonia or free nitrous acid concentration: for *Nitrospira*, a nitrite-oxidising bacteria as the *Nitrobacter*, inhibitory condition are found if FA concentration exceeds about $0.04\,g_{NH_4^+-N}.m^{-3}$ to $0.08\,g_{NH_4^+-N}.m^{-3}$. These values can be found at pH of 7.5 and at a temperature of 20 °C for an ammonium concentration of $3.5\,g_{NH_3-N}.m^{-3}$ to reach the lower bound of the inhibition threshold ranges.

FNA concentration of about $0.03\,\mathrm{g_{HNO_2^- - N}.m^{-3}}$ will lead to approximately 50% inhibition of nitrite oxidation. This FNA concentration found below neutral pH values. At neutral pH and a temperature of 20 °C a concentration of $50\,\mathrm{g_{NO_2^- - N}.m^{-3}}$ would be required to reach the 50% inhibition level. That kind of conditions could be easily reached in high strength nitrogen wastewater treatment processes. It could be more critical particularly since the process operate at pH values below 7.0 (Blackburne et al., 2007). At lower values of pH the nitrification rates are much slower but the benefit is that the NOB and AOB have equal production rates, thus the process becomes more stable.

In the literature, NH_4^+ can be considered as substrate for biomass growth but this expression can only be used if the pH is constant and the ratio between the NH_3 and NH_4^+ concentration is thereby constant (Hellinga et al., 1998). Since the proton is produced from the ammonium nitrification during the first step, it always creates acidic environment. Furthermore, the proton concentration influences the activities of AOB and NOB (Udert et al., 2003a). At the pH of 5.5, the inhibition occurs. In some references, it is explained that the most common AOB are incapable of oxidizing ammonium at pH below 5.5 (Udert, Larsen, and Gujer, 2005). However, in some conditions, some acid tolerant AOB could grow at these acidic pH values (Fumasoli et al., 2017). More recently, an explanation has been given by Fumasoli, Morgenroth, and Udert, 2015: the decrease of ammonia oxidation at low pH is not due to inhibition or limitation of enzymes but to an energy constraint. The energy available from the proton motive force is too small for the NADH production in *Nitrosomonas* and related AOB causing an energy limited state for bacterial growth.

In addition, the formed nitrite from the first step of nitrification is also involved in an acid/base couple to produce FNA. It is postulated that FNA and FA can also inhibit the nitrification process (Anthonisen et al., 1976a). The acid/base chemical equilibrium between nitrous acid and nitrite ion is written as follows (Udert, Larsen, and Gujer, 2005):

$$\mathrm{HNO_2 + OH^- \rightleftharpoons NO_2^- + H_2O} \tag{2.3}$$
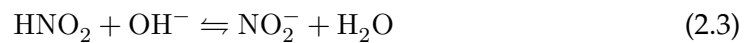
For the nitrification process to operate in a stable manner the activity of the AOB and NOB need to be in balance. Fluctuating pH is a sign of process instabilities and may be caused by changes in bacterial activity and nitrogen load. To enhance NOB growth, thus lowering the risk of NO_2^- accumulation, it is recommended to keep a relatively low pH and temperature (Edefell, 2017; Udert and Wächter, 2012).

All this factors reveals the importance and the effect of pH on both chemicals speciation in the liquid phase and so substrate concentrations, thus an impact in the biological nitrogen removal performance and in the inhibitory conditions of the process.

2.1.2 Inhibition

Generically, the growth rate of biomass and the influence of limiting nutrient or substrate concentrations can be modelled using Monod kinetics (equation 2.4) as presented by Carstensen (1996).

$$\frac{dX_B}{dt} = \mu_{max} \frac{S_\mathrm{n}}{S_\mathrm{n} + K_\mathrm{S}} X_\mathrm{B} \tag{2.4}$$

where:

- S_n: the concentration of the rate limiting nutrient or substrate;

- X_B: the concentration of active biomass;

- μ_{max}: the maximum specific growth rate of biomass;

- K_n: the appropriate half-saturation constant.

Purely inhibitory compounds

Some compounds which are not toxic to the biomass inhibits the biological processes causing the rates of the processes to decrease when they are present in a high quantity. The inhibition by a given material can be modelled by multiplying the rate expression with the "switch" term (equation 2.5) as presented by Roš, Dular, and Farkas (1988).

$$\frac{K_I}{K_I + S_I} \qquad (2.5)$$

where:

- S_I the concentration of the inhibiting material;

- K_I the appropriate half-inhibition constant.

Substrate inhibition

Sometimes, when the substrate concentration is too high, bacterial growth inhibition can also appear. This is expressed in analog manner by a substituting the Monod term in equation 2.4, which gives equation 2.6 as presented by Anthonisen et al. (1976a):

$$\frac{dX_B}{dt} = \mu_{max} \frac{S_n}{S_n + K_S + \frac{S_n^2}{K_I}} X_B \qquad (2.6)$$

Inhibitions in the nitrification process

The nitrifying organisms can encounter substrate limitation and the main substrates are NH_3 for the AOB and NO_2 for the NOB (Suzuki, Dular, and Kwok, 1974). The nitrifying bacteria can also be inhibited by their products where both AOB and NOB are strongly inhibited by nitrous acid (Suzuki, Dular, and Kwok, 1974). The NOB are on the other hand rarely inhibited by NO_3^- (Anthonisen et al., 1976b), but inhibition by FA can also occur (Batstone et al., 2015).

Compounds produced during the entire process of nitrification, or even intermediates substances can also have an inhibitory effect, especially NH_2OH which inhibits the growth of NOB (Udert et al., 2003a). Nitrite accumulation is generally explained as the result of different growth rates of the AOB and NOB. The NH_4^+ and NO_2^- concentration is however not responsible for the nitrification inhibition, rather the free ammonia (FA) and free nitrous acid (FNA) inhibit the organisms. According to Anthonisen et al. (1976b) the *Nitrosonomas* were inhibited when FA ranged between $10\,g_{NH_3-N}.m^{-3}$ to $150\,g_{NH_3-N}.m^{-3}$ and for *Nitrobacters* the range was between $0.1\,g_{NH_3-N}.m^{-3}$ to $1\,g_{NH_3-N}.m^{-3}$. The nitrifying organisms started to get inhibited by FNA at concentrations between $0.22\,g_{HNO_2^--N}.m^{-3}$ to $2.8\,g_{HNO_2^--N}.m^{-3}$.

NOB can use nitrous acid (HNO_2) as substrate rather than NO_2^- (Udert, Larsen, and Gujer, 2005). However, NOB is more sensitive to FNA and FA than AOB (Udert, Larsen, and Gujer, 2005). Research of Vadivelu et al. (2006), showed that FNA is the major factor to inhibit NOB: at concentration exceeding $90\,g_{NO_2^- - N}.m^{-3}$ or $0.011\,g_{HNO_2^- - N}.m^{-3}$($0.8\,\mu M$) inhibition was observed to start, NOB is completely inhibited at approximately $0.023\,g_{HNO_2^- - N}.m^{-3}$. These results are different from other authors such as (Hellström, Johansson, and Grennberg, 1999; Prakasam and Loehr, 1972) who proposed a limit value of $0.07\,g_{HNO_2^- - N}.m^{-3}$ and $0.34\,g_{HNO_2^- - N}.m^{-3}$ respectively, while this number in Anthonisen et al. (1976a) was $0.22\,g_{HNO_2^- - N}.m^{-3}$.

2.1.3 Temperature

The general rule is that the nitrification rate increases with temperature. In liquids between $10\,°C$ to $25\,°C$ the nitrification rate will double for every $8\,°C$ to $10\,°C$ increase in temperature (EPA, 2009). NOB can be favoured over AOB in lower temperatures (Egli et al., 2003). According to Hellinga et al. (1998) NOB grow faster than AOB at temperatures around $16\,°C$ and with increasing temperature the AOB grow faster than NOB. This means that it is easier to run a stable nitrification process with limited NO_2^- accumulation at lower temperatures.

In fact, the nitratation process becomes less effective than the nitritation process when the temperature is high. At normal temperatures in wastewater treatment plants ($5\,°C$ to $20\,°C$) nitrite oxidizers grow faster than ammonium oxidizers, which means that ammonium is completely oxidized to nitrate. On the other hand, temperature in the range of $30\,°C$ to $40\,°C$ is optimal for maximum growth rate of ammonium oxidizers and NOB are inhibited (Hellinga et al., 1998). In another published paper, treating high-strength ammonium wastewater mixed with an industrial wastewater that contained mainly organic matter (concentrations variate from $4000\,g_{NH_4^+ - N}.m^{-3}$ to $6000\,g_{NH_4^+ - N}.m^{-3}$ and $13\,000\,g_{COD}.m^{-3}$ to $15\,000\,g_{COD}.m^{-3}$), it was shown that at the temperature of $15\,°C$, the NLR was clearly higher than the Maximum Nitrification Rate (MNR) thus the accumulation of ammonia occurred (Carrera et al., 2003).

2.1.4 Dissolved Oxygen

The nitrifying bacteria use oxygen as an electron acceptor thus they are heavily dependent on adequate oxygen supply. The growth rate of the nitrifiers starts to decline at dissolved oxygen (DO) concentrations below $3\,g_{O_2}.m^{-3}$ to $4\,g_{O_2}.m^{-3}$, or even higher and the rate decreases significantly at levels below $2\,g_{O_2}.m^{-3}$ (EPA, 2009). As the oxygen supply represents a very important cost in most WWTPs, the DO concentration is usually maintained at a low level (around $2\,g_{O_2}.m^{-3}$) but in lab-scale, we maintain the continuous aeration with DO above $3\,g_{O_2}.m^{-3}$ to enhance the nitrification.

Some species of NOB have lower affinity to oxygen compared to the AOB (Udert et al., 2003a). The NOB generally need a higher oxygen concentration for the complete oxidation to be successful. Thus, the nitratation process can be limited when the oxygen concentration in the reactor is low, since its oxygen affinity constant is higher than the one in the nitritation process. Hence, the nitratation step is more influenced by oxygen limitations than the nitritation step (Guisasola et al., 2005). At DO lower than $1\,g_{O_2}.m^{-3}$, nitratation rate dropped sharply (Guisasola et al., 2005) . This means that a too low oxygen concentration can result in NO_2^- accumulation.

2.1.5   High salt concentration effects and ionic strength effects

In addition to the high nutrient content, urine is also characterized by high concentration of dissolved salts (section 1.1.1). Conductivity is a measure of ions in a solution and can be an approximation of the concentration of nitrogenous ions and salt during urine nitrification. Salt has an inhibitory effect on AOB and NOB and is most likely due to IS, where divalent cations have a larger impact than monovalent cations (Moussa et al., 2006). Several species within the group of nitrifiers are adapted to marine environments, which could be of interest in the process of urine nitrification from source-separated sources. The genus *Nitrosococcus* consist of two known species that have a strong salt requirement, where the optimum sodium chloride ($NaCl$) concentration is $17\,550\,g_{NaCl}.m^{-3}$ to $23\,400\,g_{NaCl}.m^{-3}$ and the substrate (NH_3) affinity K_S value is reported $50\,\mu M$ to $52\,\mu M$ (Luo et al., 2016). The salt concentration in a solution can affect the oxygen solubility by the "salting out effect", where an increase in salt concentration decreases the solubility of neutral species (Moussa et al., 2006).

Several studies assessed the impact of salinity on MBR performances(De Temmerman et al., 2014; Luo et al., 2015; Yogalakshmi and Joseph, 2010; Zhang et al., 2014). Luo et al. (2015) considered these effects up to a $NaCl$ concentration of $16.5\,kg\,m^{-3}$. In fact, neither AOB nor NOB can perform their oxidation processes at high salt concentrations. No AOB has been found growing at salt concentrations above $150\,kg\,m^{-3}$ and no NOB has been found growing at salt concentrations above $50\,kg\,m^{-3}$ (Oren, 2011). The main conclusions are as follows:

- the removal of organic pollution (Total Organic Carbon (TOC), COD) in a reactor operating in saline conditions is similar to that observed in the control reactor up to a salt concentration of $10\,kg\,m^{-3}$. Above this value, however, TOC elimination drops to about 80%. This decrease is probably due to the inhibitory effect of salinity on biomass. However, a high treatment yield (99%) is recovered when the $10\,kg\,m^{-3}$ concentration is maintained for two weeks. This recovery could be attributed to the adaptation of biomass to saline conditions (Hong et al., 2013).

- The elimination of TAN appears to be more sensitive to increased salinity: it decreases from 99% in the control reactor to 38% when the $NaCl$ concentration increases to $6\,kg\,m^{-3}$ (inhibition of metabolic activity and nitrifying growth rate). However, similar to what is observed for organic pollution, an adaptation of biomass to saline conditions (Zhang et al., 2014) seems to occur as nitrification performance improves and reaches 80% when saline conditions are maintained for more than 38 days.

- Salinity has a negative impact on membrane clogging, through the release of soluble microbial products and exo-polymers (Zhang et al., 2014). There is also an increase in the viscosity of activated sludge and a reduction in oxygen solubility and transfer rate.

The main influence of the high salt concentration in the biological process is the influence of the IS on the real activity of the ionic species, in other words the difference between the real and the ideal state equilibrium of the different dissolved species. As presented briefly in the chapter 1, the incorporation of activity coefficients based on the IS of the solution is necessary to correctly determine the speciation of the acid-base substances related to pH prediction. To account for this behaviour, the molar concentration is corrected by a factor known as the activity

coefficient. The modified ionic concentration is called the active concentration, as determined in the following expression:

$$\alpha_i = \lambda_i.[X_i] \tag{2.7}$$

where

α_i = active concentration of ion i
$[X_i]$ = molar concentration of ion Xi
λ_i = activity coefficient of ion i

Activity coefficients are estimated in the general pH model using the Davies equation, which is a simplification of the extended Debye-Hückel law. The activity coefficient (λ_i) for each ion *i* in solution is determined as follows (Curl, 1979):

$$log\lambda_i = -0.5Z_i^2.\left(\frac{\sqrt{I}}{1 + \sqrt{I}} - 0.2.I\right) \tag{2.8}$$

where,

Z_i = ionic charge of ion i
I = IS of solution

The expression for IS is as follows:

$$I = 0.5\sum_{i=1}^{n}[X_i]Z_i^2 \tag{2.9}$$

where,

n = the number of ionic species in solution

One physical parameter than can be related to this IS is the Electrical Conductivity (EC). This is the specific conductance of an aqueous solution and it could be calculated indirectly by empirical methods, or by diffusion coefficient-based methods. In the present work, this EC is the only experimental value than helps to fit the influence of the ionic species in the model. Thus, its numerical prediction will be incorporated in the model to highlight the influence of the ions concentration in all the physico-chemical equilibria. Equilibrium expressions for the acid-base systems included in the model are presented in section 2.3.

It is important to take into account the IS to correctly determinate species distribution in the liquid phase. As presented in the figures (with a ratio $\alpha=NH_4/NH_3$) 2.2 and 2.3, IS impact directly over the pKa value for the couple NH_4/NH_3 and thus the speciation in the solution could be different for a same pH. The two figures present the pKa for a IS with a low influence in the speciation 5point A in the figure around 9.24) and one IS ten times more important to show the influence of ionic species concentration decreasing the pKa value (point B in the figure around 9.1), leading to a FA concentration more important in the liquid phase for a same pH value (α ratio more important for a same pH). In other words by neglecting the IS interaction, the prediction of inhibitory conditions and substrate availability could be seriously compromised.

2.1.6 Calculation of electrical conductivity from the model

Calculation of the EC will be done by two methods:
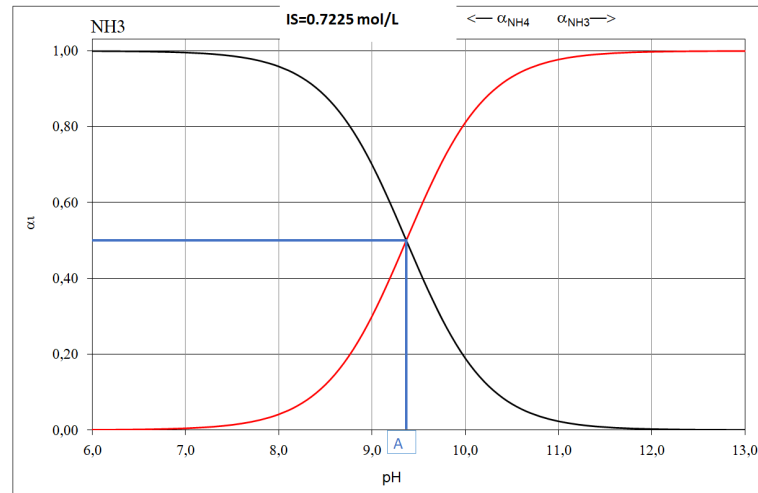
FIGURE 2.2: Ammonia species distribution for a IS of 0.7225 mol/kg
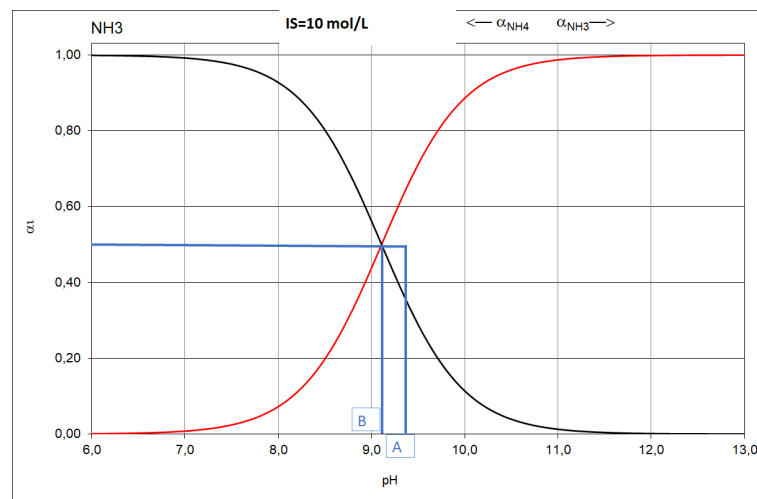
FIGURE 2.3: Ammonia species distribution for a IS of 10 mol/kg

1. the pseudo-linear approach according to Call, 1892; McCleskey, Nordstrom, and Ryan, 2012,

2. the diffusion coefficient-based method according to the Nernst-Einstein equation.

For the first method, the effective IS is closely related to the conductivity of a solution. Experimentation with soil solutions has indicated that the Marion–Babcock equation:

$$log_{10}I = 1.159 + 1.009 log_{10}EC \tag{2.10}$$

is accurate for ISs up to about 0.3 mol/L and the units for EC are in dS/cm. The arrangement of the equation 2.10 yield to:

$$EC(\mu S/cm) = 6.67 * 10^4 * [I(mol/L)]^{0.991} \tag{2.11}$$

The equation 2.11 is called pseudo-linear due to the larger prefactor and also as the inverse Marion & Babcock as the arrangement of the equation is EC=EC(I).

The second method is based on the Nernst-Einstein equation that establish a physical relationship between the molar limiting conductivity $\lambda^0_{m,i}$ and the diffusion coefficient D_i for a given ion i. The principle of the calculation is that the molar conductivity of a solute species and its diffusion coefficient are related by:

$$D_i = \frac{RT}{z_i^2 F^2} \Lambda^0_{m,i} \tag{2.12}$$

where
D_i the diffusion coefficient (m^2/s)
$\Lambda^0_{m,i}$ is the molar limiting conductivity ($S/m/(mol/m^3)$)
z the charge number (-)
F is Faraday's constant ($Coulomb/mol$)
R the ideal gas constant ($J/K/mol$)
T the absolute temperature (K)

Multiplying the molar conductivity with the concentration c_i and summing up for all the solutes, gives an estimate of the specific electrical conductance of the solution. Then, for an ideal aqueous-solution in the limit of infinite dilution (non-interactive ions) the EC is calculated on diffusion coefficients:

$$EC^0 = \sum_{i=1}^{n} (\Lambda^0_{m,i} c_i) = \left(\frac{F^2}{RT}\right) \sum_{i=1}^{n} D_i z_i^2 c_i \tag{2.13}$$

But for a realistic case of the non-ideal solutions, the method becomes more elaborated. The Nernst-Einstein equation is restricted and valid only for molar limiting conductivities $\Lambda^0_{m,i}$. In contrast, the EC of real aqueous solutions rest upon molar conductivities $\Lambda_{m,i}$:

$$EC = \sum_{i=1}^{n} (\Lambda_{m,i} c_i) \tag{2.14}$$

The only problem is that the molar conductivity changes with the concentration. According to McCleskey, 2018 the EC could be expressed as:

$$EC = \sum_{i=1}^{n} (\Lambda^0_{m,i} \lambda_{corr} c_i) \tag{2.15}$$

Here the correction factor λ_{corr} takes into account the ion-ion interaction:

$$ln_{\lambda_{corr}} \simeq -(K/\Lambda^0_{m,i})|z_i|^{1.5}\sqrt{I} \tag{2.16}$$

This ion-ion correction is similar to the simplified activity model of Debye-Hückel in the equation:

$$ln_{\lambda_i} = -(ln_{10})Az_i^2\sqrt{I} \tag{2.17}$$

with A = 0.5085 $M^{(-1/2)}$.

The activity constant λ is a quantity that belongs to the standard repertoire of hydrochemical models anyway (available for each ion and aqueous species). By defining the parametrization factor α as:

$$\alpha = \frac{ln_{\lambda_{corr}}}{ln_{\lambda_i}} = \frac{K}{\Lambda^0_{m,i}(ln_{10})A|z_i|^{0.5}} \tag{2.18}$$

The EC calculation could be presented as:

$$EC = \sum_{i=1}^{n}(\Lambda^{0}_{m,i}(\lambda corr^{\alpha})c_i) \tag{2.19}$$

$$EC = \left(\frac{F^2}{RT}\right)\sum_{i=1}^{n}D_i z_i^2(\gamma_i)^{\alpha}c_i \tag{2.20}$$

In this case the EC is calculated at a defined temperature T. The EC of most natural waters, including seawater and thus wastewater, increases with temperature 1-3% per degree Celsius. Measured EC values are usually referred to 25°C – often indicated by EC_{25}. For standardizing the EC at 25 °C, nonlinear compensation or linear approximation could be used. The nonlinear T compensation is based on a nonlinear model, as an outcome of the physical relationship between EC, diffusion coefficients and the viscosity of water. The equation is given by:

$$EC_{25} = 1.125 * 10^{-A/B} * EC \tag{2.21}$$

with the two parameters taken from Hinshelwood (1945):

$$A = 1.37023 * (T - 20) + 8.36 * 10^{-4}(T - 20)^2$$

$$B = 109 + T$$

With T in °C

In the linear approach, linear formulas are in widespread use. The most common type of a linear expression is obtained from the equation 2.21 by Taylor series expansion:

$$EC_{25} = \frac{EC}{1 + a(T - 25)}$$

with $a = 0.020\,°C^{-1}$ and T in °C.

Between 0 and 30 °C there is no difference between the linear and the non-linear approaches for the temperature compensation. Thus for our case, the linear approximation is applied.

2.1.7 Complete sludge retention and aeration

The complete retention by the membrane is a physical separation that has at the same time two influences. The first one is a direct influence related to complete retention of all the components of the mixed liquor and the second one is related to the full decoupling of SRT and HRT. SRT is a measure of the time sludge solids remain in a system and is calculated as the total amount of sludge solids divided by the rate of loss of sludge from the system. Within the studied MBR, no biomass is taken out, this leads to a very significant increase in the concentration of sludge in the biological reactor.

The hydrodynamics of the system will also be affected by this increase in the MLSS concentration (direct impact on mixing) and thus will have a direct influence on biological mechanisms: the higher concentration of MLSS usually found in MBRs will modify the rheological properties of the suspension and thus aeration process

(for oxygen transfer and membrane scouring). As a result, the oxygen transfer coefficient is greatly reduced. This issue was considered in the project but was not in the scope of the present thesis.

In terms of gas-liquid mass transfer, possible ammonia stripping has also to be considered if the air inflow conditions allows to strip soluble NH_3: for high pH, the ammoniacal nitrogen will be in the form of ammonia in significant proportion. This compound is volatile and will be subject to transfer to the gas-liquid interface. It will be necessary to take into account phenomenon in the model in order to predict and to prevent the possible problems of odors related to this ammonia stripping and obviously to take into account this quantity of ammonium stripped into the overall nitrogen balance.

The biokinetic model developed must make it possible to describe these phenomena, in interaction with any hydrodynamic optimization of the aeration technology, integration the main phenomena and process parameters to characterises them.

A number of recent studies have suggested that the decomposition of very long-lived sludge from sludge results from the degradation of the non-biodegradable particulate fraction X_u (non-biodegradable compounds coming from the waste water X_i and endogenous X_p decay products) (Habermacher et al., 2016). These studies consider reducing excess sludge produced in WWTPs by working at high solids retention (> 30 days) for CAS processes and (> 100 days) for MBR processes (Spérandio et al., 2013). Although, our project is a case study very close to a MBRs system with a few weeks of autonomous operation and for this a model of correct prediction of these solids becomes necessary to understand to what extent and for which kinetics the fraction of particles not biodegradable becomes biodegradable.

Effect in kinetic models Literature reports several cases where an overestimation of sludge production by ASM models compared to experimental measurements have been reported. This phenomenon is particularly obvious in the case of MBRs (Lubello et al., 2009). One of the main reasons for such behavior may be related to the approach used in ASM models to predict the behavior of particles produced by the endogenous decay of heterotrophic and autotrophic (X_p) biomass. In fact, it must be considered that the X_p fraction consists of organic matter derived from the decay of biomass. Therefore, the assumption that a fixed part of the biomass (indicated as f_p in the models) can no longer be biodegraded, can only be considered correct for limited sludge age values (Spérandio and Espinosa, 2008).

Another reason is that the experimental procedure definitions which estimate the inert particulate COD fraction of the influent wastewater (f_{XI}) are very uncertain, but the respirometric measurements of this fraction are not entirely adequate for the following reasons:

- Respirometry tests are short term and therefore, part of the hydrolyzable fraction is identified as an inert particulate matter.

- In the case of very slowly hydrolyzable fractions, the exogenous and endogenous OURs can not be adequately distinguished using the measurement and analysis techniques used in the respirometric assays

The inclusion of a degradation rate for components traditionally considered non-biodegradable (X_u) may lead to a modification of some wastewater fractionation parameters and/or kinetic and stoichiometric parameters of the mode (Spérandio et al., 2013).

2.1.8 Enhancement of nitrification in MBRs

Between diverse results found in the literature one observation is particularly interesting. MBRs usually lead to an increased selectivity of microorganisms by increasing the bioavailability of substrates (due to smaller floc size). The physical separation within the MBR allows clusters of nitrifying bacteria to grow at the surface of the low density flocs so its population enrich over time as it has been remarked by Fenu et al. (2010b). For more details about the influence of the MBR technology over the nitrification see Section 1.4.1.

2.2 Biological processes included in the model

This literature review highlights the most important parameters to consider when modeling a MBR with complete sludge retention treating urine. Accordingly, the processes presented in table 2.1 were included in our biokinetic model. The following sections will go through each of these processes in order to describe them and present their related mathematical expressions. The main characteristics of the model are as follows:

- It considers heterotrophic activity with limitations by not only the organic substrate but also by ammonia and alkalinity (Jubany et al., 2005; Udert and Wächter, 2012);

- It considers the nitrification process for high strength ammonia influent: therefore, nitrification is described in two steps and the inhibitions of AOB and NOB by their substrates/products are taken into account (Fumasoli et al., 2016; Jubany et al., 2008);

- The influence of pH on the bacterial processes is taken into account: the speciation of TAN and TNN is derived from the pH value and dissociation constants. This affects the availability of NH_3 and HNO_2 substrates for nitrifying bacteria;

- The impact of bacterial growth on pH is modeled: protons, CO_2, HCO_3^- and CO_3^{2-} are included as state variables. Each biokinetic process is associated with the production or consumption of these compounds. In combination with the description of chemical equilibrium, the makes possible to describe the fate of protons and therefore the pH evolution.

- the recovery of phosphorus was not in the scope of the repsent study. Therefore, the corresponding processes (speciation, biological reactions, precipitation) have not been included in order to limit model complexity.

2.2.1 Growth of heterotrophs

Description

Organisms that use organic matter for the formation of new biomass are called heterotrophs, compared to autotrophs that derive carbon for biomass production from carbon dioxide (Eddy, 2003). Autotrophs need to spend more of their energy when converting carbon dioxide for cell growth which generally results in lower growth rates compared to heterotrophs. COD is a measure of the organic content in terms of biodegradable and non-biodegradable compounds (Dubber and Gray, 2010) and can therefore be an estimation of the heterotrophic activity. COD gives a measure

TABLE 2.1: Processes included in the biokinetic model

N∘	Process	N∘	Process
1	Aerobic S_S Heterotrophic oxidation with S_O	11	Hydrolysis of entrapped organic nitrogen
2	Anoxic S_S Heterotrophic oxidation with S_{NO_2}	12	Degradation endogenous residues
3	Anoxic S_S Heterotrophic oxidation with S_{NO_3}	13	Particulate inert organic solids degradation
4	Aerobic AOB growth	14	Oxygen transfer
5	Aerobic NOB growth	15	CO_2 equilibrium
6	Heterotrophic Biomass decay	16	CO_3 equilibrium
7	AOB Biomass decay	17	NO_2 equilibrium
8	NOB Biomass decay	18	Ammonium equilibrium
9	Ammonification	19	CO_2 and NH_3 transfer liquid / air
10	Hydrolysis of entrapped organics	20	H_2O equilibrium

of the amount of organics in the water hence a lower effluent COD indicates higher heterotrophic activity.

Nitrifying bacteria are chemolithoautotrophic and utilize energy from inorganic nitrogen components and use carbon dioxide (CO_2) as carbon source. This is unlike heterotrophic bacteria (heterotrophs), which utilize organic carbon as energy- and carbon source (Ebeling, Timmons, and Bisogni, 2006). Ammonium and nitrite are weaker electron donors than organic carbon sources such as acetate (CH_3COO^-) and glucose ($C_6H_{12}O_6$). Oxidation of glucose, acetate, ammonium and nitrite and associated E_0 (standard reduction potential) are presented below.

$$C_6H_{12}O_6 + 6O_2 \xrightarrow{E_0=0.82-(-0,43)=1.25} 6CO_2 + 6H_2O \qquad (2.22)$$

$$CH_3COOH + 2O_2 \xrightarrow{E_0=0.82-(-0.28)=1.10} 2CO_2 + 2H_2O \qquad (2.23)$$

$$NH4^+ + 1.5O2 \xrightarrow{E_0=0.82-(+0.43)=0.48} NO_2^- + H_2O + 2H^+ \qquad (2.24)$$

$$NO_2^- + 2H^+ + O_2 \xrightarrow{E_0=0.82-(+0.34)=0.39} NO_3^- + H_2O \qquad (2.25)$$
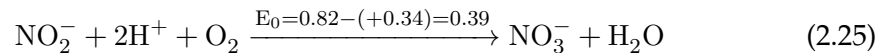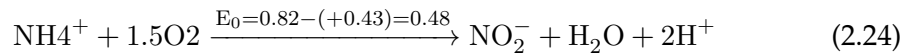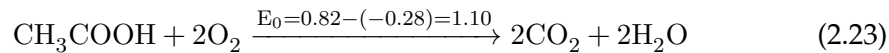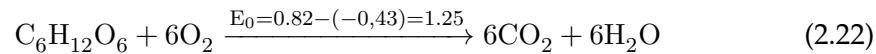
Weaker electron donors give lower free energy (ΔG), since E_0 is proportional with ΔG. This results in lower growth yield for the nitrifying bacteria than the heterotrophic bacteria (Zhu and Chen, 2001). As a consequence, nitrifying bacteria have up to 5 times slower growth rate than the heterotrophic bacteria.

Readily biodegradable substrate is considered to be the only substrate which can be used for growth of biomass. The readily biodegradable material consists of small organic molecules like acetic acid, methyl alcohol, ethyl alcohol, propionic acid, glucose etc. The assimilation of organic matter by heterotrophic bacteria in the presence of dissolved oxygen can be represented by the following reaction (Zhou, 2001):

$$C_{18}H_{19}O_9N + 0.74NH_4^+ + 8.80O_2 \rightarrow 1.74C_5H_7NO_2 + 9.30CO_2 + 4.52H_2O + H^+ \qquad (2.26)$$
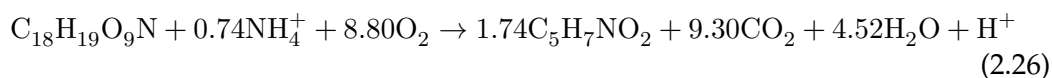
According to equation 2.26, in addition to the removal of organic matter, some ammonia is removed because it is necessary for growth of heterotrophic bacteria (as a cell constituent for e.g. proteins...). The growth of biomass is related to a proportional consumption of nutrients and substrates and the proportion of biomass produced ΔX_H to nutrient or substrate removed $-\Delta S$ is called the observed yield coefficient Y_{obs} (equation 2.27). The formation of a typical biomass compound ($C_5H_7NO_2$)

from a typical substrate ($C_{18}H_{19}O_9N$) as showed in the equation above has a typical yield coefficient.

$$Y_{obs} = -\frac{\Delta X_H}{\Delta S_s} \tag{2.27}$$

In practice, the aerobic heterotrophic yield of biomass with no limitations to growth of bacteria is in the range of $0.5\,\mathrm{g_{COD_{biomass}}\,g^{-1}_{CODsubstrate}}$ to $0.7\,\mathrm{g_{COD_{biomass}}\,g^{-1}_{CODsubstrate}}$ which makes the bacteria very fast growing. Particularly, in the ASM1 model this value is equal to $0.67\,\mathrm{g_{COD_{biomass}}\,g^{-1}_{CODsubstrate}}$ (Henze, 2007). The growth rate of biomass and the influence of limiting nutrient or substrate concentrations can be modelled using Monod kinetics that takes into account the influence of a single limiting nutrient concentration, described in equation 2.28.

$$\frac{dX_H}{d_t} = \mu_{max_H} \frac{S_s}{S_s + K_S} X_H \tag{2.28}$$

where:

- S_s: the concentration of carbonaceous substrate as COD;

- X_H: the concentration of heterotrophic active biomass;

- μ_{max_H} the maximum specific growth rate of biomass;

- K_S the substrate half-saturation constant.

Kinetic expression used in the model

Multiple limitations on the growth rate can be modelled by multiplying the right-hand side of the equation 2.28 with the appropriate number of Monod terms of the limiting substrate (oxygen, or nutrient concentrations).

The growth rate of heterotrophic biomass is described in our model in terms of oxygen and organic substrate as limiters of the process as follows:

$$\mu_{max_H} X_H \frac{S_O}{K_{O,H} + S_O} \frac{S_s}{K_s + S_s} \tag{2.29}$$

Stoichiometry

The combination of the equation 2.28 as a process rate (ρ_j) and the correct stoichiometric parameters (as the observed yield 2.27 for the growth 2.26 equation), allows to describe the kinetic of consumption/generation of each particular component involved in the describe process (e.g heterotrophic growth)

Component (i) →	1	3	10	14	16	18
Process (j) ↓	S_{co_2}	S_H	S_{NH_4}	S_O	S_s	X_H
Aerobic S_s Heterotrophic oxidation	$(alphaC_{S_s}/(Y_H*1.79/1.61) - alphaC_{X_H})/1.61$	$i_{xb}/14$	$-i_{xb}$	$-(1-Y_H)/Y_H$	$-1/Y_H$	1

By multiplying the process rate and the stoichiometric coefficient for the soluble ammonium component, we obtain the differential equation that characterises the consumption of ammonium linked to the heterotrophic growth process described in equation 2.26

$$-i_{xb}\mu_{max_H} X_H \frac{S_O}{K_{O,H} + S_O} \frac{S_s}{K_s + S_s} \tag{2.30}$$

That is how i.e. the pH contribution of the heterotrophic growth described in the equation 2.26 could be taken in to account for the overall pH prediction, as it is the case for for each concerned process inside the biokinetic model.

$$\mu_{\max_H} X_H \frac{S_O}{K_{O,H} + S_O} \frac{S_s}{K_s + S_s} \frac{i_{xb}}{14} \tag{2.31}$$

2.2.2 Anoxic heterotrophic oxidation-Denitrification

Description

Even if for the particular conditions of our biological system the oxygen level will be at the maximum level during operation and also we are in a situation of low levels of organic carbon, it is also important to take into account denitrification from nitrites or nitrates to prevent the response of the system in extreme aeration cases, like a failure in the air supply for example.

Denitrification is a microbiological heterotrophic process transforming nitrate into nitrogen gas using nitrate instead of oxygen as the oxidation agent. The conditions during which this process occurs are called anoxic because oxygen is not present and some heterotrophic bacteria are able to respire over nitrates. Denitrification is also well known from the biosphere where it is common in soil and stationary waters beneath the surface.

For removal of high amounts of nitrate in the wastewater, the nitrification process is connected to the denitrification process in the biological treatment step. Denitrifying bacteria is a large group of facultative aerobic heterotrophic bacteria and facultative aerobic autotrophic bacteria that step-wise reduce the metabolic end-product (nitrate) from nitrifying bacteria to nitrogen gas (Wilsenach and Loosdrecht, 2006). The denitrification step is either before (pre-denitrification) or after (post-denitrification) the nitrification step in a wastewater plant. Optimal conditions for denitrifying bacteria are low oxygen and high organic carbon concentrations.

Most of the heterotrophic bacteria are optional to the use of oxidation agent but the energy yield of using nitrate is less than using oxygen. Thus, if oxygen is present the bacteria prefer to use oxygen. In practice denitrification only takes place at low oxygen concentrations. The overall mechanism can be described by a typical microbial reaction of a saccharide with nitrate. The heterotrophic denitrification reaction is (Zhou, 2001):

$$5CH_3COO^- + 8NO_3^- + 3H^+ \rightarrow 10HCO_3^- + 4N_{2(g)} + 4H_2O \tag{2.32}$$

The stoichiometric chemical equations with microbial biomass in the equation above were not strictly determined separately for nitrate reduction (first stage) and nitrite reduction (second stage). The following equations take into account the stoichiometry of nitrate and nitrite reduction with ethanol as the carbon source (Vavilin and Rytov, 2015):

$$\frac{1}{12}(5.3C_2H_6O + 12NO_2^- \rightarrow 1.2C_5H_7O_2N + 5.4N_2 + 4.6CO_3^{-2} + 2.8OH^- + 10.3H_2O) \tag{2.33}$$

$$\frac{1}{12}(5.3C_2H_6O + 12NO_2^- \rightarrow 1.2C_5H_7O_2N + 5.4N_2 + 4.6CO_3^{-2} + 2.8OH^- + 10.3H_2O) \tag{2.34}$$

$$9.83C_2H_6O + 12NO_3^- \rightarrow 2.52C_5H_7O_2N + 4.74N_2 + 4.94CO_3^{-2} + 2.12HCO_3^- + 19.61H_2O \tag{2.35}$$
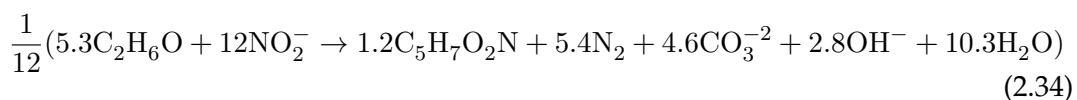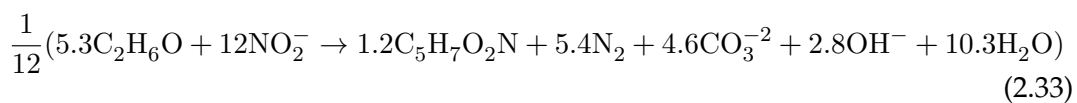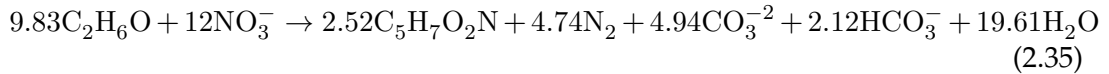
Kinetic expression used in the model

For each one of these reactions, the anoxic growth of heterotrophic bacteria are represented as an oxygen, organic substrate and specific nitrogen substrate (TNN or NO_3^-) as limiters of the process:

$$\mu_{\text{max}_H}\eta_g X_H \frac{K_{OH}}{K_{OH} + S_O} \frac{S_s}{K_S + S_s} \frac{S_{TNN}}{K_{s,TNN,H} + S_{TNN}} \tag{2.36}$$

$$\mu_{\text{max}_H}\eta_g X_H \frac{K_{OH}}{K_{OH} + S_O} \frac{S_s}{K_S + S_s} \frac{S_{NO_3}}{K_{s,NO_3,H} + S_{NO_3}} \tag{2.37}$$

Where ηg ; $K_{s,TNN,H}$; $K_{s,NO_3,H}$ represents the affinity constants.

Stoichiometry

The stoichiometric coefficients related with this respiration over NO_2 or NO_3 are described bellow.

Component (i) $\rightarrow$	12	13	16	18
Process (j) $\downarrow$	S_{NO_2}	S_{NO_3}	S_s	X_H
Anoxic S_{NO_2} Heterotrophic oxidation	$-(1 - Y_{H_{anoxic}})/(1.14 * Y_{H_{anoxic}})$		$-1/Y_{H_{anoxic}}$	1
Anoxic S_{NO_3} Heterotrophic oxidation		$-(1 - Y_{H_{anoxic}})/(1.14 * Y_{H_{anoxic}})$	$-1/Y_{H_{anoxic}}$	1

2.2.3   2-stage nitrification

Nitrification is a two step microbiological process transforming ammonia into nitrite and subsequently into nitrate. The process is well known from the biosphere where it has a major influence on oxygen conditions in soil streams and lakes. The nitrifying bacteria are divided into two groups, NH_3 oxidisers (AOB) and NO_2^- oxidisers (NOB), based on their main function in the nitrification process (Roš, Dular, and Farkas, 1988). The most important groups of organisms involved in nitrification are the lithoautotrophic. Soluble ammonia serves as the energy source and nutrient for growth of biomass of a AOB e.g. *Nitrosomas* that oxides ammonium into nitrite. The intermediate formation and removal of this nitrite is made by NOB e.g. *Nitrobacter*. Biological nitrification requires optimized management of interactions between AOB and NOB. This aspect is particularly critical for effluents with a high nitrogen content, such as urine (Udert et al., 2003a; Udert and Wächter, 2012). For practical reasons, the "traditional" models of the ASM family describe nitrification and denitrification as one-step processes (Henze, 2007). Indeed, these facilities are unlikely to face inhibition of nitritation. This one-step process incorporates kinetic parameters for the total process. The reaction for total nitrification is considered as (Ahn, Yu, and Chandran, 2008):

$$NH_4^+ + 1.86O_2 + 1.98HCO_3^- \rightarrow 0.020C_5H_7NO_2 + 0.98NO_3^- + 1.88H_2CO_3 + 1.04H_2O \tag{2.38}$$
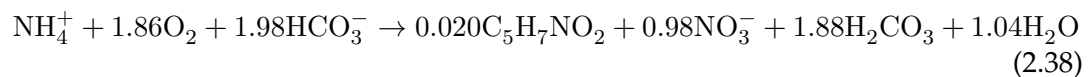
According to equation 2.38, the conversion of 100 mg ammonium to nitrate yields 17 mg nitrifying biomass as a whole. The total oxygen consumption is $4.27\,g_{O_2}$ for

nitrification of $1\,\mathrm{g_{NH4_+^-N}}$ to $NO_3^- - N$. This equation also indicates that nitrification of 1 g ammonium requires 7.07 g of alkalinity (as $CaCO_3$) or 12 mg (as $NaHCO_3$). In the context of influent heavily loaded with reduced nitrogen, it is necessary to describe these processes in two stages to reproduce the nitrite accumulation phenomena which is likely to occur, as well as the fate of alkalinity as a rate limiter substrate.

The lithoautotrophs rely on the oxidation of inorganic compounds as their characteristic energy source (Roš, Dular, and Farkas, 1988). They cooperate in the process where NH_3 is oxidised to NO_2 (first step) then NO_2 is oxidised to NO_3^- (second step). These steps are as follows:

First step (Anthonisen et al., 1976a; Zhou, 2007):

$$NH_4^+ + 0.75O_2 \rightarrow NO_2^- + 2H^+ + H_2O \tag{2.39}$$

or

$$NH_4^+ + 1.5O_2 + 2HCO_3 \xrightarrow{\mathrm{E_0=\ 0.82-(+0.43)=0.48=-235\,kJ\,mol^{-1}}} NO_2^- + 2H_2CO_3 + H_2O \tag{2.40}$$
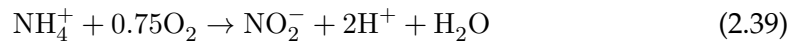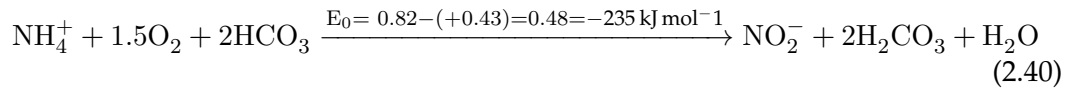
Second step (Udert et al., 2003a):

$$NO_2^- + 0.5O_2 \xrightarrow{\mathrm{E_0=\ 0.82-(+0.34)=0.39=-54\,kJ\,mol^{-1}}} NO_3^- + H_2O \tag{2.41}$$
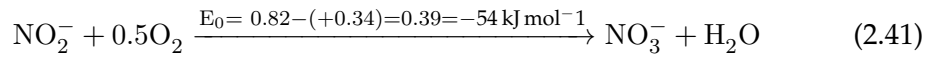
In terms of redox equations, the chemical reactions mechanisms of this process can be written (Rosenberg et al., 2013):

$$NH_3 + 0.5O_2 \rightarrow NH_2OH \tag{2.42}$$

$$0.5O_2 + 2H^+ + 2e^- \rightarrow H_2O \tag{2.43}$$

$$NH_3 + O_2 + 2H^+ + 2e^- \rightarrow NH_2OH + H_2O \tag{2.44}$$

$$NH_2OH + H_2O \rightarrow HNO_2 + 4H^+ + 4e^- \tag{2.45}$$
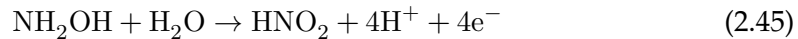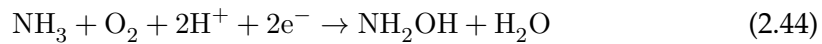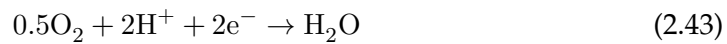
Equations 2.42 to 2.44 describes the reaction of ammonia oxidation to the intermediate hydroxylamine (NH_2OH). For the second step hydroxylamine oxidation, no oxygen is consumed in equation 2.45). Subsequently two electrons are transferred back to reaction mechanism and the remaining two electrons pass to the respiratory chain and finally nitrous acid is oxidised to nitrate. There is no acid production when nitrite is oxidized to nitrate:

$$HNO_2 + H_2O \rightarrow NO_3 + 2H^+ + 2e^- \tag{2.46}$$
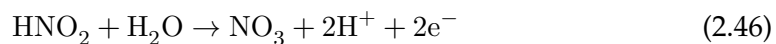
Because the processes in the two step nitrification only give a small energy yield the (E_0) (see Section 2.2.1), nitrifying bacteria are characterized by a low biomass yield. This is an essential problem for the nitrification process in biological nutrient removal systems. The observed yield coefficients for *Nitrosomonas* and *Nitrobacter* are typically significantly smaller compared to those of the heterotrophic bacteria which makes the nitrifying bacteria a rather slow growing population.

2.2.4   Growth of AOB: Nitritation

Description

The AOB bacteria count with 25 cultured species (Koops and Pommerening-Röser, 2001), among the principal ones we find five different genera; *Nitrosomonas*, *Nitrosococcus*, *Nitrosospira*, *Nitrosolobus* and *Nitrosovibrio* (Koops et al., 2006). The most common genera of AOB in many WWTP are *Nitrosomonas* (Koops et al., 2006). In a pilot-scale reactor for nitrification of urine over high ammonia concentrations, the AOB was shown to belong to the *Nitrosomonas europea* lineage (Fumasoli et al., 2016). When pH is low, around 5.8, the more acid-tolerant *Nitrospira* is selected over *Nitrosomonas* (Fumasoli et al., 2016).

Suzuki, Dular, and Kwok (1974) reported that it is ammonia (NH_3) rather than ammonium ion (NH_4^+) which is serving as the substrate of ammonium oxidizers. If the chemical equilibrium discussed in the Introduction chapter is considered, at a high pH condition, the concentration of unionized ammonia NH_3 (FA) would increase, which actually improves the nitritation rate. However, on the other hand, the activities of oxidizers responsible for nitritation would be inhibited by FA when FA concentration ranges from $0.1 \, g_{NH_3-N}.m^{-3}$ to $10 \, g_{NH_3-N}.m^{-3}$ (Anthonisen et al., 1976a). Hence, ammonia is the substrate for nitritation but also the inhibitor.

The global stoichiometric reaction described in equation 2.38 can be written now for the first step nitrification path, for the AOB activity, which is an extended version of the equation 2.39 (Ahn, Yu, and Chandran, 2008):

$$
\begin{aligned}
NH_4^+ + 1.98HCO_3^- + 1.38O_2 \rightarrow \\
0.0182C_5H_7O_2N + 0.98NO_2^- + 1.04H_2O + 1.89H_2CO_3
\end{aligned}
\tag{2.47}
$$
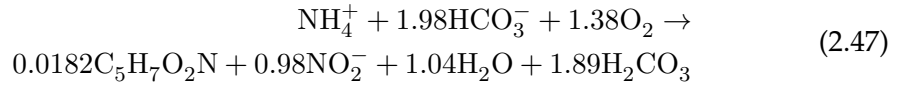
Kinetic expression used in the model

The nitritation kinetic is written in the model as follows presented in equation 2.48. Here the alkalinity effect on the nitrification could be represented as a Monod type equation (according to Biesterfeld et al. (2001)):

$$
\mu_{max_A} X_A \frac{S_O}{K_{O,A} + S_O} \frac{FA}{K_{S,FA,A} + FA + FA^2/K_{i,FA,A}} \frac{K_{i,FNA,A}}{K_{i,FNA,A} + FNA} \frac{S_{alk}}{K_{alk,A} + S_{alk}}
\tag{2.48}
$$

Stoichiometry

Component (i) →	1	3	10	12	14	17
Process (j) ↓	S_{CO_2}	S_H	S_{NH_4}	S_{NO_2}	S_O	X_A
Aerobic AOB growth	$-alpha_{C_{XA}}$	$(2/Y_A - i_{xb})/14$	$-(1/Y_A) - i_{xb}$	$1/Y_A$	$-(3.43 - Y_A)/Y_A$	1

According to the stoichiometric equation 2.39 and 2.47 the pH contribution of this process is described by:

$$
\mu_{max_A} X_A \frac{S_O}{K_{O,A} + S_O} \frac{FA}{K_{S,FA,A} + FA + FA^2/K_{i,FA,A}} \frac{K_{i,FNA,A}}{K_{i,FNA,A} + FNA} \frac{S_{alk}}{K_{alk,A} + S_{alk}} \left(\frac{2/Y_A - i_{xb}}{14} \right)
\tag{2.49}
$$

The others component such as CO_2 are taken into account as they are related with the inorganic carbon presence/needs (production/consumption) all over the nitrification stage, thus a correct alkalinity prediction could be made knowing the chemical equilibrium between the different species of carbon present in the medium (see Subsection 2.3.2).

2.2.5 Growth of NOB: Nitratation

The NOB, which are responsible for the nitrite oxidation, are divided into 8 cultured species but four are the most common: *Nitrobacter*, *Nitrococcus*, *Nitrospina* and *Nitrospira* (Rosenberg et al., 2013). The most common NOBs in WWTPs are *Nitrospira* and *Nitrobacter*. *Nitrospira* constitutes the main part of the NOB in WWTPs (Vadivelu, Keller, and Yuan, 2007). *Nitrospira* and *Nitrobacter* are favored by different nitrite concentration, in fact *Nitrobacter* is better adapted to high nitrite concentrations than *Nitrospira*. At low nitrite concentration, *Nitrospira* constitutes the main part of the NOB population and at high nitrite NOB *Nitrobacter* is the most common NOB (Kim, Lee, and Keller, 2006; Noguera, Araki, and Rittmann, 1994). *Nitrobacter* grow faster but have a lower affinity for oxygen than *Nitrospira* (Koops et al., 2006).

During the oxidation of ammonium ions to nitrite, protons (H^+) are released. Nitrite (NO_2^-) will exist in equilibrium with unionized nitrous acid HNO_2 (FNA) as showed in equation 2.68. The reduced pH in turn increases FNA concentration, thus triggering inhibition of nitritation by FNA when it falls in the range of $0.22\,g_{HNO_2^--N}.m^{-3}$ to $2.8\,g_{HNO_2^--N}.m^{-3}$ (Anthonisen et al., 1976a).

The global stoichiometric reaction described in equation 2.38 can be written now for the second step nitrification path, for the NOB activity, which is an extended version of the equation 2.39 (Ahn, Yu, and Chandran, 2008):

$$NO_2^- + 0.02H_2CO_3 + 0.49O_2 + 0.005NH_4^+ + 0.005HCO_3^- \rightarrow \\ 0.005C_5H_7O_2N + NO_3^- + 0.015H_2O \tag{2.50}$$
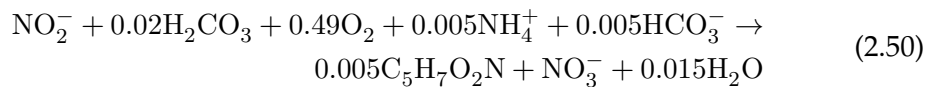
Kinetic expression used in the model

NOB growth can be limited by DO (Monod term). The substrates necessary for the growth are FNA (Vadivelu et al., 2006) (substrate inhibition) and FA acts as a pure inhibitor (Vadivelu, Keller, and Yuan, 2007). The nitritation kinetic is written in the model as follows (equation 2.51):

$$\mu_{max_N} X_N \frac{S_O}{K_{O,N} + S_O} \frac{FNA}{K_{S,FNA,N} + FNA + FNA^2/K_{i,FNA,N}} \frac{K_{i,FA,N}}{K_{i,FA,N} + FA} \frac{S_{alk}}{K_{alk,N} + S_{alk}} \tag{2.51}$$

Stoichiometry

Component (i) →	1	3	10	12	13	14	20
Process (j) ↓	S_{CO_2}	S_H	S_{NH_4}	S_{NO_2}	S_{NO_3}	SO	X_N
Aerobic NOB growth	$-alpha_{C_{X_N}}$	$i_{xb}/14$	$-i_{xb}$	$-(1/Y_N)$	$1/Y_N$	$-(1.14 - Y_N)/Y_N$	1

According to the stoichiometric equation 2.41 and 2.50, the pH contribution of this process is described by:

$$\mu_{\max_N} X_N \frac{S_O}{K_{O,N} + S_O} \frac{FNA}{K_{S,FNA,N} + FNA + FNA^2/K_{i,FNA,N}} \frac{K_{i,FA,N}}{K_{i,FA,N} + FA} \frac{S_{alk}}{K_{alk,N} + S_{alk}} (i_{xb}/14)$$

$$(2.52)$$

2.2.6   Decay of biomass and Endogenous respiration

Description

Biomass is lost by decay which incorporates a large number of mechanisms including endogenous metabolism, death, predation and lysis (Van Loosdrecht and Henze, 1999). The death regeneration concept is applied to describe the different reactions that take place when organisms die. The traditional endogenous respiration concept describes how a fraction of the organism mass disappears to provide energy for maintenance. In the death regeneration concept oxygen consumption is not directly associated with microbial decay, this one is assumed to be the result of the release of slowly biodegradable substrate that is recycled back to soluble substrate and used for more cell growth. Thus, the oxygen utilisation normally associated directly with decay is calculated as if it occurs indirectly from growth of new biomass on released substrate. In fact, bacterial decay is the transformation of active biomass into slowly biodegradable substrate as illustrated in figure 2.1.

Kinetic expression used in the model

In the death regeneration model, one unit of biomass lost (as COD) results in the formation of one unit of COD from readily biodegradable substrate minus the formed inert particulate products $(1 - f_p)$. Part of the bacterial decay is usually considered inert (f_p) because the hydrolysis process is too slow relative to the sludge retention time of a typical WWTP. The decay of biomass is described as a first order kinetic process.

$$b.X \qquad\qquad (2.53)$$

where b is the decay rate (b>0) The decay rate is assumed to be affected by environmental factors as temperature, oxygen concentration, nutrients and substrates.

Stoichiometry

Component (i) →	17	18	20	21	22	23	24
Process (j) ↓	X_A	X_H	X_N	X_{nd}	X_{ni}	X_p	X_s
Heterotrophic Biomass decay	-1			$i_{xb} - f_p * i_{xp}$	$f_p * i_{xp}$	f_p	$1 - f_p$
AOB Biomass decay		-1		$i_{xb} - f_p * i_{xp}$	$f_p * i_{xp}$	f_p	$1 - f_p$
NOB Biomass decay			-1	$i_{xb} - f_p * i_{xp}$	$f_p * i_{xp}$	f_p	$1 - f_p$

2.2.7   Degradation of the endogenous residue

Within MBRs, the endogenous residue formed during biomass decay can be considered as very slowly biodegradable: a small first order biodegradation constant for X_P ($0.007\,\mathrm{d^{-1}}$) was suggested as a good estimate of the first order constant for

X_P degradation under aerobic conditions (Jones et al., 2012a; Ramdani et al., 2012; Spérandio et al., 2013) and with a high SRTs.

The kinetic expression used in the model is therefore:

$$0.007 * X_p \tag{2.54}$$

The stoichiometric factor associated is the consumption of this 'unbiodegradable' component X_P occurring at high SRT:

Component (i) $\rightarrow$	3	23
Process (j) $\downarrow$	S_S	X_p
Degradation of the endogenous residue	1	-1

2.2.8 Ammonification

Description

Urine contains urea which suffer ureolysis and form ammonia. Ureolysis is caused by both urease active bacteria and dissolved urease. The urease activity is often considered as independent of the pH in the system (Udert, Larsen, and Gujer, 2003). However, recent research showed that this not essentially true (Randall et al., 2016). The enzyme urease converts urea and water to ammonia and carbamate (see Section 1.1.1 and equation 2.55). The carbamate molecule then undergoes spontaneous hydroxylation to ammonia and carbonic acid (equation 2.56). Ammonia can both evaporate and form ammonium in function of the pH of the system. According to the equation 2.57, more ammonia is present the equilibrium goes to the right side of the equation an this leads to an increase in ions OH^- that causes a consequent increase in pH (equation 2.70) (Mobley and Hausinger, 1989). The decomposition rate of urea in a storage container could thus be followed (at least qualitatively) by measurements of pH (Hellström, Johansson, and Grennberg, 1999).

$$CO(NH_2)_2 + H_2O \rightarrow NH_3 + H_2NCOOH \tag{2.55}$$

$$H_2NCOOH + H_2O \rightarrow NH_3 + H_2CO_3 \tag{2.56}$$

$$NH_3 + H_2O \rightarrow NH_4^+ + OH^- \tag{2.57}$$
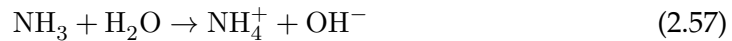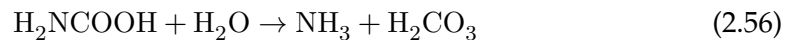
Kinetic expression used in the model

Urea as biodegradable soluble organic nitrogen (S_{ND}) is converted to ammonia nitrogen (S_{NH}) in a first order process. Hydrogen ions consumed in this conversion process result in an alkalinity change as showed previously in equations 2.55 and 2.56 (detailed representation of equation 1.1).

$$k_a S_{nd} X_H \tag{2.58}$$

Component (i) →	1	3	8	10
Process (j) ↓	S_{CO_2}	S_H	S_{ND}	S_{NH_4}
Ammonification	6/14	-1/14	-1	1

Stoichiometry

According to the stoichiometric equation 1.1 and 2.56 the pH contribution of this process is described by:

$$- \left(\frac{1}{14} \right) k_a S_{nd} X_H \tag{2.59}$$

2.2.9   Hydrolysis of particulate material

Description

Under the ASM approach, as showed in the section 1.4.1, the biodegradable organic matter is normally divided into two groups; soluble readily biodegradable (S_S) and slowly biodegradable (X_S) substrate (even if some of the slowly biodegradable matter may actually be soluble) (Henze, 2007; Spérandio, Heran, and Gillot, 2007). The readily biodegradable substrate is assumed to consist of relatively simple molecules that may be taken in directly by heterotrophic organisms and used for growth of new biomass (see equation 2.28). On the contrary, the slowly biodegradable substrate consists of relatively complex molecules that require enzymatic breakdown before being an accessible substrate. This process is achieved via hydrolysis where slowly biodegradable substrate (X_S) from the sludge is broken down producing readily biodegradable substrate (S_S). Hydrolysis is an enzymatic accelerated process transforming larger organic molecules, including both soluble and particulate organic materials, into smaller readily biodegradable molecules (Morgenroth, Kommedal, and Harremoës, 2002). The hydrolysis process rate is slow compared to the rate of growth of biomass and it will be the rate limiting factor for the growth of biomass if the substrate in the raw wastewater primarily consists of large organic molecules (Spanjers and Vanrolleghem, 1995a).

Kinetic expression used in the model

Because hydrolysis is a generic term for a great number of different biochemical processes, it is modelled on the basis of surface reaction kinetics and occurs in both aerobic and anoxic conditions. The hydrolysis rate is reduced under anoxic conditions in the same way as anoxic growth, by applying a correction factor η_h (<1). The rate is also first order with respect to the heterotrophic biomass concentration but saturates as the amount of entrapped substrate becomes large in proportion to the biomass. The rate of the total process is then given by a first order kinetic expression (Morgenroth, Kommedal, and Harremoës, 2002):

$$k_h \frac{X_s/X_H}{K_X + X_s/X_H} \left[\frac{S_O}{K_{O,H} + S_O} + n_h \frac{K_{O,H}}{K_{O,H} + S_O} \right] X_H \tag{2.60}$$

The biodegradable nitrogen matter is subdivided into ammonia nitrogen (S_{NH}), nitrate nitrogen (S_{NO_2}), nitrite nitrogen (S_{NO_3}), soluble organic nitrogen (S_{ND}) and particulate organic nitrogen (X_{nd}) (Henze, 2007; Spérandio, Heran, and Gillot, 2007). This particulate organic nitrogen is hydrolysed to soluble organic nitrogen in parallel with hydrolysis of the slowly biodegradable organic matter (X_S) (either present in

the wastewater or produced via the decay process). (Morgenroth, Kommedal, and Harremoës, 2002)

$$k_\text{h} \frac{X_\text{s}/X_\text{H}}{K_\text{X} + X_\text{s}/X_\text{H}} \left[\frac{S_\text{O}}{K_\text{O,H} + S_\text{O}} + n_\text{h} \frac{K_\text{O,H}}{K_\text{O,H} + S_\text{O}} \right] X_H \frac{X_\text{nd}}{X_\text{S}} \qquad (2.61)$$

Stoichiometry

Component (i) →	8	16	21	24
Process (j) ↓	S_nd	S_s	X_nd	X_s
Hydrolysis of entrapped organics		1		-1
Hydrolysis of entrapped organic nitrogen	1		-1	

2.2.10 Hydrolysis of inert COD fraction

Description

In our model, similarly to the degradation of the endogenous residue of biomass decay (X_p), the inert particulate fraction will be considered very slowly degradable. This comes from the fact that the particulate organic matter from the influent originates mainly from toilet paper i.e. cellulose (see Section 1.4.1 (Reijken et al., 2018)):

Kinetic expression used in the model

$$0.007 * X_i \qquad (2.62)$$

Stoichiometry

Component (i) →	3	19
Process (j) ↓	S_S	X_i
Inert COD fraction hydrolysis	1	-1

2.3 Physicochemical processes included in the model

2.3.1 pH prediction

The ASM1 model utilize a global alkalinity state variable (S_alk) at constant pH. In this approach, it is not considered that some of the acids/bases species are weak and therefore only partially contribute to the alkalinity dynamics (as could be the case of sodium acetate pair strong base and weak acid). The contribution to the alkalinity gave by to the strong acids/bases as bicarbonate (weak carbonic acid and weak bicarbonate base) is poorly consider and so the dynamics associated with alkalinity variations are not enough predicted. This have a direct impact on the performance of the reactor. Processes such as nitrification (acid producing) will decrease alkalinity, while processes such as ammonia release (base producing) will increase it. In the ASM1 model the alkalinity state variable provides an approximation that indicates whether pH is near neutrality, or well below it (Henze, 2007). The advantage of this approach is its simplicity, however several problems are present. In the case where

alkalinity is depleted, pH will drop dramatically also and this a situation which the ASM1 model cannot predict directly.

Wastewater usually contains enough alkalinity to meet the need showed in equation 2.38, mainly because all the influents are mixed and there is an important dilution of contents in the inlet. Even with this dilution and the additional alkalinity from the tap water, some wastewater treatment facilities require the addition of alkali compounds to maintain desirable pH levels for nitrification as HCO_3.

One of the possible strategies is to integrate environmental models to supply this lack of integrated knowledge. One particular model is the the RWQM No. 1 (Reichert et al., 2001). This model uses the same structured modeling approach as the ASM series. There are included chemical reactions (chemical equilibrium, calcium carbonate precipitation as well as phosphate sorption and desorption on organics). In order to properly represent the process of 2-steps nitrification and the associated inhibitions, pH need to be calculated an not only represented as a alkalinity state variable. For the development of our model, acid-base equilibrium and gas transfer were inspired by the RWQM No. 1, but precipitation was not taken into account.

For example, as presented by Sharma, Ganigue, and Yuan (2013) nitrogen content of the wastewater is the most influential factor causing pH variation in fresh sewage, the total ammonium concentration variation well correlated with the pH variation for this particular case based on the concept of charge balance for pH prediction (Sharma, Ganigue, and Yuan, 2013). This prediction of pH and quantification of its impact in the biological process takes more relevance when treating with high ammonium content wastewater and the need for models capable to predict pH variation in wastewater became crucial. Particularly, if the optimization and operation of a strategy like biomass acclimation are really sensitive to pH changes. Further, the lack of pH prediction resulted in the inability of these models to consider the effect of pH variation on the rates of biological (e.g. nitrification), chemical (e.g. nitrous acid inhibitory concentrations) and physical (e.g. ammonia stripping) processes (Anthonisen et al., 1976a; Fumasoli, Morgenroth, and Udert, 2015; Jubany et al., 2005; Udert, Larsen, and Gujer, 2006; Udert and Wächter, 2012), leading to possibly inaccurate prediction of the system performances.

The contribution of each biological process described in section 2.2 to the pH prediction is taken into account here to analyse the impact of physical and chemical equilibrium on the over biokinetics. The change in pH affects the rates of biochemical processes. Thus, the acid-base equilibrium for several parameters in the present model is essential to understand the dynamics, nature and behaviour of the system.

2.3.2   Acid-base equilibrium

The importance of the gas/liquid transfer will be highlighted in section 2.3.3. In this section the interaction in the liquid phase of the substance is presented. Those combined interaction are necessary to correctly quantify and describe the substrate availability. From urea hydrolysis to the availability of substrate for nitrification as FA and FNA, the chemical equilibrium reactions involved are:

$$(NH_2)_2CO + H_2O \rightarrow 2NH_3 + CO_2 \tag{2.63}$$

$$2NH_3 + 2H_2O \rightleftharpoons 2NH_4^+ + 2OH^- \tag{2.64}$$

$$CO_2 + H_2O \rightleftharpoons HCO_3^- + H^+ \tag{2.65}$$

$$H^+ + OH^- \leftrightharpoons H_2O \tag{2.66}$$
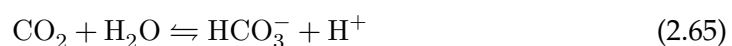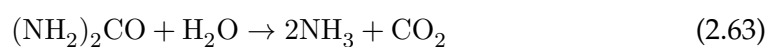
As seen in section 2.2, the real substrate for AOB is FA (Koops et al., 2006) and the substrate for NOB is nitrite (Rosenberg et al., 2013). FA and nitrous acid can inhibit both types of bacteria (Anthonisen et al., 1976a; Vadivelu, Keller, and Yuan, 2007). Temperature and pH determine the relationship between ammonium and ammonia (equation 2.67) and between nitrite and nitrous acid (equation 2.68).

$$NH_4^+ + OH^- \leftrightharpoons NH_3 + H_2O \tag{2.67}$$

$$H^+ + NO_2- \leftrightharpoons HNO_2 \tag{2.68}$$
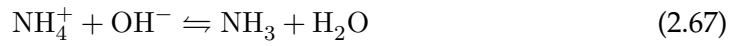
(Anthonisen et al., 1976a)

Most of these reactions are acid-base reactions, in fact they are extremely rapid reactions, occurring in the liquid phase between a weak acid and its conjugate base. The concentration of the acid can be related to the concentration (or more correctly, the activity) of his pair base from the equilibrium relationship for given as:

$$aA + bB \leftrightharpoons cC + dD \tag{2.69}$$

From a given chemical equation as 2.69 the equilibrium constant is defined as:

$$K_c = \frac{\alpha_C^c \alpha_D^d}{\alpha_A^a \alpha_B^b} \tag{2.70}$$

If the total (acid+base) concentration is known for each component present, the concentration of each acid and base can be solved via the equation 2.70. This provides a solvable set of non-linear implicit algebraic equations which can be solved together with the differential equations from the biochemical processes.

Kinetic expressions used in the model

All the chemical equilibrium reactions to describe the equilibria between CO_2 and HCO_3^-, HCO_3^- and CO_3^{-2}, HNO_2 and NO_2^-, NH_3 and $NH4^+$ and finally between H_2O and H^+ and OH^- are represented in the next equations:

$$(\lambda_{CO_2} S_{CO_2} - (\lambda_{HCO_3} S_{HCO_3} * \lambda_H S_H / Ka_{CO_2})) * k_{eq1} \tag{2.71}$$

$$(\lambda_{HCO_3} S_{HCO_3} - (\lambda_{CO_3} S_{CO_3} * \lambda_H S_H / Ka_{HCO_3})) * k_{eq2} \tag{2.72}$$

$$(\lambda_{HNO_2} S_{HNO_2} - (\lambda_{NO_2} S_{NO_2} * \lambda_H S_H) / Ka_{HNO_2}) * k_{eq2} \tag{2.73}$$

$$(\lambda_{NH_4} S_{NH_4} - (\lambda_{NH_3} S_{NH_3} * \lambda_H S_H) / Ka_{NH_4}) * k_{eq2} \tag{2.74}$$

$$(1 - (\lambda_H S_H * \lambda_{OH} S_{OH} / K_{eqw})) * k_{eq2} \tag{2.75}$$

Component (i)→	1	2	3	4	5	6	9	10	12	15
Process (j) ↓	S_{CO_2}	S_{CO_3}	S_H	S_{H_2O}	S_{HCO_3}	S_{HNO_2}	S_{NH_3}	S_{NH_4}	S_{NO_2}	S_{OH}
CO_2 equilibrium	-1		1/12	-1/12	1					
HCO_3 equilibrium		1	1/12		-1					
NO_2 equilibrium			1/14			-1			1	
Ammonium equilibrium			1/14				1	-1		
H_2O equilibrium			1	-1						1

Stoichiometry

2.3.3   Gas transfer

The dissolved gases are also acids or bases and hence the acid-base subsystem is important to calculate gas transfer, while gas transfer has a significant impact on the acid-base subsystem through its effect on pH. That is why stripping of CO_2 and NH_3 should consider the speciation of the substrates (CO_2, HCO_3 etc..) together with the pH influence.

Oxygen, carbon dioxide and ammonia dissolved in the waste water and in the mixed liquor inside the reactor are in physical equilibrium with the gaseous phase. The mass transfer that characterises these exchanges could be described by the thermodynamic equilibrium for the saturation values and the double layer theory between the liquid and the gas phase for the kinetics of the transfer. In other words, there will be a maximum and constant concentration of these compounds in the liquid phase (called saturation value), determined by a partial pressure and a thermodynamic solubility constant K_0 in the Henry's law. This one is influenced by total pressure, temperature and composition of both liquid and gas phases. According to Mook W (2000) for a particular compound α his thermodynamic solubility constant is calculated as:

$$K_0 = \frac{\alpha}{P_\alpha} \tag{2.76}$$

where α is the activity of the component in the liquid phase and P_α is the partial pressure in atm$^-$1.

The partial pressure of each component on an ideal gas mixture could be calculated using the Ideal Gas Law. If the volume and temperature are considered to be constant, partial pressure of component i could be calculated as (according to Griffith (2016)):

$$p_i = y_i P_{Total} \tag{2.77}$$

with :
p_i in atm
y_i : as a molar or volumetric ratio v/v
P_{Total} : in atm

When considering gas mixtures, the most important is our atmosphere, which consists of approximately 78% nitrogen, 21% oxygen and 1% other gases. Those percentages are both the volumetric percentages and the mole percentages. Expressed as a molar or volumetric ratio, the concentration of O_2 at the atmospheric pressure is 20.9% v/v. The partial pressure is related to the total atmospheric pressure. That one change from place to place as the altitude over the sea level. The correction of

the air pressure above sea level can be calculated with (according to Griffith (2016)):

$$p = 101325(1 - 2.2557710 - 5h)^{5.25588} \tag{2.78}$$

where: 101325 = normal temperature and pressure at sea level (Pa)
p = air pressure (Pa)
h = altitude above sea level (m)

Solubilities and dissociation constants dependent of temperature and solute concentrations. This concentration in the liquid phase is in equilibrium with the other species in function of the pH via the acidity constants as explained in the last subsection.

Solubilities

Oxygen In the case of the oxygen, the saturation concentration is also influenced by salinity. Therefore, it could be estimated according to the Weiss equation (Chifflet, Gerard, and Fichez, 2004) as a function of both salinity conditions and the temperature:

$$S_o^* = O_{2_{sat}} = 1.429 e^{g(Sal,Temp)} \tag{2.79}$$

$$g_{(Sal,Temp)} = -173.4292 + 249.6329 * \frac{100}{T} + 143.3483 * \log\left(\frac{T}{100}\right) - 21.8492 * \frac{T}{100}$$

$$+ Sal * \left[-0.033096 + 0.014259 * \frac{T}{100} - 0.0017 * \frac{T}{100}^2 \right] \tag{2.80}$$

with :
$O_{2_{sat}}$ in $g_{O_2}.m^{-3}$
Sal : Salinity (Practical Salinity Scale 1978 (PSS) 78)
T : Temperature in Kelvin

The PSS is based on an equation relating salinity to the ratio K_{15} of the electrical conductivity of seawater at 15°C to that of a standard potassium chloride solution (KCl) in which the mass fraction of KCl is 32.4356^{-3}, at the same temperature and pressure (Lewis and Perkin, 1981). The K_{15} value exactly equal to 1 corresponds, by definition, to a practical salinity exactly equal to 35. A standard seawater of 35 has by definition a conductivity ratio of unity at 15°C with a KCl solution containing a mass of 32.4356 g KCl in a mass of 1 kg of solution (Chifflet, Gerard, and Fichez, 2004). Practical salinity should be expressed by dimensionless number only and should be written as, *e.g.* S = 35.034.

The oxygen saturation concentration could be then calculated and the $K_L a$ is measured experimentally for different configuration of inlet gas pressure in the reactor working with clean water and with sludge. An alpha factor $\alpha_{K_L a}$ (Eckenfelder and Cleary, 2013), which is the main transfer rate in wastewater $K_L a$ divided by the main transfer rate in clean water, could be determined and the influence of the

turbulence and sludge characteristics in the aeration system could be identified.

$$\alpha_{K_L a} = \frac{K_L a_{sludge}}{K_L a_{clean\ water}} \tag{2.81}$$

In fact, several factors as the geometry of the reactor, as well as the presence of surface active agents, solids accumulation, biomass concentration in the gas-liquid interface have an influence in the oxygen transfer (increasing or deceasing it in a range from 0.4 to 1.2 according to (Eckenfelder and Cleary, 2013)).

Carbon dioxide   For the CO_2 the apparent acidity (dissociation) constant is (Harned and Davis, 1943):

$$pK_1 = \frac{3404.71}{T} + 0.032786 * T - 14.8435 \tag{2.82}$$

The equilibrium aqueous concentration found with this equation (see Section 2.3.2) could be linked to the thermodynamic Henry coefficient by the equation (Buhr and Miller, 1983):

$$(K_H)_{CO_2} = exp^{(-8.1403+842.9/(T+151.5))} \tag{2.83}$$

where $(K_H)CO_2$ is expressed in mol/L/atm and T is expressed in °C

At normal conditions the atmosphere (dry atmosphere at sea level) has a composition, or partial pressure, in carbon dioxide 450 ppm according to Calvin et al. (2009). This partial pressure will be used to determinate the carbon dioxide saturation concentration.

Free ammonia   The FA thermodynamic molar constant could be calculated by a simpler relation presented by Bates and Pinching (1949): for solutions of ammonia in watern high salt solutions and constant IS (ammonia concentrations from 0.59 mole per liter to at least a few tenths), the Henry's law constant,K_0, for partial pressures P_{NH_3} in mmHg, appears to be about $12.9\,\text{mol}\,\text{L}^{-1}\,\text{mmHg}^{-1}$ to $13.4\,\text{mol}\,\text{L}^{-1}\,\text{mmHg}^{-1}$ at 25 °C. The normal ammonia concentration in the atmospheric air is really low, around traces to 0.0000003% according to Warneck (1988), so for better calculation of the ammonia stripping this partial pressure is used to calculate FA saturation concentration. A correct and more accurate estimation of the Henry's constant is made by the equation (Dasgupta and Dong, 1986):

$$(K_H)_{NH_3} = exp^{(-5.31+2864/(T+273.15))} \tag{2.84}$$

where $(K_H)_{NH_3}$ is expressed in mol/L/atm and T is expressed in °C

Kinetic expression used in the model

Thus, for the dynamic of the exchange between phases, the transfer could be understood and modelled as the product of a $k_L a$ coefficient times the driving power given by the difference between the real liquid concentration and the saturation one for each compound.

Notwithstanding, the current $k_L a$ approach used in our model (first order equilibrium driven transfer) is effective to describe O_2 transfer as the $k_L a$ value of oxygen is based on physical measurement (see Section 4.2). The determination of the mass transfer coefficient $k_L a$ depends on the hydrodynamics and configuration of

the system. But for the CO_2 and FA, there is currently no reliable method to estimate correctly the transfert coefficient based on measurable physical properties.

According to Boogerd et al. (1990), when the transfers of CO_2 and O_2 are compared under the same experimental conditions of temperature and salinity content, it seems valid to assume that the k_La for carbon dioxide equals 0.893 times the k_La for oxygen. K_La_C for carbon dioxide was not determined experimentally and flowing the results from Boogerd et al. (1990), Fumasoli, Morgenroth, and Udert (2015) determined according to the penetration theory a value of 0.89 times the k_La for oxygen.

For the free ammonia, Stenstrom et al. (1989) cited a value of 0.943 times the k_La for oxygen. According to Benjamin and Lawler (2013), in biological treatment systems, although absorption of oxygen into the water is usually the primary gas transfer goal, stripping of carbon dioxide, ammonia and/or volatile trace organic compounds occurs simultaneously. For the particular case of ammonia, diffusive transport through the interfacial region on the gas side of the interface is the rate-limiting step in the overall process. In other words, free ammonia volatilization is governed by the gas throughput and not by the gas transfer from water to air. As this requires more detailed analyse of the gaseous phase (thus more equations, variables and computational time), purely for modelling purposes we decide to use the k_La approach in this work.

$$K_La * (S_o^* - S_O) * \lambda_{O_2} \tag{2.85}$$

$$K_La_C * (S_{CO_2} - S_{CO_2}^*) * \lambda_{CO_2} \tag{2.86}$$

$$K_La_N * (S_{NH_3} - S_{NH_3}^*) * \lambda_{NH_3} \tag{2.87}$$

Stoichiometry

Component (i) $\rightarrow$	1	9	14
Process (j) $\downarrow$	S_{CO_2}	S_{NH_3}	S_O
O_2 transfer air/liquid			1
CO_2 transfer liquid/air	-1		
NH_3 transfer liquid/air		-1	

2.4 Conclusion

In this chapter, the biological and physico-chemical processes occurring in a MBR treating urine have been presented. The different processes that were selected to represent the nitrification (and possibly denitrification) of highly ammonia loaded wastewater are presented. The corresponding rate equations and stoichiometric matrix are derived from a literature based approach (table 2.2). The major characteristics of this model are:

- 2-steps nitrification: the respective growth rates of AOB and NOB are described, making it possible to predict autotrophs inhibitions and system instabilities e.g. nitrite peaks;

No	Process	Rate equation
1	Aerobic S_S Heterotrophic oxidation	$\mu_{max_H} X_H \frac{S_O}{K_{OH}+S_O} \frac{S_s}{K_s+S_s} \frac{S_{alk}}{K_{alk,H}+S_{alk}}$
2	Anoxic S_S Heterotrophic oxidation with S_{NO_2}	$\mu_{max_H} \eta_g X_H \frac{K_{OH}}{K_{OH}+S_O} \frac{S_s}{K_s+S_s} \frac{S_{TNN}}{K_{a,TNN,H}+S_{TNN}}$
3	Anoxic S_S Heterotrophic oxidation with S_{NO_3}	$\mu_{maxH} \eta_g X_H \frac{K_{OH}}{K_{OH}+S_O} \frac{S_s}{K_s+S_s} \frac{S_{NO3}}{K_{s,NO3,H}+S_{NO3}}$
4	Aerobic AOB growth	$\mu_{max_A} X_A \frac{S_O}{K_{OA}+S_O} \frac{FA}{K_{S,FA,A}+FA+FA^2/K_{i,FA,A}} \frac{K_{i,FNA,A}}{K_{i,FNA,A}+FNA} \frac{S_{alk}}{K_{alk,A}+S_{alk}}$
5	Aerobic NOB growth	$\mu_{max_N} X_N \frac{S_O}{K_{ON}+S_O} \frac{FNA}{K_{S,FNA,A}+FNA+FNA^2/K_{i,FNA,A}} \frac{K_{i,FA,A}}{K_{i,FA,A}+FA} \frac{S_{alk}}{K_{alk,N}+S_{alk}}$
6	Heterotrophic Biomass decay	$b_H.X_H$
7	AOB Biomass decay	$b_a.X_A$
8	NOB Biomass decay	$b_n.X_N$
9	Ammonification	$k_a S_{nd} X_H$
10	Hydrolysis of entrapped organics	$k_h \frac{X_s/X_H}{K_X+X_s/X_H} \left[\frac{S_O}{K_{O,H}+S_O} + n_h \frac{K_{O,H}}{K_{O,H}+S_O} \right] X_H$
11	Hydrolysis of entrapped organic nitrogen	$k_h \frac{X_s/X_H}{K_X+X_s/X_H} \left[\frac{S_O}{K_{O,H}+S_O} + n_h \frac{K_{O,H}}{K_{O,H}+S_O} \right] X_H \frac{X_{nd}}{X_s}$
12	Degradation of endogenous residues	$0.007.X_p$
13	Particulate inert organic matter degradation	$0.007.X_i$
14	Oxygen transfer	$K_L a\,(C_s - S_O)$
15	CO_2 equilibrium	$(S_{CO_2} - (S_{HCO_3} * S_H/Ka_{CO_2})) * keq_1$
16	CO_2 equilibrium	$(S_{HCO_3} - (S_{CO}3 * S_h/Ka_{HCO_3})) * keq_2$
17	NO_2 equilibrium	$(S_{hno_2} - (S_{NO_2} * S_H)/Ka_{HNO_2}) * keq_3$
18	Ammonium equilibrium	$(S_{nh4} - (S_{NH_3} * S_H)/Ka_{NH_4}) * keq_4$
19	NH_3 transfer liquid / air	$Kla_N * (S_{NH_3} - NH_{3_{sat}})$
20	CO_2 transfer liquid / air	$Kla_C * (S_{CO_2} - CO_{2_{sat}})$
21	H_2O equilibrium	$(1 - (S_h * S_{OH}/K_{eqw})) * keq2$

TABLE 2.2: Summary of process rate equations included in the model.
For the stoichiometric matrix, refer to Appendix A

- impact of pH on biomass growth: the pH effect on autotrophic biomass growth is taken into account by considering the HNO_2/NO_2 and NH_3/NH_4^+ acid-base concentrations as substrates/inhibitors;

- pH prediction: the pH is predicted by modelling the consumption or production of acid/base compounds and protons during biological processes. Associated with the computation of chemical equilibrium for nitrogenous species as well as inorganic carbon, this allows to predict pH variations;

- degradation of endogenous residue and inert particulate fractions: as the MBR will operate with an infinite SRT, these fractions were considered as very slowly degradable with a first order hydrolysis rate.

This model contains a large number of parameters, which makes its calibration challenging. The next chapter will now present the pilot experiments that were conducted to acclimate biomass to urine treatment. Then, chapter 4 will present the estimation of parameters related to nitrifying biomass using respirometric techniques.

Chapter 3

Biomass acclimation for urine treatment in a MBR: pilot-scale studies

3.1 Introduction

The process of nitrification is based on the activity of autotrophic AOB and NOB. They are slow growing organisms compared to heterotrophic bacteria, and are characterized by low growth yield and maximal growth rate. These organisms are also more sensitive to substrate inhibition (see Section 2.2). Since approximately 90 to 97% of the conventional AS bacteria are heterotrophs, autotrophic nitrifying bacteria are relatively weak in the competition for oxygen and substrates (Moussa et al., 2006). Thus, in order to nitrify high nitrogen load contents from wastewater streams, conventional AS must be adapted or acclimated to avoid nitrification complications.

These problems originate from the differences in bacterial activity of the autotrophic strains due to unfavourable growth conditions, or to the particular concentration of some inhibitory compounds (excess of substrate FA or necessary compounds that contain inorganic carbon for example). Substrates FA and FNA can affect both AOB and NOB (Anthonisen et al., 1976a). High FA loads in the inlet can cause AOB inhibition, and nitrite accumulation inside a biological process. Inhibition can also occur if AOB activity increases more rapidly than NOB activity, thus high FNA concentrations can restrain NOB growth.

The presence of inorganic carbon can also influence autotrophic activity. Ammonia oxidation requires a large amount of oxygen, produces a small amount of biomass, and leads to alkalinity consumption due to the production of hydrogen ions (see Section 2.2). Ammonia-oxidizing bacteria (AOB) require approximately two moles of HCO_3^- per mole of NH_4^+, while NOB require a lower alkalinity level. AOB are more sensitive to the concentration of HCO_3^-, which for AOB acts as a carbon source for AOB biomass, and as a acidification buffer for the hydrogen ions produced by ammonia oxidation.

For the following research, it is necessary to understand the correct acclimation process of classical AS biomass, and the influence of the different factors disturbing the bacterial activity. This chapter presents, and compare two different strategies to acclimate biomass to high nitrogen content influent. First, external, and operational parameters are discussed, followed by analysis of the experimental campaigns with regards to operational feasibility and quality treatment goals.

3.1.1   Alkalinity, and pH importance

During nitrification, only around 10% of inorganic carbon is assimilated into biomass, with the majority of the HCO_3^- being used for neutralisation of hydrogen ions. This neutralisation is at the origin of the pH variations. As previously presented in chapter 2, pH regulates the chemical speciation of the inhibitory substances FA and FNA. As a result, the response of nitrifiers to the concentration of inorganic carbon is difficult to establish and these constraints could be the main cause of the decreasing activity of nitrifying bacteria (Biesterfeld et al., 2001; Whang et al., 2009). Although the exact mechanisms are not yet clear, some authors have chosen to add external chemicals to overcome this limitation of inorganic carbon and to better control pH levels. Whang et al. (2009) reported improved nitrification performance when swapping $NaOH$ with inorganic carbon-containing Na_2CO_3 buffer for controlling the pH. The microbial community structure of nitrifiers was affected as well. In this example, the easiest technical solution for controlling pH levels with external chemicals hampered the understanding of the biological phenomena. This is particularly important when correct knowledge about the fate of inorganic carbon and the bidirectional influences with the biomass on the inorganic carbon is required.

We hypothesized that the hydrogen ion concentration (pH) is the most effective control factor among various conditions such as nitrogen-loading rate, DO, HCO_3^- concentration, HRT, sludge retention time (SRT), and temperature. With inorganic carbon limiting the conditions for nitritation, lower pH levels prevent further ammonia oxidation. Thus, the precisely controlled pH inside the reactor could result in the optimal ratio of NO_3^--N/NH_4^+-N for the next stage of the treatment process. However, this strategy does not necessarily guarantee total nitrification until nitrate since no external source of alkalinity is included (see Chapter 1). HCO_3^- is not a limiting substrate for nitrite oxidation by NOB. The problem is to achieve the stoichiometric HCO_3^- quantity necessary for the AOB to completely oxidize the ammonia. To avoid nitrite build-up, additional decisive factors controlling the activity of AOB and NOB should be verified. For this purpose, the selective enrichment of AOB and AOB was conducted at infinite SRT, the highest nitrogen-loading rate possible, and without limitations of DO.

3.1.2   Complete biomass retention effect

Besides HCO_3^- limitations and avoiding nitrite build-up, a long SRT is also necessary to operate a stable and effective total nitrification process due to the slow growth rate of AOB. With regard to a high SRT, different complete biomass retention technologies have been used in the recent years (Bae et al., 2014; Udert and Wächter, 2012). Complete biomass retention is an advantageous technique because with complete retention (high SRT), a high concentration of biomass can be reached. Fixed-growth technologies and bacteria agglomeration in a biofilm can make nitrifiers more resistant to inhibitory substances and to the variations of operational conditions (Bassin, Dezotti, and Sant'Anna, 2011). Fro the reactor design point of view, the complete retention simplifies the management of wastewater treatment by solving operational problems including fouling, channeling, reduced mass transfer and high head loss (Bassin, Dezotti, and Sant'Anna, 2011; ROUSE et al., 2004). Finally, a long SRT favors the development of a selectively adapted microbial community structure for nitrification (Rusten et al., 2006). The nitrogen conversion rate of total nitrification largely depends on the biomass concentration of AOB. In this respect, the efficiency of a

MBR could be significantly improved by enhancing the bio-flocs produced inside the reactor (Lim et al., 2011; Machdar et al., 2018).

Acclimation goal and start-up

For the reasons discussed before in the literature review section, (see 1.2) start-up is the most challenging step when operating biological nitrification of source-separated urine. It is desirable to minimize the time required to establish a stable nitrifying biomass (Fumasoli et al., 2016; Udert and Wächter, 2012; Young et al., 2017) without jeopardising treatment goals for the specific kind of wastewater to be process. Acclimation strat-up also depends on the chosen BNR technique. For some authors like Udert and Wächter (2012) who worked with a MBBR, it is important to have a longer start-up period with very low and gradual increase in NLR. The contrary will cause instability in the system with high NO_2 concentrations causing process inhibition (Rusten et al., 2006). According to these authors, it is crucial to enhance the bio-floc formation. For this purpose, some technical and operative conditions must be optimised, such as the control of the Fed to micro-organism ratio (FM), the SRT and the NLR imposed to the reactor.

The inoculum type and quality are equally important because classical sludge from Activated Sludge Processes (ASP) can not be adapted in its normal state to such high concentration of nutrients and salt found in source separated urine. For some authors, the biomass acclimation strategy is different for the start-up of a urine nitrification process. Edefell (2017) suggested that the incoming urine solution should be highly diluted and then gradually increased in strength to give the bacterial population an opportunity to adapt to the substrate in a MBBR. However, Udert and Wächter (2012) found that by feeding with undiluted urine, it is possible to reach $270 \, g_N.m^{-3} \, d^{-1}$ in a hybrid membrane aerated biofilm reactor at pH 7.

Regarding the salt content, (see section 2.1) Cui et al. (2014) and specifically acclimated freshwater microorganisms to relatively low saline wastewater, Rusten et al. (2006) discovered that with higher salinity, (relative to freshwater) the start-up stage takes significantly longer. Also, they determined that nitrification rate reaches 60% of a similar freshwater system when the salinity is 21%-24%.

In summary, a controlled and gradual increase of NLR seems to be an appropriate strategy for acclimating biomass. In all of these approaches, nitrification rate is expected to be very low at the beginning and then an adaptation of bacteria culture may occur. The ratio between the food (nitrogen) to microorganisms F/M could be controlled by decreasing the inlet rate. In the beginning of the acclimation process, there is not enough biomass to face this high nitrogen load because nitrifying biomass content in the inoculum is low. Even with typical values of NLR encountered in CAS, bacteria will need time to adapt to high nitrogen concentrations and growth.

3.1.3 Applied acclimation strategies

This section concerns the investigation and optimisation of the start-up and operation of an MBR for urine nitrification based on previous research (Edefell, 2017; Fumasoli et al., 2016; Udert et al., 2003a; Udert and Wächter, 2012). Given the context presented in Chapter 1, the most challenging stage in BNR of high-strength ammonium wastewater is the start-up of the acclimation process. The nitrification process must be carried out in conditions where inhibition can potentially occur after ammonium and/or nitrite is accumulated in the reactor. As it was presented in chapter

1, pH is one of the indicators for the inhibition that must be examined. Furthermore, if the start-up conditions are not appropriate, loss of biomass or instabilities could occur which might restrain the nitrification efficiency (Jubany et al., 2008). This particular situation might unfold when the nitrogen loading rate (NLR) is higher than the MNR as described by Carrera et al. (2003).

Biomass acclimation was achieved by other authors in different technologies as MBBR, SBR and membrane biofilm reactors. Specifically for MBR systems, only Sun et al. (2012) achieved nitrification in this kind of reactors, but treating synthetic high ammonium content wastewater. In our particular case of a MBR treating source separated urine, the optimal acclimation protocol has to be defined. The scientific questions that will be investigated here are:

- Is it possible to link in a reliable way the pH variations to the acclimation degree of the biomass?

- Is this acclimation directly related to the applied NLR?

- Are there differences between biomass acclimated via chemical control of pH or via the inlet urine flow control?.

- Which are the best conditions to handle the source separated urine, to obtain a stable effluent from the reactor?

For these scientific questions some technical challenges have to be tackled:

- The origin and the quantity of AS inoculum to be used in order to treat yellow wastewater in the specific MBR conditions;

- The degree of ammonification of the urine fed to the reactor, thus the storage time and conditions of the source-separated urine.

- The urine dilution factor to achieve a controlled NLR.

- The best pH set range to obtain a stable quality effluent and a self-controlled MBR operation during acclimation.

In order to address these issues, two different approaches for reactor start-up were assessed:

1. The first one is using a progressive increase of the NLR. The fresh inlet urine has been diluted initially by a factor 20. The pH inside the reactor is controlled with the wastewater inlet flow (section 3.2);

2. The second one is also using a progressive increase of the NLR. The urine was stored before injection in order to promote ammonification. The urine was diluted by a factor 5 to keep a higher TN concentration value (section 3.3).

In both cases, automatic feeding control via the Programmable Logic Controller (PLC) allowed to reach the desired pH range in the reactor while regulating operational conditions as a function of inlet flow and HRT

The following sections present and describe the results and the conclusions of these experimental campaigns.

All the experimental data concerning the entire operation (eleven months in total for the two campaigns) of the MBR are available by clicking on the next link for open consultation. The online measured values of DO, pH, temperature and conductivity are presented daily for all the presented operational time-set.

3.2 Acclimation with fresh highly diluted urine

3.2.1 Introduction

Following the different possible strategies to acclimate biomass and in order to find the most reliable and stable start-up and operation protocol, one lab-scale MBR was operated in the ICube laboratory. The first objective is to acclimate biomass to treat and stabilise yellow wastewater. The second objective is to use the experimental data from the pilot and the acclimated biomass to calibrate the biokinetic model presented in chapter 2 (see Chapter 4).

In order to achieve this objective, it is necessary to identify and avoid the main causes of pilot's malfunctioning or inhibitory conditions to the biomass. To avoid the inhibition, a proper start-up strategy should be developed. A detailed analysis was presented in section 2.1 about this subject. Different inhibitors were indicated such as FNA and FA (Svehla et al., 2014). Although the inhibitory effect of FA on NOB has been widely reported (Balmelle et al., 1992; Philips, Laanbroek, and Verstraete, 2002), it has been proved that AOB, even being inhibited by FA, has some activity at pH below 5.5 (Fumasoli, Morgenroth, and Udert, 2015). It should be pointed out that these acid-tolerant AOB are from a different strain than at nearly neutral pH.

The main point to be retained from section 2.1 is that growth rates differences between AOB and NOB can lead to FNA accumulation: this represents the main cause of inhibition in the system (Udert and Wächter, 2012). We know now that the principal causes of this malfunctioning or disturbance in the biological activity are the pH and the temperature.

Eventually the nature and the concentration of the raw waste water to be treated has a high importance too. For source separated urine, the causes for pH limitations has been discussed widely by different authors (Fumasoli et al., 2016, 2017; Udert and Wächter, 2012; Van Hulle et al., 2010; Wett and Rauch, 2003). For a classical ASP, nitrification is usually performed in the range of 7.5–8.5 (Balmelle et al., 1992; Sharma, Ganigue, and Yuan, 2013). A high nitrogen content wastewater (yellow wastewater) contain less alkalinity than the one required for total ammonium nitrification. Thus, the optimal pH value for nitrification could be affected by the degree of ammonification of the yellow wastewater (see Section 1.2). This optimal pH (as a particular set-point or as a range) could be successfully controlled by adding external alkali compounds as shown in different studies presented by Sun et al. (2012) or Jacquin et al. (2018). The last one was also conducted in the framework of the CARBIOSEP project and the acclimated biomass characterised in the Appendix B by the author of this thesis. This external chemicals addition will also supply the necessary additional alkalinity to complete ammonium oxidation. Our project, on the other hand, is looking for controlling pH by the yellow wastewater itself and not adding external chemicals. In order to carry out appropriate start-up conditions, the

impact of pH dynamics and the origins of these dynamics are investigated in this experimental work.

For this first pilot-scale trial, it was first decided to evaluate the potential influence of specific factors on the operation of the MBR and more precisely over the pH dynamics inside it. The idea is to assess the most known factors identified by others researchers (Coppens et al., 2016; Cui et al., 2017; Edefell, 2017; Fumasoli et al., 2016; Jacquin et al., 2018; Olofsson, 2016; Rieger, 2013; Udert et al., 2003b; Udert and Wächter, 2012; Young et al., 2017) and particularly the suggestions of the VUNA project (Etter, Udert, and Gounden, 2014). This will help to investigate the reproducibility and the influence of those factors under the particular conditions of our system (*i.e.* volume of the reactor, type of filtration, type of technology, non external chemicals addition, etc...). The biomass quantity and the procedure to inoculate the reactor, the concentration of urine in the inlet, the dynamics of the pH following the set-range imposed to the PLC, were the three main factors to be investigated in our MBR.

3.2.2 Material and Methods

Pilot-plant description

A MBR with the characteristics presented in table 3.1 was operated as a semi-continuous reactor ruled by an on/off control strategy for feeding. Aeration by a membrane diffuser at the bottom of the reactor is ensured permanently (only stirring/mixing technique in the reactor).

TABLE 3.1: MBR lab-scale pilot description.

MBR volume	34 L
Pore size	0.04 µm
Membrane area	1.5 m²
Desired HRT	30 h
Input	Source-separated urine
SRT	Infinite
pH control	Inlet flow

The treatment process layout is presented in the figure 3.1. Its first element is a 400 L urine storage tank. Urine dilution with tap water was performed in this tank. It was refrigerated at 6°C. From this tank, a peristaltic pump (MasterFlex LS Economy Drive) allowed to feed the MBR aerobic reactor at $350 \, \text{ml min}^{-1}$ flow-rate. The biomass was kept inside the reactor as the biomass separation was performed by an ultrafiltration membrane (complete sludge retention).

The first experiment ran for 5 months. The reactor was equipped with DO probe (WTW Oxi 340i CellOx 700), a pH probe (WTW SensorLyt® ECA 109 117) and a temperature sensor. They were connected to a PLC (SOFREL S500) which actuated as a closed loop pH controller within the reactor as follow: The pH was measured every 25 seconds and the process computer activated the influent injection pump if pH was under the lower pH set-point or deactivated input pump if pH was above the high set-point. During pumping, the pH increases due to the alkalinity of the urine and when pump is stopped, the pH decreases due to nitrifying activity of AOB. The PLC is linked to a computer which was in charge of monitoring and recording the key process parameters (DO, pH, temperature, flow-rates and conductivity). The
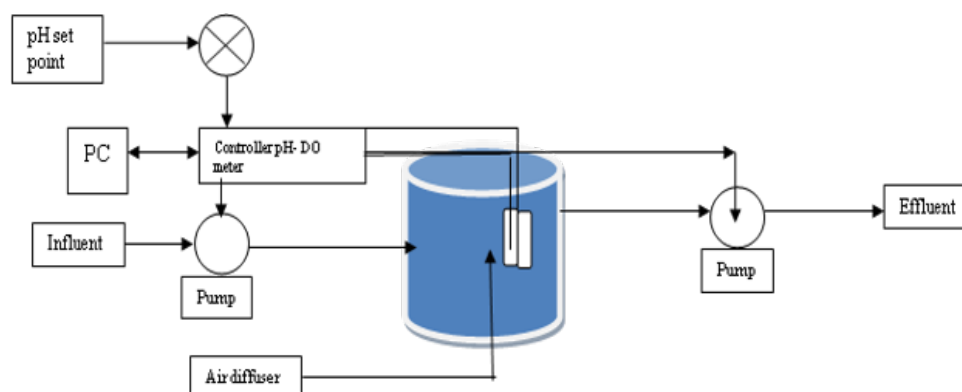
FIGURE 3.1: MBR pilot scheme

reactor was aerated by an air compressor which was fixed at 0.4 bar through an air-diffuser placed at the bottom of the reactor. The DO fluctuated between $5\,g_{O_2}.m^{-3}$ to $9\,g_{O_2}.m^{-3}$ depending on the inlet compressed air pressure, adjusted in function of the solids retention inside the reactor.

In order to prevent inhibition by temperature, knowing that it cannot be controlled in our laboratory, the pilot was kept indoors at room temperature ($23 \pm 3\,°C$) to reduce the impact of ambient variations. However, during heat waves, indoor temperature could be higher for some days. Therefore a shock in the MBR operation was observed.

The operation of the pilot was inspired by VUNA Project (Etter, Udert, and Gounden, 2014) recommendations in terms of the desired and advised pH range 6.00-6.25. Nevertheless, in order to ensure the impact of this narrow range on the reliability of the pH probe to detect small changes and evaluate the overall dynamic of the system, we decided to enlarge this pH range from 6.20 to 6.50 at the beginning. It was then decreased over the time. To better understand the influence of the inlet characteristics, the feeding started with an urine diluted 50 times with tap water and this dilution factor was decreased over the time (lowest value 16 times).

All nitrogen species in the influent and effluent were measured three times per week. The NLR was changed according to the behaviour of the reactor: increased if the percentage of nitrification was satisfactory or decreased if undesirable compounds concentrations raised (e.g. FNA concentration peaks).

Inoculum

To acclimate biomass, sludge from a municipal WWTP was used to inoculate and start the reactor. The inoculation method used in this first campaign did not exactly follow the VUNA (Etter, Udert, and Gounden, 2014) guidelines, as in their case the MBBR was inoculated with diluted AS. For our MBR, inoculum was 100% activated sludge taken from the WWTP and was not diluted. The idea was to start from more concentrated biomass in order to decrease start-up time and also to better assess biomass activity. The inoculum sludge was sampled in the Strasbourg WWTP performing nitrification/denitrification and carbon removal of the domestic wastewater of the municipality. Its characteristics are described in Table 3.2.

Diluted urine characteristics

Urine was collected from an urinal that was set-up in our laboratory. There was no flush in order to collect pure urine. Therefore, it consisted only of male urine.

TABLE 3.2: Composition of inoculum sludge for the first campaign.

Activated sludge liquid	34 L
Tap water	0 L
Urine (nitrogen source)	Dilution of 50 times
MLSS	4318 $g_{MLSS}.m^{-3}$
MLVSS	3520 $g_{MLVSS}.m^{-3}$
$OUR_{endogenous}$	0.3244 $g_{O_2}.m^{-3}h^{-1}$
$OUR_{exo,max}$ for nitrification	5.88 $g_{O_2}.m^{-3}h^{-1}$
pH	7.66

Source-separated urine was stored at 6 °C in the 400 L tank to equalize and also control the dilution ratio. The mean values of the principal characteristics of diluted urine over the 155 days of operation are presented in table 3.3.

TABLE 3.3: Diluted urine average characteristics during all campaign (mean values and relative standard deviations, n=55).

pH	7 ± 0.3
NH_4 (mg/L)	150 ± 114
NO_2 (mgN/L)	0,2 ± 0.31
NO_3 (mgN/L)	0,04 ± 0.1
TKN (mg/L)	307.5 ± 175
NH_4/TKN	0.5 ± 0.25
χ (μS/cm)	948 ± 205
O_2 (mg/L)	5.8 ± 0.8
Alkalinity (mg $CaCO_3$/L)	983 ± 546

The urine was fed to the mixing tank within 24 hours after recovering it from the source separation system. The initial idea was to feed the system with almost fresh urine in order to evaluate the fate of urea hydrolysis occurring inside the bioreactor on system performance. This allows to evaluate the necessity to have or not this equalization/storage thank for the real scale application. The storage tank temperature of 6 °C was chosen in order to minimize urea hydrolysis as this tank was here only used to store urine: the hydrolysis should happen mostly inside the bioreactor.

Analytical methods

Triplicate samples of the sludge mixed liquor were grabbed weekly to measure suspended solids (MLSS) and volatile suspended solids (MLVSS) concentrations following standard methods (Apha, 2005).

Samples from the inlet feeding urine tank and the permeate outlet of the reactor were taken 3 days per week. They were analysed by ionic chromatography (Metrohm, Switzerland) to determine the concentrations of anions and cations of interest (ammonium, nitrite, nitrate, chloride etc...). TKN was measured after selenium mineralization and distillation (ISO, 1984). These measurements were essential because in the fresh urine the nitrogen is mainly present in form of organic nitrogen urea, which cannot be detected by ionic chromatography analysis.

COD values were measured using Micro tubes test kits NANOCOLOR Test 0-29 06.18 COD 100 $g_{COD}.m^{-3}$ to 1500 $g_{COD}.m^{-3}$ to confirm the correct overall carbon removal. The reference method is the ISO 15705 (November 2002) and according

to Rodier, Legube, and Merlet (2016) chloride is the principal interference for the measure, at concentrations above 1000 mg/L.

3.2.3 Results and Discussion

The next paragraphs present the results of the first campaign carried out with the pilot MBR designed in ICube laboratory. First, the impact of the urine inlet dilution ratio is analysed. Then, the overall nitrification yield and the effluent quality are discussed. Finally, the biomass acclimation according to a series of operational parameters is investigated. These parameters derive from the evolution of the semi-continuous regime controlled by the pH range set values: HRT and NLR mainly.

It is important to keep in mind the semi-continuous operation regime in the system: the NLR calculated from equation 3.1 represents the equivalent of a daily inlet flow (Q_{in}) calculated from the quantity of batches feed per day. $N_{Kjeldahl}$ represents the inlet TKN concentration for the particular day and the volume of the reactor was eventually constant over time (no volume change means that no fouling phenomena during the operation time was detected).

$$NLR = \left[(N_{Kjeldahl} * Q_{in})/(V_{reactor} * 1000) \right] = \left[\frac{mg/l * l/day}{L} \right] = \left[\frac{kgN}{m^3 day} \right] \qquad (3.1)$$

To analyse the factors that influence the NLR calculated from equation 3.1 let us first take a look at the inlet characteristics: highly diluted urine with the shortest as possible storage time after source separated collection.

Inlet urine dynamics

Variations of nitrogen inlet concentrations are presented in figure 3.2. Obviously, the organic nitrogen variations are important in the source separated urine as a function of his origin and storage time. Even if the urine was highly diluted at a constant ratio for a long period of time as shown in the figure 3.3, variations were really important in terms of nitrogen, ammonium, total alkalinity (and also pH).

Thus, the additional alkalinity contribution and the dilution effect of tap water are not the source of these variations. This shows clearly why urea hydrolysis dynamics in the urine is the parameter that affect the most the characteristics of the urine to be treated. If this is evident for a high urine dilution operation, it highlights the fact that working with less important dilutions and more concentrated urine, the effect will be even more important.

One interesting phenomenon that can be observed and discussed from the figure 3.3 is that the NH_4/TKN ratio was decreasing all over the experimental campaign even if the dilution was constant. This means that the urea present in the source collected urine was less and less hydrolyzed. The proportion of organic nitrogen over the free ammonia is not stable and increase slightly over time, even if the urine dilution rate is constant. This could be explained only by the storage conditions of the collected urine before being mixed with water, that changes abruptly every time that the storage tank is filled in not regular periods. This lead us to think that the best way to handle this variation could be to establish a same storage time for the source-separated urine before being mixed with tap water in the tank. Also this mixing should be dome at regular periods to not perturb directly the MBR performance. Storage time of source separated urine before mixing with tap water is the most

important parameter that influences the inlet characteristics and not only the tap water dilution ratio.
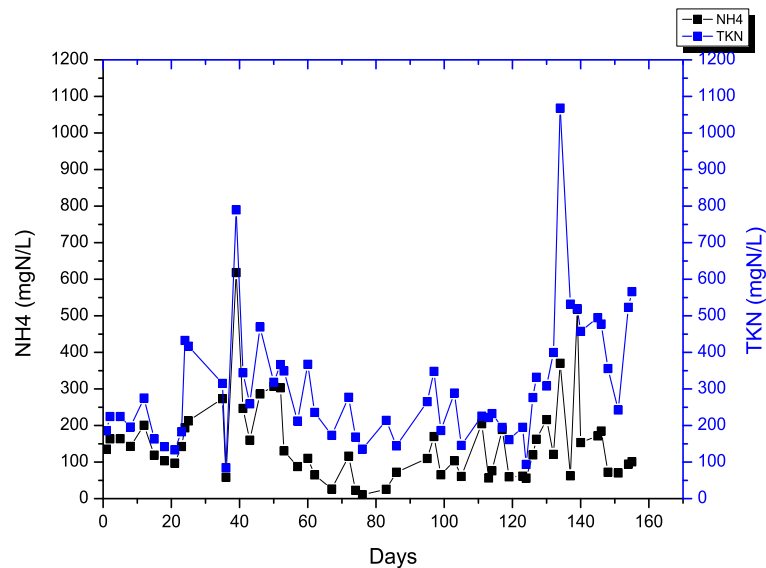
FIGURE 3.2: Inlet urine TKN and TAN evolution over time of the first campaign

Ammonia conversion efficiency

The quality of the effluent is presented in figure 3.4 in terms of nitrogen species. Here, every change in the operational pH set range in delimited by a continuous black line, as it is the case for the others figures in this section.

From this figure, one can observe two operational days where a nitrite accumulation was detected at days 40 and 100 (shown as A and B in the figure). Also, accumulation of ammonium was observed during startup, in particular at days 35-40 with a very important peak (C in the figure).

After the first nitrite peak (point A in the figure), reactor was washed out (by taking out permeate continuously without any feed and then completing the volume with tap water) to reduce nitrite content by at least 50% and let the biological nitrification do the remaining work. When the second peak (point B in the figure) occurred, the reactor was again washed following the same procedure. The pH operational set range was also decreased to reduce the quantity of diluted urine injected to the reactor at each feeding event. When the nitrification conditions were stable, the pH range was finally set to the one reported by Etter, Udert, and Gounden (2014), but few days latter a new nitrite peak was observed and the pilot was stopped.

During the first 100 days, the pH set range was constant between 6.2-6.5: the quantity of urine for each batch feed to the reactor was probably too high. In fact, the necessary quantity of urine to rise the pH to 6.5 is mainly dependent of the inlet urine alkalinity. As presented in the figure 3.3, both alkalinity and TKN varied a lot: the risk of injecting too much ammonium in the reactor is potentially higher. This is evidenced in figure 3.7: during this first 100 days period, the variation of HRT and NLR is more important than in the other two operative ranges. This could be the cause of such an important quantity of nitrite present in the first operative days, as well as the remaining ammonium concentration. This indicates a off-tuning of
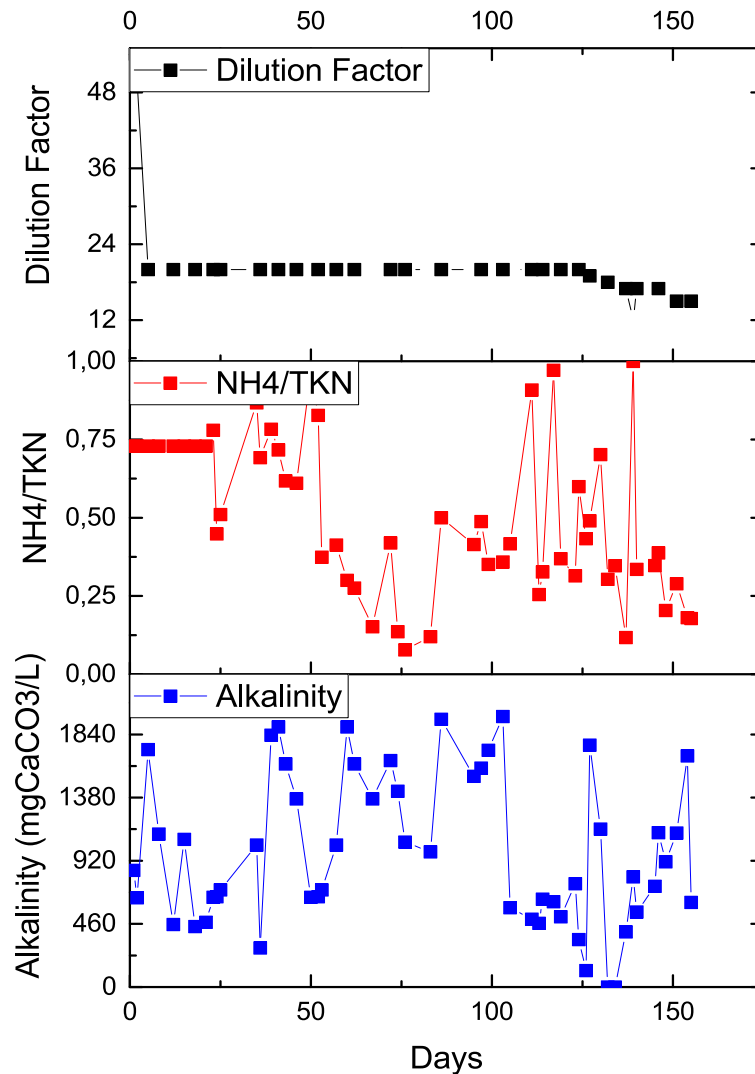
FIGURE 3.3: Effect of the inlet urine dilution over the NH_4/TKN ratio
and Alkalinity evolution over time of the first campaign

the AOB activity, that potentially need to handle punctual and too high ammonium loads.

By decreasing the pH operative set values, HRT seem to find more stable values but once again the variations in the incoming TKN lead to abrupt changes in the NLR.

Nevertheless, the effluent ammonium/nitrate ratio was constantly increasing over almost 45 days, the nitrite concentration varied to a less extent (figure 3.4), as well as the nitrification yield (figure 3.5).

For the final operative days, the pH operative set was adjusted to the desired range with a 0.05 units variation. The PLC continued to work for few days and then the reactor was stopped when nitrite content increased again. During these last operative days, the produced effluent had a stable ammonium/nitrate ratio of around 1:1 but the instabilities due to the presence of nitrite were also very clear. Thus as a conclusion, a stable effluent could be produced but with a very high risk of nitrite build-up that will affect NOB activity.

The overall nitrification yield over time is presented in Figure 3.5. The mean
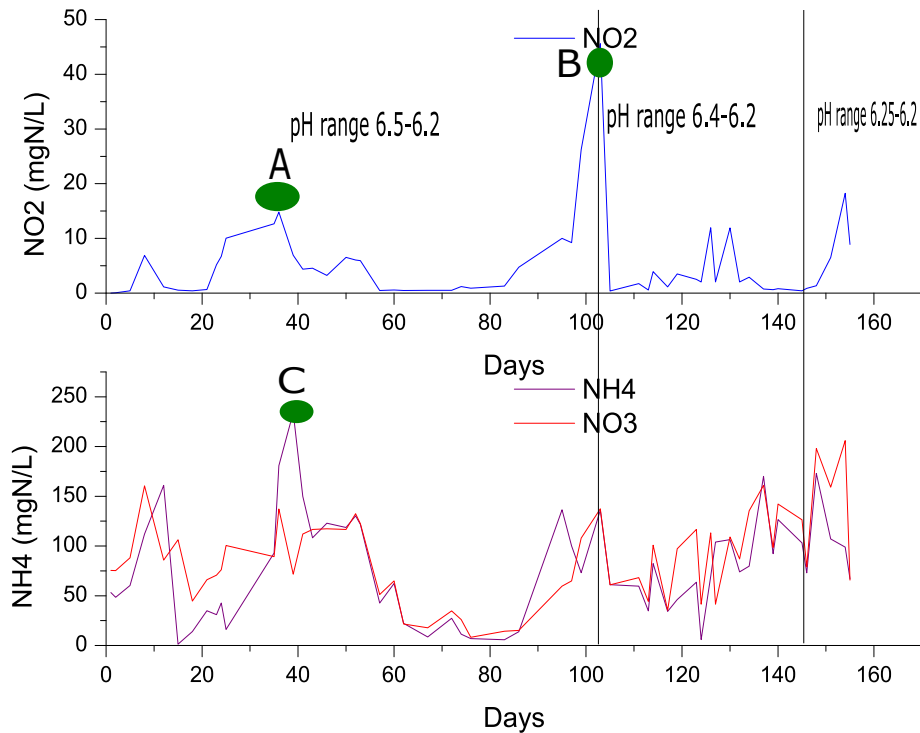
FIGURE 3.4: (a) NO_2, (b) NH_4 and NO_3 concentration in the outlet over time of the first campaign

value (53%) was expected for a yellow wastewater with alkalinity limitation problems for total nitrification (Udert and Wächter, 2012) (as presented in the section 1.1.1).

By analysing the figure 3.5, it can be observed that the variations of the nitrogen conversion efficiency are related with the variation of the NH_4/TKN presented in the figure 3.2.

This analyse could be corroborated by quantifying the outlet organic nitrogen content as presented in the figure 3.6.

The trend of the organic nitrogen presented in this figure is very similar to the one for the couple ammonium/nitrate in figure 3.4. The higher concentrations are present at days 40 and 100, which coincides with the nitrite peaks: the nitrification yield is only about 20%.

Biomass acclimation

The evolution of biomass concentration, as well as HRT and NLR evolution over time are presented in the figure 3.7.

For the first 100 days of operation, the variations of HRT and NLR are way more important and the shock on the biomass is strong. The change of C:N:P ratio from the typical domestic wastewater to urine influent, produce an impact on the biomass concentration after 20 days. Most likely the heterotrophic bacteria population is drastically decreasing. After that period, NLR starts to increase very fast. From day 35, the inhibitory influence of the increased NH_4 concentration (showed in figure 3.4) and the direct shock in the biomass decay is clear. Since no nitrite accumulation was observed, the decrease in the MLVSS could be related to the AOB bacteria impacted by ammonium accumulation and also the normal heterotrophic decay expected during the acclimation period.
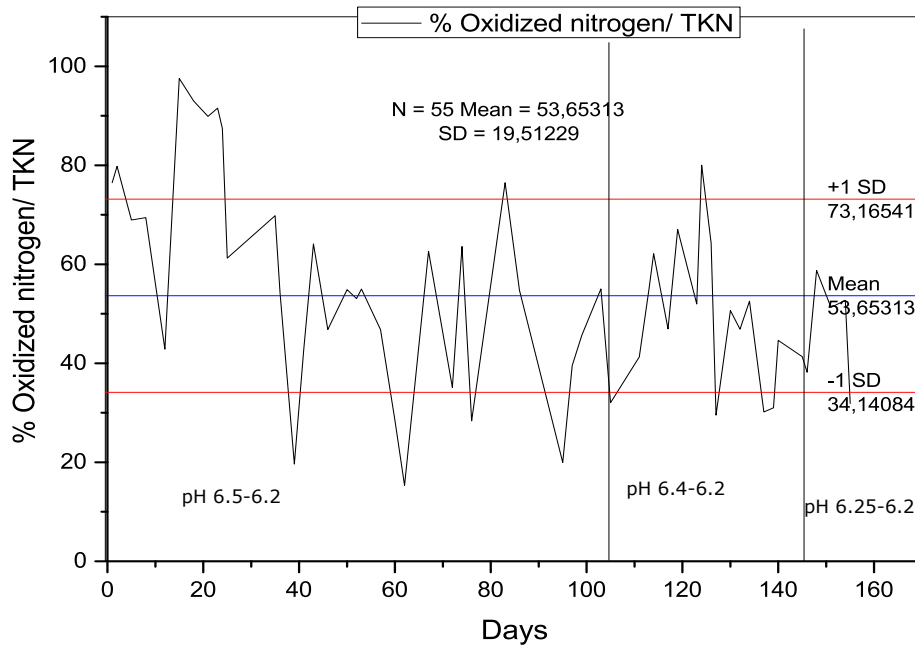
FIGURE 3.5: Nitrification yield evolution over time for the first campaign
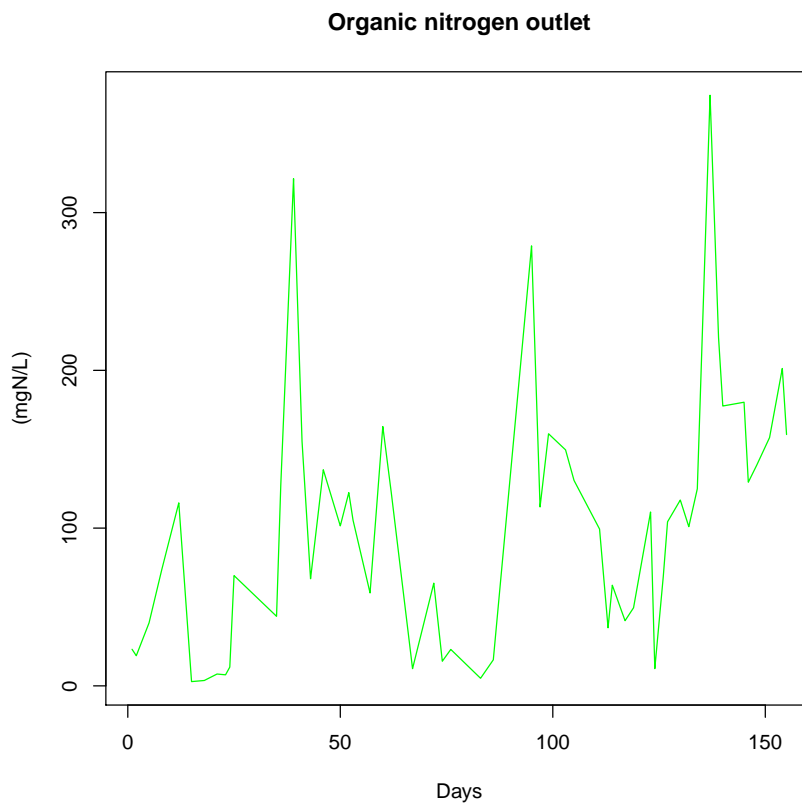
FIGURE 3.6: Remaining organic nitrogen in the outlet of the first campaign

Biomass acclimated better during the second pH operative range set as MLVSS increased almost by a factor 3 during 45 days, keeping low concentration of nitrite
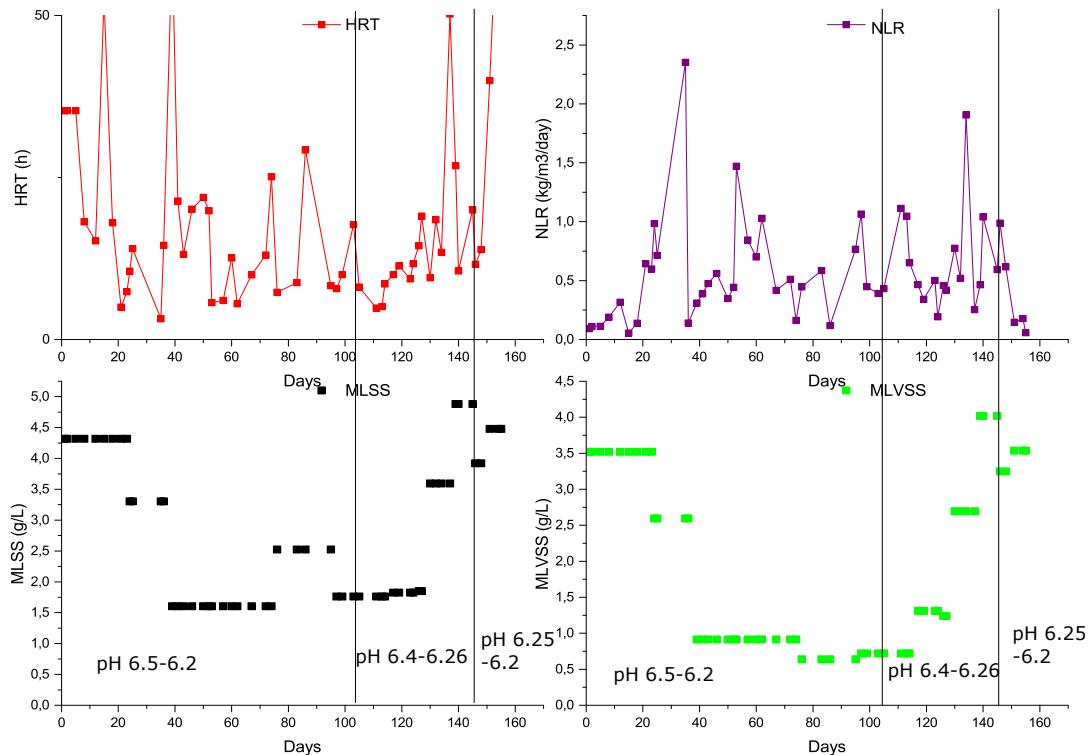
FIGURE 3.7: (a) ALR, (b) HRT , (c) MLSS and (d) MLVSS in the MBR over time of the first campaign

and producing a constant ammonium/nitrate ratio in the outlet (see Figure 3.4).

Since the first nitrite peak at day 40, it took more than 100 days to recover more or less the initial concentration of biomass (MLVSS), which makes us consider that dilution of urine in the acclimation campaign leads not only to instabilities in the MBR operation, but also that this strategy yields long acclimation periods.

MBR dynamics

The figures in the appendix D present the total campaign data of the four online measured variables: DO, pH, temperature and conductivity over the six months of operation of this first campaign. The first days corresponding to the inoculation time are not presented. The first operative day presented when the PLC start governing the urine inlet flow control. The figure 3.8 present an example of the evolution of pH during the first operative days of the MBR (first operative day 04-12-2018).

From the figure 3.8, for every single operative day, we can highlight the maximum and the minimum pH, thus the number of defection points of the pH dynamics curve can be derived (corresponding to feeding events). The beginning of the on/off feeding strategy can be distinguished. At the day-scale, the number of feeding events progressively increased. For these first days of operation, the pH range was 6.2-6.5 as explained in the last section. The figure also allows us to interpret qualitatively pH dynamics for the first month and invite us to analyse quantitatively this pH dynamics. The aim is to check its relation to the quantity of urine fed to the reactor (HRT) and thus the nitrogen load (NLR).

influence of pH dynamics over NLR and the HRT

For a particular operation day, pH dynamics behave as shown in figure 3.8.
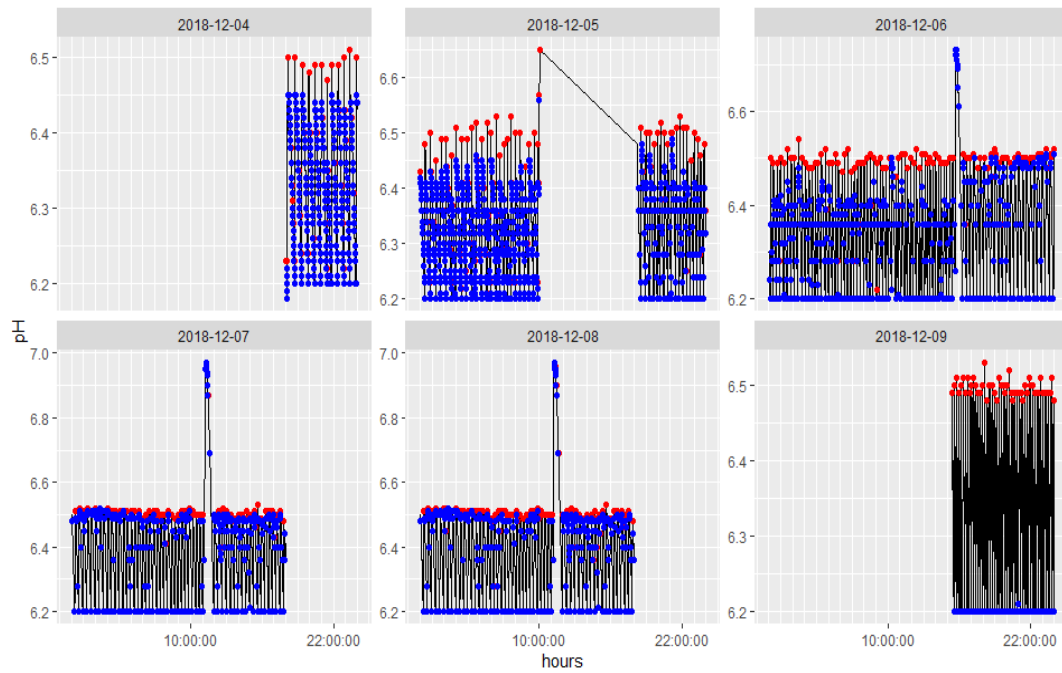
FIGURE 3.8: Maximum and minimum values identification for pH
dynamics of the first campaign
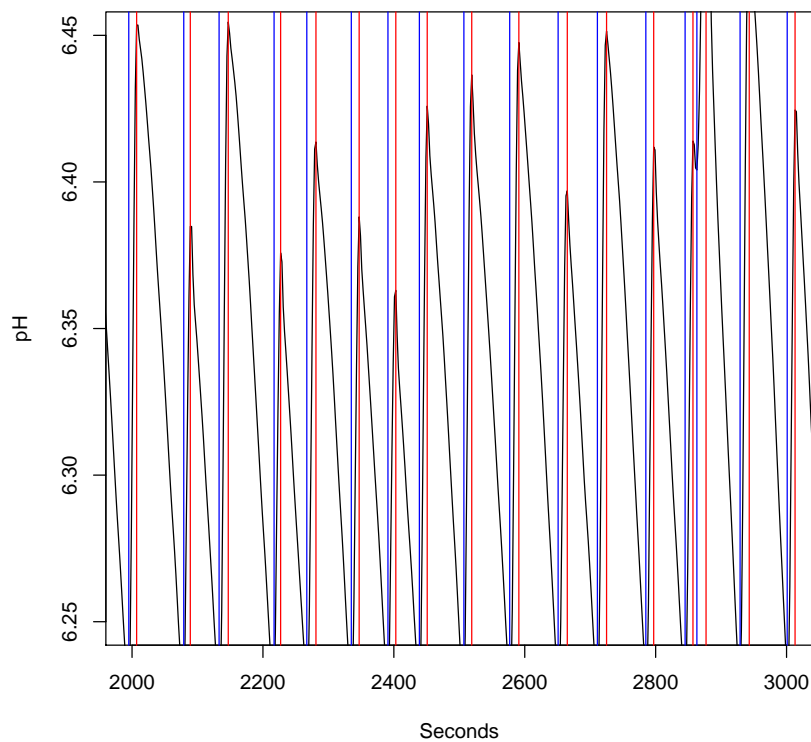
FIGURE 3.9: pH dynamics example during reactor start-up of the first
campaign

As expected, pH increased when pump starts to inject urine until the maximum pH set value (in red scatter). This is due to the inlet alkalinity that increased the overall pH inside the reactor. When the high pH set-point (6.5) is reached, the pump stops. Then, due to biological nitrification and specifically AOB activity, pH decreases until the lower set-point (6.2) (in blue scatter) where the PLC triggers the influent pump again. The balance between these two phenomena is at the core of pH dynamics understanding inside the system.

In order to quantitatively assess these pH dynamics, the derivative of pH evolution over time was calculated. The figure 3.9 allows to identify every maximum and minimum from the signal response of pH. Due to the high data quantity available (online monitoring during five months), the derivative of pH was approximated by a straight line and the slope could be calculated for each feeding/nitrification cycle.

For instance, the line between the first minimum and the next maximum point represents the alkalinity effect of the urine increasing the pH. On the contrary the point between the maximum and the next minimum represents the nitrification effect acidifying the medium by proton's production. In other words it is possible to determinate each effect by approximating delta pH as linear variations and calculating the positive (named afterwards "Delta up") and the negative (named afterwards "Delta down") slopes.
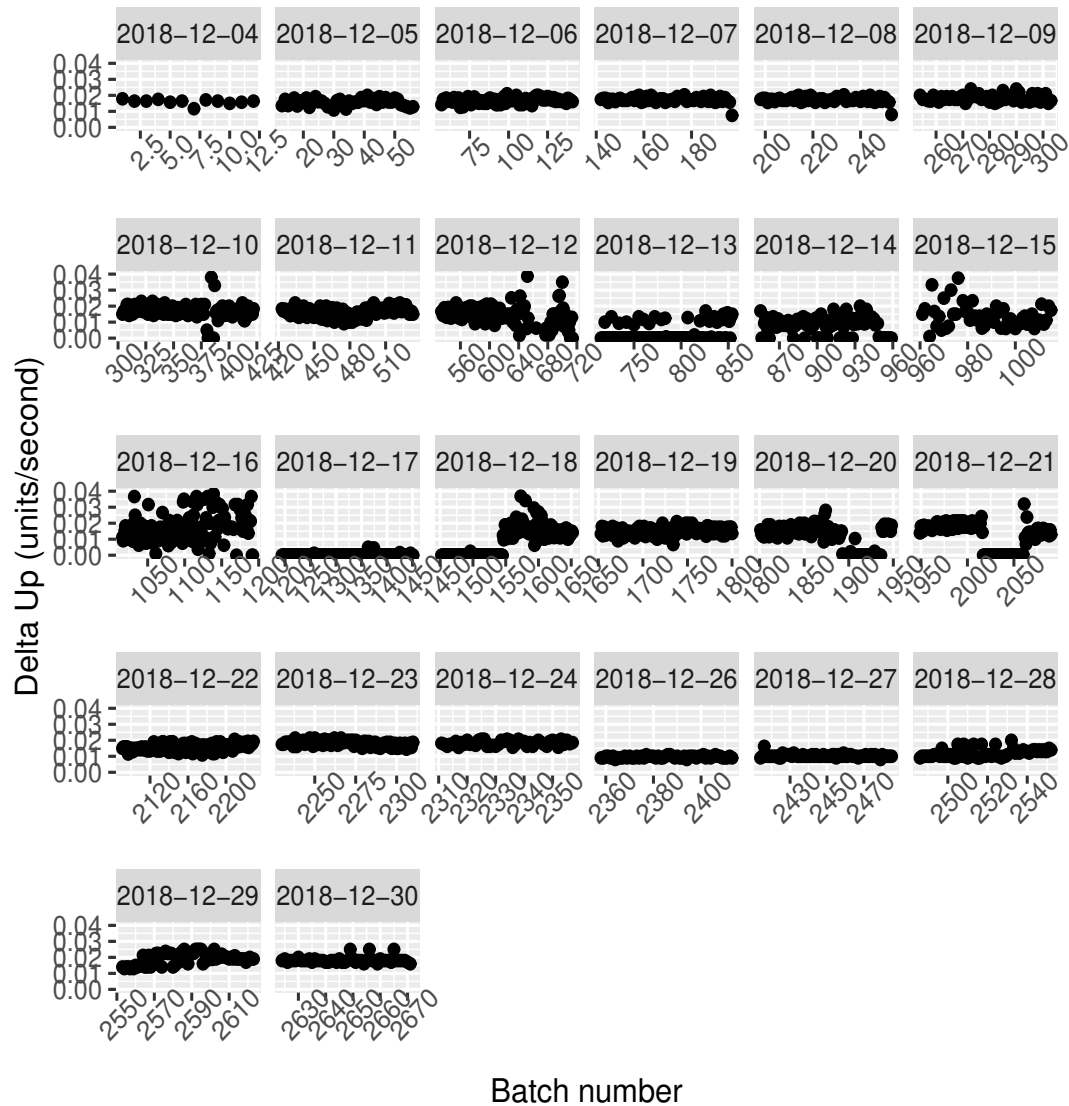
FIGURE 3.10: Delta up pH dynamics over time for the first month of
the first campaign

By evaluating the time derivative of pH value for each batch feed to the reactor
(dpH_{UP}/dt and the dpH_{DOWN}/dt) for each pumping period in each particular operation day, the two phenomena can be quantified over the experimental campaign period. Then, we can link their variation to the real impact on both NLR and HRT. Figures 3.10 and 3.11 help to clearly quantify each phenomena of pH dynamics presented for the each operative day, as the number of batches increase. It could be also presented for the totality of the operative months as in the figures 3.12 and 3.13.
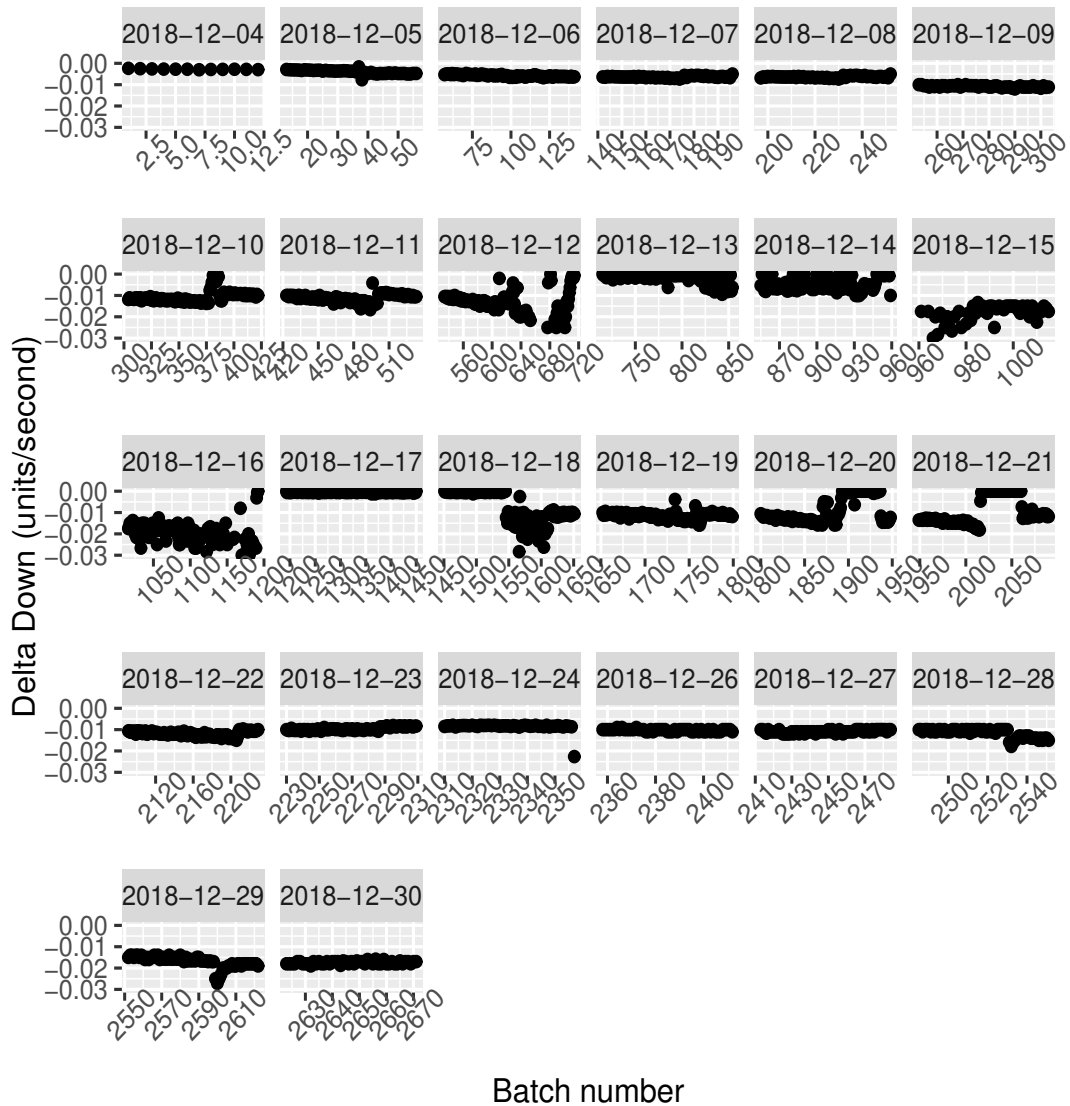
FIGURE 3.11: Delta down pH dynamics over time for the first month
of the first campaign

To enable the interpretation and to identify and differentiate the impact of each phenomena on pH dynamic, the Figures 3.14 and 3.15 were constructed. The Figure 3.14 represent the daily average delta up and delta down of the pH dynamics, all over the total experimental time of the campaign (150 days). As the delta up has no clear trend to analyse, the Figure 3.15 was build to compare and analyse the interactions between the HRT and the daily average delta down for each pH set range used.
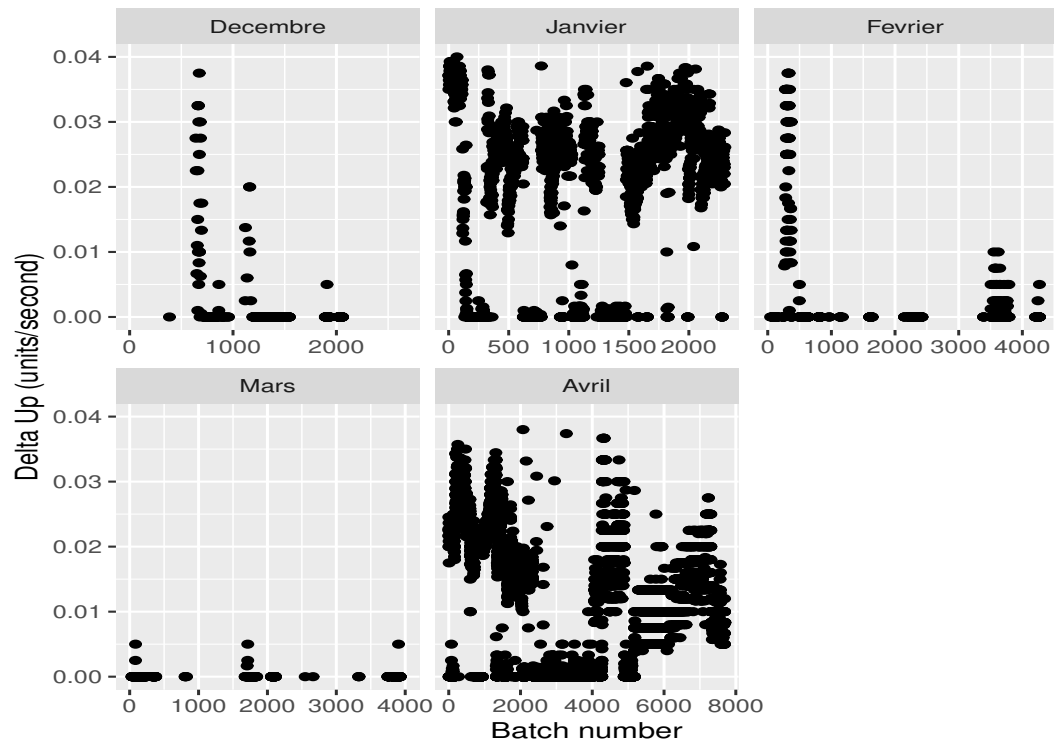
FIGURE 3.12: Delta up pH dynamics over time for the first campaign
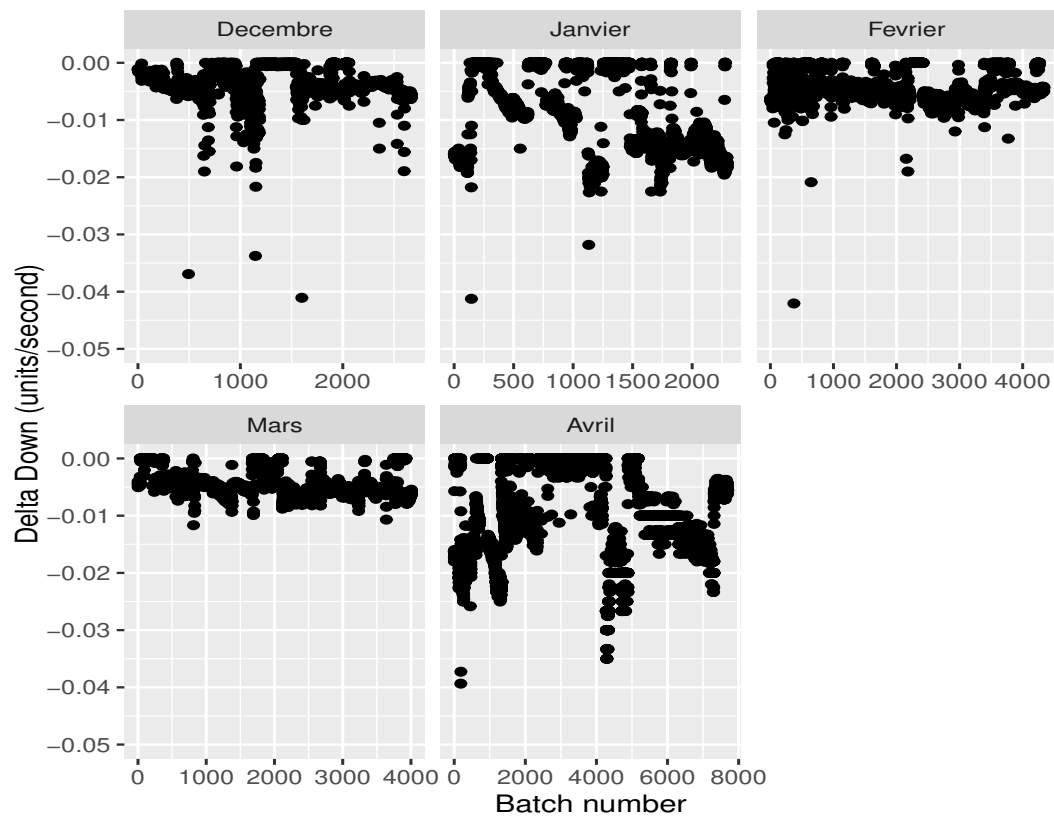
FIGURE 3.13: Delta down pH dynamics over time for the first campaign
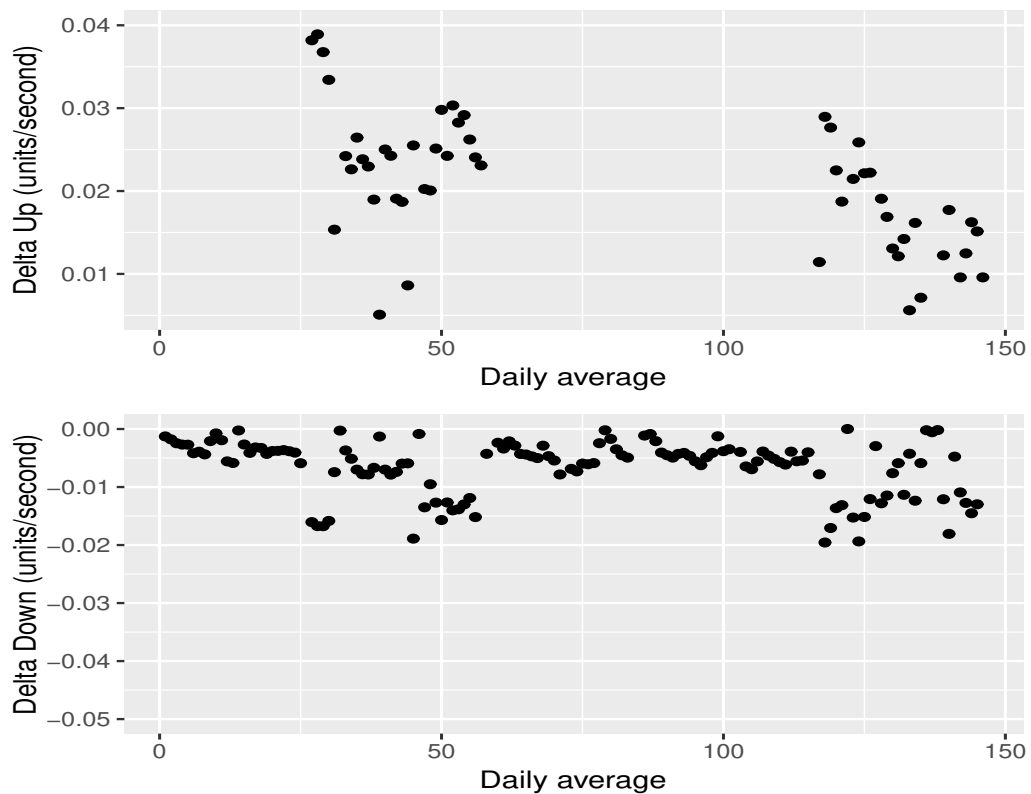
FIGURE 3.14: Average delta up/down pH over time of the first campaign

From the figures 3.14 and 3.15 it can be observed that the HRT is more affected by the delta down (due to biological activity) than the delta up (due to the alkalinity in the inlet). While the delta up remains almost constant for a long period of time (which is normal due to the non variation of the dilution factor over that period), the delta down governed the dynamics of HRT. Eventually, a slight trend is observed but with a lot of dispersion and incertitude.

3.2.4 Conclusion

One strategy to acclimate biomass to a high ammonium content inlet was applied in laboratory conditions. The semi-continuous feeding of the MBR was controlled via a PLC in function of a desired pH set range value. The influent consisted of fresh urine that was highly diluted (dilution factor from 50 to 20). No external chemicals were used to control the pH inside the reactor, only the closed loop strategy controlled by the PLC trigger or stop the feeding to control pH.

Overall, good nitrification performances were obtained with around 50% of ammonia conversion to oxidized form. However, the reactor experienced a lot of instabilities with several nitrites peaks that were detected. The pH set range was adjusted in order to try to overcome these instabilities. The difference between lower and higher pH set-points was decreased from 0.3 to 0.05 pH units but instabilities were still occurring.

For this first campaign as urine was highly diluted and the results shows that many perturbances were found: variations of both TKN concentration and NH_4/TKN
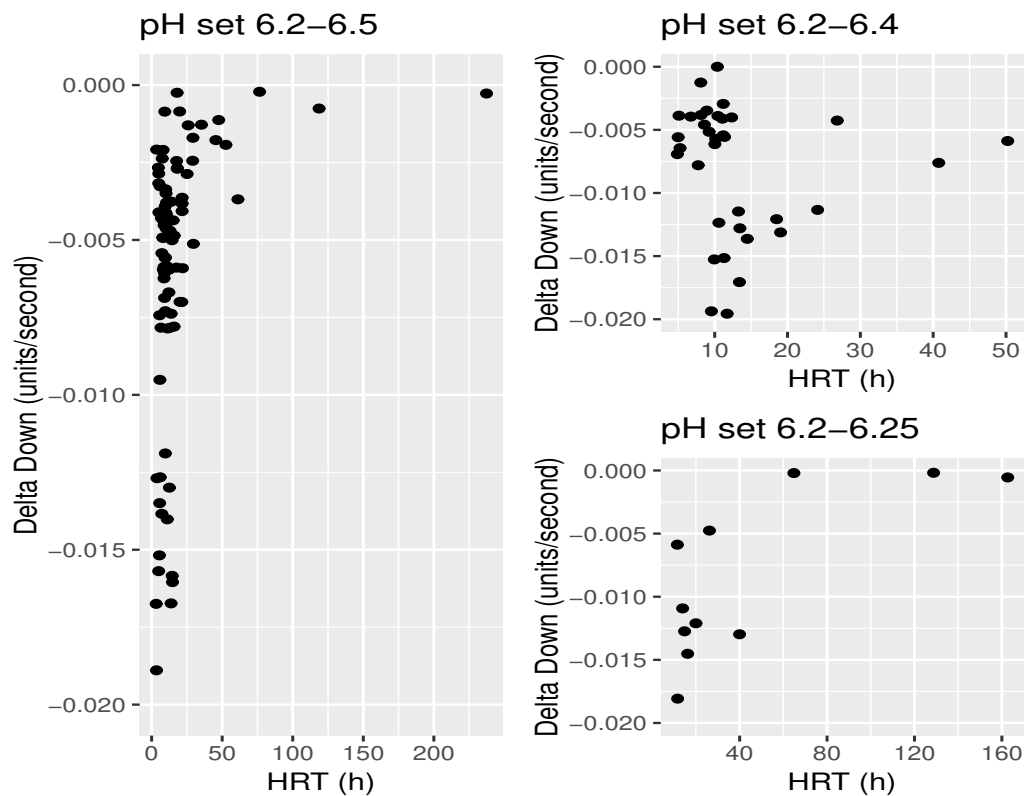
FIGURE 3.15: Average delta down pH vs HRT for each pH range set
of the first campaign

ratio in the inlet, tap-water alkalinity, operational problems... This directly affects the operation in the system, which was difficult to control in terms of NLR.

Indeed, for a given feeding event, the volume of injected urine is controlled by the expected pH elevation due to the incoming urine. However, the high variability of inlet diluted urine properties as well as its variable degree of ammonification induced high variations of inlet alkalinity and pH. Therefore, the NLR was not really controlled here. It was strongly dependent on the urea hydrolysis dynamics in the storage tank. Analysing these pH dynamics, a high variations are observed. It is represented by the high influence over the HRT, that can not hep to optimally control the NLR. This lets the system more open to the presence of nitrite build-up.

Thus, it seems more appropriate to enhance efforts towards a better understanding of ureolysis and other external parameters impacting on the urine characteristics (section 1.1.1) before just focusing on increasing the NLR over time. In other words, its seems more important to ammonify the urine inlet first to better control the nitrogen load in the MBR. A possible solution to better control this urea hydrolysis will be to increase the storage time of urine collected at the source. Nevertheless, another complementary study is necessary in order to optimize this residence time, and try to identify whether or not urea hydrolyse is the rate limiting step of the biological process. Also, increasing the temperature in the equalization tank, in order to have the maximum of ammonium and alkalinity and the lower level of non-hydrolysed urea. This means that the presence of the equalization tank reveals to be necessary for the operation of the real scale reactor, not for urine dilution purposes but to comply urine ammonification time requirements.

In order to improve reactor performance and having these conclusions in mind,

it was decided to operate the reactor with a more concentrated stored urine. The following section presents the results of this second trial.

3.3 Acclimation with concentrated stored urine: EAWAG inspired protocol in Strasbourg (ICUBE)

3.3.1 Introduction

Following the previous experimental campaign, a second experimental campaign was developed following the same principles described in section 3.2. Starting from the lessons and conclusions from the first campaign, one new protocol to acclimate biomass to high nitrogen influent was tested. The main differences are related to:

- the inoculum and the start-up of the system;

- the optimization of the pH range value to operate the reactor;

- the concentration and storage of the inlet urine.

The recommendations of the MBBR VUNA project were followed. The aim is to assesss the reproducibility and the influence of factors conceived for an application in a MBBR under the particular conditions of our MBRsystem (i.e. volume of the reactor, type of filtration, type of technology, non external chemicals addition etc...). The inoculation procedure and the pH range for inlet control were the main focus of this second campaign.

Some causes of reactor malfunction or inhibitory conditions to the biomass were identified in the first experimental campaign 3.2. To avoid inhibition, it is necessary to optimize start-up strategy. It was shown that the nature and the concentration of the raw wastewater to be treated has a high importance too. The yellow wastewater contain less alkalinity than required for total ammonium nitrification even with high dilution with tap water.

As it was proved in the first experimental campaign, urea excess has an impact in the dynamics of HRT and NLR via the biological activity of AOB. The inhibitory conditions observed were linked mainly to the differences in pH dynamics to control the NLR properly. This failure is not detected following pH variations and the system continues to feed and operate normally. However, the pH evolves due to the over activity of AOB bacteria and the NLR increases, leading to frequent nitrite peaks.

To better understand this influence and the consequent inhibitory conditions by the accumulation of FNA, this second campaign also search for an optimal pH range for the nitrification process. This optimal pH was found in literature to be in the range of 7.5–8.5 (Balmelle et al., 1992; Sharma, Ganigue, and Yuan, 2013), but that could change from system to system according to ammonia concentration, type of bioreactor and the application (Fumasoli et al., 2016, 2017; Udert and Wächter, 2012; Van Hulle et al., 2010; Wett and Rauch, 2003).

This optimal value could also be affected as a function of the degree of ammonification of urine (see Section 3.2). The operational objective is to reach an optimal pH (as a particular set-point or a range) without adding external alkali compounds (as performed by Jacquin et al. (2018)): pH should be controlled by the inlet yellow wastewater flow itself. Three different pH values were tested during the 150 days trial to better understand the influence of pH dynamics and the possible origins of this dynamics.

To better control the degree of ammonification of urine, source separated urine was now collected and stored for at least 1 week at room temperature in order to allow as much urea as possible to hydrolyze. The dilution factor of injected urine

was between 3 and 5. This dilution was adjusted to the maximum quantity of source separated urine collected at the time of the experience.

3.3.2 Material and Methods

The material and methods were exactly the same as described in section 3.2. The start-up experiments were performed in the pilot-scale reactor and followed the guidance of VUNA Project (Etter, Udert, and Gounden, 2014). There were three tested ranges of pH during the operation of the pilot; 6.20-6.25 for the first phase, 5.80-5.85 for the second phase and 7.00 - 7.05 for the third phase. The pilot plant is located indoor and operated (60+at room temperature.

Inoculum

Activated sludge was taken from metropolitan Wantzenau WWTP in the region of Strasbourg. It was used to inoculate the pilot plant for the start-up experiments. This WWTP was performing nitrification at the time of biomass collection. The applied NLR 29 $g_N.m^{-3}d^{-1}$ was low compared to the target of our project . This implies that the proportion of nitrifying bacteria was also low in the sludge. However, following the guidance of VUNA project, the inoculation procedure was followed with the indication described in Table 3.4.

The initial urine concentration in the mixed liquor was adjusted to 100 $g_N.m^{-3}$ in order to remain in the same order of magnitude than the domestic wastewater that fed the WWTP.

TABLE 3.4: Composition of inoculation sludge before dilution inside the reactor for the second campaign.

Nitrifying sludge liquid	6.8 *L*
Tap water	27 *L*
Urine (inside the reactor)	Calculated to have 100 $g_N.m^{-3}$
Urine (nitrogen source)	Dilution of 3 to 5 times
MLSS	4074 $g_{MLSS}.m^{-3}$
MLVSS	2634 $g_{MLVSS}.m^{-3}$
$OUR_{endogenous}$	0.36 $g_{O_2}.m^{-3}h^{-1}$
$r_{Nitrogen}$	5.2 $g_N.m^{-3}h^{-1}$
pH	8.5

After the inoculation procedure, pH was 8.5 while the pH range controlling influent pumping was set at 6.20-6.25. It took 24 hours to start running automatically. This delay was due to the low activity of AOB which produces protons when oxidizing ammonium from the urine present in the medium.

Inlet urine characteristics

In order to feed the most hydrolysed urine to the system, the urine was poured to the mixing tank at least one week after recovering it from the source separation system. It was stored at room temperature in plastic bottles during this period.

Then, it was injected and diluted with tap-water within the 400 L tank to equalize and control the dilution ratio. In this tank, the storage temperature of 10 °C was chosen in order to enhance ureolysis kinetics compared to the previous campaign but with a trade-off with bad-smell problems.

The mean values of the principal characteristics of concentrated urine over the 148 operation days are presented in table 3.5.

TABLE 3.5: Urine characteristics (mean values and relative standard deviations, n=36).

pH	8.5 ± 0.3
NH_4 (mg/L)	970 ± 303
NO_2 (mgN/L)	0,009 ± 0,04
NO_3 (mgN/L)	0,11 ± 0,32
TKN (mg/L)	2287 ± 1202
NH_4/TKN	0,523 ± 0,26
χ (μS/cm)	11211 ± 2340
O_2 (mg/L)	5.8 ± 0.8
Alkalinity (mgCaCO3/L)	4147.2 ± 1690

Analytical methods

The analytical methods were exactly the same as described in section 3.2 for measuring nitrogen species, TKN, COD and biomass concentration.

3.3.3 Results and Discussion

The next are the results of the second campaign performed with the pilot-scale MBR built at the ICube laboratory. First, the impact of the urine inlet dilution ratio is analysed. Then, the overall nitrification yield and the quality of the effluent are discussed. Finally, the biomass acclimation according to a series of operational parameters is dissected (HRT, NLR, pH set value).

To analyse the factors that exert an influence over the NLR calculated from equation 3.1, lets take a look first at the inlet characteristics consisting of slightly diluted urine with the maximum possible storage time after source separated collection.

Inlet urine dynamics

The variations in the nitrogen inlet concentration in the diluted urine are presented on figure 3.16. It can be observed that the organic nitrogen variations in the incoming urine are more controlled than with the high dilution strategy implemented in the first campaign (see Figure 3.2). In fact, the concentrations obtained in this new campaign are more or less stable from day 20 to day 50, with dilution factor of 3 and really very stable from day 50 when the dilution ratio was set to 5. The total alkalinity and the ratio NH_4/TKN are also more stable as shown in figure 3.17.

Ammonification was very significant from day 50 (more than 80%). This is due to the fact that the feeding tank was not entirely emptied all over the operation time of the reactor. Therefore, the development of some microbial activity probably accelerates ureolysis in the tank.

To conclude, urea hydrolysis dynamics can be better controlled by enhancing the storage time of the source separated urine either inside the feeding tank, either in another additional storage item that provides at least one week of HRT. This strategy proves to be interesting even for dilution up to 5 to 3 times, which is really close to the real case application of the CarbioSep project.
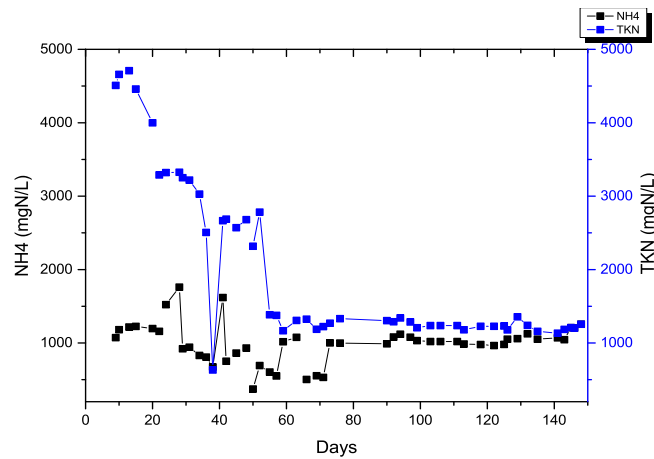
FIGURE 3.16: Inlet urine TKN and TAN evolution in the diluted urine over time of the second campaign
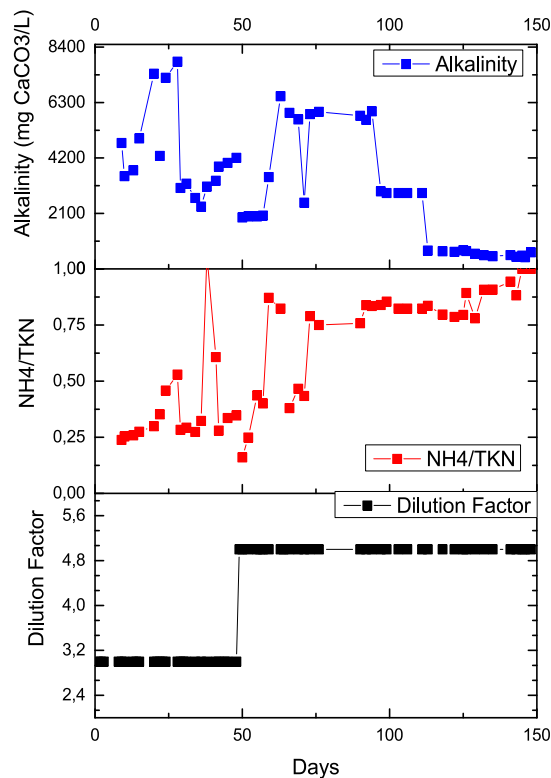
FIGURE 3.17: Effect of the inlet urine dilution over the NH_4/TKN ratio and Alkalinity evolution over time of the second campaign

Keeping urine concentration at high levels seems a good strategy to acclimate biomass if there is enough time to hydrolyze the urea present in the urine before entering the reactor. Since this is strongly dependent of the urea hydrolysis dynamics in the urine itself, the best way to optimize it will be to enhance at the maximum the ureolysis as explained is section 1.1.1, while avoiding problems as bad odours, precipitation and stripping (Udert, Larsen, and Gujer, 2006).

From an operational point of view, this reassert the fact that an equalization tank is necessary before feeding the concentrated urine to the reactor, in order to achieve urine ammonification time requirements.

Another interesting point to be analyse in the future is the influence of the storage temperature. In this campaign storage temperature was increased to $10\,°C$ in order to have the maximum of ammonium and alkalinity and the lower level of unhydrolysed urea. It is not easy to compare with the first campaign since the urine concentration in the tank was not the same, but it seems that the higher temperature enhance urea hydrolysis into a more stable process.

Nitrogen conversion efficiency

The quality of the effluent is presented in figure 3.18 in terms of nitrogen species. Here, every change in the operational pH range in delimited by a continuous black line, as it is the case for the others figures in this section.

Several days of poor operation can be observed where either ammonium or nitrite was accumulated inside the reactor. In order to overcome this, pH operational ranges were adjusted. For instance, after the continuous ammonium increase observed during the first 20 days, the change in the pH operational range leads to a stable nitrification yield as shown in the figure 3.19 but an increase in the nitrite concentration. This highlights a failure in the NOB performances most likely due to lower pH. It is easy to identify the three operational days where a nitrite accumulation was detected (days 30, 50 and 75) with concentration higher than $50\,g_{NO_2^- -N}.m^{-3}$.

After this first nitrite peak, reactor was washed (taking out permeate continuously without any feed and then completing the volume with tap water) to reduce ammonium content by at least 50% and let the biological nitrification perform the remaining work. Afterwards, nitrification yield remains stable but nitrite levels remained high. When a new nitrite pic was observed, we decided to get back to the initial pH operational range. However, during this period, biomass decay was too important (figure 3.20) and combined with a drastic fall in the nitrification yield. The operational pH range was finally fixed at neutral value of 7. This value allows to recover a good biomass growth, with a correct nitrification yield and much lower levels of nitrite in the effluent.

Apparently, the nitrogen mass balance between the inlet and outlet is not closed as much less nitrogen was detected in the permeate. Numerous tests and dilution series were performed to exclude measurement errors. Several phenomena explain this behavior:

1. The HRT was very high, in particular during the three first phases of operation. Therefore, the outlet sample of one day doesn't fit to the inlet sample of the same day. For example, for the first days of operation, only 250 mL of urine was injected in the reactor.

2. The influence of HRT and subsequent dilution in the reactor was enhanced by the washing procedure performed in case of nitrite peaks.

3. A part a nitrogen is assimilated by the biomass (8% of produced biomass)

4. Water evaporation is not negligible and can, depending on the air flow rate, amount to more than 20% of the influent flow when operating a 34 l lab-scale reactor at $20\,°C$. Because of this evaporation the influent and effluent flow rates would differ. This evaporation phenomena is often found in this type of pilot scale applications with high oxygen levels, as it was also noticed by Fux et al. (2002).
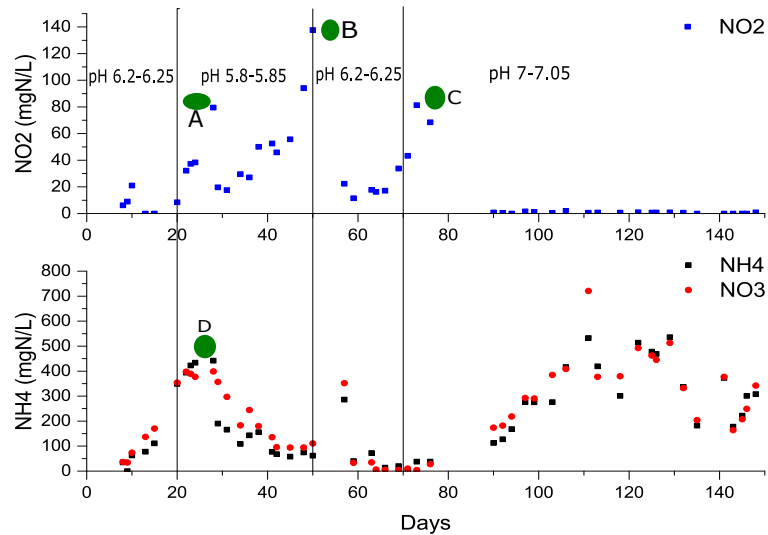
FIGURE 3.18: (a) NO_2, (b) NH_4 and NO_3 concentration in the outlet over time of the second campaign.

The overall nitrification yield over time is presented in figure 3.19. The mean value is 57%, which is consistent for the nitrification of a yellow wastewater with alkalinity insufficiency problems (Udert and Wächter, 2012). As in the first campaign 3.2 no external alkali was added to the system.
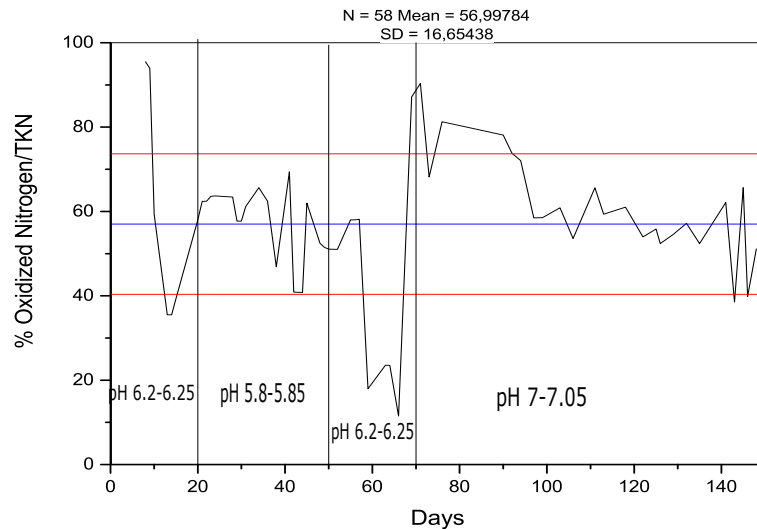
FIGURE 3.19: Nitrification yield evolution over time for the second campaign

This, plus the alkalinity needs and stability of the ratio evidenced in figure 3.17 lead us to prove that concentrated and long term stored urine (so almost completely ammonified) is a good way to better control the acclimation strategy. This validates the fact that enhancing urea hydrolysis leads to a better control of the system performances (i.e. from day 70 in the figure 3.19), as it was suggested as a conclusion of the first experimental campaign.

Biomass acclimation

The evolution of biomass concentration and its relation to the HRT and NLR evolution over time are presented in figure 3.20.
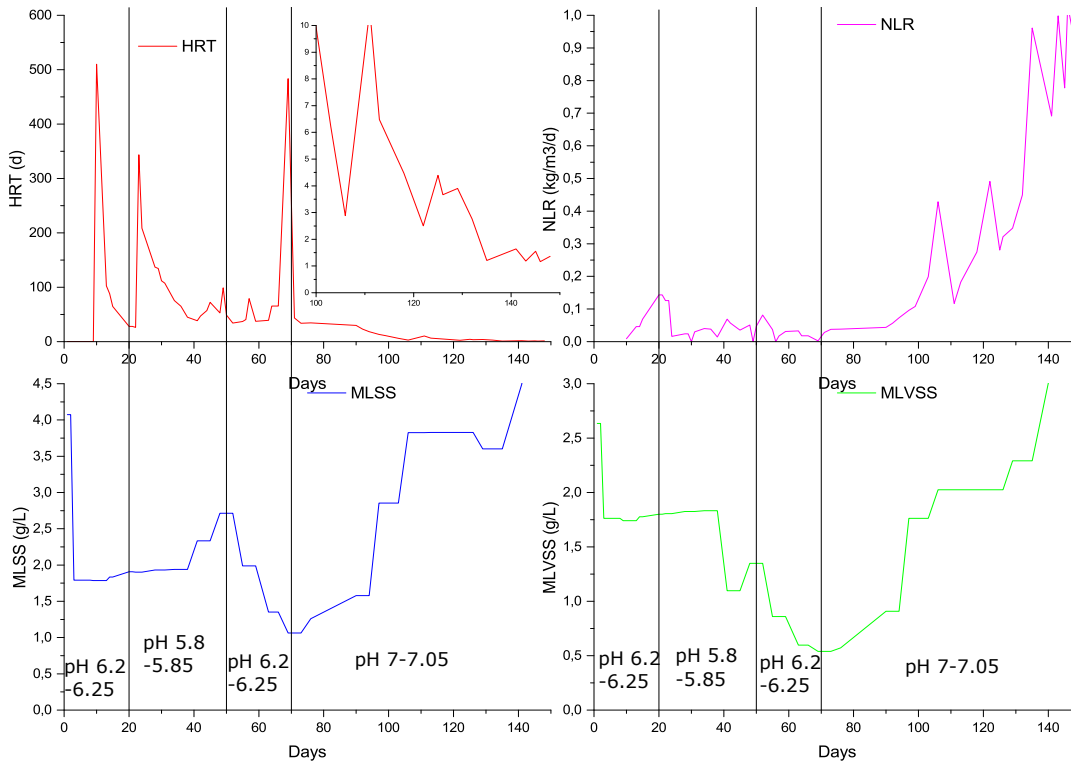
FIGURE 3.20: (a) HRT, (b) NLR , (c) MLSS and (d) MLVSS in the MBR
over time of the second campaign

Here we can distinguish the four different periods of the biomass acclimation:

- in the first stage, using the same pH range set from the previous campaign, the biomass concentration was almost stable. The change in the habitual C:N:P ratio influent wastewater from the AS treating domestic wastewater did not affect significantly biomass concentration after 20 days. NLR regularly increased during this period but nitrification yield decreased too.

- in the second stage from the day 20, a new pH range set wanted to be tested. pH was fixed to 5.8-5.85 in order to enhance NOB activity. A first nitrite peak appeared around day 30 (point A in figure 3.18). Even after washing out from the reactor the nitrite excess (point D in the figure 3.18), the nitrate and ammonium content started to decrease progressively.

- another nitrite peak appeared at day 50 (point B in the figure 3.18) and this time even after washing out the reactor, the damaging impact in the biomass was stronger. The biomass (MLVSS) started to decrease also, a change in the pH range was operated .pH was fixed again to 6.20-6.25 to enhance AOB activity.

- by the day 70, after attaining low concentrations of ammonium and nitrate another nitrite peak appeared (point C in the figure 3.18). After washing out the reactor, this time the pH was definitively fixed to the range 7.00-7.05. Then, it took more than 50 days to recover more or less the initial levels of active biomass. During this period, no nitrite peaks occurred anymore and both NLR

and nitrification yield began to increase progressively together. The acclimation process was more controlled and stable successfully stable.

From day 70 of operation, the optimal conditions for biomass acclimation were achieved. Stability of inlet NH_4/TKN ratio was observed and ammonification was maximal. This seems to affect positively the operation of the system. This confirms that urea ammonification in the source separated urine is one important parameter to better control the acclimation phase in the MBR. This is the case even when variations in the alkalinity content are also present (as is the case in figure 3.17 from the day 70 at a constant dilution factor).

MBR dynamics

Similarly to the first campaign, the analysis of pH dynamics in the reactor was carried out by calculating the "delta up" and "delta down" *i.e.* the derivative of pH during feeding and reacting events respectively.
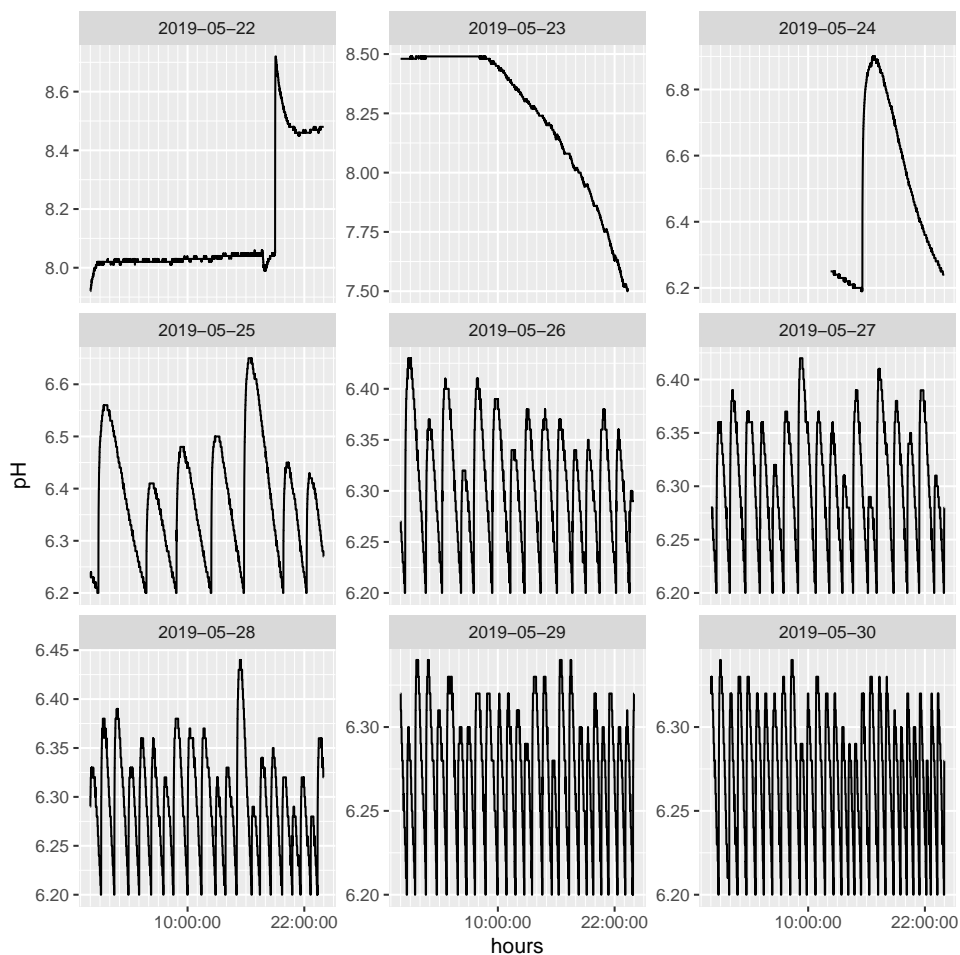
FIGURE 3.21: pH dynamics over the first operative month of the second campaign

Figure 3.21 presents an example of the evolution of pH during the first operative days of the MBR. The figures in the appendix D present the total campaign data of the four online measured variables, DO, pH, temperature and conductivity over the six months of operation. The first three days correspond to the inoculation time and the subsequent time to let the PLC start governing the urine inlet flow.

The figure 3.21 shows the evolution of pH over the first month (first operative day 23-05-2019). From the figure, we can highlight the maximum and the minimum values, thus the number of defection points on the pH curve can be derived. The beginning of the on/off feeding strategy can be distinguished. The quantity of feeding events per unit of time progressively increased afterwards. For this first operative days, the pH range was 6.20-6.25 as explained in the last section. The figure also allows to interpret qualitatively pH dynamics for the first week and invite us to analyse it quantitatively this pH. Teh could allow to relate its variations to the quantity of urine injected in the reactor (and thus HRT) as well to NLR.

Effect of pH dynamics over NLR and the HRT

It is possible to understand the impact of the variation of some operational parameters over the effluent quality and the stability of the system, if we define the relation between pH dynamics and those parameters. Particularly the analysis can be done over the NLR and the HRT. If for a particular operation day we have the shape of pH dynamics presented in figure 3.22 we can deduce the dynamics of pH increase during influent pumping due to the alkalinity mainly and also the dynamics of pH decrease due to nitrification.
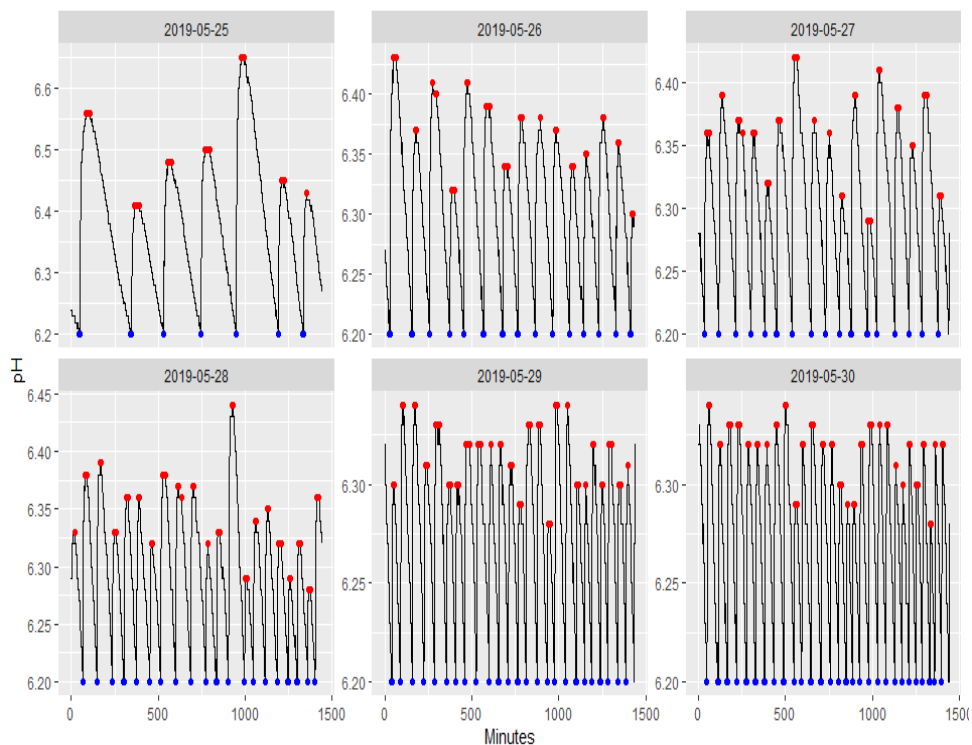
FIGURE 3.22: Maximum and minimum values identification for pH dynamics
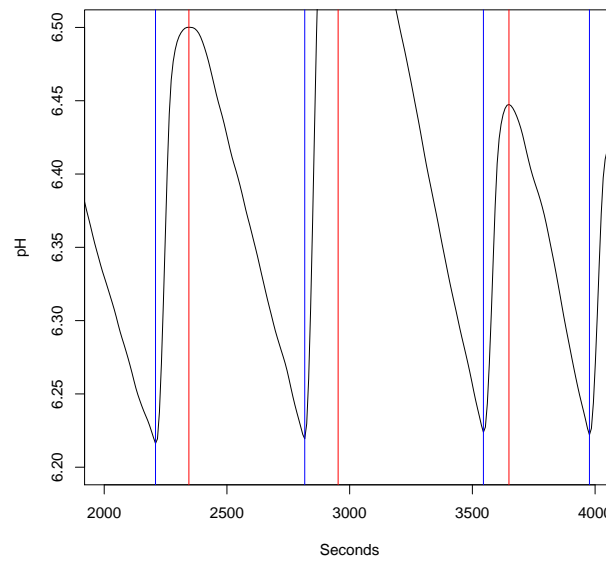
FIGURE 3.23: pH dynamics for reactor start-up of the second campaign
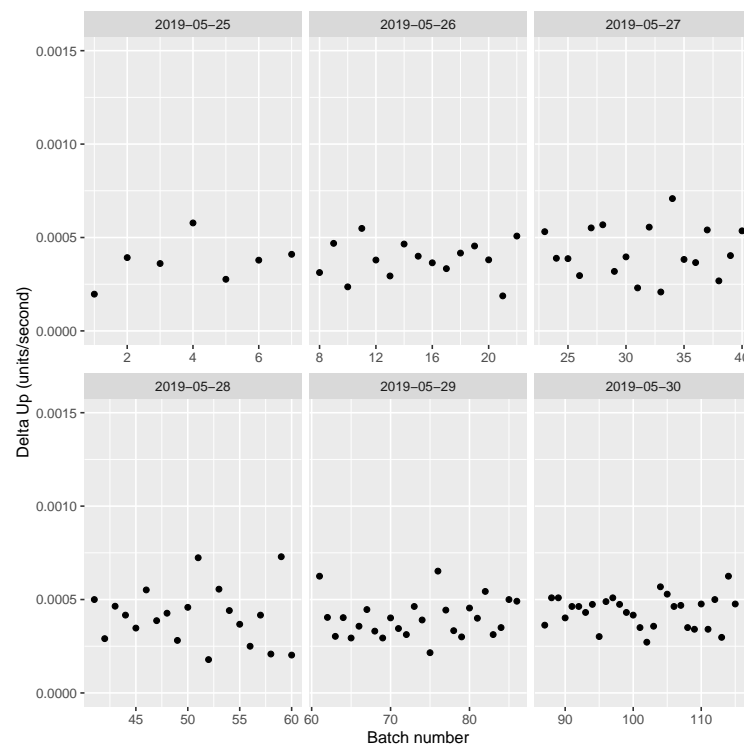
FIGURE 3.24: Delta up pH dynamics over the first operative month of the second campaign

From the figure 3.23 we can identify one first phenomena that increases the pH when pump starts to feed until a maximum pH set value (in red scatter). This is due to the alkalinity in the inlet that induces the pH increase inside the reactor. When the high pH set-point (6.25) is reached, the pump stopped. Then, due to biological nitrification and specifically AOB activity, pH decreases until the lower set-point (6.2) (in blue scatter) where the PLC triggers the influent pump again. The balance between these two phenomena is at the core of pH dynamics inside the system. The figure 3.23 allows to identify every maximum and minimum form the signal response of pH.

For instance between the first minimum and the next maximum point represents the alkalinity effect of the urine increasing the pH and on the contrary the point between the maximum and the next minimum represents the nitrification effect acidifying the medium by proton's production. In other words it is possible to determinate each effect by approximating delta pH as linear variations and calculating the slope going up and down in each section.
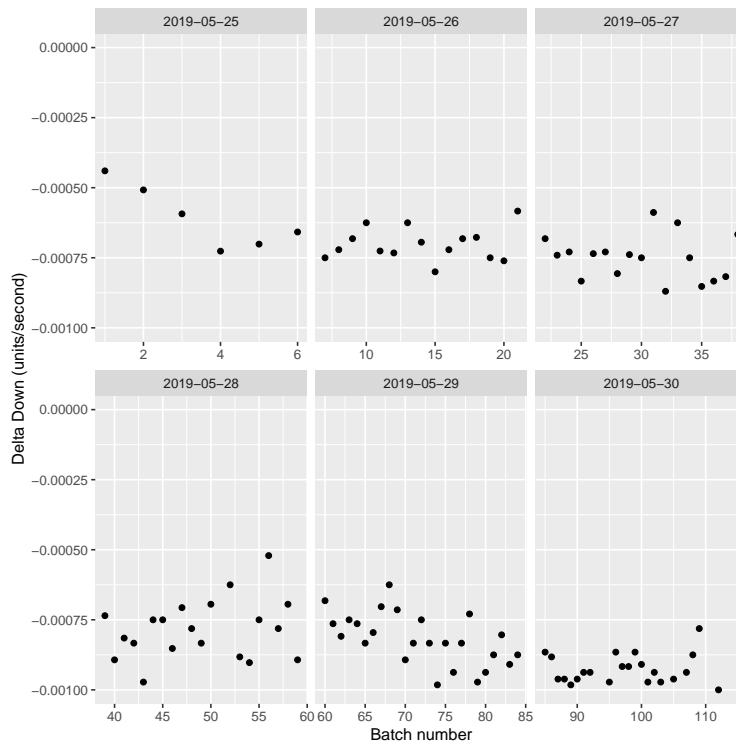
FIGURE 3.25: Delta down pH dynamics over the first operative month
of the second campaign

By evaluating the time derivative of pH value for each batch fed to the reactor (dpH_{UP}/dt and the dpH_{DOWN}/dt) for each pumping period in each particular operation day, the two phenomena can be quantified over the experimental period. Then, we can link their variation to the real impact on both NLR and HRT. Figures 3.24 and 3.25 were build to calculate pH each day in function of the accumulated batches quantity.

To enable the interpretation and to identify and differentiate the impact of each phenomena on pH dynamic, the Figures 3.26 and 3.27 were constructed. They present the total trend all over the duration of the second campaign (150 days).

Similarly to what was observed during the first pilot-scale trial, the pH increased due to the inlet urine. Then, due to biological nitrification and specifically AOB activity, pH decreased (figure 3.23).
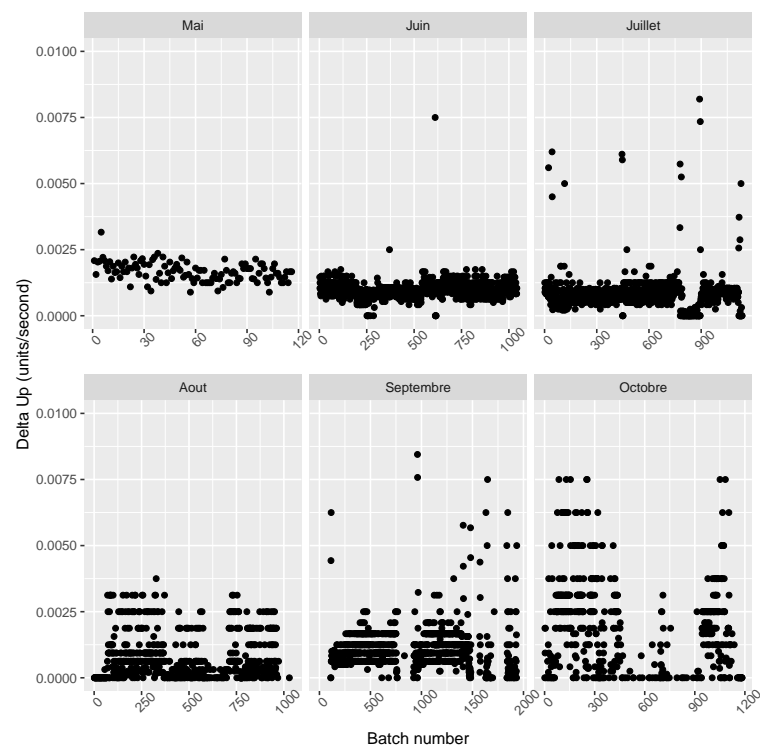
FIGURE 3.26: Delta pH up dynamics achieved over the total campaign
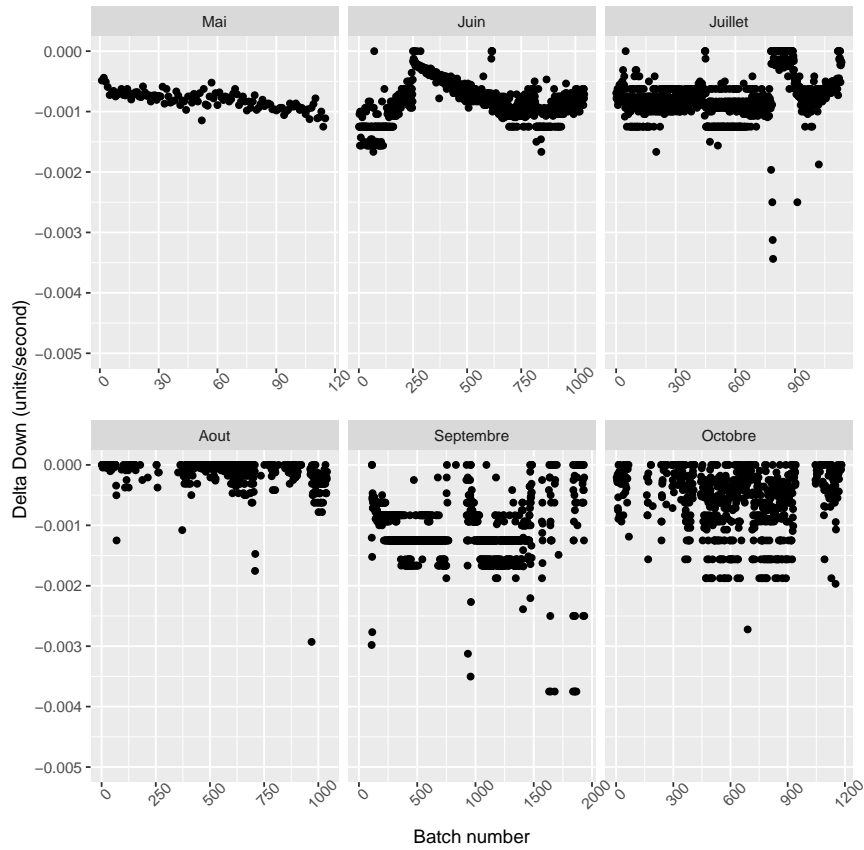
FIGURE 3.27: Delta pH down dynamics achieved over the total campaign

The Figure 3.28 represent the daily average delta up and delta down of the pH dynamics, all over the total experimental time of the campaign (150 days). As the delta up has no clear trend to analyse, the Figure 3.29 was build to compare and analyse the interactions between the HRT and the daily average delta down for each pH set range used.
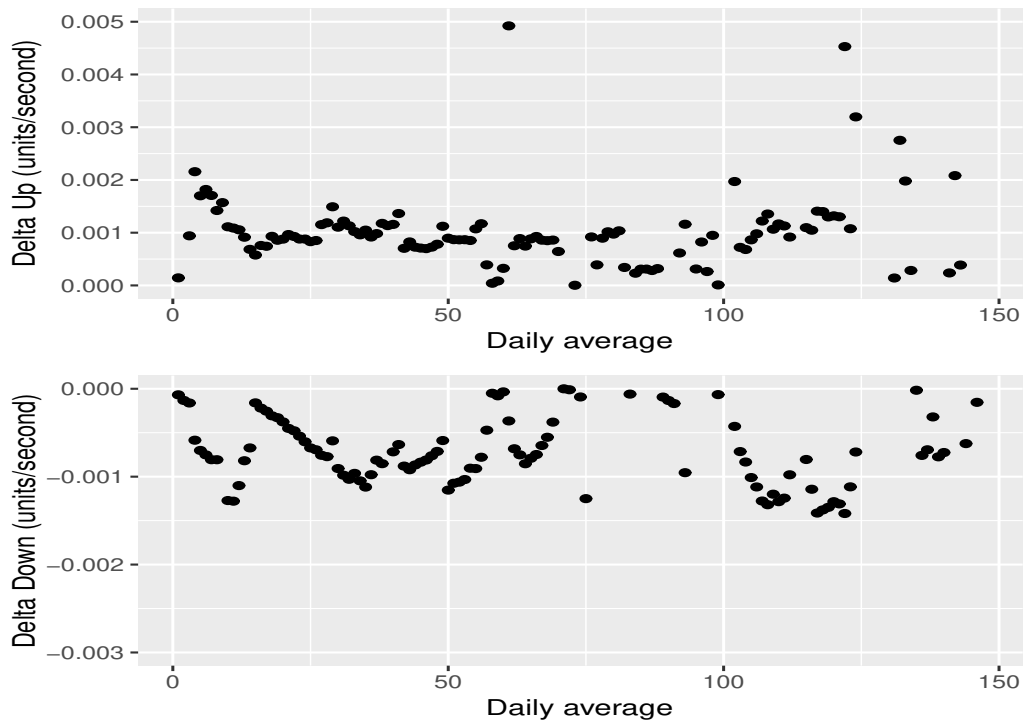
FIGURE 3.28: Average delta up/down pH over time
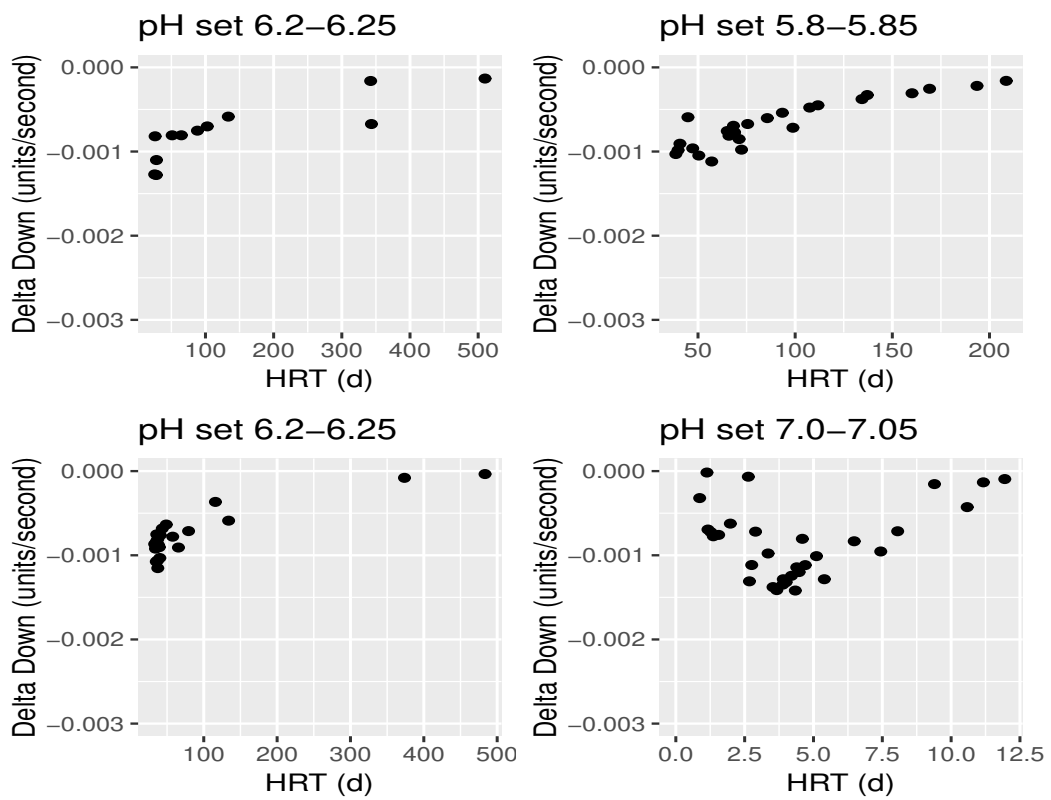
FIGURE 3.29: Average delta down pH vs HRT for each pH range set

It must be noticed that the dynamics in the figure 3.28 are way more slower comparing to the ones in the first campaign. Indeed, the slope was presented for both campaigns in units/second and in the second one the calculated delta is 10 times lower relative to the first campaign, and not in the same order of magnitude (see Section 3.2). Finally, when biomass acclimation was performed, the HRT decreased following both feeding events duration increase (more volume injected by the pump each time) as well as the decrease of the duration between two feedings.

Delta up value was relatively constant over the time (Figure 3.28). Simultaneously, the HRT decreased in each different pH set range. This is related to the inlet alkalinity and NH_4^+/NH_3 content (Figure 3.17): at the beginning, the PLC is injecting very few quantity of effluent, thus the HRT is really high. This influent alkalinity is very high but the AOB activity is still low. Therefore, pH increased quickly and the feed event duration is short. Then, as nitritation activity increased, the related protons production compensates for this, leading to slower pH increase: the feed duration increased and partly explains the decrease in HRT. The delta down is directly influenced by the AOB activity. When the NLR started to raise significantly during the last phase, biomass activity increased and directly induced quicker pH decrease between two successive feeding events. It means that the duration between two feedings decreased also.

3.3.4 Conclusion

One strategy to acclimate biomass to a high ammonium content inlet was tested in laboratory conditions, using a semi-continuous influent feeding. The influent injection was controlled via a PLC as a function of desired pH set range value. The influent consisted of urine diluted with tap water by a factor 3 or 5 depending on the period (mainly because of source separated urine limitations). No external chemicals were used to control the pH inside the reactor, only the closed loop strategy controlled by the PLC trigger or stop the feeding to control pH. Three different pH ranges were tested and the influence of each variation was ascertained.

After a trial and error period in order to find the optimal pH range and following a good level of ammonification in the diluted urine storage tank, acclimation was successful and the NLR dramatically increased up to $1.05 \, kg - Nm^{-3} day^{-1}$ with a final biomass production of $3.1 \, g_{MLVSS}.m^{-3}$.

pH dynamics throughout the operation were analysed to derive the kinetics of elevation during feeding period and decrease during nitrification. It was shown that the more concentrate and ammonified the urine is, the better the control of the HRT. This cause the pH variation are lower and HRT is high, the control of the acclimation is more reliable and progressive. and most of all, figure 3.29 validates the fact that the decrease in HRT is correlated to he nitrification rate of each batch feed to the reactor, thus pH variations are way more representative of the real nitrified nitrogen, in other words the biomass acclimation.

The strategy of hydrolyzing at maximum the urine in the storage tank allows to better stabilize and control the quality of the inlet in terms of NH_4, TKN and alkalinity concentrations. Hydrolyzed urine is a good solution to keep alkalinity to NH_4 ratio in an appropriate range to ensure 50% ammonium oxidation.

This means that the strategy of using stored source separated urine has a positive impact in the behaviour of the system, first because there is a better stability since the initial ratio $NH_4/$TKN of the highly concentrated urine as can be seen in the figure 3.17 and secondly because the pH dynamics .

Finally, the presence of a storage tank before the feeding is necessary to let ammonification happens to the highest extent. Thus, the variation of HRT inside the reactor will be properly controlled by the pH set range and resulted in the NLR increase.

3.4 General conclusions

A fully automated control of the influent flow to the MBR was achieved to acclimate biomass to high nitrogen content influent and to stabilise this source separated yellow wastewater into an equal ammonium/nitrate ratio effluent. This was achieved avoiding the use of external chemicals and understanding the influence of several parameters over the process dynamics.

Two experimental campaigns were performed in order to investigate the influence of four important parameters namely inoculation start-up, urine inlet concentration, preliminary ammonification and the influence of the pH range imposed for the feeding closed-loop strategy. We can conclude for each of this parameter important points in terms of operational parameters, technical issues and impact on the effluent quality coming out from the MBR.

1. From the results shown in figures 3.7 and 3.20, it is noticeable that the first phase of the acclimation will present a biomass decay. This is probably due to a variation in the biomass proportion between heterotrophic and autotrophic bacteria, linked to the differences in the C:N:P ratio of the new yellow wastewater influent to be treated. This adaptation of the biomass was quicker for the second experimental campaign, were the initial amount of activated sludge was lower (see Table 3.4). This probably helps to better control the competition between the two bacterial strains and let the AOB and NOB better be adapted to the high nitrogen content (with an initial concentration of $100\,g_N.m^{-3}$).

2. Using highly diluted fresh urine to feed the reactor does not allow to efficiently control the initial NH_4/TKN ratio of the urine. These objectives were better achieved by keeping a lower dilution rate of 5 times, which is in fact closer to the technical objective of the real scale system of treating mainly yellow wastewater with an approximate dilution factor of 3 times. Achieving the ammonification of organic nitrogen in the inlet allows to have less disturbances for the progressive increase in the NLR necessary to acclimate biomass. In these conditions, the alkalinity of the influent will raise the pH in the bioreactor proportionally to its nitrogen concentration during feeding. During the reaction phase, pH decrease will be more closely related to the nitrifying activity without significant ammonification inside the reactor.

3. The optimal set range of the pH value to optimize the acclimation of the biomass using complete hydrolyzed urine highly concentrated to be treated is found to be between 7.00 - 7.05. Nevertheless, care must be taken to generalize this optimal pH for any kind of urine, the best pH value must be evaluated experimentally.

4. The analysis of pH dynamics performed in this study opens perspectives for the future development of more advanced control strategies and failures detection.

In both pilot-scale experiments, the feeding events duration as well as the interval between two of them was highly dependent on several factors and variables: inlet concentrations of nitrogen, degree of ammonification, alkalinity, gas-liquid mass transfer of CO_2 and possibly NH_3. The risk of inhibition and nitrite and/or ammonia accumulation was important, in particular for the first campaign with less controlled influent. Despite the detailed analysis of pH dynamics, it is very difficult to de-correlate the influence of each operational parameter on this behavior. Simulation of the reactor start-up using the model developed in Chapter 2 should help. This will be the subject of Chapter 5 which deals with scenarios analysis using the model. Before, the model must be calibrated: the first part of Chapter 5 proposes a sensitivity/identifiability analysis. Part of those parameters where calibrated using respirometric techniques in Chapter 4: acclimated sludge from the second trial is used to perform these tests.

Chapter 4

Characterization of acclimated biomass biokinetic parameters by respirometry

Respirometers are devices that measure the "respiration" of living organisms and are used to measure and interpret the oxygen uptake rate of activated sludge. All types of respirometers consist of a reactor in which activated sludge from different wastewater sources and a specific substrate are brought together as well as a device measuring the rate at which the biomass takes up oxygen. The oxygen is usually measured in the liquid phase with an electrochemical or optical DO sensor. The oxygen uptake rate is then calculated by making a general mass balance for oxygen over the liquid phase (Gernaey et al., 2001; Kong et al., 1996).

Respirometric methods are used in this thesis as a tool to analyse high nitrogen acclimated sludge activity. At the same time, the calibration of the proposed bio-physical model (chapter 1) is performed. According to previous works (Jubany et al., 2008), one protocol has been adapted for testing the oxygen consumption rate (OUR) of the enriched biomass. Respirometric data obtained will be compared with a control sample consisting of extended aeration activated sludge sample.

This protocol is based on controlled doses method. It was developed to characterize biomass enriched on autotrophic bacteria. It links the OUR measured in the mixed liquor for specific conditions and different amounts/types of substrate addition: some particular and sensitive parameters could thus be identified. These conditions allows to evaluate substrate excess inhibition, inhibitory concentrations of byproducts...

4.1 Fundamentals of respirometry

In general terms, the DO concentration in the bioreactor is determined by two competing processes, namely Oxygen Transfer Rate (OTR) supply by continuous aeration and microbial OUR for exogenous respiration. Let us consider a system consisting of a liquid phase, containing biomass and a gas phase both being ideally mixed and having an input and output (Figure 4.1). It is assumed that the DO concentration in the liquid phase can be measured. By a mass balance in the liquid phase we have:

$$\frac{dS_O}{dt} = OTR - OUR \qquad (4.1)$$

With

$$OTR = kla * (S_O^{eq} - S_O) \tag{4.2}$$

as OTR rate by aeration. S_O^{eq} is the equilibrium concentration at which the oxygen transfer rate is equal to the oxygen uptake rate linked to the maintenance of the biomass (endogenous OUR). It is determined by aerating the mixed liquor in the reactor for approximately 30 min until a stable equilibrium concentration is reached. At this equilibrium point the OTR is equal to the OUR and the there is no change in the DO over time.

Thus, after these considerations, the final DO mass balance over the liquid phase is then given by equation 4.3:
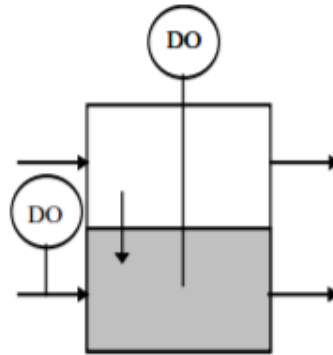
FIGURE 4.1: Respirometer, Liquid phase principle, Flowing gas, Flowing liquid (LFF) (Sheng, Yu, and Li, 2010)

$$\frac{d(V_L S_o)}{dt} = Q_{in} S_{O,in} - Q_{out} S_O + V_L K_L a (S_O^{eq} - S_O) - V_L \text{OUR} \tag{4.3}$$

Where:

- S_O: DO concentration in the liquid phase

- S_O^{eq}: equilibrium DO concentration in the liquid phase

- $S_{O,in}$: DO concentration in the liquid phase entering the system

- $K_L a$: volumetric oxygen gas/liquid mass transfer coefficient (based on liquid volume)

- Q_{in}: flow rate of the liquid entering the system

- Q_{out}: flow rate of the liquid leaving the system

- V_L: volume of the liquid phase

- OUR: respiration rate of the biomass in the liquid

In most systems Q_{in} and Q_{out} will be equal so that the liquid volume is constant. In what follows it is assumed that the liquid volume is constant, so that the terms in 4.3 can be divided by V_L. Equation 4.3 becomes:

$$\frac{dS_o}{dt} = \frac{Q_{in}}{V_L}(S_{O,in} - S_O) + K_L a (S_O^{eq} - S_O) - \text{OUR} \tag{4.4}$$

Depending on the boundary conditions, respirometric measurements can be classified depending on the presence or not of a liquid or gas flow (Spanjers and Vanrolleghem, 1995a). Among the different possibilities, two were applied in this study. They are presented below.

4.1.1 Static gas, static liquid (LSS)

One approach is to use a method without liquid flow and oxygen mass transfer. Even if a gas phase is present, no mass transfer from the gas phase into the liquid phase is considered (no bubbling). In practice, to prevent input of oxygen into the liquid, the gas phase may be absent. Then, the first three terms on the right-hand side of equation 4.4 fall away and the mass balance reduces to:

$$\frac{dS_\mathrm{o}}{dt} = -\mathrm{OUR} \tag{4.5}$$

Hence, to obtain the respiration rate only the differential term must be determined. This can be done by measuring the decrease in DO as a function of time due to respiration, which is equivalent to approximating the differential term with a finite difference term: $\Delta S_\mathrm{O}/\Delta t = -\mathrm{OUR}$.

In order to monitor OUR for a long period, this method requires successive aeration/no-aeration cycles.

4.1.2 Flowing gas, static liquid (LFS)

The disadvantage of the need for successive re-aerations can be eliminated by continuously aerating the biomass. Then, the oxygen mass transfer term must be included in the mass balance coming back to equation 4.4 without the inlet/outlet term:

$$\frac{dS_\mathrm{o}}{dt} = K_\mathrm{L}a(S_\mathrm{O}^{eq} - S_\mathrm{O}) - \mathrm{OUR} \tag{4.6}$$

To obtain OUR, both differential and mass transfer terms must be determined. To calculate the latter, the mass transfer coefficient $K_\mathrm{L}a$ and the DO equilibrium concentration (S_O^{eq}) must be known. These coefficients must be determined regularly because they depend on environmental conditions such as temperature, barometric pressure and the properties of the liquid. The simplest approach is to determine them by using separate re-aeration tests and look-up tables. Another approach is to estimate the coefficients from the dynamics of the DO concentration response by applying parameter estimation techniques. The advantage of the latter method is that the values of the aeration coefficients can be updated relatively easily.

4.2 Experimental setup

4.2.1 Respirometers description

The materials used include:

- Two vessels (respirometric devices) with appropriate readout and sample capacity of 250 mL. Each vessel has an oxygen supply system with constant air flow and a magnetic stirrer (air pumps and diffusers initially used for aquariums)

- Two probes with an oxygen-sensitive electrode (galvanic) – WTW CellOx® 325 and optical probes (Portavo 907 MULTI and WTW 3630 IDS) for Strasbourg trials.

- pH probe (WTW 3630 IDS)

- Data acquisition system consisting of a personal computer with the appropriate software from probes manufacturers.

4.2.2 Reagents

Measurement of OUR is performed after selective addition of organic carbon or nitrogen substrates at controlled doses. Specific inhibitors (N-allylthiourea (ATU) for the AOB activity and Sodium Azide (NaN_3) for the NOB activity) are used when necessary.

The solutions to be prepared are mainly:

- Sodium Acetate $NaCH_3COO^-.7H_2O$: $12.06\,\mathrm{kg\,m^{-3}}$

- Ammonium chloride NH_4Cl: $19\,\mathrm{kg\,m^{-3}}$

- Sodium Nitrite $NaNO_2$: $11.61\,\mathrm{kg\,m^{-3}}$

- ATU (allylthiourea): $6.25\,\mathrm{kg\,m^{-3}}$

- NaN_3 : $1\,\mathrm{kg\,m^{-3}}$

4.2.3 Procedure

The following are the main steps of the procedure:

1. Calibrate each oxygen probe and meter according to the method given by the supplier.

2. Determine the MLVSS of the biomass in the pilot reactor (Apha, 2005).

3. Sample the appropriate volume of mixed liquor in the reactor and prepare it to suit the requirements of the measurements taking into account that :

   (a) As the reactor is not performing complete nitritation, the level of residual TAN may be too high to obtain endogenous conditions within a reasonable time. Residual ammonium oxidation would lead in these conditions to an extra oxygen consumption.

   (b) In that situation, it was decided to wash the biomass five times using the following protocol: mixed liquor was settled in a 1 liter graduated cylinder, the supernatant was discarded and replaced by a saline solution ($NaCl$ at the same conductivity than in the pilot). This procedure was repeated five times. The last iteration allowed to adjust the biomass concentration (e.g. concentrate it by a factor two).

4. let the sample under aeration in the respirometer for 24h in order to reach endogenous conditions.

5. activate probe data acquisition and magnetic stirrer (adequate mixing is essential, mainly for suspensions with high concentrations of suspended solids).

6. start the experiment: after meter reading has stabilized, record initial DO and start timing device. Record appropriate DO data at appropriate time intervals depending on rate of DO consumption.

4.2.4 Controlled doses method

For both respirometry techniques (LSS and LFS), we implemented a controlled dosage of a specific substrate to evaluate the response of a specific bacterial population via the OUR (OURend and Exogenous Oxygen Uptake Rate (OURexo)). This dosage varied according to particular medium characteristics or by simply increasing the substrate concentration. This technique is available for using any kind of specific substrate and even inhibitory or toxic compounds. It allows to control the conditions inside the respirometer such as pH, temperature, as well as the presence and concentration of external chemical compounds.

The principle is always the same: after a starvation period (endogenous conditions), the biomass will respond to specific doses of particular compounds. The change in respiration and thus oxygen consumption due to the presence of this compound will affect the equilibrium of dissolved oxygen concentration. Increasing these controlled doses allows to evaluate the impact of substrate or specific chemical compound in terms of saturation, competitive and noncompetitive inhibition, toxic effects, etc... via the Monod or Haldane type equations (see Section 2.1.2).

The measure of the concentration of the specific substrate to be added before and after the controlled doses is performed in order to check both the endogenous state and the total consumption at the end of the respirometric test. This also allows to monitor substrate concentration in the respirometer.

4.2.5 Kla measurement in sludge

According to Loosdrecht et al. (2016), the respirometric test for oxygen transfer process will be evaluated in first step by Flowing gas – static liquid technique (LFS). During this type of respirometric analyses the batch reactor is continuously aerated. The mass balance in the liquid phase follows equation 4.6.

The Kla value is determined by a dynamic gassing out method. First, the aeration is stopped until a dissolved oxygen concentration of $1.5\,\mathrm{g_{O_2}.m^{-3}}$ to $2\,\mathrm{g_{O_2}.m^{-3}}$ is reached (Bandyopadhyay et al., 2009), then the aeration is activated until the oxygen's equilibrium value (S_O^{eq}). This method is used as many times as necessary during one test.

Accurate determination of Kla is very important for the evaluation of many other respirometric parameters. Numerous factors, such as gas flow, bubble size, reactor dimensions, stirring of mixed liquor (turbulence), temperature of mixed liquor, MLSS and air pressure, etc. have a major influence on Kla. Therefore, the following conditions must be ensured during the determination of this parameter (Roš, Dular, and Farkas, 1988):

1. A constant airflow throughout the whole experiment

2. A reactor with known volume and shape must be used for all measurements

3. Constant stirring must be provided

4. Constant temperature of mixed liquor during the measurements

The Kla measurement is performed several times with different air inflow configurations and different agitation speed and then the average Kla value is evaluated for each configuration to identify its variation that will be used for further calculations. As it was demonstrated in previous works, the volumetric transfer coefficient must be determined and calculated for every specific experiment set in order to optimize the controlled doses method (Guisasola et al., 2005; Jubany et al., 2008; Spanjers and Vanrolleghem, 1995a).

4.3 Respirometry in high nitrogen acclimated sludge

For the measurements of oxygen dynamics in acclimated sludge, samples of mixed liquor were taken from the MBR. Then, the respirometric tests were carried out in LFS mode for each sample.

The OUR was calculated according to equation 4.6. This equation includes a gas/liquid transfer term and the OUR by the microorganisms. The OUR is the sum of the OURend and OURexo. OURend is the oxygen uptake rate related to maintenance in absence of readily biodegradable substrate while the exogenous oxygen uptake rate is the oxygen uptake required to degrade a substrate (Capodici et al., 2016).

When substrate is lacking, OURexo becomes zero and only OURend is present. In this case, continuous aeration allows the oxygen concentration in the reactor to reach a steady oxygen level, representing the equilibrium between oxygen transfer and endogenous respiration.

4.3.1 Estimation of endogenous activity and oxygen transfer coefficient

The oxygen uptake rate measured before the addition of substrate is due to the endogenous respiration of the activated sludge. The endogenous respiration is often defined as the oxygen consumption of microorganisms in the absence of substrate, but many mechanisms and processes are included in the concept of endogenous respiration. Van Loosdrecht and Henze (1999) have described the phenomena in more details and tried to organize the mechanisms and processes involved in microbial endogenous respiration.

According to Loosdrecht et al. (2016), the respirometric test for endogenous activity will be evaluated in the first step by LSS method. This type of test is performed without aeration. The mixed liquor of the membrane bioreactor from the pilot is aerated until a dissolved oxygen concentration of $6\,g_{O_2}.m^{-3}$ to $8\,g_{O_2}.m^{-3}$ is reached. After the aeration is stopped, the decline in oxygen concentration with time due to respiration was monitored. During this type of experiment the mass balance of equation 4.5 becomes (Drtil, Németh, and Bodík, 1993; Gernaey et al., 2001):

$$\frac{dS_o}{dt} = -OUR_{end} \qquad (4.7)$$

This is a very simple equation since the aeration terms can be omitted. The relationship between the decrease in oxygen concentration and time is normally found to be linear and the oxygen uptake rate is determined by calculations of the slope of the curve. If the oxygen uptake rate is related to the MLVSS, the specific oxygen uptake rate is obtained.

By alternating the aeration of the sludge in intervals it is possible to follow the OUR during a longer period. A typical respirogram in these conditions is shown in Figure 4.2.
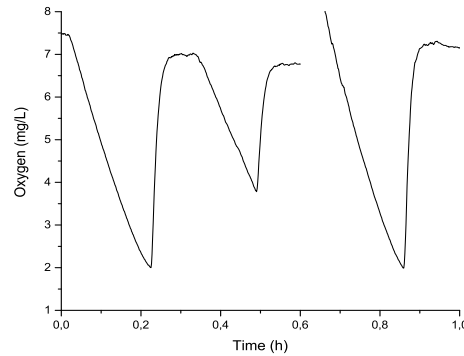
FIGURE 4.2: Respirogram representative of one trial for OURend measurement and Kla adjustment.

Then, each time that the OURend is measured, the re-aeration period just after until reaching the equilibrium concentration could be used to calculate Kla as described in section 4.2.5 as many times as necessary.

4.3.2 Estimation of Exogenous activity

When the bacteria activity has to be measured, the best way to do it is after a starvation time were all the substrate present in the sludge was already consumed and then the cellular maintenance is the only priority for the bacteria (endogenous metabolism). In this situation, any addition of external nutrients will generate a DO variation, only due to the consumption of this specific substrate. This selectivity can be exploited by controlling exactly the type, physical phase, concentration and quantity of this substrate to be injected. This can be repeated as meany times as necessary and it correspond to a controlled doses method that can be implemented in order to characterises any type of bacteria strain, from heterotrophs to AOB and NOB bacteria.

For example concerning heterotrophic bacteria, when an easily biodegradable carbon source is added to activated sludge, the OUR will increase and when the carbon source is consumed, the OUR will return to approximately its initial level in a constant DO equilibrium level. The more easily degradable a carbon source is, the higher the OUR becomes, until it reaches its maximum for the activated sludge. The maximum uptake rate is reached when all bacteria capable of utilizing the organics grow at maximal speed.

To measure the exogenous activity of heterotrophic and autotrophic bacteria, two diverse types of substrate were used, a carbonaceous and a nitrogenous one. The respirograms were derived from equation (4.8).

$$OUR_{\text{exo}} = kla * (S_O^{eq} - S_O) - \frac{dS_O}{dt} - OUR_{\text{end}} \qquad (4.8)$$

The controlled doses method comprises additions of specific substrates:

- NH_4Cl for nitrogen source for the AOB bacteria,

- $NaNO_2$ as nitrogen source for the NOB bacteria,

- Sodium Acetate as carbon source for heterotrophic bacteria.

Between each specific substrate addition, endogenous activity and Kla adjustment are evaluated for correct interpretation of the results.

By measuring the oxygen uptake rates in the presence and absence of a specific inhibitor (e.g. ATU for the AOB activity or NaN$_3$ for the NOB activity), the total heterotrophic and the two steps nitrification oxygen uptake rates can be calculated. Thus, for both organic carbon oxidation (heterotrophic) and ammonium oxidation (nitrification), OUR is calculated in the usual way. The results could be calibrated against the proposed two steps nitrification model predictions.

The exogenous oxygen uptake rate curve reflects the kinetics of aerobic biodegradation of C and N substrates by heterotrophic and autotrophic microbes of the acclimated sludge. In most cases, these processes are independent and their oxygen uptake rates may be added up as indicated in the Equation (4.9)

$$OUR_T = r_H + r_A + r_N \tag{4.9}$$

It is demonstrated that the OUR profile for a single substrate contains the same type of information as the Monod growth curve in defining the relationship between growth rate (μ) and substrate concentration(S) (Kong et al., 1996). This is because one batch experiment covers a range of substrate concentrations, making it possible to evaluate the "growth rate-substrate concentration" relationship.

Carbon degradation and the two steps nitrification process the nitrogen consumption are described according to the model described in chapter 2. Taking into account the process rates and the Petersen matrix presented in section 2.2, it is possible to represent the rate of oxygen consumption for each particular substrate addition in the controlled doses method as follows:

$$r_H = -(1 - Y_H)\frac{dS_C}{dt} = \frac{-(1 - Y_H)}{Y_H}\mu_{maxH}X_H\frac{S_O}{K_{OH} + S_O}\frac{S_s}{K_S + S_s} \tag{4.10}$$

$$r_{AOB} = -(3.43 - Y_A)\frac{dS_{FA}}{dt} = \frac{-(3.43 - Y_A)}{Y_A}\mu_{maxA}X_A\frac{S_O}{K_{OA} + S_O}\frac{FA}{K_{S,FA,A} + FA + FA^2/K_{i,FA,A}}\frac{K_{i,FNA,A}}{K_{i,FNA,A} + FNA} \tag{4.11}$$

$$r_{NOB} = -(1.14 - Y_A)\frac{dS_{FNA}}{dt} = -\frac{(1.14 - Y_A)}{Y_A}\mu_{maxN}X_N\frac{S_O}{K_{ON} + S_O}\frac{FNA}{K_{S,FNA,A} + FNA + FNA^2/K_{i,FNA,A}}\frac{K_{i,FA,A}}{K_{i,FA,A} + FA} \tag{4.12}$$

The substrate degradation rate r and substrate concentration (S_s, FA or FNA), are related to the measured OURexo. It is important to remark that the biomass growth due to the substrate addition is negligible within the time frame of the test. Indeed, it was showed in the literature that for example an addition of only $5\,g_{COD}.m^{-3}$ $+ 20\,g_{NH_4^+-N}.m^{-3}$ results in a biomass growth of approximately $0.035\,g_{MLVSS}.m^{-3}$ which is very insignificant compared to the usual active biomass concentration (gVSS/L) already present in the mixed liquor inside the respirometer vessel (Jubany et al., 2005; Roš, Dular, and Farkas, 1988).

From the respiration rate determination, most of the model's parameters can be estimated (Kong et al., 1996). Only μ_{maxH} μ_{maxA} and μ_{maxN}, cannot be specifically estimated and their values must be obtained separately. The fractions of autotrophic biomass concentration X_A and X_H were not determined separately, therefore, in what follows, the kinetics are related to the total biomass concentration and the specific growth rate togetherμX. The parameters or parameter combinations that can be identified from Equations (4.10) to (4.12) are mainly μ_{maxA} X_A, $K_{s,FA,A}$ $K_{i,FA,A}$ $K_{i,FNA,A}$ for the AOB stub and μ_{maxN} X_N $K_{s,FNA,N}$ $K_{i,FNA,N}$ $K_{i,FA,N}$ for the NOB stub.

4.3.3 Parameters estimation: stoichiometric coefficients

The structural identifiability of Monod-based activated sludge models was studied by Petersen (2000): only some parameters combinations were identifiable if only OUR measurements were available. Most of these combinations contained the biomass growth yield and the initial substrate concentration. To avoid identifiability problems in this experimental work and decrease the error propagation, the growth yields were determined first with specific experiments and then they were used in the respirometric determination of other parameters such as affinity constants for substrate or inhibition coefficients.

Following a controlled doses method developed for the particular needs of our project (see Section 4.2), stoichiometric coefficients for heterotrophic bacteria are measured by several COD, TAN or TNN pulses for heterotrophic, AOB and NOB bacteria respectively. They are all performed with different known injected reagent concentrations. According to the mass balance for the oxygen consumption, the growth yield for each kind of bacterial strain is defined as the biomass produced as COD per either oxidized carbon either oxidized nitrogen sources. This definition must be considered for the parameter determination and correct model calibration.

The controlled doses method allows to determinate the impact of a specific substrate by following the DO concentration and calculating the Oxygen Consumption (OC) associated to each dose. Each dose produces a curve between the time of substrate addition and the end of the OURexo curve where the DO reaches its initial concentration. By calculation of the area under this curve, it is possible to calculate the amount of oxygen used for decomposing the added substrate or chemical compound, according to the integration of equation 4.5:

$$OC = \int_{t_1}^{t_2} OUR.dt = kla \int_{t_1}^{t_2} (S_O^{eq} - S_O).dt \qquad (4.13)$$

4.3.4 Biokinetic parameters estimation

The parameter estimation was performed using the yield coefficients for the heterotrophic and autotrophic biomass calculated as explained in the previous paragraph. For each dose, knowing substrate concentration (S_s and S_{NH} at several times), the biokinetic parameters (μ_{max} and the several Monod and inhibition constants) for both organic carbon and nitrogen bio-degradation processes can be obtained by fitting the OUR calculated with the proposed model (in this case just the equations 4.10 to 4.12) to the experimental OUR data.

With these considerations, biokinetic parameters estimation is performed by fitting the experimental OUR values with the modelled ones. The estimated parameters are:

- μ_{maxH} X_H, K_s for the heterotrophic stub,

- μ_{maxN} X_N, $K_{s,FNA,N}$, $K_{i,FNA,N}$, $K_{i,FA,N}$ for the NOB stub.

This parameters estimation could be carried out by graphics interpretation with Origin software, or with the help of the AQUASIM software (the non-linear parameter estimation is based on the DASSL algorithm automatically integrated in the software).

The objective function to be minimized in AQUASIM is the sum of the squares of the weighted deviations between measurements and calculated model results:

$$\chi^2(\rho) = \sum_{i=1}^{n} \left(\frac{y_{(meas,i)} - y_i(\rho)}{\sigma_{(meas,i)}} \right)^2 \tag{4.14}$$

In this equation y_{meas_i} is the it_h measurement, σ_{meas_i} is its standard deviation, $y_i(\rho)$ is the calculated value of the model variable corresponding to the ith measurement and evaluated at the time and location of this measurement, $\rho = (\rho 1, ::: \rho m)$ are the model parameters and n is the number of data points.

It is possible to improve the precision of parameter estimation by optimal experimental design procedures.(Spanjers and Vanrolleghem, 1995b) demonstrated for example that the accuracy of the parameter estimation may be increased by a factor of 2 through an additional pulse of substrate given at an appropriate time during a respirogram. That is why our procedure includes LFS respirometry with several pulses of carbon and nitrogen substrates in a classical way, but also in the particular experimental conditions that allow to highlight the influence of a particular process.

Therefore, for specific substrate and saturation/inhibition constants (K_s and K_i), specific experimental design procedures should be used to control external factors and better determinate sensitive parameters. This is particularly true for the estimation of NOB biokinetic parameters.

For each pulse in the controlled doses method, the maximum OUR could be calculated for one specific dose of substrate. Knowing substrate concentration, it is possible to reach the saturation zone of the substrate for the particular bacteria strain. It is then possible to establish a relation between the rate of particular substrate consumption and the substrate concentration. This relation is normally linearly proportional when the concentration is small. But at higher concentrations the rate of consumption becomes independent of the substrate concentration. The Monod equation could take into account this kinetic characteristics:

$$V = V_{max} \frac{S}{S + K_m} \tag{4.15}$$

Applied to the specific substrate consumption equation 4.15 could be written as:

$$OUR = OUR_{max} \frac{S}{S + K_{sat}} \tag{4.16}$$

Where K_{Sat} represents the substrate concentration at which the reaction rate is half of its maximal value. OUR_{max} and K_S could be determined by varying the substrate concentration. They can be readily derived from OUR measured at different concentrations.

For a more detailed inhibitory terms, for example to describe the inhibitory effect of an substrate in excess, the Haldane-type equations are more reliable than the simple Monod approach. These more complex terms are carefully detailed in Chapter 2.

4.3.5   Parameters for heterotrophs

As no interference problems are related to the COD addition, it is not necessary to inhibit the autotrophic biomass, thus the controlled doses method could be used as many times as necessary without jeopardising the biomass taken from the pilot.

In our work, heterotrophic strain is not a major point of interest. Carbon removal in the MBR was just only verified weekly. The initial ratio C/N of the urine injected to the reactor, was not considered as a parameter to study. Specific parameters for heterotrophs where measure only once for the acclimated sludge of Jacquin et al. (2018) (presented in the Appendix B, in order to verify that in acclimated sludge, parameters for heterotrophs do not change from the classical sludge.

Growth yield

Y_H was estimated using LFS respirometry. Controlled specific COD pulses are performed with different known injected Sodium Acetate concentrations (COD_{pulse} of 2.5, 5, 12.6, 25.3, 38 mg/L) according to the controlled doses method. In theory, this could be achieved with only one pulse because only total OC and COD pulse concentration are required. But it would result in too much uncertainty on the yield calculation because of the sensitivity of this parameter to the OC and COD pulse values.

Substrate saturation/inhibition

For each pulse added for yield identification, the substrate specific consumption could be correlated to a Monod relation to determine the half-saturation constant K_s.

4.3.6   Parameters for NOB

NOB activity is given by equation (4.12). The evaluated parameters include apparent decay and growth rates (expressed as a product of the constant and the specific biomass value) and the half saturation constant for the TNN substrate. In this case, we are trying to determine the activity related to the second step of the nitrification process, that is why the first step due to the AOB activity must be eliminated to characterise correctly the NOB activity. This could be achieved by adding the necessary quantity of ATU to inhibit the AOB activity according to Ginestet et al. (1998). The necessary final concentration of ATU inside the respirometer is $10\,g_{ATU}\,m^{-3}$. This inhibition is toxic, what makes each one of the respirometric analysis a destructive one, as the biomass could not be re-injected to the MBR. This inhibition allows to correctly measure the nitratation biokinetic and stoichiometric specific parameters.

For the acclimated sludge in Strasbourg, one particular LFS test was performed after many hours of continuous aeration without substrate additions, to evaluate in a correct way the growth and decay terms.

Growth yield

Y_N was estimated using LFS respirometry. Controlled TNN pulses are performed with different known injected sodium nitrite $NaNO_2$ concentrations presented in the last section according to the controlled doses method. In theory, this could be achieved with only one pulse because only total OC and TNN pulse concentration are required. But it would result in too much uncertainty on the yield calculation because of the sensitivity of this parameter to the OC and TNN pulse values.

FNA saturation/inhibition

For each pulse added for yield identification, the substrate specific consumption could be correlated to a Monod relation to determine the half-saturation constant $K_{S_{FNA,N}}$. If enough excess quantity of substrate is presented, inhibitory conditions could be reached and the associated parameter could be estimated. In that case, the more reliable inhibitory term is the Haldane equation, that takes into account both, half-saturation and inhibition constants. In function of the results obtained, one of the inhibitory terms would be used.

FA inhibition

In order to determine the inhibitory effect of FA over NOB, specific OC was evaluated for a particular dose of TNN in a respirometer initially free of FA. Then, for the same dose of TNN, controlled and increasing doses of FA are added to the medium in order to evaluate each time the impact of this external concentration on the specific OUR for the specific TNN substrate quantity. Figure 4.10 represents better an example of this procedure.

Alkalinity half-saturation constant

As nitritation does not consume alkalinity at the same level as the nitritation, the estimation of the alkalinity related parameters is only feasible for the AOB bacteria via respirometric measures.

4.3.7 Parameters for AOB

AOB activity is given by equation (4.11). The evaluated parameters include apparent decay and growth rates (expressed as a product of the constant and the specific biomass value) and the half saturation constant for the TAN substrate. In this case we are trying to determinate the activity related to the first step of the nitrification process, that is why the second step due to the NOB activity must be eliminated to characterise correctly the AOB activity. This could be achieved by adding the necessary quantity of sodium azide NaN_3 to inhibit the NOB activity according to Ginestet et al. (1998). The necessary final concentration of NaN_3 inside the respirometer is $1.56\,g_{NaN_3}.m^{-3}$. This inhibition is toxic, what makes each one of the respirometric analysis a destructive one, as the biomass could not be re-injected to the MBR. This inhibition allows to correctly measure the nitritation biokinetic and stoichiometric specific parameters.

Growth yield

Y_A was estimated using LFS respirometry. Controlled TAN pulses are performed with different known injected ammonium chloride NH_4Cl concentrations according to the controlled doses method. In theory, this could be achieved with only one pulse because only total OC and TAN pulse concentration are required But it would result in too much uncertainty on the yield calculation because of the sensitivity of this parameter to the OC and TAN pulse values.

FA saturation/inhibition

For each pulse added for yield identification, substrate specific consumption could be correlated to a Monod relation to determine the half-saturation constant $K_{S_{FA,A}}$.

FNA inhibition

The procedure is similar to the one used to evaluate the FA inhibition over the NOB bacteria. In order to determine the inhibitory impact of the FNA over the AOB, specific OC was evaluated for a particular dose of TAN in a respirometer initially free of FNA. Then, for the same dose of TAN, controlled and increasing doses of FNA are added to the medium in order to evaluate each time the impact of this external concentration on the specific OUR for the specific TAN substrate quantity.

4.4 Results

The following results originate from from the respirometric analysis of the sludge obtained from a MBR without external chemicals addition for pH control, treating high nitrogen content wastewater and not performing complete nitrification (as described in section 3.3). All the parameters were determined using LFS respirometry in the respirometer with biomass withdrawn from the pilot plant. The pilot plant was operating as a 50% nitrification system with high concentration of TAN and TNN in the first reactor and producing an effluent with equal parts of TAN and TNN for more than 50 days (see Section 3.3). The respirometric protocol was the one described in section 4.2.

For the heterotrophic strain, one interesting analyse is presented in the appendix B. Indeed, as explained in the results in the appendix, it was demonstrated that no major changes were found in the parameters of heterotrophic bacteria. In fact, yield growth was found unchanged from the classical value and only biokinetic parameters were different. This is expected as the sludge was acclimated with a lower level in the ratio C/N of the urine. This ratio was an important operational parameter in the Jacquin et al. (2018) MBR pilot.

Inside the scope of the thesis, heterotrophic biomass was not characterized. The results presented here are related to the AOB and the NOB activity, nitrifying species that are the principal objective of the acclimated biomass.

4.4.1 Protocol specific features

Due to the fact the sludge analysed in this campaign comes from the pilot described in section 3.3, some characteristics of the respirometric protocol must be analysed.

Incomplete nitrification First, the incomplete nitrification regime inside the reactor leads to high remaining concentrations of ammonium that could eventually affect the execution of the controlled doses method. Thus, in order to achieve the endogenous state two options are possible:

- adding external alkalinity and wait the necessary time to consume the remaining ammonium,

- perform a solid/liquid separation method based on settling in a graduated cylinder to get rid of the excess ammonium by multiple washes.

The details are specified in section 4.2. The second protocol allows to reach quickly the endogenous state keeping the same conductivity as in the pilot (by dilution with saline solution) and also concentrating the biomass to compensate the potential loss in the supernatant during this "washing" protocol.

Alkalinity Secondly, the mixed liquor taken from the pilot displays a inorganic carbon limitation. This allows to implement a controlled doses method taking the bicarbonate as a reagent as described in equation 2.41. Hence, it can be considered as a pseudo-respirometric-titrimetric protocol. As no acid is added to keep the pH constant, this is not strictly a classical titrimetric protocol, but the pH evolution is followed according to the bicarbonate doses added to the respirometer. In these conditions of ammonium excess, the controlled doses method could be used to obtain half saturation constant for the bicarbonate as the main alkali component in the inorganic carbon.

Protocols assessment To compare the two proposed methods and analyse the impact or the possible perturbations of this washing protocol, two samples of biomass were taken to apply the same respirometry protocol. The first biomass was adjusted with the washing protocol to reach rapidly the endogenous state. The second one was taken weeks before and all the remaining ammonium substrate was consumed by controlled doses of bicarbonate. When the ammonium levels became very low AOB bacteria were inhibited to apply the respirometric test and compare with the first biomass sample. At the same time, the second biomass allows to evaluate the half saturation constant for the bicarbonates under an excess of ammonium substrate for the AOB bacteria.

4.4.2 NOB bacteria

To characterise the nitratation step, ATU was used as inhibitor of the AOB activity according to the concentration of $86\mu M$ presented by Ginestet et al. (1998). Even if the controlled doses method for the NOB bacteria implies the use of specific nitrite substrate that is supposed to inhibit the AOB bacteria, we prefer to avoid this interaction by inhibiting completely nitritation step. Two parallel respirometers were evaluated as explained before. The first one is evaluated with the respirometric test just after the "washing" protocol was implemented. The second biomass enters in decay regime following a long starvation period and then can be used to estimate correctly the autotrophic decay parameters.

The results of the controlled doses method are presented in the respirograms obtained in figures 4.3 and 4.4 respectively for the "washed" sludge and the old sludge where decay was relatively more important.

The OURexo associated to these figures are presented in figures 4.5 and 4.6. Here, several nitrite pulses were performed with different known injected sodium nitrite concentrations. For the first biomass, the eleven pulses were $NaNO_2$pulse= 0.5, 1.25, 2.5, 5, 7.5, 10, 15, 20, 25, 30, 50 mg/L. For the second biomass with more aeration time, the eight pulses were $NaNO_2$pulse= 0.5, 1.25, 2.5, 5, 15, 20, 25, 50 mg/L. All the batch tests were carried out at 23 °C and pH of 7.6 with biomass taken from the pilot plant.

At first view, the results of the calculated OURexo for the fresh biomass are almost four times bigger than the ones for the old biomass. This indicates already that some differences can be found between the two protocols to get rid of the ammonium excess described in section 4.2.
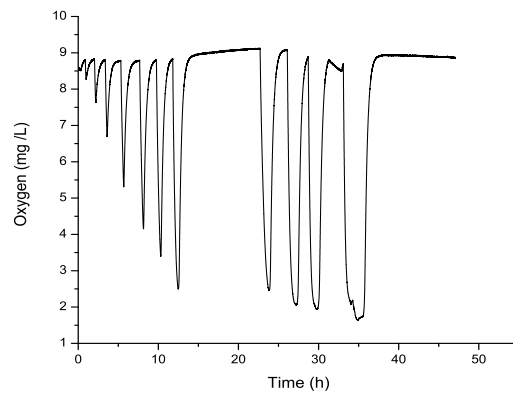
FIGURE 4.3: Respirogram for NOB bacteria for eleven doses of TNN over time in fresh "washed" sludge
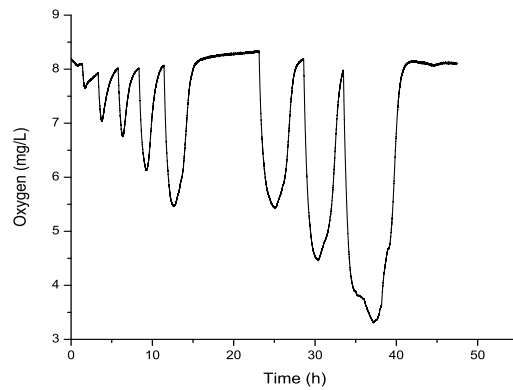
FIGURE 4.4: Respirogram for NOB bacteria for eight doses of TNN over time in old sludge
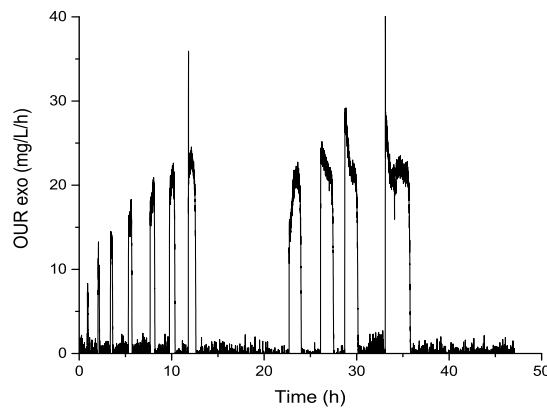
FIGURE 4.5: OURexo determination for NOB bacteria for eleven doses of TNN over time in fresh sludge.

Growth yield

After the controlled doses method, the total OC could be calculated as the area under the curve for each dose of TNN in the respirograms 4.5 and 4.6. The results are presented in figure 4.7. From this figure, the linear regression between the OC and the TNN quantity is obtained for each biomass and the NOB yield is calculated from
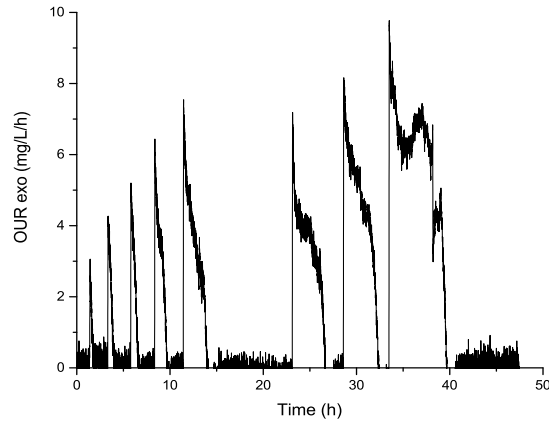
FIGURE 4.6: OURexo determination for NOB bacteria for eight doses of TNN over time in old sludge.

equation 4.17.

$$\frac{OC}{TNN_{\text{pulse}}} = \frac{(1.14 - Y_{\text{N}})/Y_{\text{N}}}{1/Y_{\text{N}}} = \frac{OC}{TNN_{\text{pulse}}} = 1.14 - Y_{\text{N}} \tag{4.17}$$
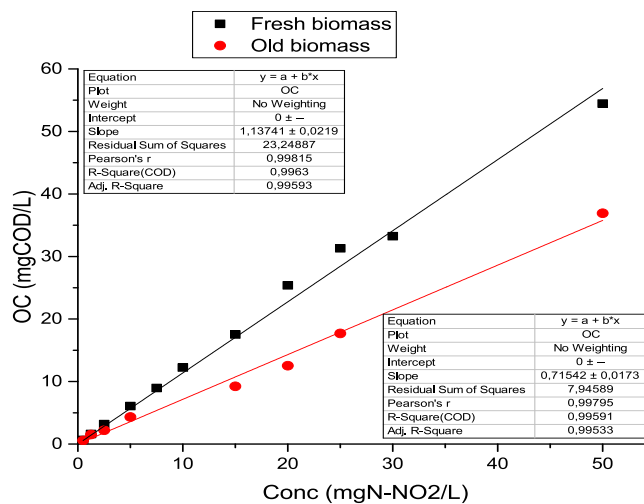
FIGURE 4.7: Biomass yields determination for NOB activity in fresh and old sludge: OC as a function of the TNN pulses for Y_{N} determinations

Figure 4.7 highlights a clear difference in the metabolic behaviour of the bacteria between the two sludges: the slope for the old one is significantly lower compared to the fresh "washed" biomass. The slope obtained from the linear regression was $1.0952 \, \text{mg}_{O_2} \, \text{mg}_{N-NO_2}^{-1}$ for the fresh biomass and $0.7154 \, \text{mg}_{O_2} \, \text{mg}_{N-NO_2}^{-1}$ for the "old" one. Therefore, Y_{N} is calculated considering biomass as $C_5H_7NO_2$):

- $(0.0448 \pm 0.0008) \, \text{gCOD} \, \text{gN}^{-1}$ or $(0.0315 \pm 0.0005) \, \text{gVSS} \, \text{gN}^{-1}$ for the fresh biomass,

- $(0.4246 \pm 0.0105) \, \text{gCOD} \, \text{gN}^{-1}$ or $(0.2990 \pm 0.0071) \, \text{gVSS} \, \text{gN}^{-1}$ for the old biomass.

The first impression is that the yield growth calculated for the old biomass is way to far from the normal values found in the literature (see Table 4.2). The different is almost 10 times the value calculated for the fresh biomass and the order of magnitude is to different to be compared directly with the values from the literature.

It is not easy to assess the origin of such big difference. The old biomass seemed to have a more important decay effect as the activity is lower: less oxygen is consumed to degrade a same dose of TNN if we compare to the "fresh" sludge. This means that the quantity of nitrogen assimilated by NOB biomass i_{xb} in this sludge should be taken into account for the calculations of Y_N (see Table 4.2 for more details).

These results validate somehow the "washing protocol" as a method to apply controlled doses in a sludge coming from a non complete nitrification reactor: the performance of the biomass is still good, the excess ammonium and nitrite compounds were effectively washed. Furthermore, the Y_N value was in the same order of magnitude than literature values.

FNA saturation/inhibition

The kinetic parameters of NOB $K_{S,FNA,N}$ and $K_{I,FNA,N}$ were determined in the acclimated biomass with TNN as the only substrate after AOB inhibition with ATU.

Increasing amounts of TNN were progressively added to the reactor. For every substrate concentration, OUR was determined. From the experimental data, one can establish the better inhibitory relation, in order to estimate the OURmax and the parameters $K_{S,FNA,N}$ and $K_{I,FNA,N}$.

Model	MichaelisMenten
Equation	y = Vmax * x / (Km
Plot	OURmax
Vmax	28,01437 ± 1,1255
Km	5,6826E-4 ± 1,1170
Reduced Chi-	3,44599
R-Square(CO	0,93305
Adj. R-Square	0,92562
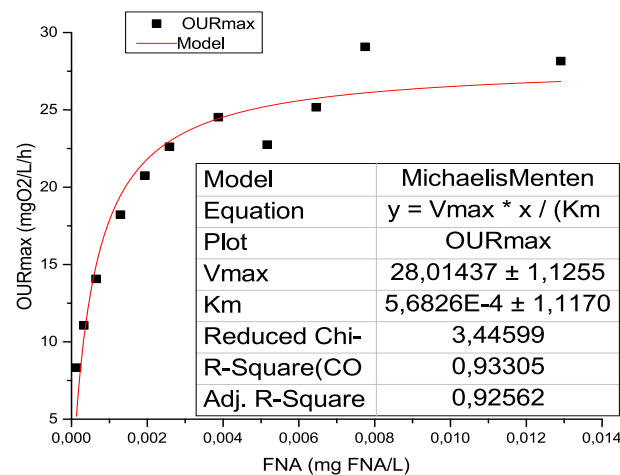
FIGURE 4.8: Experimental data for $K_{S,FNA,N}$ determination with LFS respirometry in fresh sludge.

Experimental data reveals that the inhibitory conditions were not reached for either of the biomass analysed. As shown in figure 4.8, for fresh sludge, the inhibitory concentration could not be reached completely. Therefore the protocol does not allow to estimate $K_{I,FNA,N}$ correctly. Thus, for a better identification of remaining parameters, the Haldane expression was simplified to a Monod term. This allowed to estimate the half saturation constant value like presented in equation 4.15. However, the value obtained for the parameter $K_{S,FNA,N}$ 5.683×10^{-4} $g_{HNO_2^- -N}.m^{-3}$ has over 20% of incertitude.

For the old biomass the figure 4.9 shows that the inhibitory zone was also not reached for this biomass, thus a calculation of the $K_{S,FNA,N}$ was made by fitting the Monod equation to the experimental data using the Origin Software tools.

From the results presented in figures 4.8 and 4.9, it is clear that the old biomass has a decreased activity. For a same TNN dose, the reached OURmax for the old
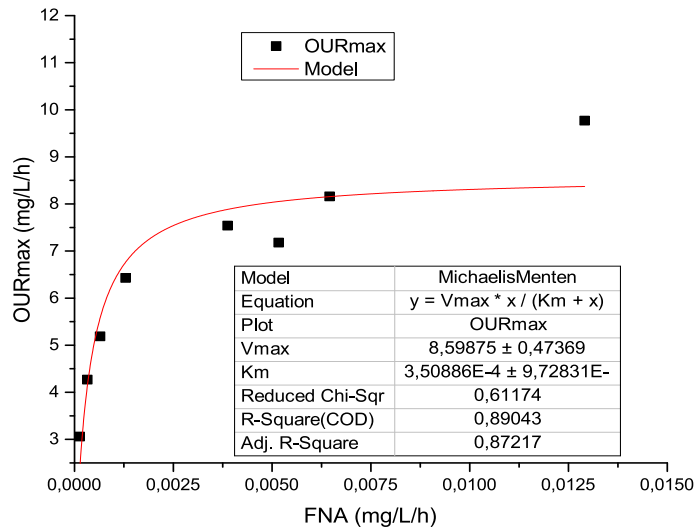
FIGURE 4.9: Experimental data for $K_{S,FNA,N}$ determination with LFS respirometry in old sludge.

biomass is lower than the one obtained with the fresh biomass. One can express this difference in terms of model's parameters.

For several authors in the literature (Antileo et al., 2002; Pambrun, Paul, and Spérandio, 2006), substrate affinity and inhibition coefficients can vary depending on the biomass acclimation protocol. This variations could be specifically related to substrate and the inhibitory compounds and/or to the biomass composition.

Comparing the calculated half saturation values obtained for the two biomass, it should be noticed that each strategy affects differently the NOB behaviour. The yield growth, the half-saturation constant and the OURmaximum obtained for the NOB in the old biomass are way to far from the expected literature values (see Table 4.2). Adding the necessary external alkalinity to consume the ammonium excess, leaving the biomass without controlled alkalinity doses deeply affect NOB activity. It generates an increase in the quantity of TNN in the medium and NOB are not able to handle it. This is valid inside the respirometer but also inside the reactor This fact emphasizes the importance of controlled pH ranges, to better tune both nitrifiers activity.

From now, only the fresh biomass will be characterised and the biokinetic parameters will be determined with this biomass, in order to avoid the influence of different protocols in the estimated values.

FA inhibition

The main difference between a reactor performing 100% or 50% nitrification will be the residual excess of ammonium in the medium. Thus, this FA excess could affect NOB activity. $K_{I,FA,N}$ value could probably change in function of biomass acclimation protocol, that should determinate NOB population changes.

From the controlled doses protocol presented in the beginning of the section, there is a slight change made for the FA inhibition determination. In all the graphics presented in this section the experimental conditions in the respirometric experiment were: pH = 8.6 and T 22 °C. These high pH and T were used to favor the presence of the inhibitory compound (FA) and also to avoid FNA inhibition to NOB.

ATU (10 mgL − 1) was used as specific inhibitor for AOB. The experiment consisted of successive equal TNN pulses ($10\,g_{NO_2^- - N}.m^{-3}$) with different FA concentration in the medium that was ensured by the injection of TAN into the liquid after the depletion of each TNN pulse. The first TNN pulse was carried out with the medium free of FA. Figure 4.10 shows the DO profile of some TNN pulses and the liquid FA concentration as an example of the used methodology.

Similarly to the half saturation substrate constant, the direct effect of the ammonium as inhibitor for the nitrous acid degradation could be evaluated from equation (4.12). Experimental data was fitted to equation (4.18) using Origin Software.

The experimental campaign started with two high NO_2 pulses of $50\,g_{NO_2^- - N}.m^{-3}$ to $60\,g_{NO_2^- - N}.m^{-3}$ that were applied 24 hours before the addition of FA and after adjusting the pH at 8.6 (figure 4.10).

(a) Total respirogram

(b) FA dosses
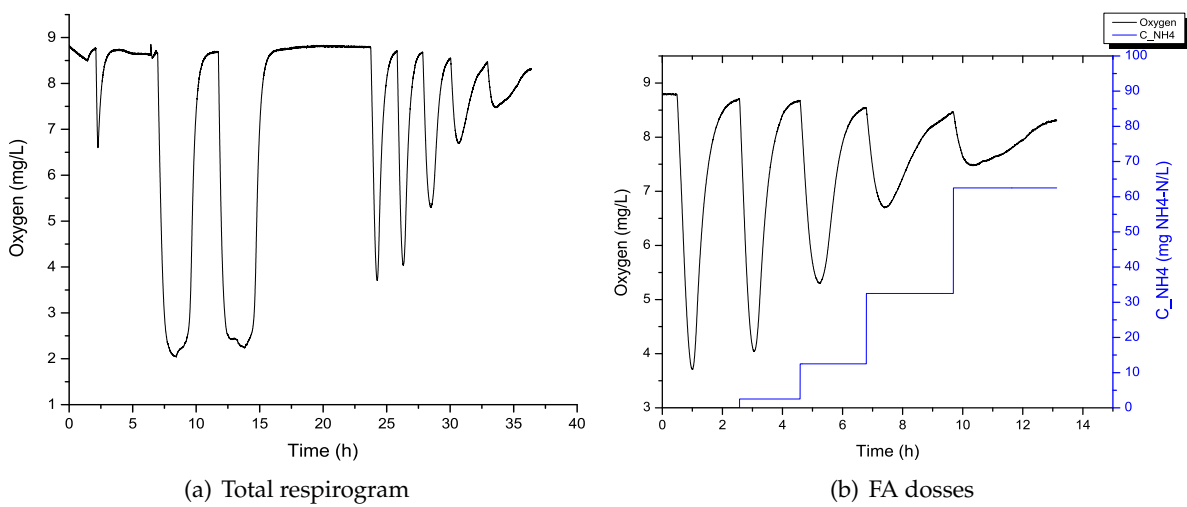
FIGURE 4.10: $K_{I,FA,N}$ determination with LFS respirometry in the respirometer DO profile and FA concentration in the medium along TNN pulses.

(a) OUR
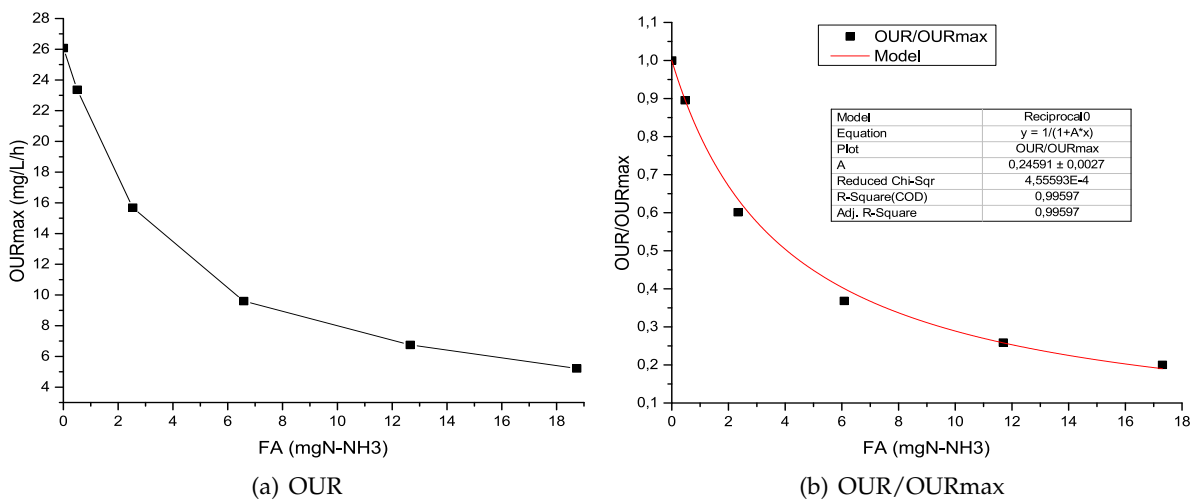
(b) OUR/OURmax

FIGURE 4.11: $K_{I,FA,N}$ determination with LFS respirometry in the fresh sludge OUR vs FA concentration, experimental data for model prediction with fitted parameter.

$$OUR/OUR_{max} = \frac{K_{(i,FA,A)}}{K_{(i,FA,A)+FA}} = \frac{1}{1 + FA/K_{(i,FA,A)}} \qquad (4.18)$$

From this procedure, we obtain for this particular acclimated sludge, a value of $4.067 \, g_{NH_3-N}.m^{-3}$ for the $K_{I,FA,N}$ constant. The value measured for the acclimated sludge of Jacquin et al. (2018) was $1.707 \, g_{NH_3-N}.m^{-3}$ with an MBR reactor controlled by external chemicals (see Appendix B). Few references are found in which this parameter was estimated. For Wett and Rauch (2003), a value of $1.9 \, g_{NH_3-N}.m^{-3}$ achieved the best fit during calibration. However, when the process (SBR with $1400 \, g_{NH_4^+-N}.m^{-3}$ to $2000 \, g_{NH_4^+-N}.m^{-3}$ in the influent) was operated under stable conditions the inhibition constant increased to $24.3 \, g_{NH_3-N}.m^{-3}$ due to sludge adaptation. In Chandran and Smets (2000), a value of $1.33 \, g_{NH_3-N}.m^{-3}$ was obtained from batch respirometric experiments. In that case the biomass had previously been enriched in nitrifying bacteria in a SBR with a $500 \, g_{NH_4^+-N}.m^{-3}$ feed. It is therefore clear that this inhibition coefficient highly depends on the population and its acclimation to FA.

Biokinetic parameters fitting

For the remaining apparent growth rate ($\mu_{max_N X_N}$) parameter, the estimation is made using the parameters obtained previously ($K_{(S,FNA,N)}$ that was estimated using Origin Software). Experimental data from the controlled doses method were fitted to a substrate saturation/inhibition equation 4.18 and parameter $\mu_{max_N X_N}$ was estimated using AQUASIM Software based on the developed model (chapter 2).

By fitting the parameters for the two high doses (pulses of $50 \, g_{NO_2^--N}.m^{-3}$ to $60 \, g_{NO_2^--N}.m^{-3}$ in figure 4.10) in the AQUASIM software as shown in the figure 4.12, it is possible to finally obtain the next set of parameters shown in table 4.1:
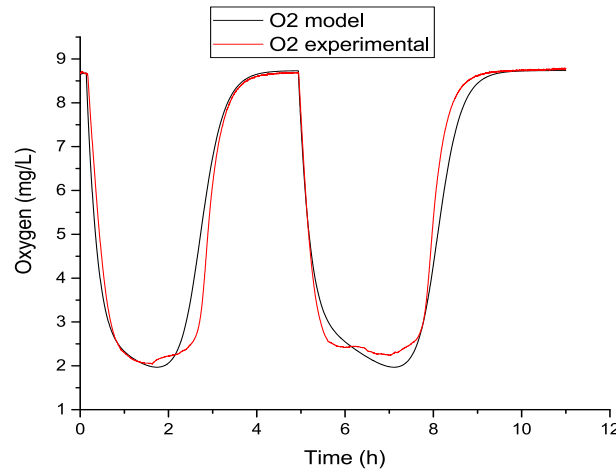
FIGURE 4.12: Parameters adjustment for NOB bacteria ($\mu_{max_N X_N}$ and $K_{(S,FNA,N)}$, $K_{(i,FA,N)}$ validation) for two TNN pulses.

The result of the estimated parameters for NOB activity under LFS respirometric test are presented in the figures 4.13 and 4.14. The summary of this parameters estimation is presented in table 4.2.

From these results, we can analyse directly the impact of the external control of pH by chemicals on the growth yield factor. It reached the maximum values when

$K_{(S,FNA,N)}$ (mg/L)	0.0005683
$\mu_{max_N}X_N$ (mg/L/h-1)	1.02

TABLE 4.1: Results of the fitting for the OUR profile with AQUASIM software
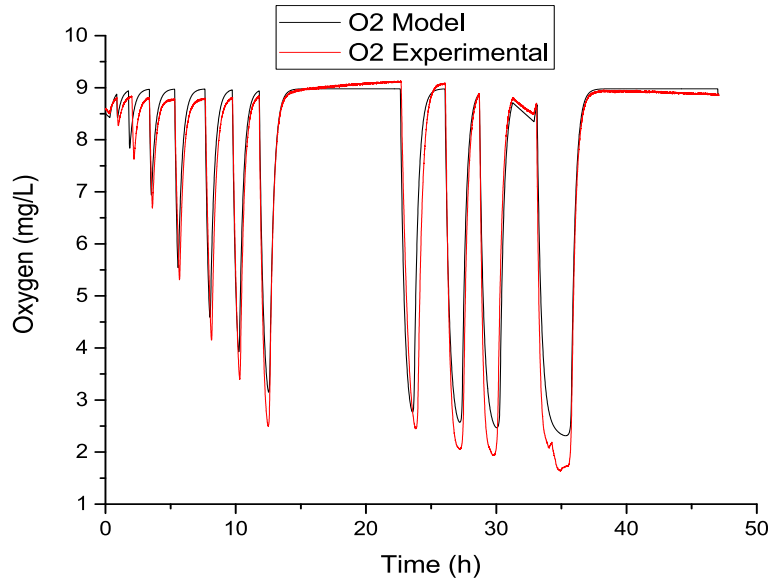
FIGURE 4.13: Parameters adjustment for NOB bacteria($\mu_{max_N}X_N$, $K_{(S,FNA,N)}$, $K_{(i,FNA,N)}$ and $K_{(O,N)}$ validation)
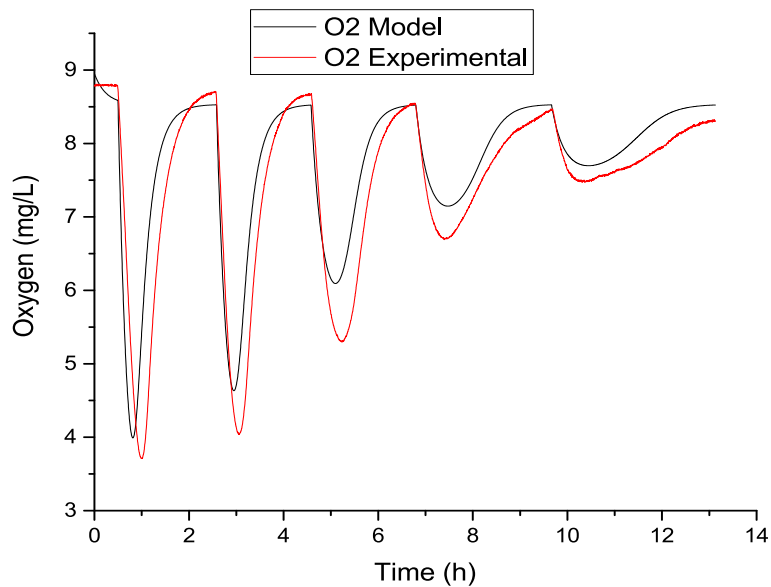
FIGURE 4.14: Parameters adjustment for NOB bacteria ($\mu_{max_N}X_N$, $K_{(S,FNA,N)}$, $K_{(i,FA,N)}$, $K_{(O,N)}$ and $K_{(i,FA,N)}$ validation)

external chemicals allows to control pH and supply the additional alkali needs to have a complete nitrification inside the reactor. From our experimental pilot performing 50% nitrification, the growth yield obtained is more or less half of the one

	Nitratation (NOB)						
	$\mu_{\max_N}X_N$	$b_N X_N$	K_{ON}	Y_N	$K_{S,FNA,N}$	$K_{I,FNA,N}$	$K_{I,FA,N}$
Jacquin et al., 2018[a]	7.2-72	-	-	0.0909	0.00131	-	1.7077
Strasbourg campaign	1.02	-	1.88	0.0448	0.0005683	-	4.067
Jubany et al. (2008)	14.875 [b]	0.17[c]	1.75	0.08	0.0081	0.45	9.5

[a]Characterised sludge see Appendix B
[b]Calculated with $\mu_{\max_N}$ value and the X_N biomass of $350\,\mathrm{g_{MLVSS}.m^{-3}}$ reported by the author
[c]b_N value

TABLE 4.2: Comparative results for NOB parameters estimation

obtained in the MBRs performing complete nitrification aided with external chemicals.

Affinity for oxygen seems to remain very similar, since the three studied reactors worked without any O_2 limitations, the NOB bacteria does not develop any kind of particular affinity at lower oxygen values.

Concerning half saturation constants, the order of magnitude differs when using or not chemicals to control pH. In the case of non total nitrification, the half saturation constant is almost 10 times lower that the ones obtained with external controlled pH. This means that in a non controlled scenario, the system will tend to be is less sensitive to nitrite accumulation: as the half saturation constant is lower, the maximum nitratation rate will be achieved at lower concentration of TNN.

In contrast, the value of $K_{I,FA,N}$ shows that the NOB acclimated with the strategy implemented in Strasbourg (see Section 3.3) would be more resilient to FA accumulation that could lead to a nitrite accumulation. In fact, the value is higher than the one obtained in the Jacquin et al. (2018) sludge, which means that more ammonium could be present inside the reactor without disturbing the NOB activity. In other words, the process is more stable since variations in FA contents can be handled without arriving directly to nitrite accumulation.

Concerning the effect of external chemical's, the inhibitory effects of FA on NOB are more important in the work of Jacquin et al. (2018) than the one from Jubany et al. (2008) ($K_{I,FA,N}$ values of 1.7 and 9.5 respectively). This could be the direct consequence of the acclimation strategy use by the two authors. Jacquin et al. (2018) increased progressively the NLR, whereas Jubany et al. (2008) used directly synthetic wastewater with high ammonium concentration $3000\,\mathrm{g_{NH_4^+-N}.m^{-3}}$.

With our strategy treating poorly diluted urine and without using external chemicals, the inhibitory impact of FA over the NOB ($K_{I,FA,N}$ value of 4.07) is in the middle of the values found in reactors performing complete nitrification but influenced by their acclimation strategy. This means that acclimated NOB are more accustomed to high FA by the fact of using concentrated and complete hydrolyzed urine to feed the reactor. Consequently, a good NOB tolerance to high ammonium environments without using external chemicals to stabilise pH.

Finally, regarding the factor $\mu_{\max_N}X_N$ the differences are clear between the MBRs with pH controlled by adding chemicals, where the activity is higher as the nitrification is completely achieved. This leads to a higher combined parameter $\mu_{\max_N}X_N$. The problem is that not differentiated analyses could be performed because the specific NOB concentration is not specifically known for each campaign (only Jubany et al. (2008) calculated it from long term TNN model fitting). Nevertheless, the MLVSS concentration reported in Montpellier (see Appendix B) were much higher than in Strasbourg: this is probably the reason explaining the higher $\mu_{\max_N}X_N$ estimated there.

It is important remember that the specific $\mu_{\max_N}$ could be influenced by temperature and pH. According to Jubany, Baeza, and Carrera (2007), the specif growth rate for both AOB and NOB bacteria is around 7.5-8 and decrease for pH above and below of this range leads to a bell-type shape that could be represented by the equation:

$$\mu_{\max_N}(pH, T) = \frac{6.69.10^7 \exp\left(\frac{-5295}{273+T}\right)}{1 + \frac{10^{-8.69}}{10^{-pH}} + \frac{10^{-pH}}{10^{-6.78}}} \tag{4.19}$$

which is the combination of (Hunik, Tramper, and Wijffels, 1994)

$$\mu_{\max_N}(T) = A\mu_{\max_N} \exp\left(\frac{-Ea_N}{R(273+T)}\right) \tag{4.20}$$

and the equation (Dochain and Vanrolleghem, 2015)

$$\mu_{\max_N}(pH) = \frac{\mu_{\max_N}(pH_{\text{opt}})}{1 + \frac{10^{-pk_1}}{10^{-pH}} + \frac{10^{-pH}}{10^{-pk_2}}} \tag{4.21}$$

Where pk_1 and pk_2 represents the high and the low pH values at which the growth is the half of the maximum growth rate $\mu_{\max_N}$ at the optimal pH (Holloway and Lyberatos, 1990).

Some differences between the measured values of the apparent growth rate and the specific growth rate in the references cited could be also related to the temperature of the test. Very slight temperature variations where observed between the respirometric test presented in this section and the one measured in the Jacquin et al. (2018) sludge (presented in the Apprendix B). The main different point is the biomass concentration ($2500\,g_{\text{MLVSS}}.m^{-3}$ for this work and $15\,000\,g_{\text{MLVSS}}.m^{-3}$ for Jacquin et al. (2018)). Specif information about Jubany et al. (2008) test conditions is available for biomass ($3000\,g_{\text{MLVSS}}.m^{-3}$) but not for temperature during the test, thus non conclusion could be made about temperature effect.

Conclusions

The impact of the two strategies for the implementation of the controlled doses method in the sludge coming from a non total nitrification reactor was evaluated in this section. The uncontrolled alkali dose method allowed to remove correctly the excess ammonium nitrogen inside the sludge but compromised the integrity of the NOB bacteria as the normal growth yield and the expected maximum OUR were seriously affected during the necessary days to consume all the remaining ammonium. In the other hand, the "washing" method allowed to remove the remaining excess of ammonium from the sludge taken directly from the reactor and seems to be a very good technique to apply efficiently the controlled dose method in this kind of sludge. Even if some of the biomass is lost in the supernatant, this is compensated by the concentration effect and then the overall biomass activity is not affected considerably. Nevertheless this is purely a practical solution, a new protocol to wash correctly the biomass is highly recommended to avoid the influence of physical separation on the parameters determination.

These respirometric protocols helps to identify stoichiometric parameters as the growth yield and some biokinetic parameters according to specific conditions inside the respirometer. The table 4.2 shows the comparative results for the obtained parameters between the two acclimated biomass characterised in this project (the first

one in this chapter, the second one in Jacquin et al. (2018) in Appendix B) and one literature source that applied a similar respirometric protocol over acclimated biomass with external chemical to control pH.

The temperature influence in the respirometer was no easy to control, as no thermostatic bath was use to control it. Respirometric protocol could be improved by adding a temperature system control that allows to minimise temperature changes inside the respirometer.

4.4.3 AOB Bacteria

In order to characterize the nitritation step, NOB bacteria were inhibited by NaN$_3$ according to the concentration of 24 μM reported by Ginestet et al. (1998). The protocol proposed by this author was followed according to the specifications, in order to avoid the NOB interference in the measured activity.

Due to some technical problems, the LFS respirometry technique could not be used during this test to evaluate the full AOB dynamics. Only the Y_A growth yield parameter could be derived. Three FA doses were successfully added to the respirometer, but at different periods of time. That is why two separate figures will be presented below.

Growth yield

The respirogram 4.15 shows the response of AOB bacteria to one dose of 2.5 $g_{NH_4^+-N} \cdot m^{-3}$ at a temperature of 27.5 °C and a pH of 7.3. From this figure, with a kla value of 4.60 h^{-1} the OC could be calculated as described in equation 4.13.
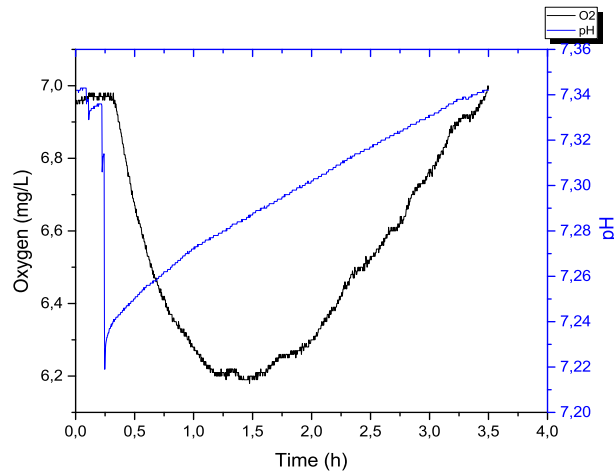
FIGURE 4.15: LFS respirometry technique for AOB growth yield estimation.

The AOB growth yield could be estimated for this particular sludge as:

$$OC = kla * \int_{t_1}^{t_2} (S_O^{eq} - S_O).dt = 4.60 * 1.71 = 7.85 mgO_2/L \tag{4.22}$$

$$\frac{OC}{TAN_{pulse}} = \frac{3.43 - Y_A}{1 + Y_A * i_{xb}} \tag{4.23}$$

The nitrogen content of the AOB nitrifiers was assumed to be $0.08\,\mathrm{g_{COD}.m^{-3}\,g_{NH_4^+-N}.m^{-3}}$ as the quantity assimilated by the biomass.

$$\frac{OC}{TAN_{pulse}} = \frac{7.85}{2.5} = 3.14 = \frac{3.43 - Y_A}{1 + 0.008 * Y_A} \tag{4.24}$$
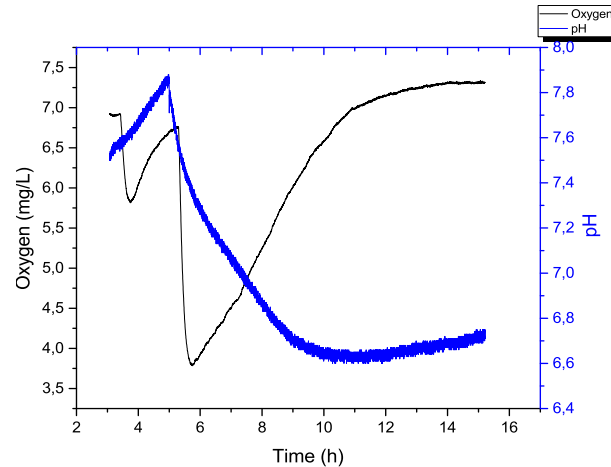
FIGURE 4.16: LFS respirometry technique for AOB parameters estimation.

From the two figures 4.15 4.16, the OC could be calculated for each dose and an arithmetical mean could be calculated to obtain the Y_a value.

The growth yield obtained from the arithmetical mean is $(0.278 \pm 0.006)\,\mathrm{gCOD\,gN^{-1}}$ or $(0.196 \pm 0.004)\,\mathrm{gVSS\,gN^{-1}}$. More doses are necessary to decrease the incertitude in the calculated parameter.

This calculated growth yield is used to estimate the other biokinetic parameters by fitting the respirogram 4.16 with the help of the AQUASIM Software.

Biokinetic parameters

From the same figure 4.16, a set of biokinetic parameters could be determinate by fitting both O_2 and pH profiles. The result of this combined fitting are presented in the figure 4.17 for the whole respirometric protocol.

The figure shows that the model predict correctly the trends of O_2 and the pH profiles, but some offset is still present, mostly for the oxygen prediction for the first dose. On the contrary, the predicted pH is really satisfactory as the proton production related to the nitritation process seems to be well predicted.

Alkalinity related parameters are more sensitive to pH variation, particularly the half saturation constant $K_{alk,a}$ and the initial value of the alkalinity inside the respirometer.

The maximum growth rate $\mu_{max_A X_A}$ and the half saturation constant for the substrate FA $K_{S,FA,A}$ were fitted against the O_2 profile using the growth yield Y_A calculated previously.

After this parameters fitting, a value of $0.282\,\mathrm{g_{NH_3-N}.m^{-3}}$ was found for the half saturation constant. This value as well as the other estimated AOB parameters are summarized and compare to literature values in Table 4.3.
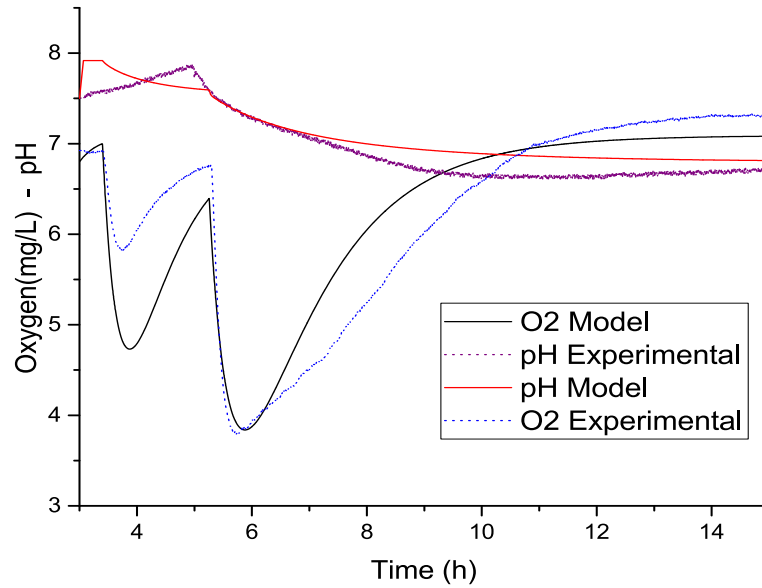
FIGURE 4.17: Parameters adjustment for AOB bacteria ($\mu_{\mathrm{max_A}X_A}$, $K_{(S,FA,A)}$ and $K_{\mathrm{alk},a}$)

Nitritation (AOB)			
	$\mu_{\mathrm{max_A}X_A}$	Y_A	$K_{S,FA,A}$
Strasbourg campaign	5.77	0.278	0.282
Jubany et al. (2008)	17.65 [a]	0.18	0.34

[a]Calculated with $\mu_{\mathrm{max_N}}$ value and the X_N biomass of $350\,\mathrm{g_{MLVSS}.m^{-3}}$ reported by the author

TABLE 4.3: Comparative results for AOB parameters estimation.

Conclusions

This respirometric campaign for estimating AOB parameters highlights some experimental difficulties. As the pilot was not performing total nitrification, the washing protocol has to be performed in order to get rid of the excess amount of ammonia. This could disturb the biomass and hampers OUR measurements. Nevertheless, it shows that the developed model has the potential to predict accurately pH variations due to AOB activity. In this respects, the alkalinity measurement is a crucial parameter to consider.

The obtained values for the AOB growth conditions, comparing particularly to the values obtained with LFS respirometry reported by Jubany et al. (2008), the AOB characteristics in this study are in similar levels. Since most of the key parameters, particularly FA inhibition constant were not able to be estimated, a careful look must be kept to forthcoming interpretations.

4.4.4   General conclusions

The results for the estimated parameters of AOB and NOB were compared to the literature values. From the references found, no acclimation strategy was similar to the one used in the present work. Nevertheless, the comparative analyse allows to highlight the importance of the acclimation protocol used in each study, over the biokinetic parameters measured.

The biokinetic parameters for NOB were compared to specif references working with biomass acclimated over an external pH control. Each acclimation strategy clearly affects the internal equilibrium between AOB and NOB. AOB activity control the pH inside the reactor, thus potentially the presence of nitrite accumulation as it was evidenced experimentally in the section 3.3. With that said, the differences in the estimated parameters could be related to the specific conditions of biomass acclimation.

Some of the scientific questions proposed in the Chapter 3 were also evidenced in the present results. To determinate whether or not there are differences between biomass acclimated via chemical control of pH or via the inlet urine flow control, the results from the present Chapter paves the way.

The parameters estimation presented here help to quantitatively assess the impact of the acclimation protocol choice, relative to the specific NOB growth and inhibition dynamics. It was evidenced that half-substrate constant, as well as the inhibitory constant by FA, were both affected by the particular conditions of the acclimated biomass. For instance, NOB acclimated in the present work was less sensible to the FA present in the reactor, relative to other authors were nitrification reached 100% without remaining ammonium. Biomass was adapted to the particular conditions of each reactor,

Finally, temperature could affect the result of the measures, principally for the apparent growth rate (as it was showed in equation 4.19). Some improvement of the respirometric protocol could be a thermostatic circulator or an alternative to better control temperature over the test.

Chapter 5

Model calibration, validation and predictive scenarios

Following biokinetic model development (chapter 2) and experimental assessment of nitrifying biomass adaptation to urine treatment in a MBR (chapters 3 and 4), this last chapter is focused on numerical studies involving the biokinetic model. First, a sensitivity analysis is performed to confirm the identifiability of parameters evaluated during respirometric tests and provide some guidance for future calibration exercise. Finally, a scenario analysis investigates the best conditions for biomass acclimation.

5.1 Identifiability and sensitivity analysis

Even an environmental model of moderate sophistication (like a classical ASM) is usually over-parametrized. This means that the measurements which are available to calibrate the model are not sufficient to determine optimal values of all model parameters. Consequently, parameter identifiability and the objective choice of "the best" sub-set of parameters for calibration is a major issue.

The model developed in this thesis has 35 parameters. In order to increase parameters identifiability, specific respirometric tests were conducted (see Chapter 4) and allowed to identify key parameters for AOB and NOB.

For the remaining ones, a methodology for parameter identification proposed by Brun et al. (2002) is used in order to identify and choose an optimal set of parameters for model calibration. It was applied prior calibration and validation steps.

5.1.1 Background

Model calibration is understood as the estimation of some of the model parameters by fitting certain set of experimental data obtained from a particular pilot study (Gernaey et al., 2004). It is necessary for carrying out the calibration to follow a single calibration protocol according to the model constraints. However, independently of the protocol, the calibration step is usually achieved through a trial and error approach by direct comparison to the experimental data. During this calibration a number of parameters are changed one at a time to fit the model. It is therefore important to select correctly the parameter subset to be tuned as the most important and sensitive ones. It is the key point, since an unsuitable parameters subset may lead to poor or incorrect fitting. Identifiability analysis is a good and well-known tool for finding an adequate parameter subset to fine-tune with.

For the sensitivity and identifiability analysis, the measurements used for model calibration have to be defined. The same measurements are used in sensitivity and

identifiability analyses. As a first step, a local (or linear) sensitivity analysis of the model parameters is performed. In local sensitivity, the effect of a parameter value in a very small region near its nominal value is estimated. The methods implemented are based in the Flexible Modelling Environment (FME) package in R and they are based on so-called "sensitivity functions" (Soetaert and Petzoldt, 2010).

5.1.2 Materials and methods

Initial parameters values

The local analysis investigates the influence of small changes of the parameter values on the model results. In contrast to a so-called global analysis, it does not account for parameter value changes within the complete range of possible parameter values. However, with a model like the one built in this thesis, the computational cost of a global sensitivity analysis would be prohibitive. Even though, a local sensitivity analysis gives very good and reliable results, if parameter values are close to their final values during sensitivity analysis (Brun et al., 2002). Thus, the initial parameters set values must be the most accurate and realistic values as possible. To accomplish this, initial values come either from the literature either from direct measurements as respirometric testing of the sludge processed in our reactor (see Chapter 4).

The sensitivity of the 35 parameters of the model was investigated. These parameters as well as there initial values are listed in Table 5.2

The main influent characteristics for the identifiability/sensibility analyse are summarized in Table 5.1.

Influent variables	Units	Identifiability
COD inlet	mg/L	500
TKN inlet	mg/L	100
TIC	gC/m3	100
X_n	mg/L	11,9
X_a	mg/L	254,66
X_h	mg/L	763,98
pH		7

TABLE 5.1: Input state variables

Identifiability analysis

First, an identifiability analysis is performed using the methodology defined in (Brun et al., 2002) which is based on a local sensitivity analysis. The objective of this analysis was to find the identifiable subset of parameters reliable enough to calibrate some of the components of biological MBR model. At the same time the results help to validate the parameter's quantification made by the direct measure in the respirometric test. Since evaluated parameters in those test are identifiable, the respirometric measures could be employed as direct calibration tools.

The first step of the identifiability analysis is the identification of the sensitive model parameters to be calibrated. For this purpose, all the parameters (all kinetic and stoichiometric parameters not depending on the temperature correction coefficients listed in Table 5.2) are selected. The identifiability analysis considered seven different outputs: NH_4^+, NO_2^-, NO_3^-, the total inorganic carbon via CO_2, HCO_3^-, CO_3^{2-} and the total protons production/consumption as pH. As a starting point, the

Name	Description	Unit	Value
$alphaC_{(S_s)}$	Carbon mass fraction of SS RWQM1 COD matrix	g C/ g COD SS	0.318
$alphaC_{(X_a)}$	Carbon mass fraction of bacteria RWQM1 COD matrix	gC/gXa COD	0.323
$alphaC_{(X_h)}$	Carbon mass fraction of bacteria RWQM1 COD matrix	gC/gX COD	0.323
$alphaC_{(X_n)}$	Carbon mass fraction of bacteria RWQM1 COD matrix	gC/gXn COD	0.323
f_p	Fraction of biomass leading to X_p	g COD/g COD	0.08
$f_{(Xi_0)}$	Percentage of inert particulate inlet COD	%	10
$f_{(Xs_0)}$	Percentage of slowly degradable inlet COD	%	29.8
$i_{(xb)}$	Nitrogen content of X_a X_n X_h	g N/g COD	0.08
$i_{(xp)}$	Nitrogen content of X_p	g N/g COD	0.06
$Kalk_a$	Affinity constant of alkalinity towards AOB	mol/m3	0.5
$Kalk_h$	Affinity constant of alkalinity towards heterotrophs	mol/m3	0.1
$Kalk_n$	Affinity constant of alkalinity towards NOB	mol/m3	0.5
keq_1	Kinetic constant for CO2 HCO3 equil.	d-1	100000
keq_2	Kinetic constant for the rest	d-1	10000
k_a	Ammonification rate	m3/g N/d	0.08
k_h	Maximum specific hydrolysis rate	g COD/g COD/d	3
$K_{i_{FA_A}}$	Inhibition constant for free ammonia of AOB	g FA/m3	7
$K_{i_{FA_N}}$	Inhibition constant for free ammonia of NOB	g FA/m3	0.95
$K_{i_{FNA_A}}$	Inhibition constant for free nitrous acid of AOB	g FNA/m3	2.044
$K_{i_{FNA_N}}$	Inhibition constant for free nitrous acid of NOB	g FNA/m3	0.13398
K_{o_A}	Affinity constant for DO of AOB	g O2/m3	0.74
K_{o_H}	Affinity constant for DO of heterotrophs	g O2/m3	0.2
K_{o_N}	Affinity constant for DO of NOB	g O2/m3	1.75
K_s	Affinity constant for S_s of heterotrophs	g COD/m3	4
$K_{s_{FA_A}}$	Affinity constant for free ammonia of AOB	g FA/m3	0.7504
$K_{s_{FNA_N}}$	Affinity constant for free nitrous acid of NOB	g FNA/m3	0.00238
K_x	Affinity constant for X_s	g COD/g COD	0.03
nu_h	Correction factor of anoxic hydrolysis		0.4
Y_a	Growth yield of AOB	g COD/g N	0.18
Y_h	Growth yield of heterotrophs	g COD/g COD	0.67
Y_n	Growth yield of NOB	g COD/g N	0.08

TABLE 5.2: Stoichiometric and kinetic parameters

relative sensitivity of each parameter j (in total 35) to each of the available measurements (henceforth called model outputs) y (seven in total) and at each time instant $i_{(S_{ij})}$, was calculated as:

$$S_{ij} = \frac{\delta y_i}{\delta \theta_j} \frac{\theta_j}{y_i} \tag{5.1}$$

From these sensitivities (S_{ij}) the sensitivity measure (δ_{yj}^{msqr}) was calculated for each parameter and output:

$$\delta_{yj}^{msqr} = \sqrt{\frac{1}{n} * \sum S_{ij}^2} \tag{5.2}$$

where n is defined as the number of measurements (at different time instants).

The equation 5.2 measures the mean sensitivity of a model output y_j to a change in the parameter θ_j (in the mean square sense). A high δ_{yj}^{msqr} means that the value of the parameter θ_j has great influence on the simulation result; a value of zero means that the simulation results does not depend on the parameter θ_j (Brun et al., 2002).

The total sensitivity of a parameter δ_{yj}^{msqr} was calculated as the sum of the parameter's δ_j^{msqr} over each output (y_j), according to Equation:

$$\delta_j^{msqr} = \sqrt{\frac{1}{n} * \sum (\delta_{yj}^{msqr})^2} \qquad (5.3)$$

The results of Equation 5.3 allow to rank the parameters with respect to their "tuning efficiency". The most sensitive parameters will be chosen for calibration.

The main criteria is that to be identifiable, a parameter subset K has to fulfil two conditions:

1. a model output $y(\theta)$ has to be sufficiently sensitive to individual changes to each parameter in K. This sensitivity is calculated by the sensitivity measure δ_j^{msqr}.

2. variations in the model output due to changes in single parameters may not be approximately cancelled by appropriate changes in other parameters. This analysis of parameter inter-dependence is addressed by the collinearity index, γ_K (elucidated in the next subsection) .

The determinant value, ρ_K, takes into account both identifiability conditions simultaneously and is, therefore, particularly suited for the assessment of the identifiability of parameter subsets.

After an identifiability analyse made with the assistance of the Rstudio software, these sensitivities ($i_{(S_{ij})}$) where obtained and the sensitivity measure (δ_{yj}^{msqr}) was calculated for each parameter and selected variable output as presented in the equation 5.1. The simulation was performed for a CSTR reactor for one day of operation (more than 20000 values) until steady-state was reached.

The results from the software simulation present a listed of absolute error (AR) ranking of roots of mean squared($r(av(SensAR^2))$), mean absolute($av(|SensAR|)$), mean ($av(SensAR)$) and maximum of sensitivities ($max(|SensAR|)$) for every single state variable of the model. The ranking is presented in the table 5.7 for the 25 most important parameters.

The global ranking summarises the next results

- L1 is the L1-norm, $\sum |S_{ij}|/n$ from the mean absolute($av(|SensAR|)$) values

- L2 is the L2-norm, $\sum S_{ij}^2/n$ from the roots of mean squared($r(av(SensAR^2))$)

- Mean: the mean of the sensitivity functions from the mean ($av(SensAR)$)

- Min: the minimal value of the sensitivity functions

- Max: the maximal value of the sensitivity functions

Parameters correlation

To analyse the correlation between the more sensible parameters identified before, a collinearity index could be calculated. The collinearity index (γ_K) is associated with a parameter subset K of size by the equation 5.4:

$$\gamma_K = \frac{1}{\sqrt{min\lambda_k}} \qquad (5.4)$$

In the equation 5.4 λ_k represents the smallest eigenvalue of the normalised determinant ρ_K. γ_K measures the degree of near-linear dependence between the sensitivity functions. It equals unity if the columns are orthogonal and it reaches infinity if the columns are linearly dependent. If the columns are nearly linearly dependent, changes in the model output, y, due to small changes in a parameter θ_j can be compensated to a large extent by appropriate changes in other parameters in K. This is indicated by a high collinearity index γ_K.

5.1.3 Results of sensitivity analysis

Set parameters identification

The results are presented in tables 5.3 to 5.6 for the single output variables NH_4^+, NO_2^-, NO_3^- and pH. It is important to note that the calculated uncertainty also depends on the initial chosen values of all other parameters.

The sensitivities for the pH, NH_4, NO_2 and NO_3 state variables are classed respectively in in tables 5.3, 5.4, 5.5 and 5.6 respectively.

	Parameter	r(av(SensAR^2))	av(|SensAR|)	av(SensAR)	max(|SensAR|)
		[gH/m3]	[gH/m3]	[gH/m3]	[gH/m3]
1	$alphaC_{Ss}$	3,0E-06	2,2E-06	2,2E-06	1,2E-05
2	keq_1	2,9E-06	8,3E-07	5,5E-09	3,7E-05
3	Y_h	2,8E-06	1,9E-06	-1,9E-06	8,4E-06
4	$alphaC_{Xh}$	2,3E-06	1,6E-06	-1,6E-06	8,5E-06
5	Y_a	1,6E-06	7,1E-07	-7,1E-07	9,3E-06
6	$K_{s_{FA_A}}$	1,1E-06	4,4E-07	-4,4E-07	8,6E-06
7	i_{xb}	6,8E-07	3,2E-07	-3,0E-07	2,7E-06
8	k_a	5,0E-07	1,5E-07	-1,5E-07	7,1E-06
9	keq_2	2,5E-07	6,8E-08	5,5E-11	8,0E-06
10	K_{o_A}	1,9E-07	8,3E-08	-8,3E-08	1,9E-06
11	$alphaC_{Xa}$	1,5E-07	6,6E-08	-6,6E-08	5,5E-07
12	f_{Xs_0}	8,9E-08	4,7E-08	4,6E-08	7,1E-07
13	$Kalk_a$	8,7E-08	2,2E-08	-2,2E-08	1,0E-06
14	K_s	4,7E-08	4,3E-09	-1,9E-09	1,8E-06
15	k_h	4,4E-08	1,7E-08	-1,2E-08	4,1E-07

TABLE 5.3: Variable: S_h (averages over 20001 values)

Taking a closer look at the first fifteen parameters in tables 5.3 to 5.6, a set of ten parameters could be identified as common for the four output state variables selected (NH_4^+, NO_2^-, NO_3^- and pH). These parameters are: Y_h, $alphaC_{Ss}$, $alphaC_{Xh}$, i_{xb}, Y_a, $K_{s_{FA_A}}$, k_a, f_{Xs0}, $alphaC_{Xa}$, K_{o_A}.

As can be observed in table 5.7 , Y_n,Y_a,$K_{s_{FNA_N}}$,$K_{s_{FA_A}}$, $alphaC_{Ss}$, Y_h, $alphaC_{Xh}$, k_a and K_{ON} are by far the most sensitive parameters. Among the others, values were lower and more uniform.

The nine parameters found to be most sensitive are all closely connected to AOB and NOB dynamics. The kinetic parameters for half saturation of both strains directly govern the access to the main substrate and also the possible inhibitory conditions for substrate consumption. Consequently, along with the stoichiometric growth yield, the former two half saturation parameters also govern the production and consumption of protons in the system.

	Parameter	r(av(SensAR^2))	av(|SensAR|)	av(SensAR)	max(|SensAR|)
		[g/m3]	[g/m3]	[g/m3]	[g/m3]
1	Y_h	1,6E+00	1,5E+00	-1,5E+00	2,6E+00
2	$alphaC_{Ss}$	1,5E+00	1,5E+00	1,5E+00	2,0E+00
3	$alphaC_{Xh}$	1,1E+00	1,1E+00	-1,1E+00	1,7E+00
4	keq_1	7,7E-01	2,3E-01	1,1E-04	9,3E+00
5	i_{xb}	4,0E-01	3,2E-01	-3,2E-01	1,0E+00
6	Y_a	2,6E-01	1,6E-01	-4,6E-02	8,8E-01
7	$K_{s_{FA_A}}$	2,2E-01	1,1E-01	1,9E-02	8,7E-01
8	keq_2	6,3E-02	2,1E-02	9,3E-05	8,7E-01
9	k_a	6,0E-02	5,2E-02	-3,2E-02	2,7E-01
10	f_{Xs_0}	5,9E-02	3,5E-02	-1,4E-02	1,9E-01
11	$alphaC_{Xa}$	4,1E-02	2,5E-02	-2,5E-02	1,1E-01
12	K_{o_A}	4,0E-02	2,2E-02	3,1E-03	1,5E-01
13	k_h	1,8E-02	7,8E-03	-7,1E-03	7,9E-02
14	$Kalk_a$	1,2E-02	4,5E-03	2,1E-03	5,7E-02
15	K_x	7,6E-03	3,5E-03	3,4E-03	3,0E-02

TABLE 5.4: Variable: NH_4 (averages over 20001 values)

	Parameter	r(av(SensAR^2))	av(|SensAR|)	av(SensAR)	max(|SensAR|)
		[g/m3]	[g/m3]	[g/m3]	[g/m3]
1	Y_h	11,40	9,28	-9,28	20,61
2	Y_a	11,17	8,80	-8,80	21,17
3	$alphaC_{(Xh)}$	8,85	7,06	-6,85	16,38
4	$alphaC_{(Ss)}$	7,30	6,04	5,70	12,83
5	$K_{s_{(FA)_A}}$	6,17	4,87	-4,87	11,69
6	$i_x b$	3,79	2,92	-2,92	7,294
7	K_{o_A}	1,34	1,07	-1,07	2,511
8	keq_1	0,94	0,68	0,05	3,625
9	Y_n	0,73	0,51	0,51	1,615
10	k_a	0,72	0,48	0,20	1,752
11	f_{Xs_0}	0,71	0,42	-0,41	1,709
12	$K_{i_{FA_A}}$	0,38	0,31	0,31	0,6901
13	K_{o_N}	0,31	0,22	0,22	0,6936
14	$alphaC_{Xa}$	0,22	0,17	-0,15	0,4536
15	$K_{i_{FA_N}}$	0,22	0,15	-0,15	0,4507

TABLE 5.5: Variable: NO_2 (averages over 20001 values)

More surprisingly, another group of parameters related to heterotrophic bacteria seems to be relatively important. $alphaC_{Ss}$ and $alphaC_{Xh}$ represent the fraction of carbon inside readily biodegradable substrate and heterotrophic bacteria respectively. The heterotrophic growth yield Y_h is also of importance. Here again we can highlight the direct link of these parameters with the quantity of inorganic carbon produced during heterotrophic growth and no sign of substrate inhibition effect could be established.

Finally the ammonification rate and the oxygen saturation constant for NOB seems to have an interesting impact also, indicating that urine dynamics and oxygen conditions are also important facts to take into account.

	Parameter	r(av(SensAR^2))	av(ǀSensARǀ)	av(SensAR)
		[g/m3]	[g/m3]	[g/m3]
1	Y_h	1,81	1,30	-1,30
2	$alphaC_{Ss}$	1,61	1,20	1,20
3	$alphaC_{Xh}$	1,46	1,05	-1,05
4	Y_a	1,26	0,88	-0,88
5	$K_{S_{FA_A}}$	0,79	0,56	-0,56
6	Y_n	0,73	0,50	-0,50
7	i_{xb}	0,53	0,36	-0,36
8	K_{o_N}	0,31	0,21	-0,21
9	$K_{i_{FA_N}}$	0,21	0,15	0,15
10	K_{o_A}	0,15	0,10	-0,10
11	$alphaC_{Xa}$	0,08	0,06	-0,06
12	keq_1	0,07	0,05	0,03
13	k_a	0,04	0,03	-0,03
14	$Kalk_n$	0,04	0,02	-0,02
15	$Kalk_a$	0,03	0,02	-0,02

TABLE 5.6: Variable: NO_3 (averages over 20001 values)

In contrast, other parameters directly related to AOB and NOB dynamics, such as inhibitory K_i constants, are quite insensitive in the tested conditions. Whit that said, it is not surprising that in the conditions presented in the Chapter 4, (where it was not possible to achieve the inhibitory conditions) it was difficult to identify and quantify clearly the inhibitory constant.

Hence, confirming the findings of Haag and Westrich (2002), the results of the sensitivity analysis highlight the importance of AOB and NOB dynamics for the inorganic carbon prediction and therefore correct pH dynamics prediction. It is noteworthy that half saturation concentrations of organic carbon, oxygen and alkalinity for heterotrophic bacteria are also quite insensitive, indicating that the concentrations of these nutrients are still in excess and do not limit heterotrophic growth. The maximum specific hydrolysis rate and the affinity constant for X_s shows intermediate sensitivity, indicating that this nutrient contribution is also important and even more in process like the one of this project that works with infinite SRT.

On the basis of this ranking, only the more sensitive parameters could be considered identifiable. There is not a clear cut-off value for the δ_j^{msq} to determinate the identifiability of a parameters set (Ruano et al., 2007). However, based on experience, a threshold value of 0.05 was chosen as a cut-off value to select the most significant parameters and reduce the computational time for further collinearity index and determinant measure calculations. As a result, a subset containing the 19 parameters presenting the higher δ_j^{msq} was selected according to equation 5.3.

Correlation between parameters

Combining the information of the parameters' sensitivity with information about their identifiability allows choosing an optimal parameter subset for calibration. A parameter can be well identified, if the effect of tuning its value (on the state variables used for calibration) cannot be compensated by changing the values of other

Ranking	Parameter	value	L1	L2	Mean	Min	Max	N
1	Y_n	8.0e-02	0.290	0.695	-5.7e-04	-2.249	2.246	7506
2	Y_a	1.8e-01	0.227	0.396	7.4e-02	-0.874	1.084	7506
3	K_sFNA_N	4.0e-04	0.166	0.39473	7.7e-04	-1.2647	1.268	7506
4	K_sFA_A	2.4e-01	0.214	0.37130	7.2e-02	-0.8021	1.010	7506
5	$alphaC_{Ss}$	5.7e-01	0.158	0.242	6.3e-02	-0.681	0.475	7506
6	Y_h	6.7e-01	0.118	0.205	-1.1e-01	-0.697	0.078	7506
7	$alphaC_Xh$	5.2e-01	0.107	0.164	-4.3e-02	-0.332	0.468	7506
8	k_a	8.0e-02	0.080	0.137	4.8e-02	-0.289	0.402	7506
9	K_{o_N}	1.8e+00	0.05827	0.122	1.4e-03	-0.3947	0.387	7506
10	$Kalk_n$	5.0e-01	0.043	0.10403	9.4e-04	-0.3891	0.389	7506
11	i_{xb}	8.0e-02	0.03132	0.05949	3.8e-03	-0.0998	0.218	7506
12	$Kalk_a$	5.0e-01	0.029	0.054	1.1e-02	-0.126	0.156	7506
13	k_h	3.0e+00	0.022	0.040	1.9e-02	-0.043	0.139	7506
14	K_x	3.0e-02	0.021	0.038	-1.7e-02	-0.138	0.060	7506
15	K_oA	7.4e-01	0.019	0.035	5.8e-03	-0.0771	0.097	7506
16	keq2	1.0e+04	0.005	0.01424	1.3e-03	-0.3683	0.37102	7506
17	i_xp	6.0e-02	0.004	0.00938	-4.2e-03	-0.043	0.000	7506
18	f_p	8.0e-02	0.004	0.00805	-5.9e-04	-0.018	0.026	7506
19	K_iFA_N	9.5e-01	0.004	0.007	2.6e-04	-0.0185	0.022	7506
20	keq1	1.0e+05	0.004	0.007	5.7e-04	-0.024	0.023	7506
21	$alphaC_{Xa}$	5.2e-01	0.004	0.007	-1.5e-03	-0.017	0.016	7506
22	$alphaC_{Xn}$	5.2e-01	0.002	0.004	-7.4e-04	-0.011	0.010	7506
23	K_iFA_A	7.0e+00	0.002	0.004	-1.7e-03	-0.015	0.010	7506
24	K_s	4.0e+00	0.001	0.003	-1.4e-03	-0.019	0.01001	7506
25	K_iFNA_A	5.5e-01	0.001	0.003	-2.0e-04	-0.015	0.010	7506
26	nu_h	4.0e-01	0.002	0.003	1.7e-04	-0.010	0.00812	7506
27	K_iFNA_N	6.0e-02	0.001	0.002	-2.6e-05	-0.007	0.006	7506
28	K_oH	2.0e-01	0.001	0.002	-7.0e-05	-0.005	0.005	7506
29	$alphaN_{Ss}$	6.0e-02	0.00034	0.0006	3.1e-05	-0.0034	0.003	7506
30	$alphaN_{Xh}$	1.2e-01	0.00023	0.0003	-1.0e-04	-0.0018	0.002	7506
31	$alphaH_{Xh}$	8.0e-02	0.00019	0.0003	-7.0e-05	-0.0019	0.002	7506
32	$Kalk_h$	1.0e-01	0.00014	0.0002	-1.0e-04	-0.0019	0.001	7506
33	$alphaH_{Ss}$	8.0e-02	0.00012	0.0002	-7.4e-05	-0.0010	0.001	7506
34	f_{Xi0}	1.0e+01	0.000	0.000	0.0e+00	0.000	0.000	7506
35	f_{Xs0}	3.0e+01	0.000	0.000	0.0e+00	0.000	0.000	7506

TABLE 5.7: Parameter significance ranking

parameters. Such information can be gained from the dependence of the parameters' sensitivity functions. The method used to determine the linear degree of dependence of the sensitivity functions is similar to the collinearity analysis applied in linear regression analysis.

This type of bivariate sensitivity analysis can also be performed on several variables. The figure 5.1 shows the results from a bivariate sensivity analyse. The zoom for the nine selected variables from the Table 5.7 is presented in figure 5.2.
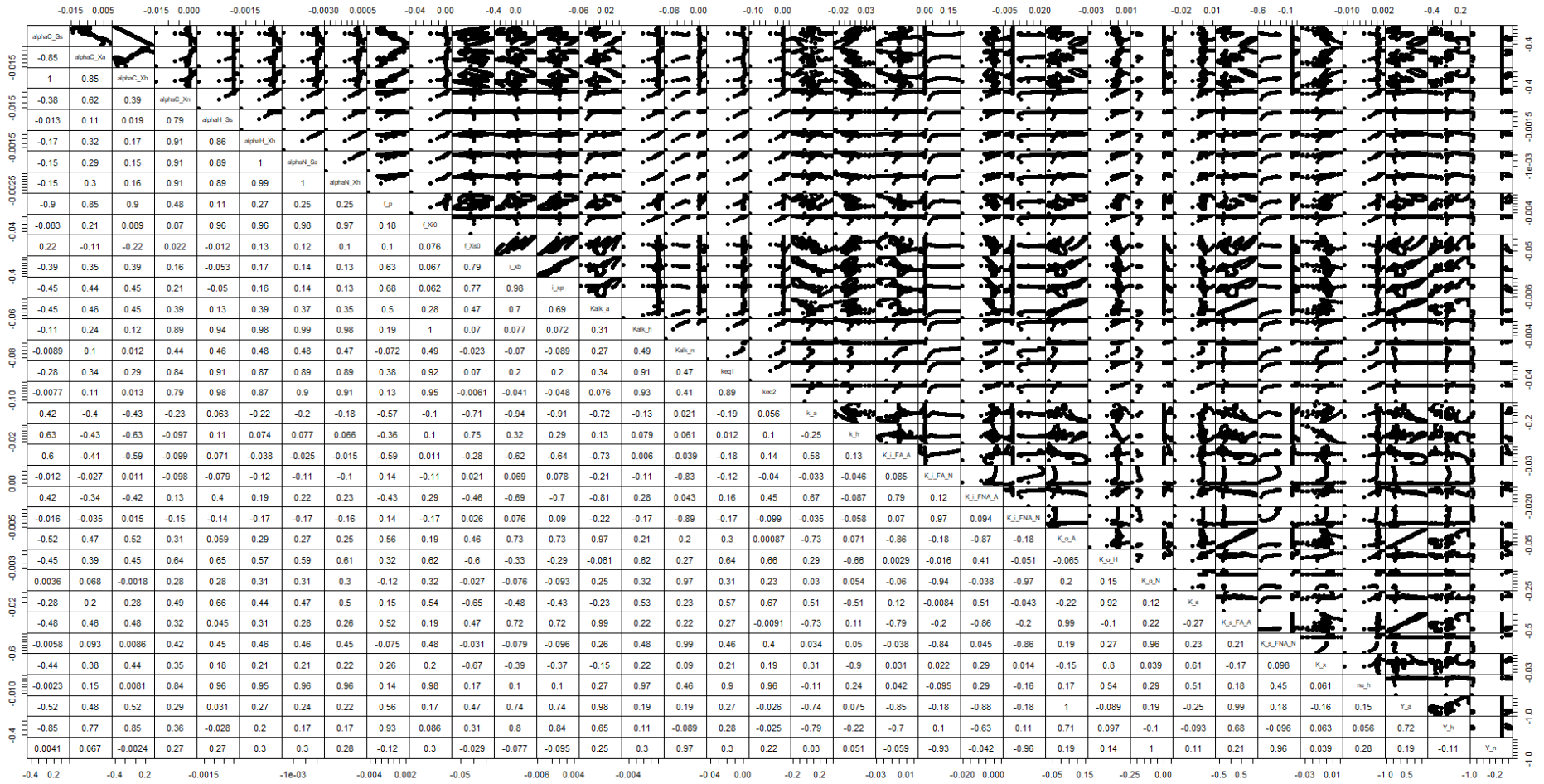
FIGURE 5.1: Pairs of sensitivity functions
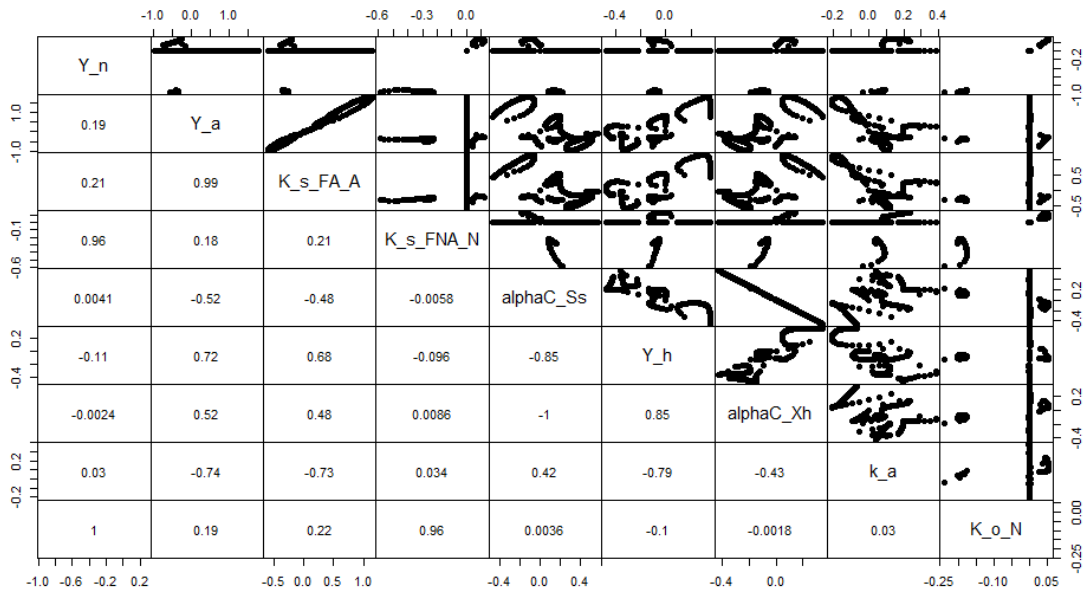
FIGURE 5.2: Pairs of sensitivity functions for the nine selected parameters

Due to their higher sensitivity, the nine parameters were further investigated with respect to their identifiability. We calculated the collinearity indices of subsets of the nine most sensitive parameters according to table 5.7. The results, starting with the most sensitive parameter and adding the other less sensitive parameters one at a time, are shown in figure 5.3.

The larger the collinearity value, the less identifiable the parameter based on the initial conditions imposed and the data. In general a collinearity value less than about 20 is considered as "identifiable". Based on experience from other authors in the literature (Brun, Reichert, and Künsch, 2001; Haag, 2006; Ruano et al., 2007), a collinearity value of 5 was chosen as the cut-off value in this study.

Figure 5.3 plots the collinearity of the nine most sensitive parameters according to table 5.7. The collinearity index is plotted as a function of the number of parameters selected. We add a line at the height of 5, the critical cut-off value.

The threshold of $\gamma = 5$ is clearly exceeded for a combination of the five most sensitive parameters $Y_n, Y_a, K_{s_{FNA_N}}$, alphaC$_{Ss}$, Y_h. This indicates that the best fit values of these five parameters cannot be simultaneously identified by inverse calibration. For the subset of the nine most sensitive parameters the collinearity index lies way above 5.

To further analyse which parameters are responsible for the high collinearity of the subset, we determined the collinearity of all possible parameter pairs within the sub-set of the nine most sensitive parameters as presented in figure 5.3. As a hint for the direction of collinearity, we also calculated the correlation coefficient (according to Pearson) of the sensitivity functions. The results of this analysis are shown in figure 5.2. The most significant collinearity (positive or negative correlation) emerges for the pairs Y_a-$K_{s_{FA_A}}$, Y_n-$K_{s_{FNA_N}}$, Y_n-K_{O_N}, alphaC$_{Ss}$-alphaC$_{Xh}$, $K_{s_{FNA_N}}$-K_{O_N}. The collinearity index for each pair is 11.89, 5.34, infinite, infinite, 5.22 respectively.

For the first pair, this very high collinearity can be explained as follows: the degree of compensation is more than 91%, *i.e.* $\gamma = 11.9$. Thus, changing simulation
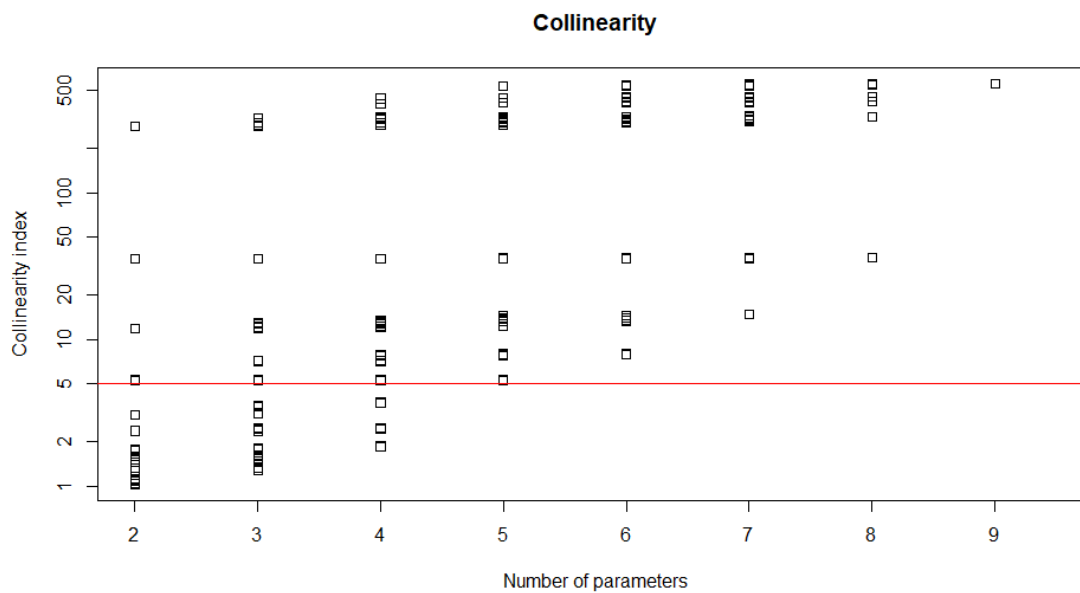
FIGURE 5.3: Collinearity analysis for the nine selected parameters

values by a modification of the AOB growth yield can be almost completely compensated by inversely varying the half saturation constant for the substrate. In conclusion, it is almost impossible to simultaneously identify the parameter set values of Y_a-$K_{s_{FA_A}}$ from inverse calibration.

Knowing their effects upon simulated concentrations, there are other pairs of parameters with a relatively high collinearity of their sensitivity functions, even infinite values. However the pairs Y_n-$K_{s_{FNA_N}}$, $K_{s_{FNA_N}}$-K_{O_N} have collinearity index of almost 5 and correlation coefficient near to one.

To finally decide on the parameters subset to be used in calibration, we use the collinearity index of various subsets of the nine most sensitive parameters presented in the figure 5.3. In order not to lose valuable information, it is important to choose the largest possible parameter subset. In this particular case, the maximum subset size accomplishing the collinearity threshold was four. The results indicate that there are some combinations of four parameters (out of the nine most sensitive parameters) with a γ less than 5. Additionally, we take the following statements into account:

- growth yield was obtained successfully from respirometric test for heterotrophic bacteria (see Appendix B) and NOB.

- half saturation constant for free nitrous acid was obtained successfully from respirometric test for NOB.

- heterotrophic bacteria carbon content $alphaC_{Xh}$ and also α carbon mass fractions of soluble carbon $alphaC_{Ss}$ came from the RWQM1 COD matrix.

Table 5.8 displays the possible four parameters sets with a γ almost equal to 5.

From the table 5.8, the possible combination of 4 parameters includes $alphaC_{Ss}$ and $K_{s_{FNA_N}}$. Thus taking into account the criteria exposed above, we decided to calibrate our model by adjusting the following kinetic parameters: Y_a, $K_{s_{FA_A}}$, k_a and K_{o_N}.

Y_a	$K_{S_{FA_A}}$	$K_{S_{FNA_N}}$	alphaC$_{Ss}$	k_a	K_{o_N}	**N**	γ
0	0	1	0	1	1	4	5.23
0	0	1	1	1	1	4	5.23
1	0	1	0	1	1	4	5.23
0	1	1	0	1	1	4	5.23
0	0	1	0	1	1	4	5.24

TABLE 5.8: Possible identifiable set parameters

Choice of parameters subset for calibration

Since the calibration method is usually performed output by output following step-wise procedures and experience based protocols (*i.e.* Insel et al. (2006) and Corominas et al. (2011)), the identifiability of the parameters subset for each output was also studied. The initial set values parameters where maintained constant (at the conditions of diluted urine), and the influence of their variation was not studied in this work. The identifiability measurements for each output were calculated independently and the results are summarised in Tables 5.9 to 5.13:

i_{xb}	k_a	K_{o_A}	N	γ
1	1	0	2	3.47
1	0	1	2	4.13

TABLE 5.9: Identifiability results pH set parameters

i_{xb}	k_a	f_{Xs0}	K_{o_A}	N	γ
0	1	1	1	3	4.29

TABLE 5.10: Identifiability results NH_4 set parameters

i_{xb}	k_a	$K_{S_{FNA_N}}$	K_{o_A}	f_{Xs0}	K_{o_N}	$K_{i_{FA_N}}$	N	γ
0	0	1	1	0	0	0	2	2.74
0	0	0	1	0	1	0	2	2.95
0	0	0	1	1	0	0	2	3.11
0	1	0	1	0	0	0	2	3.28
1	0	0	1	0	0	0	2	4.13
0	0	1	0	0	0	1	2	4.34

TABLE 5.11: Identifiability results NO_2 set parameters

$K_{i_{FA_N}}$	k_a	K_{o_A}	$Kalk_n$	i_{xb}	$K_{i_{FNA_N}}$	$Kalk_a$	N	γ
1	1	0	0	0	0	0	2	2.87
0	1	0	0	0	1	0	2	3.53
1	0	0	1	0	0	0	2	3.94
0	1	1	0	0	0	0	2	4.23
1	0	0	0	1	0	0	2	4.48
1	0	0	0	0	0	1	2	4.84

TABLE 5.12: Identifiability results NO_3 set parameters

$K_{s_{FA_A}}$	$i_x b$	K_{o_A}	k_a	f_{Xs0}	$Kalk_a$	$K_{i_{FA_A}}$	k_h	N	γ
0	0	0	1	0	0	1	0	2	2.09
0	0	0	0	0	1	1	0	2	2.57
0	0	0	0	0	0	1	1	2	2.79
0	0	0	0	1	0	1	0	2	2.86
1	0	0	0	0	0	1	0	2	2.95
0	1	0	0	0	0	1	0	2	2.97
0	0	1	0	0	0	1	0	2	3.81
0	0	1	1	0	0	0	0	2	4.04
0	0	0	1	0	0	0	1	2	4.37

TABLE 5.13: Identifiability results TIC set parameters

As can be observed, maximum subset sizes of 2, 3, 2, 2 and 2 were obtained for pH, ammonium, nitrite, nitrate and TIC respectively. With regards to nitrate, it should be noted that any combination of the most sensitive parameters accomplished the cut-off value for NO_3^- output.

Once these results were obtained, the next action was to define the possible parameter subset in order to proceed with the correct selection. Accordingly, the parameter subset accomplishing the collinearity threshold and with the highest determinant value was chosen for NH_4^+, NO_2^-, NO_3^-, TIC and pH. The selected parameter subsets are summarised in Table 5.14.

Output	**Parameter subset**	γ
pH	i_{xb}, k_a	3.47
NH_4	k_a, f_{Xs0}, K_{o_A}	4.29
NO_2	K_{o_A}, K_{o_N}	2.95
NO_3	$K_{i_{FA_N}}$, k_a	2.87
TIC	k_a, $K_{i_{FA_A}}$	2.09

TABLE 5.14: Identifiability set parameters for each variable

5.1.4 Conclusions

In this section, an identifiability study was made based on a local sensitivity analyse. Variation of the 35 parameters (initial values in the Table 5.2) that compose the physio-biological model was made, to quantify the impact in the model outputs. This influence was graded and grouped in different subset parameters. A bivariate sensitivity analysis was employed for choosing the optimal set parameters.

From Table 5.8 it could be confirm that the half-saturation parameters for AOB and NOB are identifiable and thus direct measure via respirometric test is a faithful tool for their quantification. Same could be said for the yield growth factor.

From the identifiability and sensibility analyse it could be said also that inhibitory parameters ware quite insensitive in the tested conditions. Despite the fact that no global analyse as performed, these results helps to anticipate the scenario where inhibitory conditions are reached in the respirometric test. In that particular case, it could be said that the direct measures of the inhibitory parameters is not possible as not particular identifiability is preconized.

The particular subset parameters presented in Table 5.14 paves the way to continue the analyse of the model parameters. This wok should be done via a particular

calibration campaign where each particular output state variable could be measured constantly. This path leads the way to increase the sensibility analyse ,and validate and calibrate some of the remaining most sensible parameters.

5.2 Avoiding nitrite build-up in a MBR: A simulation study

The production of an effluent with a proper nitrate to ammonium ratio is essential for the treatment goal of our process. As observed before in Chapter 3, bicarbonate content is a key parameter for controlling the degree of nitritation (also observed before by Van Hulle et al., 2005). Streams with a bicarbonate excess may also imply other consequences, such as a decrease on the inhibition pressure over NOB, due to the decrease in FA concentration, although this situation may be balanced by increasing the FNA levels.

The experimental investigations carried out in this study confirmed that stable urine nitrification in a MBR is challenging to obtain (see Chapter 3). Because of the huge variability that exists among ammonium and bicarbonate concentrations, it is crucial to identify the limits of the system to avoid at maximum nitrite build-up.

The complex interplay between acid-base equilibria and the growth of biomass makes the identification of optimal start-up conditions challenging. The model developed in Chapter 2 could help in this regard. Defining different scenarios, one can analyse the performances of the system as well as the involved mechanisms (substrate limitations or inhibitions, etc.).

Therefore, this section will investigate numerically the following issues:

1. is it possible to reliably implement the on/off control strategy that was investigated experimentally?

2. what is the optimal pH range for quicker biomass acclimation in terms of enrichment in AOB and NOB respectively?

3. what is the influence of biokinetic parameters value on the estimation of the optimal scenario?

4. what is the impact of feeding with fresh or stored urine (confirming or not the hypothesis made in Chapter 3)?

5.2.1 Material and methods

Influent conditions

In order to assess the influence of variations in ammonium and bicarbonate concentrations from source separated urine on nitrite build-up, different concentrations of both chemical species were taken up, being specifically defined for each scenario. On the other hand, only negligible concentrations of nitrite and nitrate were considered and it was also assumed that AOB, NOB and heterotrophic biomass content in the influent was insignificant.

Regarding the organic matter, an elevated organic matter concentration in the concentrated urine $1400\,\mathrm{g_{COD}.m^{-3}}$ was considered, similar to the levels reported in this work (see Chapter 3). The influent characteristics are shown in Table 5.15.

Biokinetic parameters

In order to confirm the results of sensitivity analysis and assess the impact of biokinetic parameters in combination with the control strategy, two sets of parameters were used for NOB mainly. The first one originates from respirometric tests presented in 4. The second one originates from the work of Jubany et al. (2008). Both are summarized in Table 5.16.

Parameter	Non ammonified urine	Ammonified urine
pH	7.66	8.5
TKN (mg/L)	1240	1240
NH_4/TKN	6%	84%
COD (mg/L)	1400	1400
Alkalinity (mg $CaCO_3$/L)	416	5100
χ (μS/cm)	11211	11211
T (°C)	20	20

TABLE 5.15: Inlet urine characteristics used for the simulated scenarios.

	NOB parameters				
	Y_N	$K_{S,FNA,N}$	$K_{I,FNA,N}$	$K_{I,FA,N}$	$K_{S,FA,A}$
Strasbourg campaign	0.0448	0.0005683	0.06	4.067	0.282
Jubany et al. (2008)	0.08	0.0081	0.06	9.5	0.24

TABLE 5.16: Used NOB parameters during simulations

pH **variations**

In order to assess the pH range influence, the following values were tested: 5.80-5.85, 6.20-6.25 and 7.00-7.05.

5.2.2 Model implementation

The initial conditions were defined according to a steady-sate simulation using the typical influent composition of a domestic wastewater treatment plant in France (see Appendix C). This yielded the concentrations of autotrophic biomass in the 5 times diluted activated sludge used for pilot-scale experiment inoculation procedure (see Chapter 3). The values are presented in Table 5.17.

Parameter	Unit	Value
Xa	(mg/L)	7
Xn	(mg/L)	17
Xh	(mg/L)	300
NH_4	(mg/L)	100
Alkalinity	(mg C/L)	50
χ	(μS/cm)	500
T (°C)	20	20

TABLE 5.17: Initial conditions used for the simulated scenarios.

The bioreactor was modeled as semi-continuous stirred tank reactor with complete biomass retention. Its volume was 34 L and the inlet/outlet flowrate was $30\,\mathrm{L\,d^{-1}}$ (when the pump was on according to the control strategy).

The model developed in chapter 2 was implemented in an Ordinary Differential Equations solver (Hindmarsh, 1982) allowing for setting-up the on-off control strategy to feed the reactor according to pH set values.

The results were evaluated in terms of nitrification performances, nitrite build-up and biomass growth. In order to get further insight in the mechanisms, the respective Monod and/or inhibition terms were also computed as presented in Chapter 2, paragraph 2.1.2 for AOB and NOB respectively.

5.2.3 Simulation results

Figures 5.4 to 5.18 present the simulation results obtained for the different scenarios: nitrogen species evolution, biomass concentrations, inhibition/Monod terms. Each scenario was simulated using two parameters sets (specifically for the NOB parameters came from Chapter 4 and Jubany et al. (2008)).

One first global conclusion is that the numerical implementation successfully managed to reproduce the control strategy and the gradual increase of NLR. pH variations which trigger the influent pump are well captured by the model. However, after a certain time (varying depending on the scenarios), the pH cannot reach the upper setpoint anymore, yielding a continuous pumping. This is problematic as this phenomenon was not observed experimentally (it was tending to but only at the very end of acclimation period during the experiment with stored urine, see Chapter 3). For some scenarios, this situation corresponds to an acclimated biomass (no nitrite accumulation) but in some others, NOB were already inhibited at this stage.

After some investigations varying the inlet and initial conditions in terms of inorganic carbon (results not shown), it was observed that these values were of critical importance to predict very accurately pH dynamics and ensure that the control strategy behaves as expected. Also, response time of the pH probes and PLC system was not incorporated in our model implementation: this could have an impact especially for the feeding events which can be very short.

The following subsections discuss in more details the various scenarios results.

Modelling validation of pH control

The next figure 5.4, enable to validate the experimental PLC control strategy (used in chapter 3) from a numerical point of view. In fact, the trend is correctly captured by the model, but for pH range 7.00-7.05, at some point the flow-rate became constant and makes pH decrease constantly as the pH could never reach the highest set-point. Nevertheless, it validates the fact that inlet feeding could be governed by pH measures and that the conceptualized model is able to correctly integrate this pH dynamics in common with the physico-chemical process that occurs in the liquid phase.

For the three scenario presented in the figure 5.4, the initial TIC is the same. In the inlet urine, the HCO_3 is almost 100% at pH of 8.5. At the same pH, NH_4 is the main component of the inlet nitrogen as it was consider almost completely ammonified. In hydrolysed urine the buffering capacity of bicarbonate HCO_3 demand large quantities of acid to lower the pH (Udert, Larsen, and Gujer, 2006). It means that in terms of buffer capacity, the inlet urine does not variate but only when it is mixed inside the reactor at the operative pH. As a trend evidenced in the results, it seems that this buffer intensity change with pH in the reactor impose in the acclimation protocol.

From a numerical point of view, the pH imposed to the reactor changes from a slightly acid range until a neutral one. Looking at the distribution diagrams, we are in the region of combined predominance of HCO_3 and dissolved CO_2 (pka1=6.352, pka2=10.329) as the main components of the TIC. At acid pH, alkalinity is more
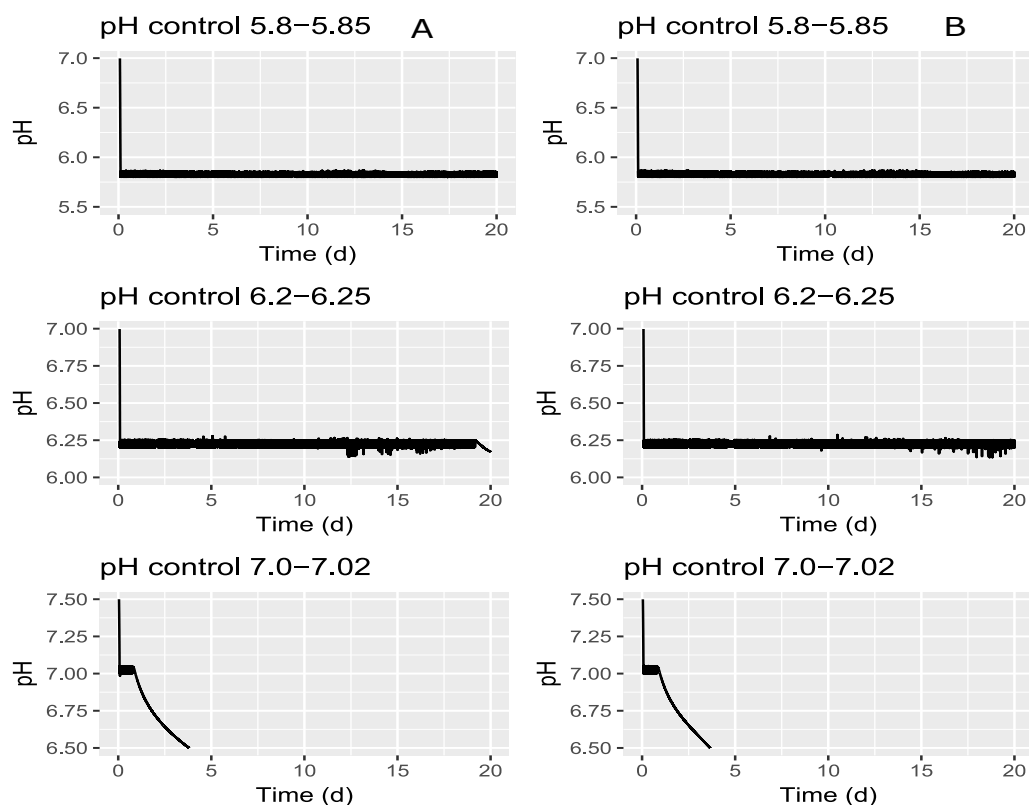
FIGURE 5.4: Model pH dynamics prediction over time. At left (A) biokinetic parameters from Jubany et al. (2008), at right (B) biokinetic parameters from the present work.

present in the form of dissolved CO_2. At neutral pH, alkalinity is present mainly as HCO_3. The buffer capacity, represents the amount of base or acid needed to change the solution pH by one unit. In fact, a minimum buffer capacity exists around pH 8.3 and at pH values less than 8, alkalinity has a significant effect on the buffer capacity (Eddy, 2003). That is the reason why during the simulation, it was observed that inlet and initial conditions in terms of inorganic carbon limitations (results not shown), were of critical importance to predict very accurately pH dynamics. At the lower pH values, buffer capacity is more important and thus more urine is needed to increase the pH inside the reactor. At neutral pH values the consumption of alkalinity in the nitrification process results in a poor buffering capacity in the reactor. pH decreasing dynamic is more important that the high buffer capacity of bicarbonate HCO_3 in the urine, even with permanent inlet flow.

Nevertheless, this numerical analyse seems contradictory to the Figure S2 in the work of Fumasoli, Morgenroth, and Udert (2015); where the buffer intensities of a synthetic urine solution with $968\,g_{NH_4^+-N}.m^{-3}$ and TIC lower than $4\,g_C.m^{-3}$, increase with the pH, passing from $0\,mmol/L$ to $2.5\,mmol/L$ between pH 5 and 7 (taking into account that ammonia and phosphate were the buffer compounds). This preliminary contradiction needs to be clarified in the upcoming works.

The acclimation strategy based on a semi-continuous operation in founded on the evolution of the pH and could be evaluated in terms of NLR increase. Thus, a calculation of the real injected volume over the time could be carried out in order to determinate punctual NLR and quantitatively assess the real input to the reactor. As an example, the Figure 5.5 presents the evolution of the simulated acclimation campaign at pH 6.20-6.25 of concentrated and highly ammonified urine. For the rest of the results in this section, the NLR results are not shown.
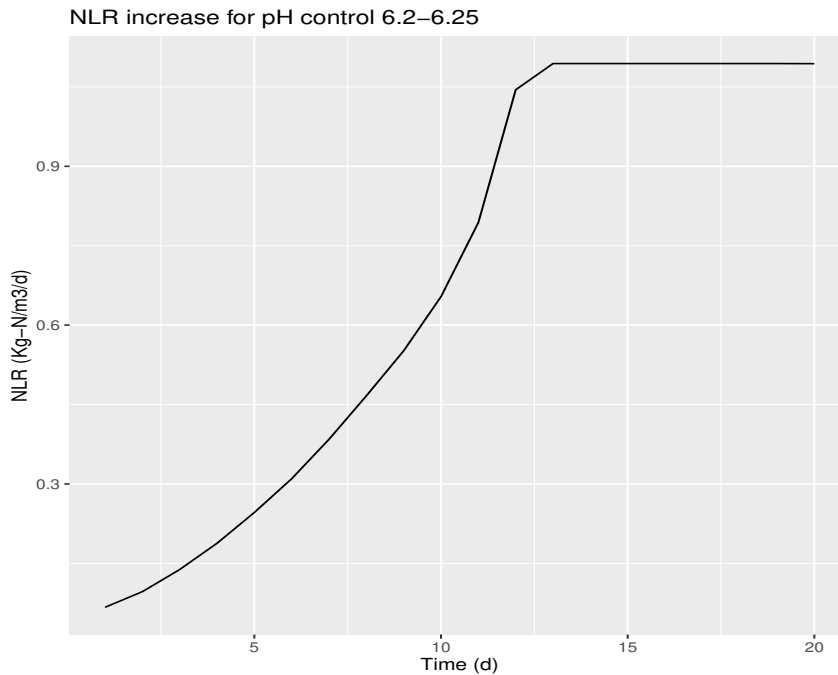
FIGURE 5.5: Example of the NLR over time for the simulated acclimation campaign.

It is important to highlight that for computational reason, the extended time in the simulation was fixed to 20 days, knowing that a constant NLR value was achieved even before the final time. Thus, this represents the results for a real acclimation protocol after the first 20 operative days. The numerical problem encounter at pH 7 will be discuss purely in a numerical approach.

Influence of pH value

The evolution of the nitrifying biomass acclimation and the necessary acclimation times are presented next in figures 5.6 and 5.7, in function of three different pH set ranges. Also, the two different biokinetic parameters sets for the NOB listed in the Table 5.16 are compared.
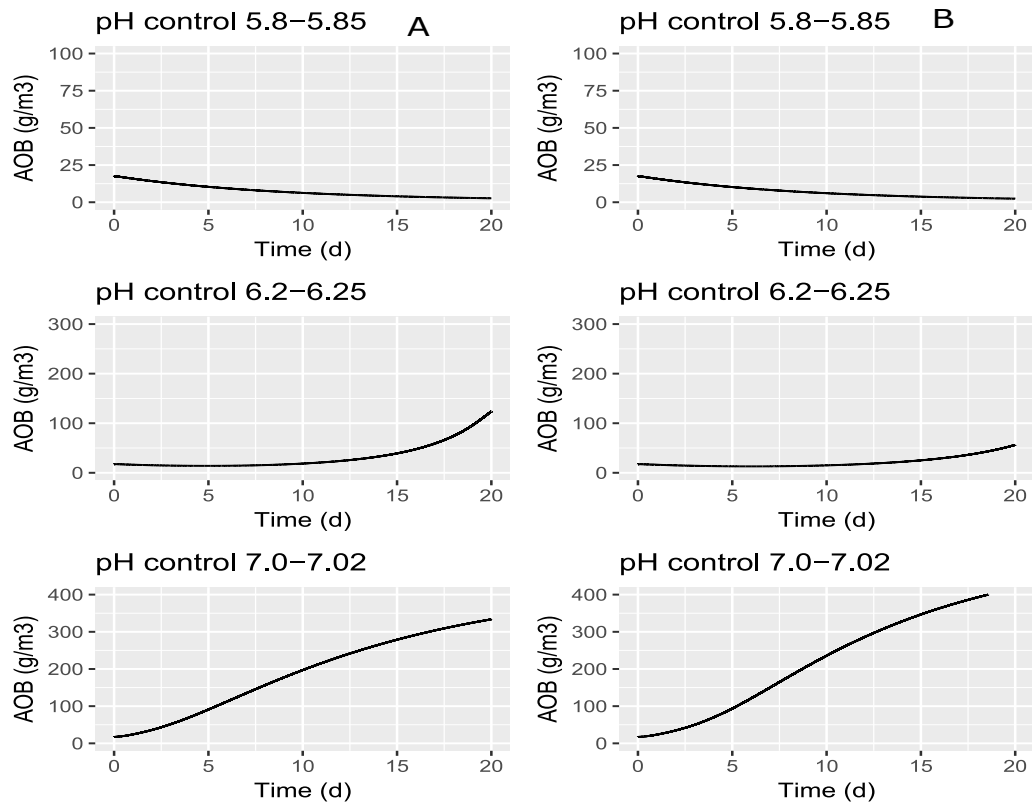

FIGURE 5.6: Predicted AOB evolution over time. At left (A) bioki-
netic parameters from Jubany, Baeza, and Carrera (2007), at right (B)
biokinetic parameters from the present work.

From the Figures 5.6 and 5.7, the total acclimation time and the maximum biomass concentration that could be obtained for each pH set range could be assessed. These figures also pinpoint the influence of biokinetic parameters on the predictions with (A) parameters from Jubany, Baeza, and Carrera (2007) and (B) parameters from the present study.

For the AOB acclimation, Figure 5.6 highlight the fact that more acid pH values resulted in a biomass washout whatever the biokinetic parameters used. In general terms, the higher the pH, the higher the AOB concentration. With Jubany, Baeza, and Carrera (2007) parameters, pH 6.20-6.25 seems to lead to the enrichment in NOB bacteria twice than with the parameters from the present work. At neutral pH, biomass result are in the same order of magnitude.

Also related to the pH dynamics, equations 4.19 to 4.20 shows that for NOB, at a same temperature $\mu_{\max_N}$ (and also valid for the $\mu_{\max_A}$) increase with the pH. This helps us to understand the why biomass washout is presented at acid pH (in addition to the alkalinity limitation and buffer intensity explained in the last subsection).

For the NOB acclimation in terms of increasing pH set-range, the situation is highly dependent on biokinetic parameters. The same behavior is observed for pH
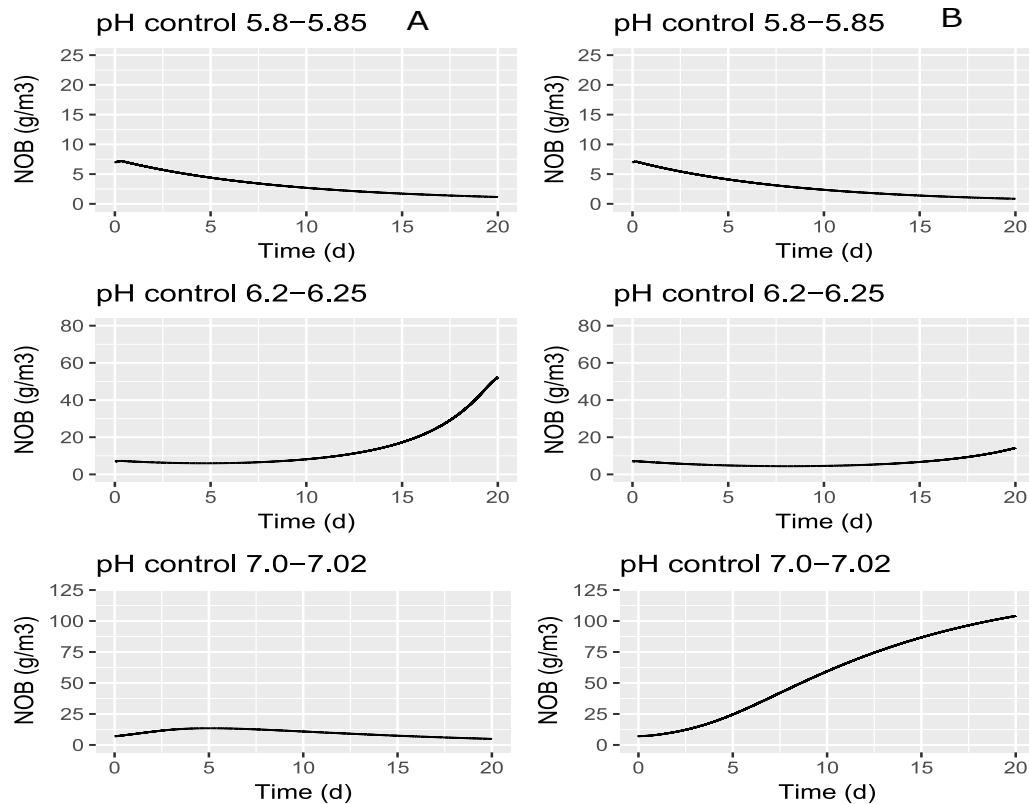
FIGURE 5.7: Predicted NOB evolution over time. At left (A) bioki-
netic parameters from Jubany, Baeza, and Carrera (2007), at right (B)
biokinetic parameters from the present work.

5.80-5.85 with a washout as the AOB washout. With Jubany, Baeza, and Carrera
(2007) parameters, pH 6.20-6.25 seems to lead to the enrichment in NOB bacteria
three times more important that the one with the parameters from this work. NOB
are progressively washed out for pH 7.00-7.05 using the Jubany, Baeza, and Carrera
(2007) parameters, whereas, with this study's parameters, pH 7.00-7.05 yields the
fastest acclimation.

   The intermediary conclusions are related to the most interesting biomass growth
conditions. The acid pH values seems to be not very well received by the autotrophic
bacteria. In fact the more neutral the pH the better the biomass growth for both AOB
and NOB. In terms of substrate affinity, it is clear that the conditions of each pa-
rameter subset are linked to the biomass prediction. For example the NOB biomass
growth is more important using the subset parameters from this work at pH 7.0,
which correspond exactly to the experimental conditions used to determinate bioki-
netic parameters values. This is a first clue to understand the variance and the im-
pact of experimental protocols to determinate biokinetic parameters.

   This numerical application highlights the importance of pH preciseness over the
global control of the systems. Therefore probes must be sensible enough and count
with a backup strategy in case of malfunctioning or unreliable measures.

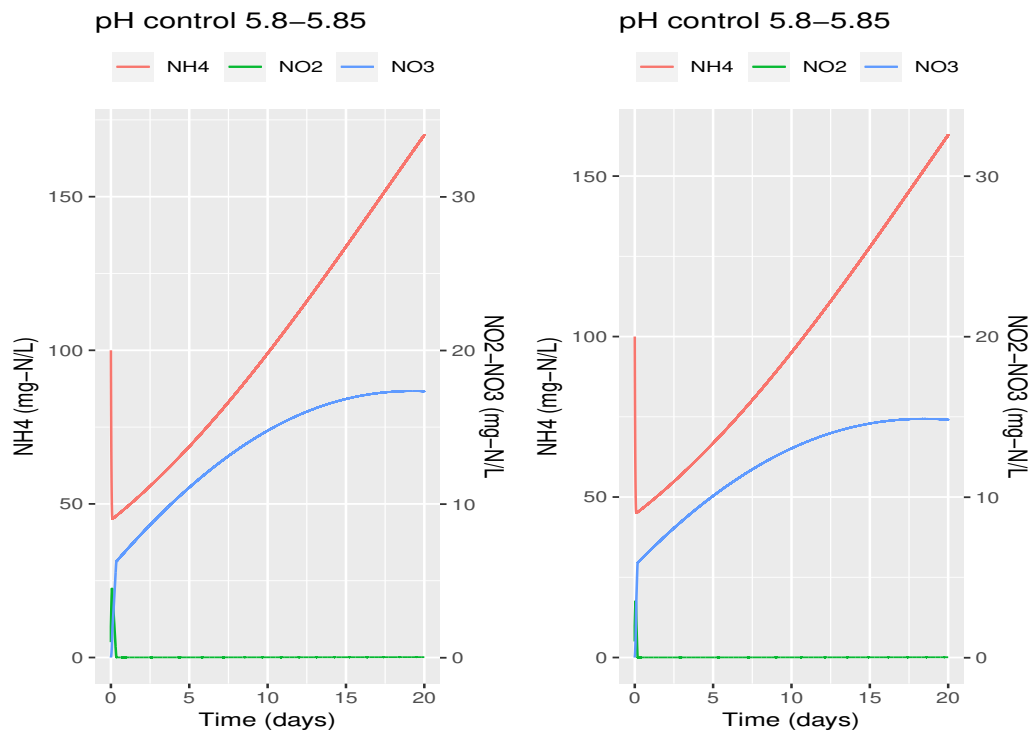The evolution of the nitrogen forms is presented in Figures 5.8, 5.9 and 5.10.

FIGURE 5.8: Nitrogen forms evolution over time for pH 5.80-5.85. At left biokinetic parameters from Jubany, Baeza, and Carrera (2007), at right biokinetic parameters from the present work.

For all conditions, the increase in NLR induces an increase in ammonium concentration with time. Nevertheless, the final quantity of NH_4 is more important as pH increase. For pH 5.80 it is normal as the AOB and NOB biomass are washout, thus FA is just accumulated and no nitrite is formed. It seems that for pH 6.20, more than 20 days of acclimation time are necessary to obtain a constant outlet NH_4 concentration. This could be also notice from the biomass acclimation results. For a pH 7, NH_4 trends to stabilisation, but more time in necessary to arrived to the steady state (as could be confirmed by the sum of outlet nitrogen).

Regarding the oxidized nitrogen, nitrate is very poorly produce at pH 5.80 as NOB biomass is been washout also. The same happens for nitrite. For pH 6.20, nitrate is produced in the both set parameters scenarios, but with the one from Jubany, Baeza, and Carrera (2007) a nitrite pic is produced at the same point where NOB increase, which lead us forecast a nitrite build-up and the logical impact in the biomass. On the contrary, with the parameters of this work, nitrate production is in the same order of magnitude and there is no sign of nitrite accumulation, anyways with a very low biomass growth.

The most interesting result is for pH 7.00-7.05 where the influence of parameters set is obvious. With Jubany, Baeza, and Carrera (2007) parameters (figure 5.10 left), NOB bacteria are quickly inhibited yielding a stable partial nitrification after 20 days. With the parameters from this study, nitrification is complete with nitrate production (Figure 5.10 right). AOB and NOB are present in an important quantity and there is no sign of nitrite build-up after 20 days.

FIGURE 5.9: Nitrogen forms evolution over time for pH 6.20-6.25. At left biokinetic parameters from Jubany, Baeza, and Carrera (2007), at right biokinetic parameters from the present work.

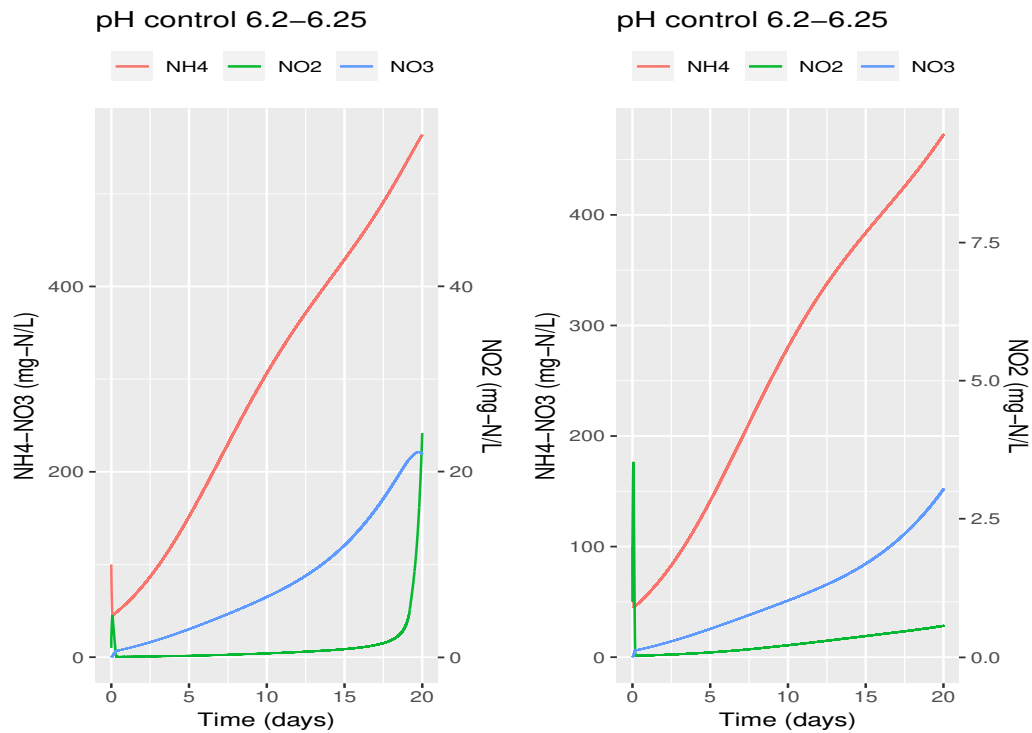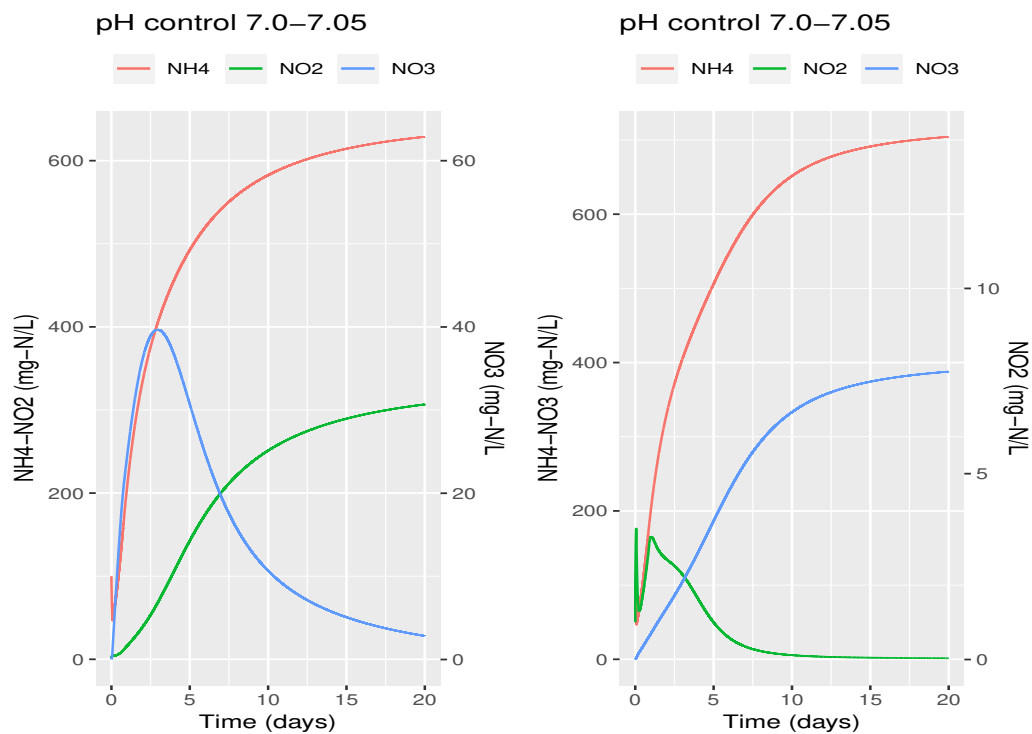FIGURE 5.10: Nitrogen forms evolution over time for pH 7.00-7.05. At left biokinetic parameters from Jubany, Baeza, and Carrera (2007), at right biokinetic parameters from the present work.

In order to correct interpret the fate nitrifying bacteria and of nitrogen forms, the Monod/inhibitory terms for AOB and NOB for the different pH set ranges tested are presented in figures 5.11, 5.12, 5.13 and 5.14.

FA inhibitory effect on Xa

| — inhib_Xa_FA pH 5.8–5.85 | — inhib_Xa_FA pH 6.2–6.25 | — inhib_Xa_FA pH 7.0–7.05 |

FA inhibitory effect on Xa

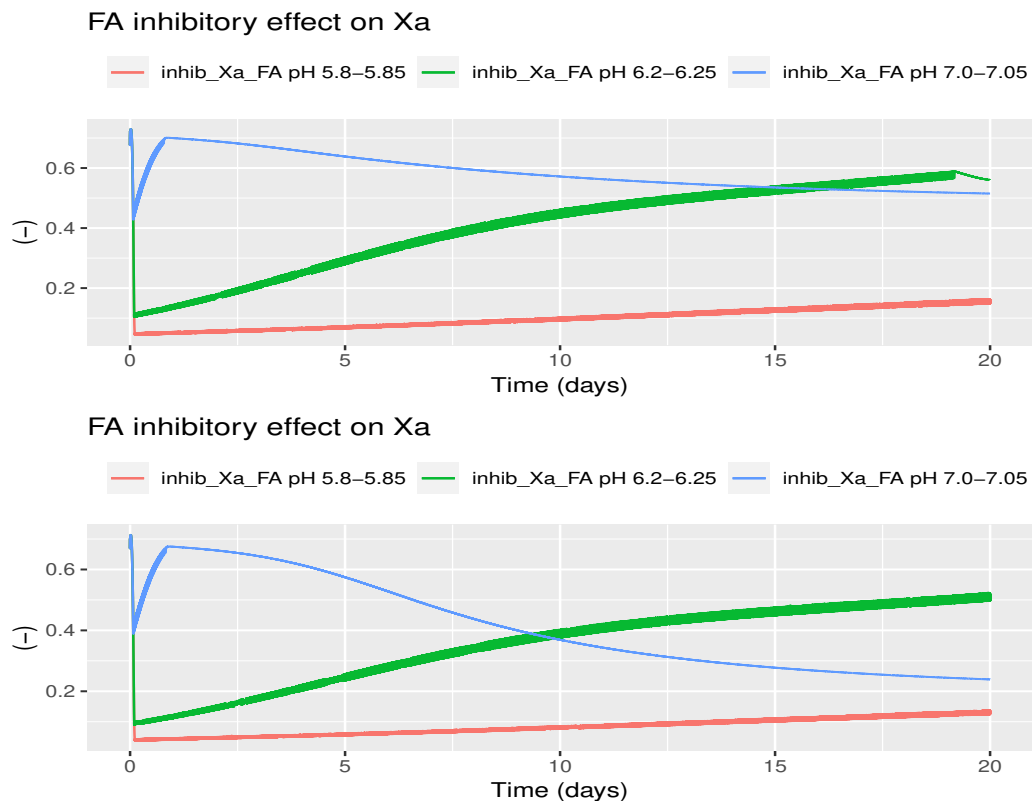| — inhib_Xa_FA pH 5.8–5.85 | — inhib_Xa_FA pH 6.2–6.25 | — inhib_Xa_FA pH 7.0–7.05 |

FIGURE 5.11: Free ammonia inhibitory terms for AOB evolution over time. At top biokinetic parameters from Jubany, Baeza, and Carrera (2007), at bottom biokinetic parameters from the present work.

As could be seen in this Figures 5.11 and 5.14, substrate inhibition for both AOB and NOB is more important as the lower the pH values whatever the biokinetic set parameters used. For AOB this is excepted as there is not enough FA, but also for the reasons explained before in this sections (alkalinity limitations, maximum specif growth rate, the consequently biomass washout).

For NOB, at pH FNA is not produced by AOB, thus inhibition is permanent. For pH 6.20, FNA inhibition increases gradually over time, acclimatization is slower but appears more stable and less dependent on kinetic parameters, as evidenced in figure 5.6 and 5.7 the trend is very similar between the two biokinetic set parameters. At pH a FNA inhibition appears quickly with the Jubany, Baeza, and Carrera, 2007 parameters but remains controlled with the parameters of this work. The evolution of this inhibition can be faster but depending on the parameters and comparing here could be risky. The differences in the biomass acclimation could be the reason of this difference. The parameters from this work came from a biomass that has undergone several weeks of acclimatization at different pH values then finally pH 7, all without chemicals. Jubany, Baeza, and Carrera (2007) work was operated with external chemical addition to maintain pH at 7.

Inhibition by the products are differently predicted by the two biokinetic set parameters. From the Jubany, Baeza, and Carrera (2007) parameters, FNA inhibition of AOB could happen after just five days of acclimation at pH 7 (80% of impact).

FIGURE 5.12: Free nitrous acid inhibitory terms for AOB evolution over time. At top biokinetic parameters from Jubany, Baeza, and Carrera (2007), at bottom biokinetic parameters from the present work.

This inhibition, as evidenced in the last subsection, is due to the nitrite build-up that overtake $10\,g_{HNO_2^- -N}.m^{-3}$ from day 5. This inhibition was not present using the biokinetic parameters of this work.

The inhibitory effect of FA over the NOB increase as the pH increase. This is normal as at higher pH, more important the FA fraction present in the reactor. Their influence in the NOB activity is more importantly predicted with the Jubany, Baeza, and Carrera (2007) parameters and more controlled with the ones from this work. Once again, this difference in difference could be explained by the acclimation protocol in both works. In the Jubany, Baeza, and Carrera (2007) study, the external alkalinity of the chemicals used to control pH at 7, lead to a 100% nitrification operation. With that said, the remaining TAN was almost insignificant and thus acclimated NOB are not use to have huge quantities of NH_4 nearby. In the present work, 50% nitrification is achieved, thus the acclimated biomass has an environment with a considerable quantity of TAN. This particular condition where achieved without nitrite build-up but after 70 days of previous experimental essays over the same biomass (see Chapter 3).
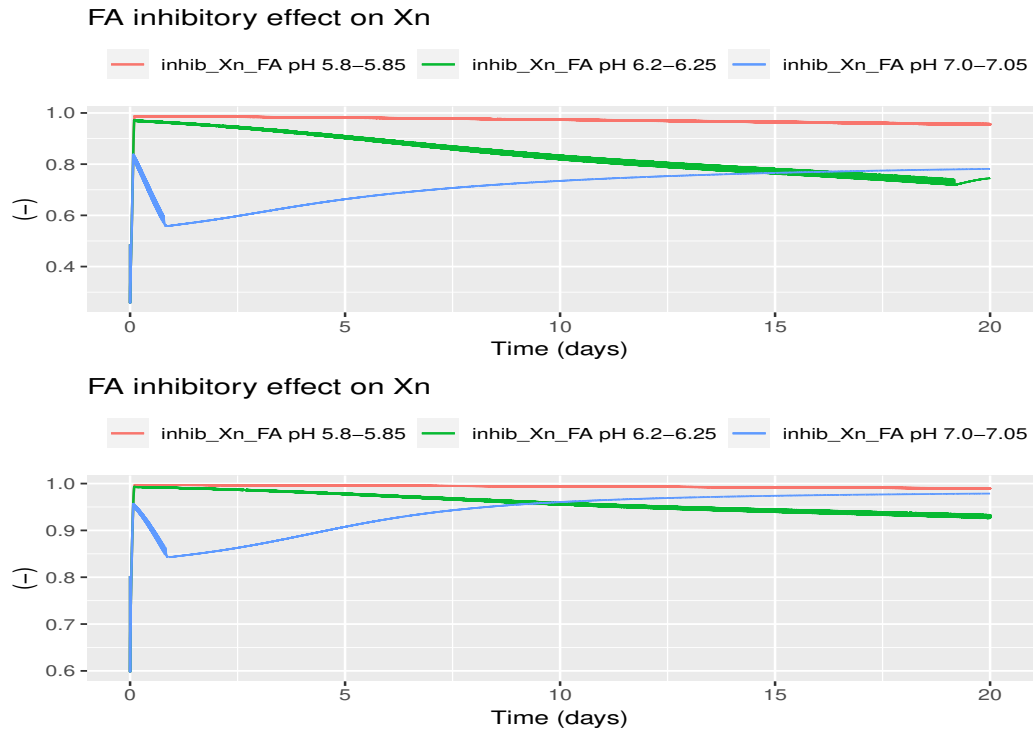
FIGURE 5.13: Free ammonia inhibitory terms for NOB evolution over time. At top biokinetic parameters from Jubany, Baeza, and Carrera (2007), at bottom biokinetic parameters from the present work.
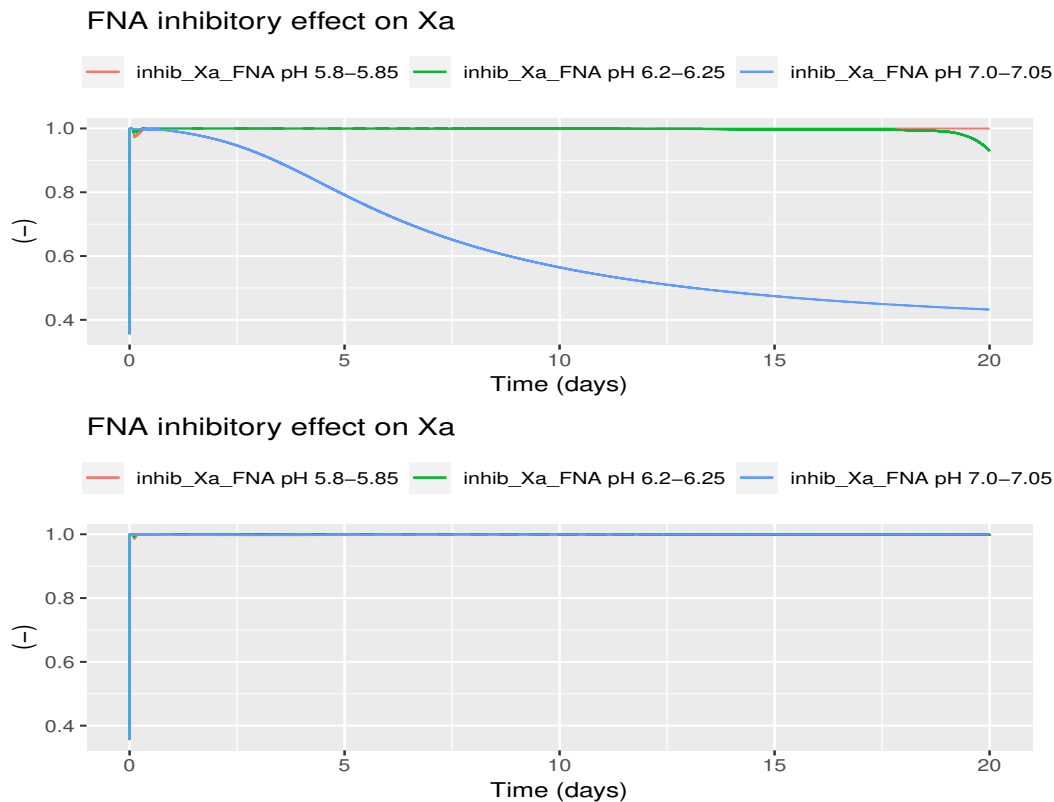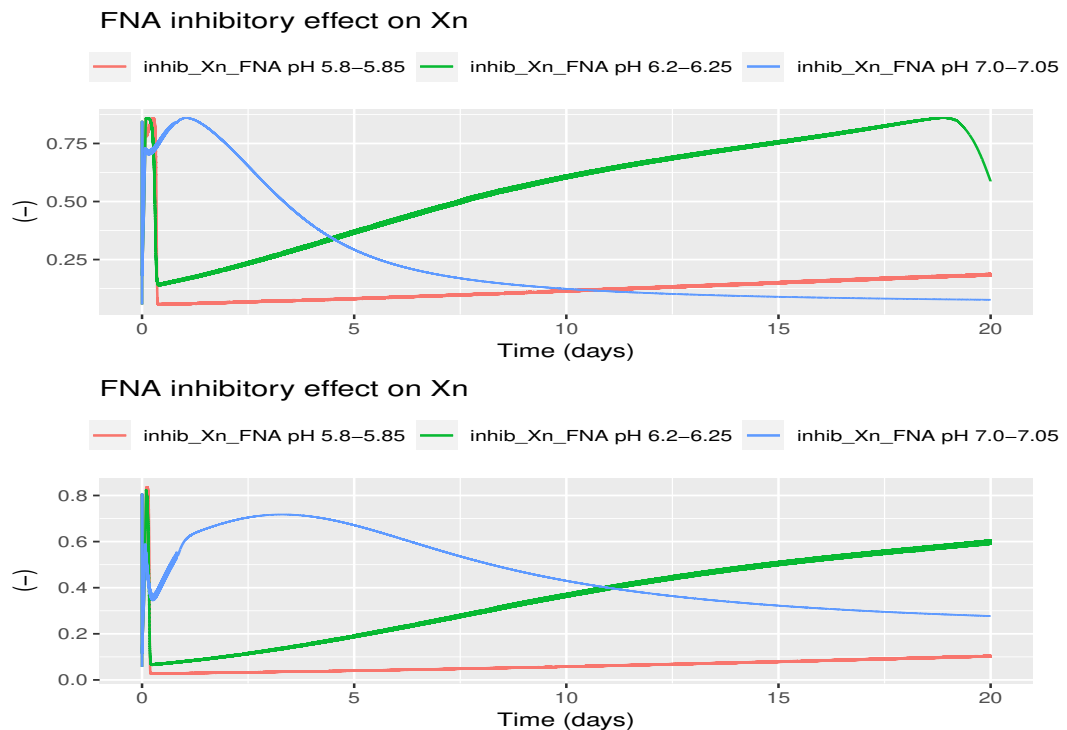

FIGURE 5.14: Free nitrous acid inhibitory terms for NOB evolution over time. At top biokinetic parameters from Jubany, Baeza, and Carrera (2007), at bottom biokinetic parameters from the present work.

Influence of preliminary ureolysis

The next are the results of the simulation of 100 operative days in this scenario, using the calibrated parameters in this work for NOB. Nitrifying biomass, nitrogen forms and the inhibitory terms are presented next. The pH set range was fixed at 6.20-6.5 to have more quantity or urine going in to the reactor.
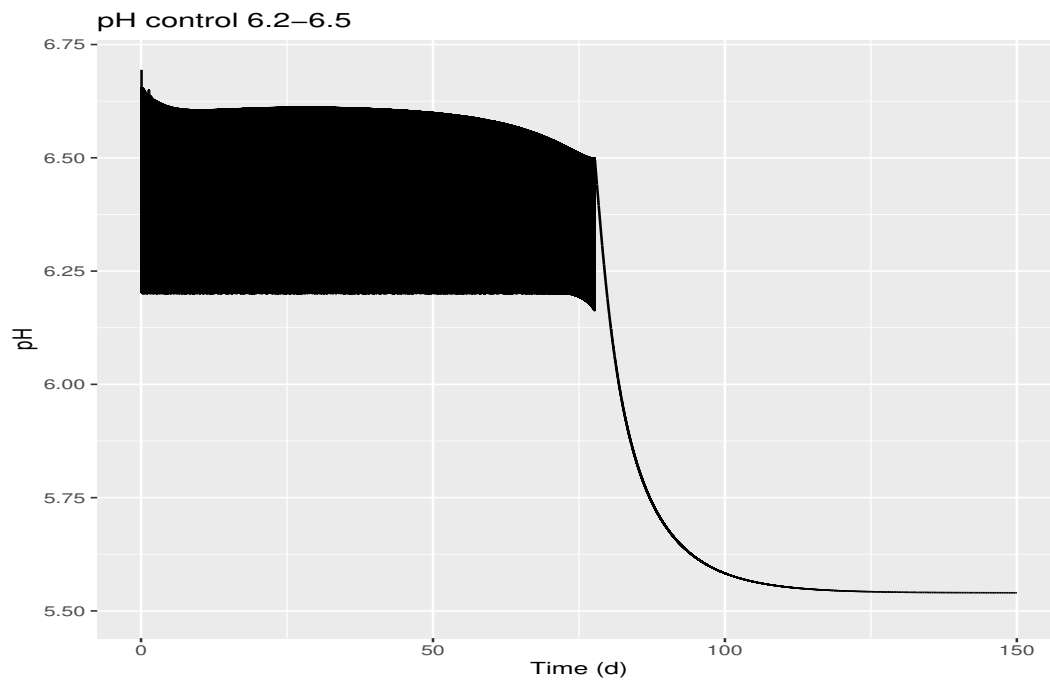
FIGURE 5.15: Model pH dynamics over time.

It is important to highlight that for computational reasons, the extended time in the simulation was fixed to 150 days and just for a one pH range set, knowing that a constant NLR value was achieved even before the final time. The 150 days was consider as the necessary time to achieve steady state process. Thus, it represents the results for a real acclimation protocol after the first 75 operative days. The numerical problem encounter after that will be discuss purely in a numerical approach.

pH control 6.2–6.25
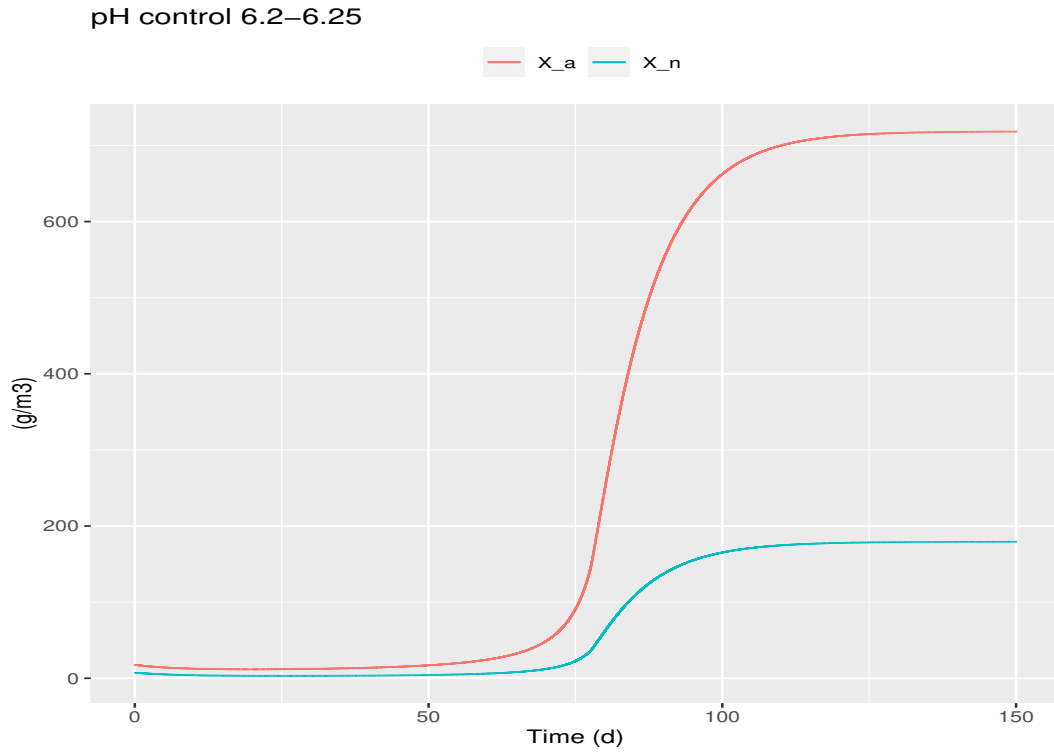
FIGURE 5.16: AOB and NOB evolution dynamics over time.

pH control 6.2–6.5
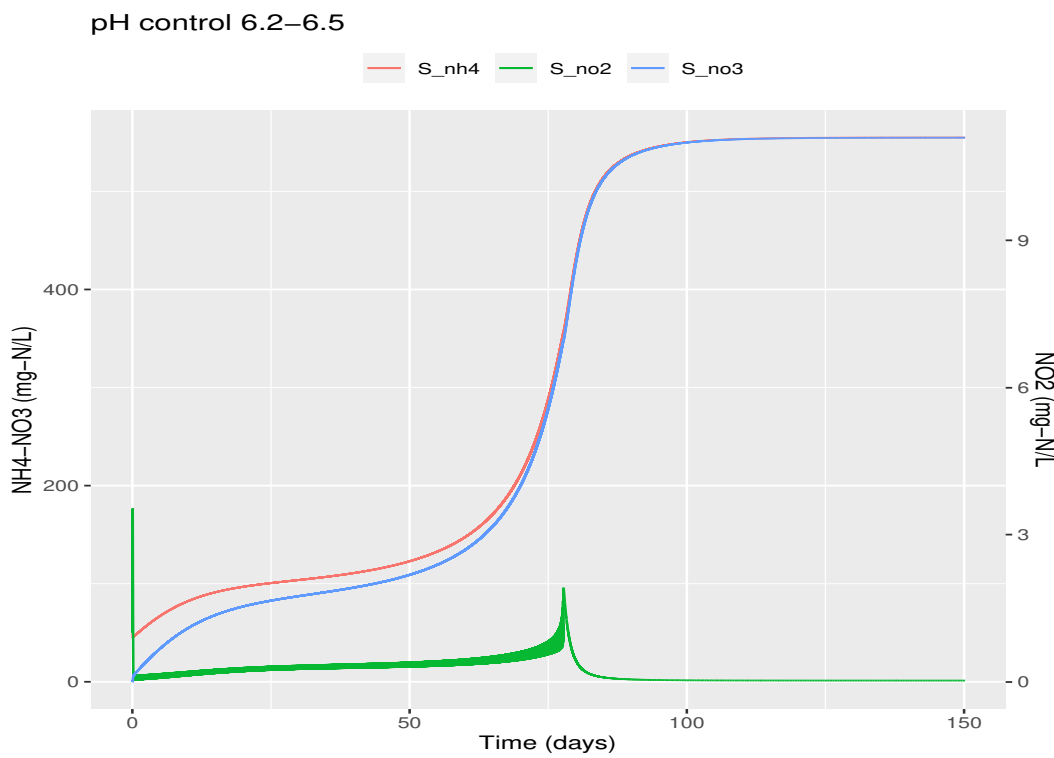
FIGURE 5.17: Nitrogen forms evolution over time.

The inhibitory terms evolution for the AOB and NOB are presented next:
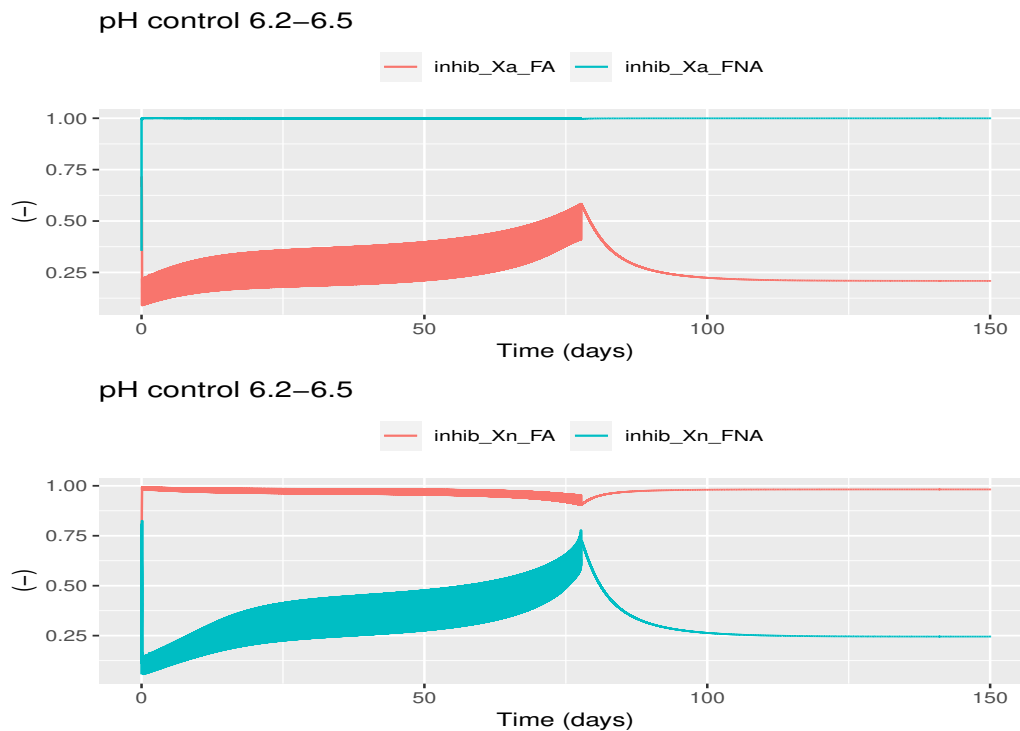
FIGURE 5.18: Inhibitory terms evolution over time. At top AOB inhibition at bottom NOB inhibition.

From the figure 5.18, it can be observed that no inhibitory conditions by the products of the nitrification is evidenced and the trend are very similar to those in figures 5.12 and 5.13. On the other hand, the inhibition by the substrates of AOB and NOB resulted in a continuous decrease over time until 50% of AOB by the day 75 and, 25% for NOB at the same day. Nevertheless, the biomass growth was to slow and as presented in the Figure 5.16 AOB was the one that adapts the better. In fact after 75 days of acclimation, we obtain a constant ratio NH_4/NO_3 with a light nitrite build-up. At that time, biomass increase four times for AOB (from $17\,g/m^3$ to $80\,g/m^3$) and three times for NOB (from $7\,g/m^3$ to $21\,g/m^3$).

By comparing this result with the biomass prediction for completely ammonified urine at the same pH value, one can remark that 20 days of acclimation time are sufficient to achieve the same order of magnitude of nitrifying biomass with completely hydrolyzed urine. This in practical terms lead to validate and affirm the results encountered during the two experimental campaigns (see Chapter 3). With that said, this proves that the biological model could be used to better guide and manage the experimental acclimation campaign.

After day 75, the inlet flow is continuous and the pH decrease until 5.5. The 50% nitrification is constant and the operation found a steady state at day 100. The inhibitory terms found also a constant 75% value for both nitrifying biomass and nitrite build-up is avoided. The final biomass concentration are $720\,g/m^3$ for the AOB and $190\,g/m^3$ for the NOB. This results are just numerical approximation of the maximum biomass concentration that could be achieved at pH fixed in 5.5 for a CSTR. In practical terms, it does not bring any interesting technical choices of the acclimation protocol.

5.2.4 Conclusions

As a conclusion of the numerical analyse, optimizing the buffer capacity inside the reactor could help to better achieve pH changes dynamics. It will also improve simulation results at different pH range and total acclimation times of the simulated campaigns.

The numerical analysis in this chapter proves that it is possible to reliably implement the on/off control strategy, that was investigated experimentally before (see Chapter 3) in a biological model. The variations of pH and the impact of biological activity in this variations are correctly capture.

For the different acclimation scenarios, it was found that the pH 7.00-7.05 propose the better global conditions for the optimal biomass growth with the less inhibitory risk. This was valid in terms of enrichment of both AOB and NOB. Some particular differences in the pH range effect were observed, like the NOB washout using the parameters from Jubany, Baeza, and Carrera (2007). This means the there is an impact of biokinetic parameters value on the estimation of the optimal scenario, and this influence could be related to the origin of those parameters.

The influence of feeding with fresh or stored urine presented in this chapter, confirms the hypothesis made in Chapter 3, as urea hydrolyse been a major condition for the overall acclimation process. As result, more scenarios should be analyse before confirming the tendencies observed here, but as previously presented, the model reveal himself as a promising tool for the following research.

The numerical results of this sections highlights the importance of biological modelling tools, relative to the real acclimation strategies campaigns. Thus, the results paves the way for choosing the better acclimation strategy to obtained acclimated biomass containing high nitrogen contents. This represents a promising technological advancement that could help to optimise the typical MBR acclimation protocols, and to avoid the problems that are usually encountered. A clear example of this could be related of using the model to better guide experimental campaigns as the one studied in the Chapter 3.

5.3 General Conclusions

A mathematical model of a partial nitritation MBR source-separated urine has been successfully constructed, calibrated by respirometry and validated using different case scenarios for biomass acclimation. The development of this model was carried out following a systematic guideline (see Chapter 2), which has been upgraded through the inclusion of an identifiability analysis step and additional statistical tests for the evaluation of the model fitting.

The calibrated MBR model is capable of accurately predicting the behaviour of the main physico-chemical outputs (NH_4^+, NO_2^-, NO_3^-, pH). Good results were also obtained, for the estimated total acclimation times. The influence of the source-separated urine ammonification (exposed already in the Chapter 3) was numerically proved in the present Chapter.

Some of the scientific questions proposed in the Chapter 3 were also evidenced in the present results. The proposed modelling scenarios lead to conclude that it is possible to link in a reliable way the pH variations to the acclimation degree of the biomass. It was proved that pH variations are correlated to the nitrifying biomass enrichment via the HRT increase and thus the NLR also. This acclimation was found directly related to the applied NLR, as was evidenced in the Figure 5.5.

Another interesting conclusion is that completely ammonified urine is one the best conditions to handle the source separated urine, to obtain a stable effluent from the reactor. The scenario that relates the nitrification of non ammonified urine, lead us to affirm the experimental conclusions from Chapter 3. Furthermore, they confirm that acclimation could be reached dealing with low ammonified urine, but with higher acclimation times and a final slight increase in nitrifying biomass. The pH set range imposed to the reactor was also in accordance to the experimental results, as pH 7.00-7.05 seems to be the one that produces the more stable effluent and the most interesting biomass enrichment.

This let us conclude that the build model paves the way about how to integrate physico-chemical phenomena and correctly represents the MBR behaviour. Also, it poses an interesting challenge in how to use it as a predictive tool, that could better guide any experimental acclimation protocol to treat yellow wastewater. This is a technological advancement that could help to safe time, resources, and improve brand new or already existing treatment systems.

Chapter 6

Conclusion

Separation of urine at source by decentralized treatment units seems to be an interesting solution, as it allows to recycle nutrients from a concentrated stream (Maurer, Pronk, and Larsen, 2006). The advantages of this decentralized treatment for source-separated urine are also related to a lower capital and operational cost, as well as a better control of the effluent quality for each particular technical solution. It allows resource recovery and reuse of water (e.g. grey water), facilitates the treatment process in the existing WWTPs by decreasing the impact of the "morning peak" and "afternoon peak", treatment effort and hygienic concerns such as the "yuck" factor. It could be also applied at a household level or even in a single household device (Larsen et al., 2016).

Among the diverse kinds of effluents management solutions available, source separation was not new, but it had long been considered as an inexpensive, rustic and environmental friendly technology mainly applied for low-income people or countries. It is also often considered as preferably suitable for rural areas, whereas simplified sewage is preferred for more densely populated areas. More recently, source separation is gaining attention as a sustainable alternative even in urban areas and industrialized countries (Harder et al., 2019; Larsen et al., 2009; McConville et al., 2017; Simha et al., 2020; Wielemaker, Weijma, and Zeeman, 2018). The technology investigated in this research work falls within this context.

6.1 General conclusions

This thesis deals with the stabilisation of yellow wastewater by nitrification in a MBR, as a preparative for a tertiary step to valorise the effluent. The results of the study have demonstrated the feasibility of this MBR technology for the treatment of source-separated urine. The work evolved with a successful long-term experiment at pilot-scale. Moreover, the thesis also includes the development, calibration by respirometric test and validation of a mathematical model of the process, aiming at increasing process knowledge.

The main target is to stabilize urine by nitrification. Due to the high-nitrogen content of urine, start-up of the reactor is challenging due to potential biomass inhibitions and interactions with physio-chemical properties (pH mainly).

6.1.1 Model conceptualization and evaluation

For better comprehension and eventual improvement of the system, an integrated physio-chemical and biological model was conceptualized following a thorough literature review of the phenomena at stake during urine nitrification within a MBR. This was performed according to the CARBIOSEP project operational objectives.

This theoretical analysis exercise yields a modified ASM model that mainly takes into account:

1. two-steps nitrification process to separately identify nitration and nitratation and the differentiated autotrophic activities of AOB and NOB,

2. description of substrate limitation/inhibition conditions for the nitrifying bacteria,

3. inclusion of physical parameters as temperature, DO, total membrane retention of solids, liquid-gas exchange and inorganic carbon impact on biomass,

4. contribution of the biomass activity over the dynamics of consumption/generation of protons inside the reactor (prediction of bacteria activity impact on pH),

5. long term degradation of "unbiodegradable" residues over the infinite SRT operation of the MBR.

The balance between pH impact on biomass and protons production from the biological activity was successfully conceptualized. pH effect on autotrophic biomass growth is taken into account by considering the $HNO2/NO_2$ and NH_3/NH_4^+ acid-base concentrations as substrates/inhibitors. pH is modelled by the consumption or production of acid/base compounds and protons during biological processes, associated with the computation of chemical equilibrium for nitrogenous species as well as inorganic carbon.

The constructed model contains a large number of parameters. The calibration of several key parameters is challenging. A combined sensitivity/identifiability analysis is proposed in order to target the most relevant parameters to identify from the experimental data available.

These parameters were mainly the ones related to the AOB and NOB growth dynamics; $Y_n, Y_a, K_{s_{FNA_N}}, K_{s_{FA_A}}$, Y_h, k_a and K_{ON}. From the same analysis, inhibitory $K_iFNA_A, K_iFNA_N, K_iFA_A, K_iFA_N$ parameters constants are quite insensitive in the tested conditions.

6.1.2   Pilot-scale experiments

In parallel, classical activated sludge was acclimated to high nitrogen influent. One pilot-scale MBR was adapted to treat source separate urine and obtain acclimated sludge. This experiment was initially aiming at producing datasets for biokinetic model calibration and validation

The operational objective was to obtain stable effluent quality during the acclimation period. No addition of external alkali should lead to the oxidation of about 50% of total nitrogen entering the system.

Two different acclimation strategies were tested and compared in order to acclimate biomass without using external chemicals. The acclimation relied on a control strategy based on the pH monitored inside the reactor. The influent pumping was controlled by an on/off regulation with high and low pH set-points.

In the first strategy, the urine was highly diluted and its degree of ammonification in relation with storage time was not really controlled. Numerous instabilities (nitrite peaks) occurred despite the multiple washings of the reactor content and changes in the operational pH range. The analysis of pH dynamics showed that they were not really correlated to the NLR and HRT observed in the reactor. Therefore,

the increase of NLR was not proportional to the maximum nitrification rate of the biomass, yielding nitrite accumulation.

The lessons learned from this first trial were applied for the second one which implied two main modifications of the protocol: use of more concentrated urine and preliminary storage of urine in order to favor ammonification. Hydrolyzing at maximum the urine in the storage tank allows to better stabilize and control the quality of the inlet in terms of NH_4, TKN and alkalinity concentrations.Furthermore, the hydrolysis of urea greatly increases the buffering capacity of urine. This point was thought crucial as ammonification will raise urine pH and inorganic carbon content, yielding quicker pH increase during influent pumping. The urine fed was kept concentrate over two dilution factors (3 and 5 times).

After several changes of the pH operational range, a fully automated control of the influent flow to the MBR was achieved during the lats 70 operative days. It resulted in a successful biomass acclimation to high nitrogen content influents, and into a stabilisation source separated yellow wastewater to produce an equal ammonium/nitrate ratio effluent. This successful biomass acclimation occurred at pH 7-7.05. The maximum NLR obtained was $1.05\,\mathrm{kg-N/m^3/d}$.

This was achieved avoiding the use of external chemicals and understanding the influence of several parameters over the process dynamics. The results showed that the best way to acclimate biomass under these conditions is feeding almost completely hydrolyzed and concentrated urine and keeping the pH at a range operational set around 7 for the better bacterial performance.

6.1.3 Respirometry

The acclimated biomass was characterized by respirometric tests in order to assess bacteria activity and mainly calibrate the half saturation and inhibition constants for the different nitrifying populations described in the model. As the reactor performed 50% nitrification of reduced nitrogen, one protocol for respirometric test in high acclimated sludge was conceived. It implies washing of the biomass by successive dilutions/concentrations with a saline solution followed by controlled addition of substrates and specific inhibitors when necessary. This protocol allowed to identify experimentally key biokinetic parameters from acclimated sludge. The results were mainly obtained for the NOB bacteria, the most sensitive to substrate accumulation and with the slowest growth rate among the nitrifying bacteria. It should be noticed that the model allowed to satisfactorily predict the dynamics of both dissolved oxygen and pH during respirometric tests.

The next are the values estimated for the NOB; Y_N=0.0488,$K_{S,FNA,N} = 0.0005683$, $K_{I,FA,N} = 4.067$. The only one estimated for the AOB is the $K_{s,FA,A} = 0.282$.

6.1.4 Scenario analysis by numerical simulation

The pilot-scale experiments alone did not allow to get a comprehensive insight of the mechanisms involved in the biomass inhibition during acclimation for various pH ranges and inlet urine characteristics. As the developed and partly calibrated biokinetic model allows to capture the processes of interest, it was used for a numerical study of biomass acclimation conditions. Operational pH ranges as well as urine ammonification level were assessed.

The model was implemented in a ordinary differential equations solver allowing for setting-up the desired on/off control strategy. The results confirmed that pre-ammonified urine yielded shorter acclimation time. The shortest acclimation period was at neutral pH (7-7.05) as observed during the experiments.

The understanding of the relation between pH and nitrifying bacteria was successful, and it helps understand and optimize sludge acclimation stage, the reactor start-up and the BNR conditions achieved with the proposed MBR technology.

6.2   Perspectives

For the further work the first objective will be to realize a complete and detailed calibration and validation of some missing parameters, especially the ones for the AOB. Also a full scale validation could be envisaged using some of the experimental data produce in this PhD work.

The conceptualized model opens perspectives on how to integrate pH as a physical variable affected by the biological activity. The first approach used a partial integration with a RWQM already developed, but some points of improvement were necessary on the path to correctly predict protons dynamics. This leads to a perspective in how to improve pH prediction, in particular in terms of better describing the inter-phase exchange that affect the chemical equilibrium in the liquid phase.

This numerical implementation should be nevertheless improved in the future by taking into account the response time of the pH probe and associated controller and by incorporating additional physio-chemical processes (fate of phosphorus, precipitation, sulfates...) that could yield a better pH dynamics description. This model opens perspectives for development of better control algorithm for urine nitrification involving only pH measurement and model predictive control.

Even if the numerical model developed in this thesis needs to be refined and some parameters validated and re-calibrated, it is a technological advancement relative to the actual modelling tools. Furthermore, this improvement should be made in order to be outperform predictive models and not for a specific scientific interest. The outcome could be a model based fault detection (online prediction of inhibition to decrease automatically the NLR), that in a technical way could be see as a soft-sensor. The advantages is that the more recent development in artificial intelligence and developed algorithms could be crucial to facilitate the computational work. From the technical point of view, pH shows itself as an operating indicator, but also as a reliable control variable in the nitrification process. For future development, a more advanced control strategy and failure detection system could be a good process engineering perspective.

The influence of urine storage, thus of the hydrolysis rate over the performance and the stability of the system over the acclimation phase, forecast to design or adapt a technical solution for accelerating urine ammonification, under controlled conditions, and with the less possible quantity or remaining urea.

Improved acclimation strategy will help to reduce the necessary time to start the system, as also to decrease the instabilities during the start-up phase. A good perspective for the autonomous and efficient operation of the real scale system. Certainly, all of this knowledge will help to avoid poor sizing of the process, to improve the design, operation and optimization of the real scale system.

The most important technical questions that this research tries to respond are based in the following analyse. The world is going in the direction of favouring

less energy intense processes and on the other side there is a general agreement in valorising the value of the waste streams.

Nevertheless, in case of an urea-rich stream treatment, a process that would stabilize the ammonia and produce water from it (coupled to a tertiary treatment) has also the economic option of recovering the Urea. If possible to recover, Urea is a very valuable material. A bibliographical review could be made to be aware of full scale processes that are able to recover it from wastewater. Even in a small scale,it does not mean that such processes do not exist. For the chosen treatment system for the Carbiosep project, taking in to account that the in the project approach water is produced and Nitrogen is a mere waste product, it will be interesting to analyse for the financial and technical aspects:

1. on one hand, the attractivity of recovered N-products (Urea or NH_4 salts);

2. on the other hand, the value of the 'harvested' water depends on the degree of the wanted tertiary treatment (which involves further costs).

This thesis work will answer some of the technical aspects about how to stabilise urine, to acclimate biomass to high nitrogen strength waste and how to deliver a stable effluent for a tertiary treatment stage. The rest of the issues are away from this thesis scope.

Appendix A

Petersen matrix of the model

Process (j) ↓	1 S_co2	2 S_co3	3 S_h	4 S_h2o	5 S_hco3	6 S_hno2	7 S_i	8 S_nd	9 S_nh3	10 S_nh4	11 S_ni	12 S_no2	13 S_no3	14 S_o	15 S_oh	16 S_s	17 X_a	18 X_h	19 X_i	20 X_n	21 X_nd	22 X_ni	23 X_p	24 X_s
1 Aerobic SS Heterotrophic oxidation	(alphaC_Ss/(Y_h*1.79/1.61)-alphaC_Xh)/1.61		i_xb/14							-i_xb				-(1-Y_h)/Y_h		-1/Y_h		1						
2 Anoxic SNO2 Heterotrophic oxidation																-1/Y_h_anoxic		1						
3 Anoxic SNO3 Heterotrophic oxidation													-(1-Y_h_anoxic)/(1.14*Y_h_anoxic)			-1/Y_h_anoxic		1						
4 Aerobic AOB growth	-alphaC_Xa		(2/Y_a-i_xb)/14							-(1/Y_a)-i_xb		1/Y_a		-(3.43-Y_a)/Y_a			1							
5 Aerobic NOB growth	-alphaC_Xn		i_xb/14							-i_xb	-(1/Y_n)	1/Y_n		-(1.14-Y_n)/Y_n						1				
6 Heterotrophic Biomass decay																		-1			i_xb-f_p*i_xp	f_p*i_xp	f_p	1-f_p
7 AOB Biomass decay																	-1				i_xb-f_p*i_xp	f_p*i_xp	f_p	1-f_p
8 NOB Biomass decay																				-1	i_xb-f_p*i_xp	f_p*i_xp	f_p	1-f_p
9 Ammonification	6/14		-1/14					-1		1														
10 Hydrolysis of entrapped organics																1								-1
11 Hydrolysis of entrapped organic nitrogen								1													-1			
12 Degradation of the endougenous residue																1							-1	
13 Hydrolysis of inert COD franction																1			-1					
14 Oxygen transfert														1										
15 CO2 equilibrium	-1		1/12	-1/12	1																			
16 HCO3 equilibrium		1	1/12		-1																			
17 NO2 equilibrium			1/14			-1						1												
18 Ammonium equilibrium			1/14						1	-1														
20 CO2 transfer liquid / air								-1																
20 CO2 transfer liquid / air	-1																							
21 H2O equilibrium			1	-1											1									

FIGURE A.1: Petersen matrix for the conceptualized model.

Appendix B

Jacquin et al., 2018 Sludge characterization by respirometry

B.1 Results obtained for the Jacquin et al., 2018 sludge

The next are the results from the respirometric analysis of the sludge obtained from a MBR with pH control by external chemicals addition and performing complete nitrification of urine as influent. To adapt the respirometry protocol and optimize the controlled doses procedure, some considerations were taken into account as described in the section 4.2. Here, the heterotrophic biomass was considered as an important bacterial strain to analyse due to the fact that the ratio C/N in the inlet was an important operational parameter of the MBR pilot in this campaign.

For some technical and logistic problems, it was no possible to characterise the AOB strain bacteria in for the particular sludge acclimated during the experimental campaign described by Jacquin et al. (2018). Two different inhibitor concentrations were used to stop the NOB bacteria activity, NaN_3 was used as Ginestet et al. (1998) suggested to reach total concentrations of 1.56 mg/L to 10 mg/L in the respirometric flask. However, neither of these concentrations allows to inhibit NOB. Thus, the results are presented just for the heterotrophic and the NOB bacteria activity.

B.1.1 Heterotrophic biokinetic parameters

Growth yield

Here, several COD pulses were performed with different known injected Sodium Acetate concentrations ($CODpulse = 2.5, 5, 12.6, 25.3, 38 \text{mg/L}$). Figure B.1 represents the results from the batch tests at 25 °C and pH of 7.5 with biomass taken from the pilot plant.

OC was calculated as the area under the exogenous OUR which was obtained from the DO profile of each batch experiment. Y_H was calculated from the slope of the linear regression of the experimental data and using equation B.1. This equation is constructed by the definition of observed yield presented in equation 2.27 and with the correct stoichiometric parameters from the Petersen matrix presented in section 2.2.

$$\frac{OC}{COD_{pulse}} = 1 - Y_H \left[\frac{gO_{2X}}{gO_{2AcNa}} \right] \tag{B.1}$$

The slope obtained from the linear regression of the figure B.2 was $0.3207 \text{ mgO}_2 \text{ mgO}_2 -1$, and this value is used to calculate Y_H according to equation B.1 as $(0.6793 \pm 0.0014) \text{ gCOD}_{XH} \text{ gCOD}^{-1}$ (or $0.48 \pm 0.01 \text{ gVSS gCOD}^{-1}$ considering biomass as $C_5H_7NO_2$).
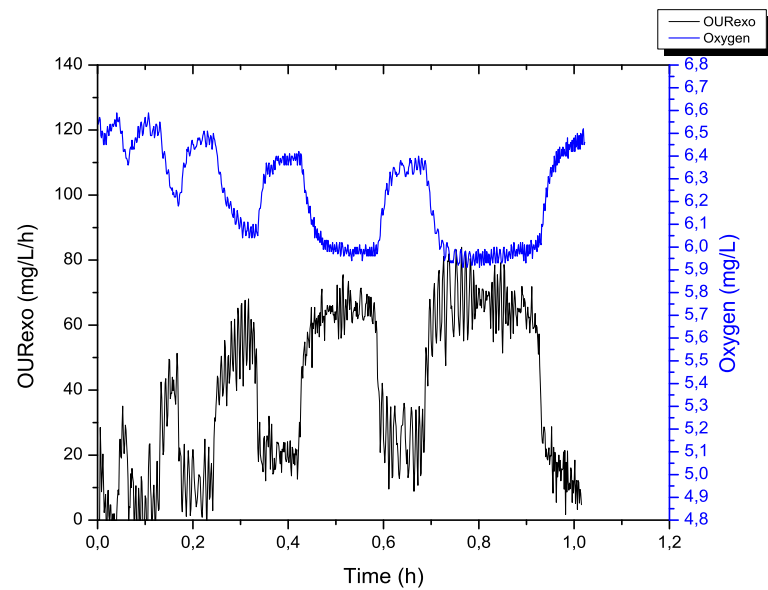
FIGURE B.1: Biomass yields determination for heterotrophic activity:
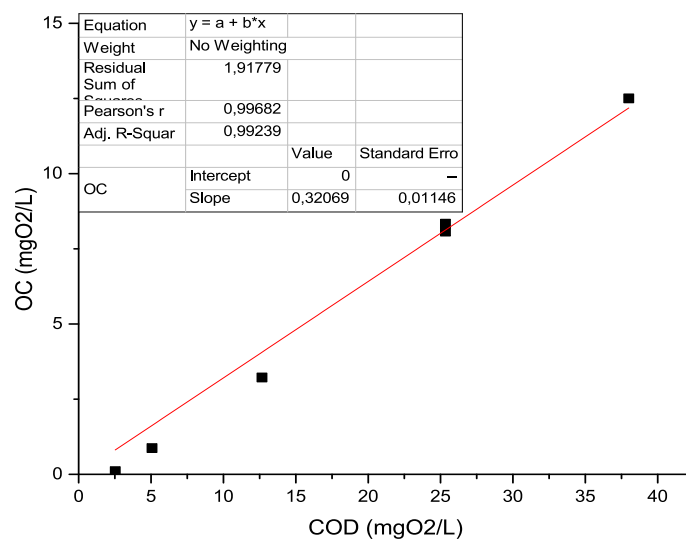OURexo calculated for five doses of Sodium Acetate.

FIGURE B.2: Biomass yields determination for heterotrophic activity:
OC as a function of the initial Sodium Acetate injections COD pulses
for Y_H determinations.

This calculated value of Y_H corresponds almost exactly to the default one presented by Henze et al. (1986) of $0.67\,\mathrm{gCOD\,gCOD^{-1}}$. This is not a surprising result, since the overall ratio C/N in the inlet reported by Jacquin et al. (2018) was 1.0 ± 0.3, which means that there were no limitations in COD substrate for the heterotrophic bacteria to grow over time.

Substrate saturation/inhibition

From the figure B.1 the OURmax for each dose could be calculated and the Michaelis-Menten relation for the substrate consumption could be established. The figure B.3

represents this relation and allows to calculate the half saturation constant K_S for the sodium acetate.

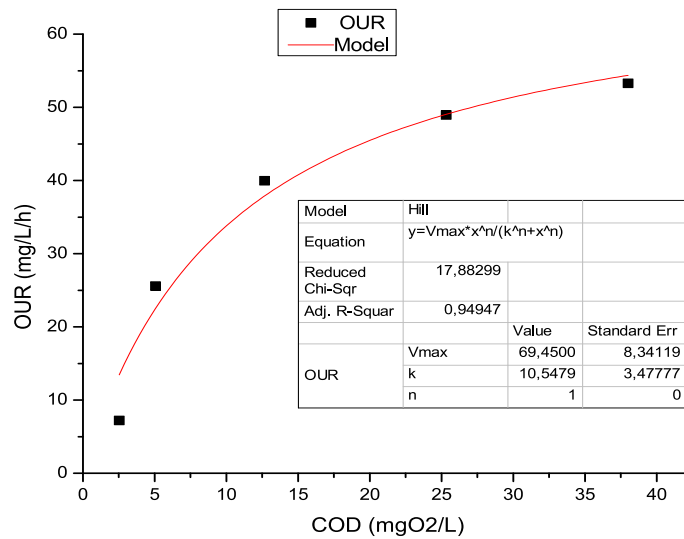FIGURE B.3: Carbonaceous half saturation constant determination for heterotrophic activity: OURexo as a function of the initial Sodium Acetate COD injections for the five doses.

From the non-linear fit of the figure B.3 it is possible to obtain a K_S of 10.54 $g_{COD}.m^{-3}$. The equation B.2 represents this relation.

$$OUR = OUR_{max} \frac{S_C}{S_C + K_s} \tag{B.2}$$

The calculated value of K_S does not correspond with the default value suggested by Henze (2007) of 20 $g_{COD}.m^{-3}$. Nevertheless, the incertitude is around 30% so this value must be interpreted carefully. This difference could be attributed to the difference in the accessibility of the substrate for the heterotrophic bacteria, which biomass decrease in proportion over the time in relation to the autotrophic strains. Also, the specifities of MBR operartion such as higher biomass concentration and mass transfer (floc intra-diffusion) could explain this.

Biokinetic parameters fitting

The result of the LFS respirometric test are presented in the figure B.1. Figure B.4 represents the test for one particular day and the figure B.5 the same LFS test with the same biomass after 16 hours of continuous aeration without substrate additions, to evaluate in a correct way the decay term.

The data is adjusted to the equation 4.10 keeping the standard value for the half saturation oxygen constant K_{OH} and using the values of Y_H and K_S previously determined. Here we can not distinguish the heterotrophic biomass from the maximum growth rate and decay rate parameters, that is why the pair of each parameter coupled to the biomass is treated as the variable to fit. The table B.1 shows the calibrated K_S and the two fitted values for the pair $\mu_{maxH}.X_H$ and $b_H.X_H$ that were evaluated within 16 hours of interval. This result shows that the biomass decreases during this
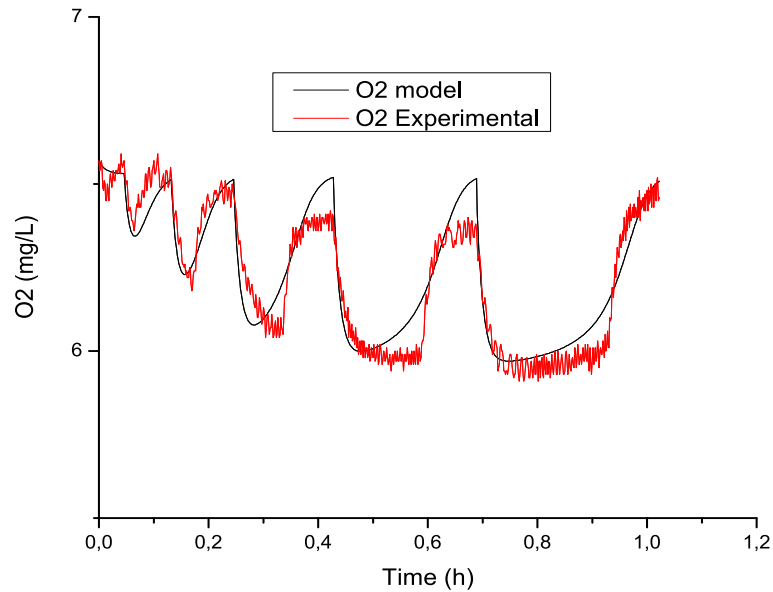
FIGURE B.4:   Parameters adjustment for heterotrophic bacteria $(\mu_{\mathrm{max_H}X_H}$ and $K_S)$
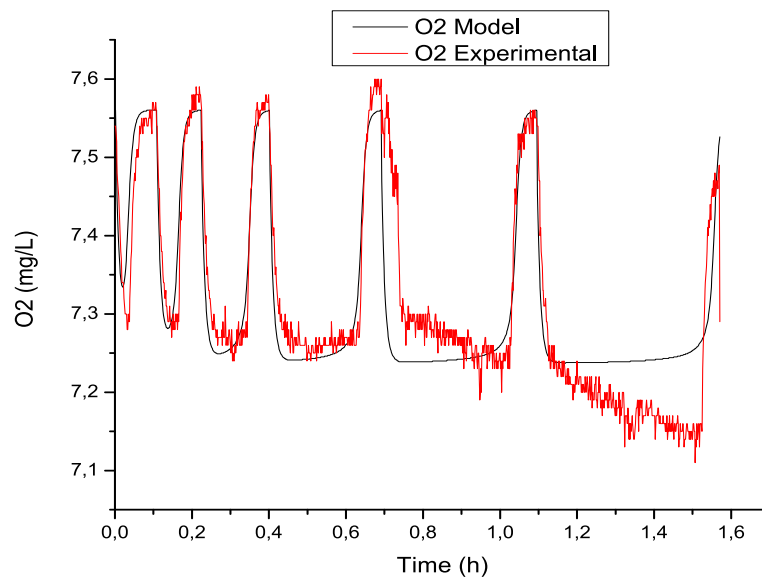
FIGURE B.5:   Parameters adjustment for heterotrophic bacteria $(\mu_{\mathrm{max_H}X_H}, K_S$ and $b_H X_H)$

time of 16 hours and so the decay becomes more important, but even in this accli-mated sludge the ratio μ_{maxH}/b_H is still in the same order of magnitude as in the conventional activated sludge.

B.1.2   Nitrite Oxidizing Bacteria biokinetic parameters

To characterise correctly the nitratation step, ATU was used as inhibitor of the AOB activity according to the concentration presented by Ginestet et al. (1998). Even if the controlled doses method for the NOB bacteria implies the use of specific nitrite

K_S (mg/L)	10.55
$b_H X_H$ (mg/L/s-1)	0.003
$\mu_{\text{max}_H X_H}$ (mg/L/s)^a	0.035
$\mu_{\text{max}_H X_H}$ (mg/L/s)^b	0.026

[a]fresh biomass
[b]old biomass

TABLE B.1: Results of the fitting for the OUR profile with AQUASIM software

substrate that does not reacts but inhibits the AOB bacteria, we prefer to avoid this interaction by inhibiting completely nitritation step.

Growth yield

In the same way as the heterotrophic growth yield was calculated from a controlled doses method, Y_N was calculated with a similar methodology: a set of experiments with different initial TNN concentrations (TNN$_{\text{pulse}}$ 0.9, 1.8, 4.5, 9, 13.5, 18 $mgN\ L^-1$) is performed at a temperature of 22 °C and a pH of 7. Here again OC is calculated as the area under the OURexo which was obtained from the DO profile of each batch experiment. Y_N is calculated from the slope of the linear regression of the experimental data and using equation B.3. This equation is the corresponding one to the equation B.1 for the NOB growth yield, which was directly obtained from the process stoichiometry for the two-step nitrification model. Expression in the numerator is the OC per unit of produced X_N (stoichiometric coefficient of DO in the NOB growth process) and the expression in the denominator is the oxidized TNN per unit of produced X_N (stoichiometric coefficient of TNN in the NOB growth process).

$$\frac{OC}{TNN_{\text{pulse}}} = \frac{(1.14 - Y_{\text{N}})/Y_{\text{N}}}{1/Y_{\text{N}}} = \frac{OC}{TNN_{\text{pulse}}} = 1.14 - Y_{\text{N}} \tag{B.3}$$
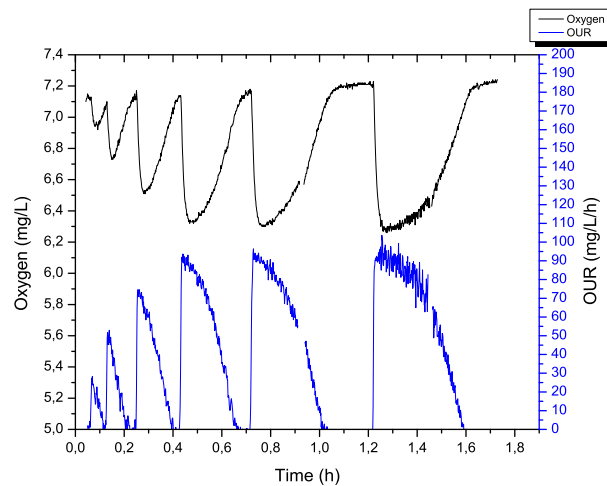

FIGURE B.6: Biomass yields determination for NOB activity: OC as a function of the initial Sodium Nitrite injections, OURexo for the six doses.
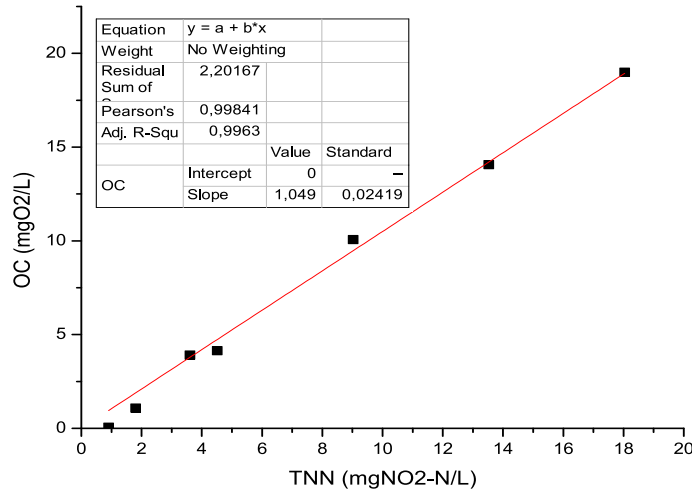
Equation	y = a + b*x		
Weight	No Weighting		
Residual Sum of	2,20167		
Pearson's	0,99841		
Adj. R-Squ	0,9963		
		Value	Standard
OC	Intercept	0	—
	Slope	1,049	0,02419

FIGURE B.7: Biomass yields determination for NOB activity: OC as a function of the initial Sodium Nitrite injections.

The slope obtained from the linear regression was $1.0491\,\mathrm{mg\,O_2\,mgN-NO_2^{-1}}$, therefore Y_N is calculated as $(0.0909 \pm 0.0400)\,\mathrm{gCOD\,gN^{-1}}$ (or $(0.064 \pm 0.028)\,\mathrm{gVSS\,gN^{-1}}$ considering biomass as $C_5H_7NO_2$.

This calculated value of growth yield will be used to estimate the biokinetic parameters presented next.

FNA saturation/inhibition

The determination of $K_{S,FNA,N}$ and $K_{I,FNA,N}$ is possible in the acclimated biomass. Nevertheless, in order to avoid any kind of perturbation, AOB bacteria was inhibited with the necessary concentration of ATU.

Increasing amounts of TNN were progressively added to the reactor and OUR was determined for every substrate concentration. Experimental data were first fitted to a Haldane-type equation (see equation (B.4)) in order to estimate parameters OURmax, $K_{S,FNA,N}$ and $K_{I,FNA,N}$ using Origin Software.

$$OUR = OUR_{max}\frac{FNA}{K_{(S,FNA,A)} + FNA + FNA^2/K_{(i,FNA,A)}} \tag{B.4}$$

It can be observed from figure B.8 that the inhibitory concentration could not be reached, therefore the protocol does not allows to estimate $K_{I,FNA,N}$ reliably. Thus, the Haldane expression was simplified to the Monod basic substrate inhibition to estimate the half saturation constant value. From the non-linear fit of the figure B.8, it is possible to obtain a $K_{(S,FNA,N)}$ of $0.001\,31\,\mathrm{g_{HNO_2^- - N}}\cdot\mathrm{m^{-3}}$. The equation B.5 represents this relation.

$$OUR = OUR_{max}\frac{FNA}{K_{(S,FNA,N)} + FNA} \tag{B.5}$$

In order to reach correctly the inhibitory zone, for the next trials, the maximal TNN will be increased twice, in order to achieve the inhibition without affecting the pH of the medium. This will help to improve the protocol for the sludge characterisation.
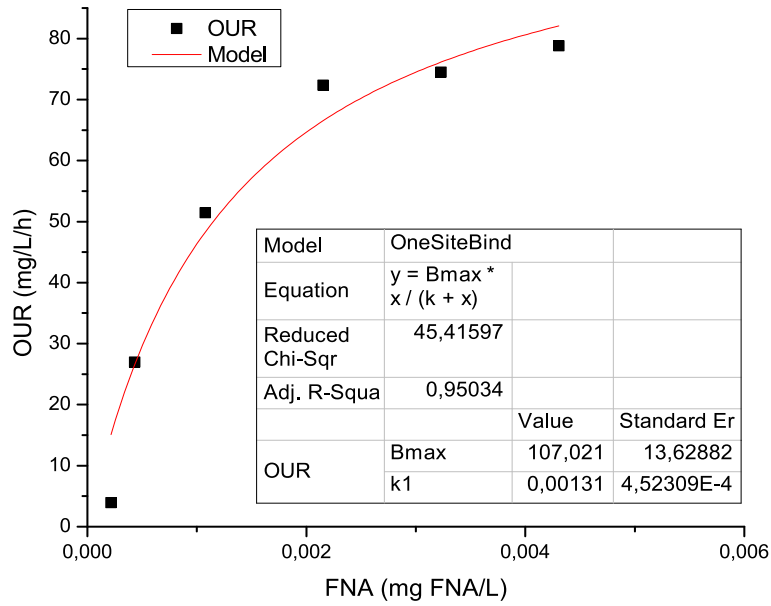
Model	OneSiteBind		
Equation	y = Bmax * x / (k + x)		
Reduced Chi-Sqr	45,41597		
Adj. R-Squa	0,95034		
		Value	Standard Er
OUR	Bmax	107,021	13,62882
	k1	0,00131	4,52309E-4

FIGURE B.8: Experimental data for $K_{S,FNA,N}$ determination with LFS respirometry in the reactor.

FA inhibition

$K_{I,FA,N}$ determination in the acclimated biomass is the only parameter left for the complete characterization of NOB-related processes. It was considered constant in terms of FA for a specific biomass although its value could probably change either due to biomass acclimation to FA or NOB population changes.

$K_{I,FA,N}$ was determined using LFS respirometry in the respirometer with biomass withdrawn from the pilot plant, and diluted with the permeate as described in section 4.2. The pilot plant was operating as a complete nitrification system with high concentration of TAN and TNN in the MBR reactor and producing an effluent free of TAN and TNN. In all the graphics presented next (figures B.9 and B.10), the experimental conditions in the respirometric experiment were: pH = 8.4 $\pm$ 0.1 and T = 26 °C. These high pH and T were used to favor the presence of the inhibitory compound (FA) and also to avoid FNA inhibition to NOB. ATU ($10\,\mathrm{mgL^{-1}}$) was used as specific inhibitor for AOB. The experiment consisted of successive equal and controlled TNN pulses ($4.5\,\mathrm{mg/L}$) with different FA concentration in the medium, concentration that was controlled by the injection of TAN into the liquid after the depletion of each TNN pulse. The first TNN pulse was carried out with the medium free of FA. Figure B.9 shows the DO profile of some TNN pulses and the liquid FA concentration as an example of the used methodology.

In the same way, the direct effect of the ammonium as inhibitor for the nitrous acid degradation could be evaluated from equation (4.12). Experimental data was fitted to equation (B.6) using Origin Software and is presented in figure B.10.

$$OUR = OUR_{max} \frac{FNA}{K_{(S,FNA,A)} + FNA} \frac{K_{(i,FA,N)}}{K_{(i,FA,N)+FA}} \tag{B.6}$$

From our parameter estimation procedure, we obtain for this particular acclimated sludge, a value of $1.7077\,\mathrm{g_{NH_3-N}.m^{-3}}$ for the $K_{I,FA,N}$ constant.

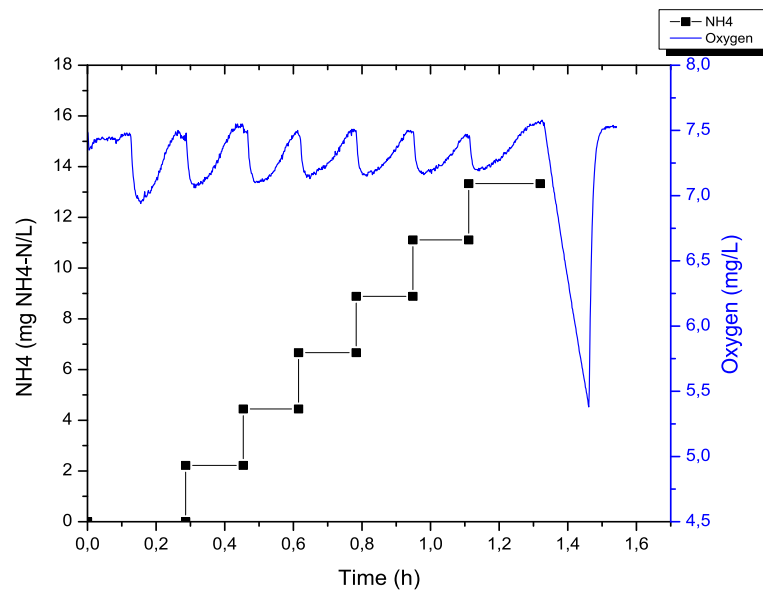Here, it is important to remark that the chosen TNN dose was not high enough to

FIGURE B.9: $K_{I,FA,N}$ determination with LFS respirometry in the respirometer DO profile and FA concentration in the medium along TNN pulses.
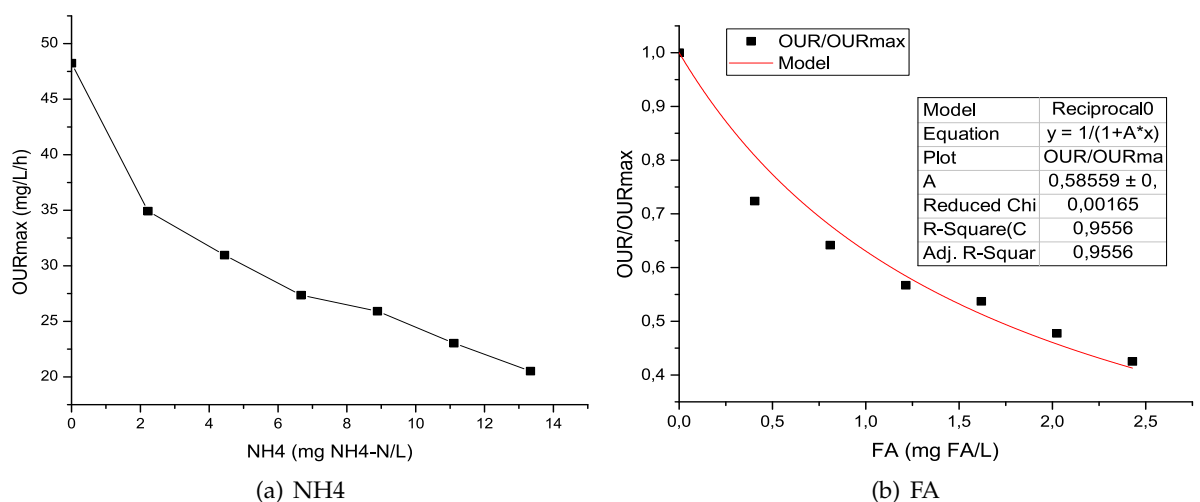

(a) NH4

(b) FA

FIGURE B.10: $K_{I,FA,N}$ determination with LFS respirometry in the respirometer OUR vs TAN and FA concentrations, experimental data for model prediction with fitted parameter.

reach a maximum nitratation rate without substrate limitations, but the quantity of FNA and the substrate half saturation constant are known, thus they can be included in the estimation. That is why the concentration and the inhibition term were also taken into account for the estimation of $K_{I,FA,N}$ constant according to the equation B.6.

For the next trial, the fixed dose will be estimated in order to being far from the substrate saturation area, in order to facilitate the determination of the FA as inhibitory compound. This will help to better adapt the protocol specially for the characterisation of sludge with no total nitrification conditions, where the remaining ammonium and nitrite concentrations can still be important.

Biokinetic parameters

For the remaining kinetic parameters estimation and the validation of the ones obtained previously ($K_{S,FNA,N}$ and $K_{I,FA,N}$ were estimated using Origin Software), experimental data from the controlled doses method were fitted to a substrate saturation/inhibition equation B.6 and parameters as $\mu_{\max_N X_N}$ were estimated using AQUASIM Software.
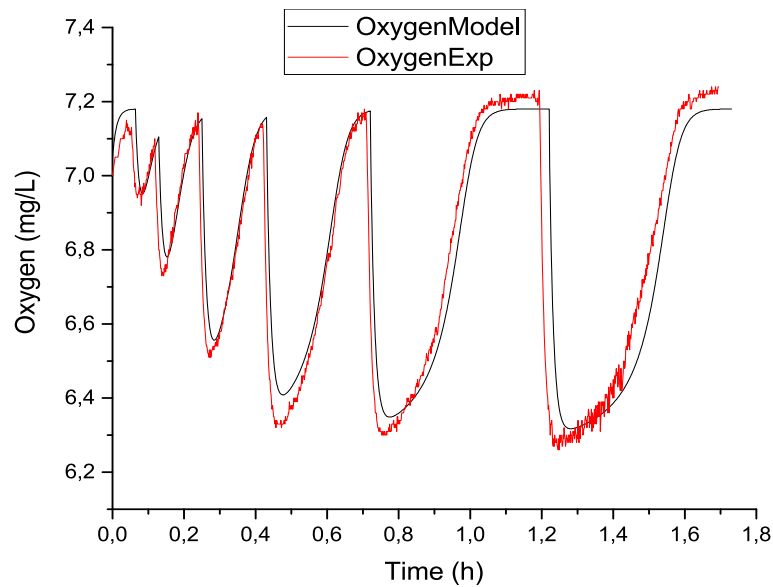

FIGURE B.11: Parameters adjustment for AOB bacteria ($\mu_{\max_N X_N}$ and $K_{S,FNA,N}$ validation)
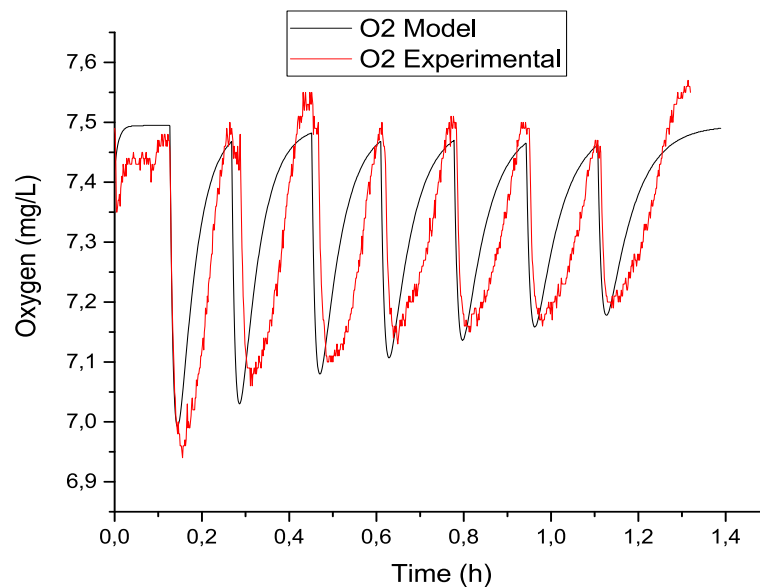

FIGURE B.12: Parameters adjustment for AOB bacteria ($\mu_{\max_N X_N}$ and $K_{S,FNA,N}$, $K_{(i,FA,N)}$ validation)

$K_{(S,FNA,N)}$ (mg/L)	0.00131
$K_{I,FA,N}$ (mg/L)	1.7077
$\mu_{\max_N} X_N$ (mg/L/s-1)	0.002 [a]
$\mu_{\max_N} X_N$ (mg/L/s-1)	0.02 [b]

[a]Without FA inhibition
[b]With FA inhibition

TABLE B.2: Results of the fitting for the OUR profile with AQUASIM software

The result of the estimated parameters for NOB activity under LFS respirometric test are presented in the figures B.11 and B.12. The summary of this parameter estimation is presented in table B.2.

As it can be seen, the parameters found for $K_{(S,FNA,N)}$ and $K_{I,FA,N}$ matched with the estimated values of $\mu_{\max_N} X_N$ for the two different scenarios, validating the estimation made with the Origin Software. The possible reason for the difference between the two estimated $\mu_{\max_N} X_N$ could be found in the direct effect of pH and temperature, under the $\mu_{\max_N}$ value. According to Jubany et al. (2008), the optimal growth rate for both AOB and NOB bacteria is for pH around 7.5-8 and decrease for pH above and below of this range leads to a bell-type shape that could be represented by the equation:

$$\mu_{\max_N}(pH, T) = \frac{6.69.10^7 \exp\left(\frac{-5295}{273+T}\right)}{1 + \frac{10^{-8.69}}{10^{-pH}} + \frac{10^{-pH}}{10^{-6.78}}} \tag{B.7}$$

which is the combination of (Hunik, Tramper, and Wijffels, 1994)

$$\mu_{\max_N}(T) = A\mu_{\max_N} \exp\left(\frac{-Ea_N}{R(273+T)}\right) \tag{B.8}$$

and the equation (Dochain and Vanrolleghem, 2015)

$$\mu_{\max_N}(pH) = \frac{\mu_{\max_N}(pH_{opt})}{1 + \frac{10^{-pk_1}}{10^{-pH}} + \frac{10^{-pH}}{10^{-pk_2}}} \tag{B.9}$$

Where pk_1 and pk_2 represents the high and the low pH values at which the growth is the half of the maximum growth rate $\mu_{\max_N}$ at the optimal pH (Holloway and Lyberatos, 1990).

Conclusions

This appendix presents the first respirometric tests performed with the sludge obtained by Jacquin et al. (2018). The respirometric protocol was tested and all the necessary adjustments were updated for the analysis of the sludge obtained later in the Strasbourg experiment. Especially, the TNN doses will be increased in order to better characterize NOB substrate inhibition.

Another important conclusion is that the heterotrophic bacteria did not suffer of great changes during this acclimation campaign in terms of growth yield. Only the biokinetic behaviour of the substrate consumption changed, which is something expected due to the biomass proportion change by treating a wastewater with different

C:N:P proportions. Thus, heterotrophic activity in the campaigns in Strasbourg were just validated from an overall carbon removal point of view in the pilot, as shown in section 3.3, but it was not characterised with respirometric techniques, as it was not part of the objectives of the acclimation campaign.

Appendix C

Numerical estimation of nitrifying biomass

C.1 Objectives

The present numerical study aims at simulating initial operation of the CarbioSep pilot. The pH dynamics and autotrophic biomass evolution following the initial seeding of the pilot are of interest.

C.2 Methodology

First, a steady-state simulation of a typical wastewater treatment plant (WWTP) (with typical pollutant loads) allows to define the initial biomass concentrations within the seed sludge (which was sampled in a WWTP). Then, simulations of the pilot reactor operation following the seed are carried out to study the impact of initial alkalinity on the establishement of nitrification, biomass inhibition, etc.

C.3 Simulation of initial biomass concentrations

A typical nitrifying WWTP was sized according to traditional design guidelines (low F/M ratio, typical pollutants loads for one people-equivalent, etc.). Results are presented in Table C.1.

A steady-state simulation was conducted using the CarbioSep biokinetic model in Aquasim. The reactor compartment is here behaving like a conventional activated sludge process with excess sludge removal.

The resulting autotrophic biomass concentrations are plotted in Figure C.1. The resulting AOB and NOB concentration are respectively 48 mg/L and 21 mg/L.

TABLE C.1: Typical nitrifying WWTP design

| Fixed parameters/hypothesis		
Volume	0,034	m3
TSS in he reactor	4,5	kg/m3
VSS/TSS	0,7	
VSS in the reactor	3,15	kg/m3
F/M	0,08	kg BOD5/kg VSS/d
TSS/BOD5 at the influent	1,2	
Flowrate per P.E.	0,2	m3/d
Design parameters calculated		
BOD5 load	8,57E-03	kg BOD5/d
TSS load	1,03E-02	kg TSS/d
Excess sludge prod.	9,42E-03	kg TSS/d
Sludge mass in the pilot	0,153	kg TSS
SRT	16	days
Capacity in P.E.	0,1428	P.E.
Inlet flowrate	2,86E-02	m3/d
Wastage flow rate	2,09E-03	m3/d
Concentrations and loads in the influent		
BOD5	300	g/m3
COD	780	g/m3
TKN	75	g/m3
N-NH4	52,5	g/m3
Norg	22,5	g/m3
NLR	63,00	g N/m3/j
	0,063	kg N/m3/j
NLRs	0,02	kg N/kg VSS/j
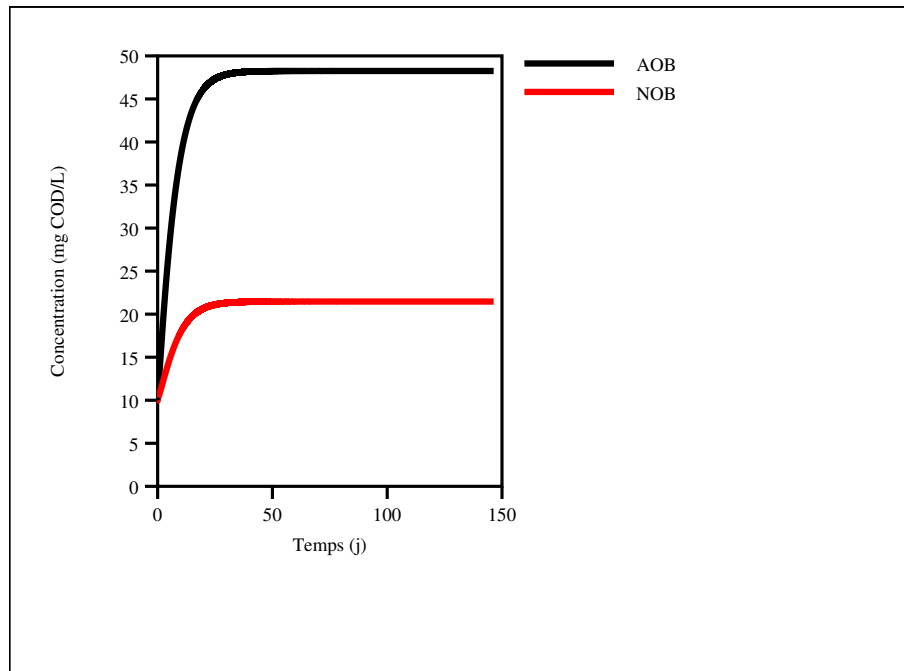
FIGURE C.1: Autotrophic biomass concentrations in the sludge from
the typical WWTP

C.4 Simulation of reactor start-up

Start-up of the reactor was simulated considering the following initial conditions:

- Activated sludge diluted 3 times: [AOB] = 17 mg/L ; [NOB] = 7 mg/L

- $N - NH_4$ = 50 mg/L

- HCO_3 = 100 mg C/L

- CO_3 = 20 mg C/L

Some kinetic parameters have been changed according to Fumasoli, Morgenroth, and Udert, 2015 and are summarized in Table C.2.

TABLE C.2: Kinetic parameters for AOB and NOB (inhibition and saturation constants)

$K_{S_{FA_A}}$	0.0000536	mol/L
	0.7504	mg N/L
$K_{i_{FNA_A}}$	0.000146	mol/L
	2.044	mg N/L
$K_{S_{FNA_N}}$	0.00000017	mol/L
	0.00238	mg/L
$K_{i_{FNA_N}}$	0.00000957	mol/L
	0.13398	mg/L

In this mode, the reactor is operated as a batch reactor (no inlet feed).

Figures C.2 and C.3 shows the results concerning the fate of nitrogen. Nitrification is starting after a few hours in the first day but at this stage, only NO_2 is formed. After a NO_2 peak, nitritation starts and NO_3 is formed while NO_2 is depleted. Due

to the initial pH which is pretty high (Figure C.4), free ammonia is significant at the beginning, explaining NOB inhibition (Figure C.5) and thus the NO_2 peak.
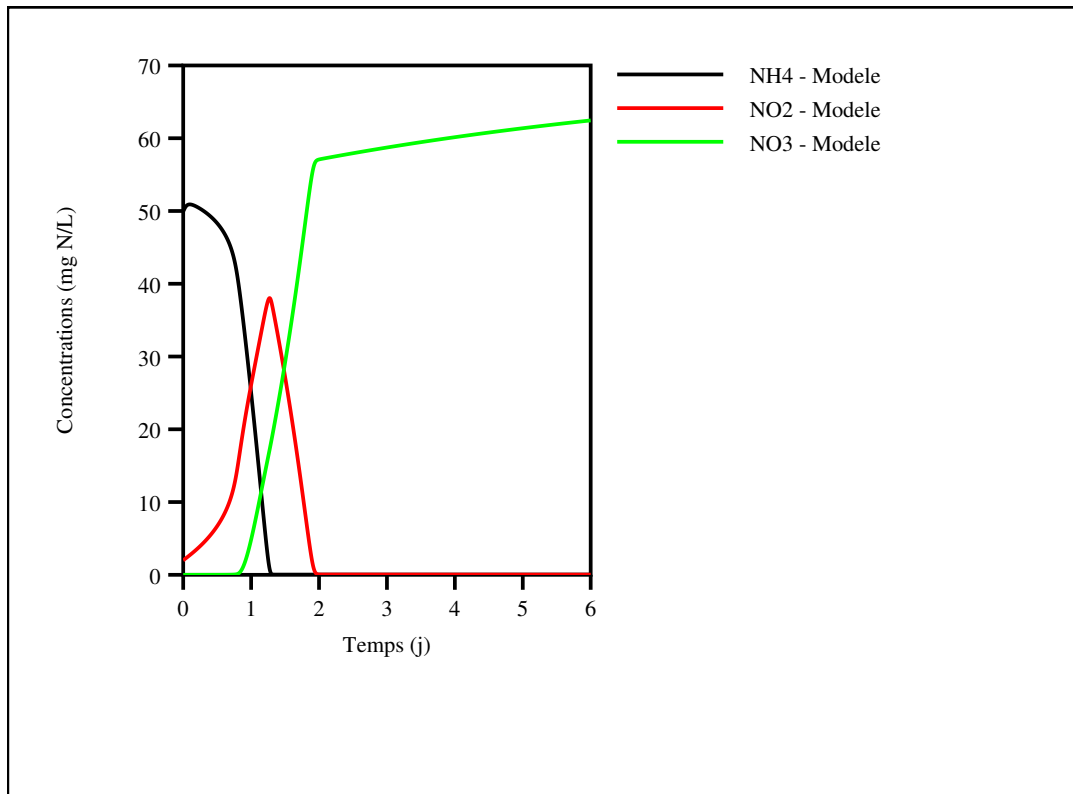
FIGURE C.2: Nitrogen species during reactor start-up

It should be noticed that in order to induce the automatic feed control with a pH range around 6, one has to wait for for more than 1 day for pH to decrease sufficiently. This is highly dependant on the initial ammonia concentration and alkalinity of the tap water used to dilute the sludge. Additional simulations have been carried out with varying HCO_3/CO_3 ratios to confirm this (results not shown).
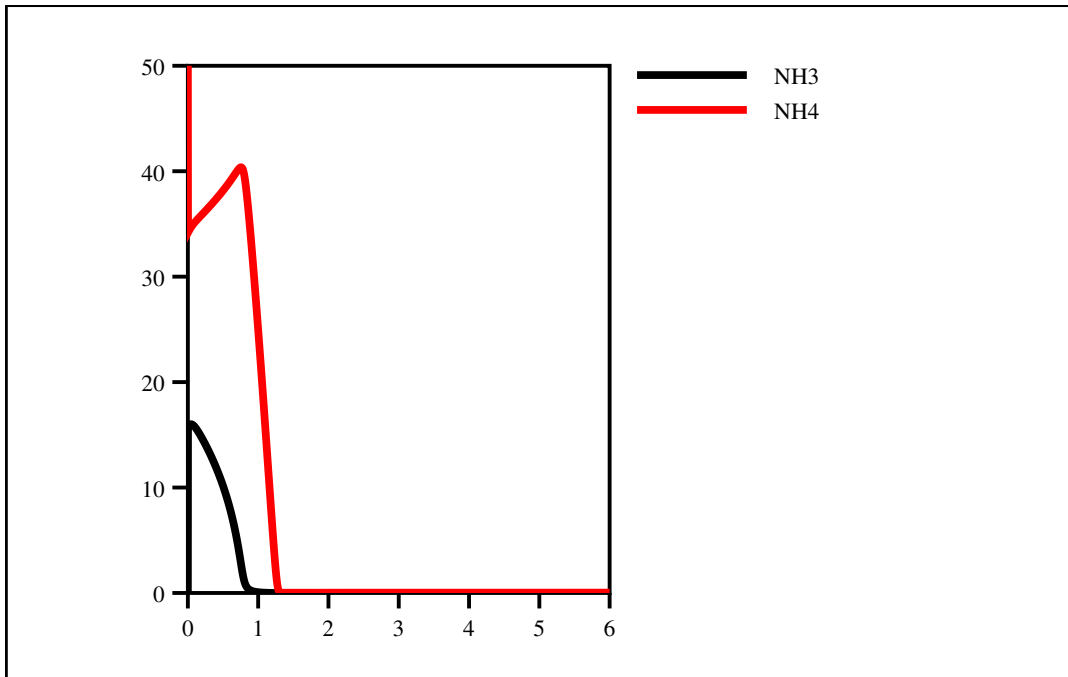
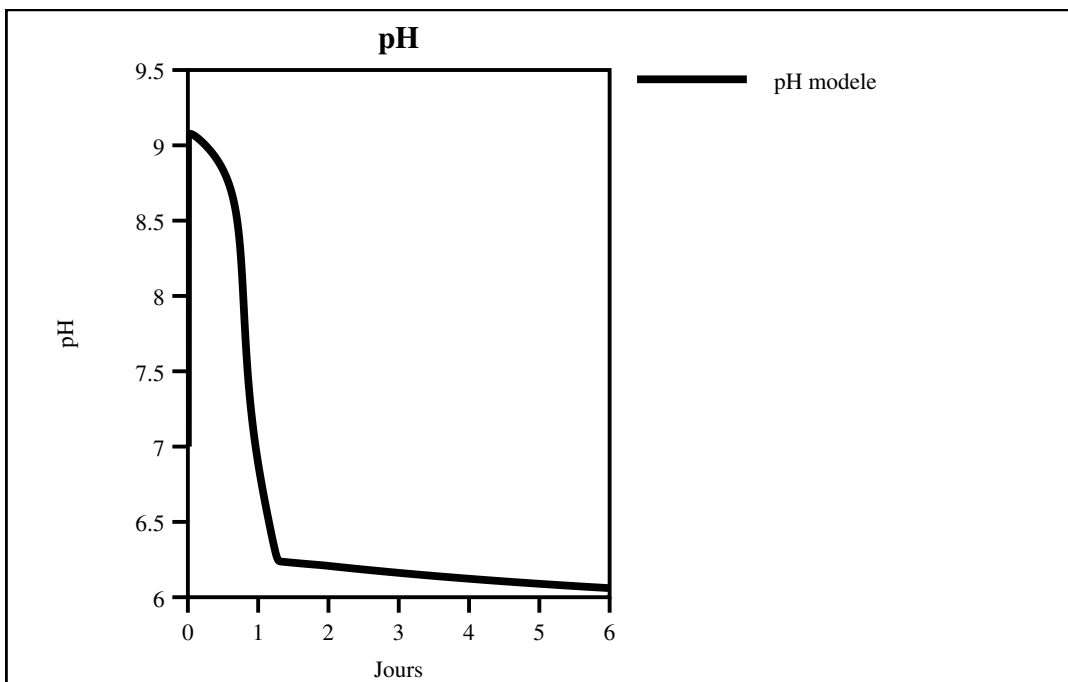FIGURE C.3: Ammonia/ammonium during reactor start-up
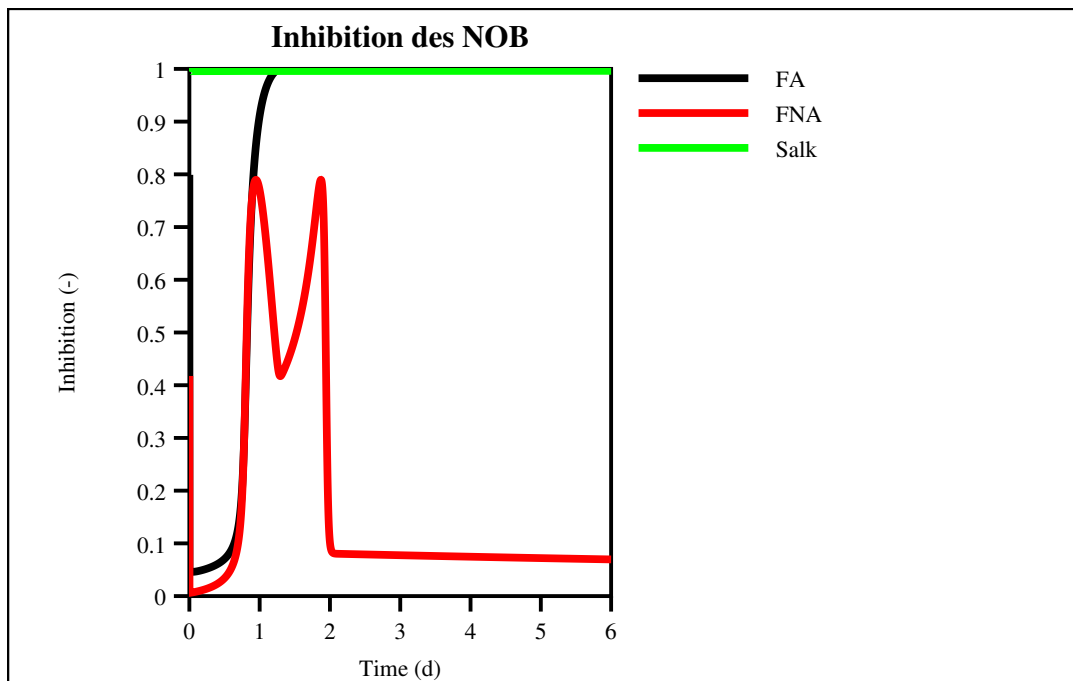

FIGURE C.4: pH evolution during reactor start-up

FIGURE C.5: Inhibition terms for NOB during reactor start-up

Appendix D

Data from the pilot

The next are the results for pH, O_2, T and Conductivity for the two campaigns.

Bibliography

Ahn, Joon Ho, Ran Yu, and Kartik Chandran (2008). "Distinctive microbial ecology and biokinetics of autotrophic ammonia and nitrite oxidation in a partial nitrification bioreactor". In: *Biotechnol. Bioeng.* 100.6, pp. 1078–1087. ISSN: 00063592. DOI: 10.1002/bit.21863.

Ahn, Y T et al. (2006). "Modeling of extracellular polymeric substances and soluble microbial products production in a submerged membrane bioreactor at various SRTs". en. In: *Water Sci. Technol.* 53.7, pp. 209–216. DOI: 10.2166/wst.2006.330. URL: http://wst.iwaponline.com/cgi/doi/10.2166/wst.2006.330.

Alleman, J. E. (1985). "Elevated nitrite occurrence in biological wastewater treatment systems". In: *Water Sci. Technol.* 17.2-3 -3 pt 1, pp. 409–419. ISSN: 02731223. DOI: 10.2166/wst.1985.0147.

Anthonisen, A C et al. (1976a). "Inhibition of nitrification by ammonia and nitrous acid". In: *J. (Water Pollut. Control Fed.*, pp. 835–852. URL: http://www.jstor.org/stable/25038971.

— (1976b). "Inhibition of nitrification by ammonia and nitrous acid". In: *J. (Water Pollut. Control Fed.*, pp. 835–852. URL: http://www.jstor.org/stable/25038971.

Antileo, Christian et al. (2002). "Nitrifying biomass acclimation to high ammonia concentration". In: *J. Environ. Eng.* 128.4, pp. 367–375. URL: http://ascelibrary.org/doi/abs/10.1061/(ASCE)0733-9372(2002)128:4(367)http://dabamirror.sci-hub.cc/737fac4c05b6c1a2d392afcfed09ba83/antileo2002.pdf.

Apha (2005). "Standard methods for the examination of water and wastewater (19th ed.)Washington". In: *Am. J. Public*.

Aquino, Sérgio F and David C Stuckey (2008). "Integrated model of the production of soluble microbial products (SMP) and extracellular polymeric substances (EPS) in anaerobic chemostats during transient conditions". en. In: *Biochem. Eng. J.* 38.2, pp. 138–146. DOI: 10.1016/j.bej.2007.06.010. URL: http://linkinghub.elsevier.com/retrieve/pii/S1369703X07002434.

Bae, Hyokwan et al. (2014). "High-rate partial nitritation using porous poly(vinyl alcohol) sponge". In: *Bioprocess Biosyst. Eng.* 37.6, pp. 1115–1125. ISSN: 16157605. DOI: 10.1007/s00449-013-1083-3.

Balmelle, B. et al. (1992). "Study of Factors Controlling Nitrite Build-Up in Biological Processes for Water Nitrification". In: *Water Sci. Technol.* 26.5-6, pp. 1017–1025. ISSN: 0273-1223. DOI: 10.2166/wst.1992.0543. URL: https://iwaponline.com/wst/article/26/5-6/1017-1025/26923.

Bandyopadhyay, B. et al. (2009). "Dynamic measurement of the volumetric oxygen transfer coefficient in fermentation systems". In: *Biotechnol. Bioeng.* 104.5, pp. 841–853. ISSN: 00063592. DOI: 10.1002/bit.22566. URL: http://doi.wiley.com/10.1002/bit.22566.

Bassin, João P., Marcia Dezotti, and Geraldo L. Sant'Anna (2011). "Nitrification of industrial and domestic saline wastewaters in moving bed biofilm reactor and sequencing batch reactor". In: *J. Hazard. Mater.* 185.1, pp. 242–248. ISSN: 03043894. DOI: 10.1016/j.jhazmat.2010.09.024.

Bates, Roger G. and Gladys D. Pinching (1949). "Acidic dissociation constant of ammonium ion at 0 to 50 C, and the base strength of ammonia". In: *J. Res. Natl. Bur. Stand. (1934).* 42.5, p. 419. ISSN: 0091-0635. DOI: 10.6028/jres.042.037.

Batstone, D. J. et al. (2015). "Platforms for energy and nutrient recovery from domestic wastewater: A review". In: *Chemosphere* 140, pp. 2–11. ISSN: 18791298. DOI: 10.1016/j.chemosphere.2014.10.021. URL: http://dx.doi.org/10.1016/j.chemosphere.2014.10.021.

Benjamin, Mark M and Desmond F Lawler (2013). *Water quality engineering: Physical/chemical treatment processes*. John Wiley & Sons.

Bernhard, Anne (2010). "The Nitrogen Cycle: Processes, Players, and Human Impact." In: *Nat. Educ. Knowl.* 3.10, p. 25.

Biesterfeld, Sidney et al. (2001). "EFFECT OF ALKALINITY TYPE AND CONCENTRATION ON NITRIFYING BIOFILM ACTIVITY". In: *Proc. Water Environ. Fed.* 2001.16, pp. 277–291. ISSN: 1938-6478. DOI: 10.2175/193864701790901951. URL: https://accesswater.org/publications/-288221/effect-of-alkalinity-type-and-concentration-on-nitrifying-biofilm-activity.

Blackburne, Richard et al. (2007). "Kinetic characterisation of an enriched Nitrospira culture with comparison to Nitrobacter". In: *Water Res.* 41.14, pp. 3033–3042. ISSN: 00431354. DOI: 10.1016/j.watres.2007.01.043.

Böhm, Lutz et al. (2012). "The importance of fluid dynamics for MBR fouling mitigation". In: *Bioresour. Technol.* 122, pp. 50–61. DOI: 10.1016/j.biortech.2012.05.069. URL: http://www.sciencedirect.com/science/article/pii/S0960852412008139.

Boogerd, F. C. et al. (1990). "Oxygen and carbon dioxide mass transfer and the aerobic, autotrophic cultivation of moderate and extreme thermophiles: A case study related to the microbial desulfurization of coal". In: *Biotechnol. Bioeng.* 35.11, pp. 1111–1119. ISSN: 10970290. DOI: 10.1002/bit.260351106.

Boyer, Treavor H. et al. (2014). "Ion-exchange softening of human urine to control precipitation". In: *Environ. Prog. Sustain. Energy* 33.2, pp. 564–571. ISSN: 19447442. DOI: 10.1002/ep.11825. URL: http://doi.wiley.com/10.1002/ep.11825.

Brun, Roland, Peter Reichert, and Hans R. Künsch (2001). "Practical identifiability analysis of large environmental simulation models". In: *Water Resour. Res.* 37.4, pp. 1015–1030. ISSN: 00431397. DOI: 10.1029/2000WR900350.

Brun, Roland et al. (2002). "Practical identifiability of ASM2d parameters - Systematic selection and tuning of parameter subsets". In: *Water Res.* 36.16, pp. 4113–4127. ISSN: 00431354. DOI: 10.1016/S0043-1354(02)00104-5.

Buhr, H. O. and S. B. Miller (1983). "A dynamic model of the high-rate algal-bacterial wastewater treatment pond". In: *Water Res.* 17.1, pp. 29–37. ISSN: 00431354. DOI: 10.1016/0043-1354(83)90283-X.

Call, R. Ellsworth (1892). *The chemistry of soils*. Vol. 20. 493, pp. 29–30. ISBN: 9780195313697. DOI: 10.1126/science.ns-20.493.29.

Calvin, Katherine et al. (2009). "2.6: Limiting climate change to 450 ppm CO2 equivalent in the 21st century". In: *Energy Econ.* 31.SUPPL. 2, S107–S120. ISSN: 01409883. DOI: 10.1016/j.eneco.2009.06.006. URL: http://dx.doi.org/10.1016/j.eneco.2009.06.006.

Capodici, M et al. (2016). "Respirometry for the Characterization of Heterotrophic Biomass Activity: Application to a MBR Pilot Plant Operated with Two Different Start-Up Strategies". In: *J. Environ. Eng.* 142.2, p. 06015009. ISSN: 0733-9372. DOI: 10.1061/(ASCE)EE.1943-7870.0001036. URL: http://dx.doi.org/10.1061/(ASCE)EE.1943-7870.0001036http://ascelibrary.org/doi/10.1061/{\%}28ASCE{\%}29EE.1943-7870.0001036.

Carrera, J. et al. (2003). "Biological nitrogen removal of high-strength ammonium industrial wastewater with two-sludge system". In: *Water Res.* 37.17, pp. 4211–4221. ISSN: 00431354. DOI: 10.1016/S0043-1354(03)00338-5.

Carstensen, Jacob (1996). "Identification of Wastewater Processes". In: 73.

Chandran, Kartik and Barth F. Smets (2000). "Single-step nitrification models erroneously describe batch ammonia oxidation profiles when nitrite oxidation becomes rate limiting". In: *Biotechnol. Bioeng.* 68.4, pp. 396–406. ISSN: 00063592. DOI: 10.1002/(SICI)1097-0290(20000520)68:4<396::AID-BIT5>3.0.CO;2-S.

Chatterjee, Pritha, M M Ghangrekar, and Surampalli Rao (2016). "Development of anammox process for removal of nitrogen from wastewater in a novel self-sustainable biofilm reactor". en. In: *Bioresour. Technol.* 218, pp. 723–730. DOI: 10.1016/j.biortech.2016.07.002. URL: http://linkinghub.elsevier.com/retrieve/pii/S096085241630966X.

Chen, Yao (2009). "Full nitrification of human urine in a sequencing batch reactor". In: URL: http://repository.ust.hk/dspace/handle/1783.1/6303.

Chifflet, Sandrine, Philippe Gerard, and Renaud Fichez (2004). "Manuel D'Analyses Chimiques Dans L'Eau De Mer". In: *Ird*.

Choubert, Jean-Marc et al. (2010). "Techniques de fractionnement de la matière organique des déchets liquides pour la modélisation des bioprocédés". In: *Tech. l'ingénieur.* URL: https://www.researchgate.net/profile/Jean-marc{_}Choubert2/publication/236001588{_}Techniques{_}de{_}fractionnement{_}de{_}la{_}matire{_}organique{_}des{_}dchets{_}liquides{_}pour{_}la{_}modlisation{_}des{_}bioprocds/links/0deec51574e6dafeff000000.pdf.

Clauwaert, Peter et al. (2017). "Nitrogen cycling in Bioregenerative Life Support Systems: Challenges for waste refinery and food production processes". In: *Prog. Aerosp. Sci.* 91.April 2017, pp. 87–98. ISSN: 03760421. DOI: 10.1016/j.paerosci.2017.04.002. URL: http://dx.doi.org/10.1016/j.paerosci.2017.04.002.

Clegg, Simon L. and Michael Whitfield (1995). "A chemical model of seawater including dissolved ammonia and the stoichiometric dissociation constant of ammonia in estuarine water and seawater from -2 to 40°C". In: *Geochim. Cosmochim. Acta* 59.12, pp. 2403–2421. ISSN: 00167037. DOI: 10.1016/0016-7037(95)00135-2.

Coppens, Joeri et al. (2016). "Nitrification and microalgae cultivation for two-stage biological nutrient valorization from source separated urine". In: *Bioresour. Technol.* 211.2016, pp. 41–50. ISSN: 18732976. DOI: 10.1016/j.biortech.2016.03.001. URL: http://dx.doi.org/10.1016/j.biortech.2016.03.001.

Corominas, Lluís et al. (2011). "Modified calibration protocol evaluated in a model-based testing of SBR flexibility". In: *Bioprocess Biosyst. Eng.* 34.2, pp. 205–214. ISSN: 16157591. DOI: 10.1007/s00449-010-0462-2.

Cui, Fenghao et al. (2017). "Experimentation and mathematical models for partial nitrification in aerobic granular sludge process". en. In: *KSCE J. Civ. Eng.* 21.1, pp. 127–133. ISSN: 1226-7988, 1976-3808. DOI: 10.1007/s12205-016-0506-5. URL: http://link.springer.com/10.1007/s12205-016-0506-5http://zeze.sci-hub.cc/bcf2e59b0f70a7e0246eef6de09ef8ae/cui2016.pdf.

Cui, Y. W. et al. (2014). "Start-up of halophilic nitrogen removal via nitrite from hypersaline wastewater by estuarine sediments in sequencing batch reactor". In: *Int. J. Environ. Sci. Technol.* 11.2, pp. 281–292. ISSN: 17352630. DOI: 10.1007/s13762-013-0190-7.

Curl, Rane L (1979). "Carbonate Chemistry of Aquatic Systems, by R. E. Loewenthal and G. v. R. Marais, Ann Arbor Science, 433 pp+ xi,$22.50". In: *AIChE J.* 25.3, pp. 557–557. ISSN: 0001-1541. DOI: 10.1002/aic.690250328. URL: https://

aiche.onlinelibrary.wiley.com/doi/abs/10.1002/aic.690250328http://doi.wiley.com/10.1002/aic.690250328.

Da Costa et all, BIPE-FP2E study (2015). "Public Water and Wastewater Services in France Economic, Social and Environmental Data 6th". In: URL: http://www.fp2e.org/userfiles/files/publication/RAPPORT{_}BIPE{_}GB{_}ENTIER.pdf.

Dasgupta, Purnendu K. and Shen Dong (1986). "Solubility of ammonia in liquid water and generation of trace levels of standard gaseous ammonia". In: *Atmos. Environ.* 20.3, pp. 565–570. ISSN: 00046981. DOI: 10.1016/0004-6981(86)90099-5.

De Silva, D G and Bruce E Rittmann (2000). "Nonsteady-state modeling of multispecies activated-sludge processes". In: *Water Environ. Res.* 72.5, pp. 554–565. URL: http://www.ingentaconnect.com/content/wef/wer/2000/00000072/00000005/art00006.

De Temmerman, L et al. (2014). "Salt stress in a membrane bioreactor: Dynamics of sludge properties, membrane fouling and remediation through powdered activated carbon dosing". en. In: *Water Res.* 63, pp. 112–124. DOI: 10.1016/j.watres.2014.06.017. URL: http://linkinghub.elsevier.com/retrieve/pii/S0043135414004461.

Delrue, F et al. (2010). "Modelling a full scale membrane bioreactor using Activated Sludge Model No.1: challenges and solutions". en. In: *Water Sci. Technol.* 62.10, p. 2205. DOI: 10.2166/wst.2010.383. URL: http://wst.iwaponline.com/cgi/doi/10.2166/wst.2010.383.

Delrue, Florian (2008). "L'UNIVERSITE BORDEAUX 2". PhD thesis. URL: http://ori-oai.u-bordeaux1.fr/pdf/2008/DELRUE{_}FLORIAN{_}2008.pdf.

Di Bella, Gaetano, Giorgio Mannina, and Gaspare Viviani (2008). "An integrated model for physical-biological wastewater organic removal in a submerged membrane bioreactor: Model development and parameter estimation". In: *J. Memb. Sci.* 322.1, pp. 1–12. DOI: 10.1016/j.memsci.2008.05.036. URL: http://www.sciencedirect.com/science/article/pii/S0376738808004754.

Di Bella, Gaetano, Michele Torregrossa, and Gaspare Viviani (2011). "The role of EPS concentration in MBR foaming: Analysis of a submerged pilot plant". en. In: *Bioresour. Technol.* 102.2, pp. 1628–1635. DOI: 10.1016/j.biortech.2010.09.028. URL: http://linkinghub.elsevier.com/retrieve/pii/S0960852410015415.

Di Bella, Gaetano et al. (2015). "Performance of membrane bioreactor (MBR) systems for the treatment of shipboard slops: Assessment of hydrocarbon biodegradation and biomass activity under salinity variation". en. In: *J. Hazard. Mater.* 300, pp. 765–778. DOI: 10.1016/j.jhazmat.2015.08.021. URL: http://linkinghub.elsevier.com/retrieve/pii/S0304389415300133.

Digiano, Francis A et al. (2004). "Membrane Bioreactor Technology and Sustainable Water". In: *Water Environ. Res.* 76.3, pp. 195–196. DOI: 10.1002/j.1554-7531.2004.tb00220.x.

Dochain, Denis and P. Vanrolleghem (2015). *Dynamical Modelling & Estimation in Wastewater Treatment Processes*. Vol. 4, pp. 9781780403045–9781780403045. DOI: 10.2166/9781780403045. URL: https://iwaponline.com/ebooks/book/151/.

Drtil, Miloslav, Peter Németh, and Igor Bodík (1993). "Kinetic constants of nitrification". In: *Water Res.* 27.1, pp. 35–39. ISSN: 00431354. DOI: 10.1016/0043-1354(93)90192-K. URL: http://dx.doi.org/10.1016/j.watres.2011.08.036{\%}5Cnhttp://dx.doi.org/10.1016/j.biortech.2010.01.038{\%}5Cnhttp://dx.doi.org/10.1016/j.biortech.2014.07.065https://iwaponline.com/wst/article/59/11/2093/15747/Biological-nitrogen-and-phosphorus-removal-inhttps:.

Du, Rui et al. (2014). "Advanced nitrogen removal with simultaneous Anammox and denitrification in sequencing batch reactor". In: *Bioresour. Technol.* 162, pp. 316–322. ISSN: 18732976. DOI: 10.1016/j.biortech.2014.03.041. URL: http://dx.doi.org/10.1016/j.biortech.2014.03.041.

Dubber, Donata and Nicholas F. Gray (2010). "Replacement of chemical oxygen demand (COD) with total organic carbon (TOC) for monitoring wastewater treatment performance to minimize disposal of toxic analytical waste". In: *J. Environ. Sci. Heal. - Part A Toxic/Hazardous Subst. Environ. Eng.* 45.12, pp. 1595–1600. ISSN: 10934529. DOI: 10.1080/10934529.2010.506116.

Ebeling, James M., Michael B. Timmons, and J. J. Bisogni (2006). "Engineering analysis of the stoichiometry of photoautotrophic, autotrophic, and heterotrophic removal of ammonia-nitrogen in aquaculture systems". In: *Aquaculture* 257.1-4, pp. 346–358. ISSN: 00448486. DOI: 10.1016/j.aquaculture.2006.03.019. URL: http://dx.doi.org/10.1016/j.aquaculture.2006.03.019.

Eckenfelder, W W and J G Cleary (2013). *Activated Sludge Technologies for Treating Industrial Wastewaters*. DEStech Publications Incorporated. ISBN: 9781605950198. URL: https://books.google.fr/books?id=3RANAQAAQBAJ.

Eddy, Metcalf & (2003). "Wastewater Engineering: Treatment and Reuse". In: *J. Phys. A Math. Theor.* 44.8. Ed. by Intergovernmental Panel on Climate Change, p. 085201. ISSN: 1751-8113. DOI: 10.1016/0013-7952(93)90087-S. arXiv: 1011.1669. URL: https://www.cambridge.org/core/product/identifier/CBO9781107415324A009/type/book{_}parthttp://www.scirp.org/journal/doi.aspx?DOI=10.4236/jwarp.2018.103020http://arxiv.org/abs/1011.1669http://dx.doi.org/10.1088/1751-8113/44/8/085201http://stacks.iop.org/.

Edefell, Ellen (2017). "Challenges during start-up of urine nitrification in an MBBR". In: URL: www.vateknik.lth.se.

Effler, Steven W. et al. (1990). *Free Ammonia and Toxicity Criteria in a Polluted Urban Lake*. DOI: 10.2307/25043912. URL: https://www.jstor.org/stable/pdf/25043912.pdf.

Egli, Konrad et al. (2003). "Community analysis of ammonia and nitrite oxidizers during start-up of nitritation reactors". In: *Appl. Environ. Microbiol.* 69.6, pp. 3213–3222. ISSN: 00992240. DOI: 10.1128/AEM.69.6.3213-3222.2003.

EPA, U.S. (2009). "Nutrient control design manual: state of technology review report. EPA/600/R-09/012 EPA/600/R-09/012. US Environmental Protection Agency." In: January.

Esculier, Fabien (2018). "Le système alimentation / excrétion des territoires urbains : régimes et transitions socio-écologiques". In:

Etter, B, K M Udert, and T Gounden (2014). "VUNA – Scaling Up Nutrient Recovery from Urine". In: *Technol. Dev. Int. Conf.* June, pp. 4–6. URL: www.vuna..

Etter, Bastian, Alexandra Hug, and Kai M Udert (2013). "Total Nutrient Recovery from Urine-Operation of a Pilot-Scale Nitrification Reactor". In: URL: https://pdfs.semanticscholar.org/c2de/cdb0c8af8a2815f8ee356bd0a44bb06703bc.pdf.

Fall, C et al. (2014). "Total solids-retention in activated sludge: modelling and simulation". In: pp. 321–332. DOI: 10.2495/WP140281. URL: http://library.witpress.com/viewpaper.asp?pcode=WP14-028-1.

Fallah, N. et al. (2010). "Long-term operation of submerged membrane bioreactor (MBR) for the treatment of synthetic wastewater containing styrene as volatile organic compound (VOC): Effect of hydraulic retention time (HRT)". In: *J. Hazard. Mater.* 178.1–3, pp. 718–724. ISSN: 0304-3894. DOI: 10.1016/j.jhazmat.2010.02.001. URL: http://www.sciencedirect.com/science/article/pii/

`S0304389410001834http://www.sciencedirect.com/science/article/pii/`
`S0304389410001834/pdfft?md5=ebd83a4c94e8cd6ae6bb3e506be9068a{\&}pid=`
`1-s2.0-S0304389410001834-main.pdf`.

Feng, Daolun, Zucheng Wu, and Shihong Xu (2008). "Nitrification of human urine for its stabilization and nutrient recycling". In: *Bioresour. Technol.* 99.14, pp. 6299–6304. ISSN: 09608524. DOI: `10.1016/j.biortech.2007.12.007`.

Fenu, A. et al. (2010a). "Activated sludge model (ASM) based modelling of membrane bioreactor (MBR) processes: A critical review with special regard to MBR specificities". In: *Water Res.* 44.15, pp. 4272–4294. ISSN: 0043-1354. DOI: `10.1016/j.watres.2010.06.007`. URL: `http://www.sciencedirect.com/science/article/pii/S0043135410003830http://www.sciencedirect.com/science/article/pii/S0043135410003830/pdfft?md5=507e2a66cf5bcb4597f66189d29076a6{\&}pid=1-s2.0-S0043135410003830-main.pdf`.

Fenu, A et al. (2010b). "Activated sludge model (ASM) based modelling of membrane bioreactor (MBR) processes: A critical review with special regard to MBR specificities". In: *Water Res.* 44.15, pp. 4272–4294. DOI: `10.1016/j.watres.2010.06.007`. URL: `http://www.sciencedirect.com/science/article/pii/S0043135410003830`.

Fenu, A et al. (2010c). "Energy audit of a full scale MBR system". en. In: *Desalination* 262.1-3, pp. 121–128. DOI: `10.1016/j.desal.2010.05.057`. URL: `http://linkinghub.elsevier.com/retrieve/pii/S0011916410003747`.

Flanagan, C. P. and D. G. Randall (2018). "Development of a novel nutrient recovery urinal for on-site fertilizer production". In: *J. Environ. Chem. Eng.* 6.5, pp. 6344–6350. ISSN: 22133437. DOI: `10.1016/j.jece.2018.09.060`. URL: `https://doi.org/10.1016/j.jece.2018.09.060`.

Flores-Alsina, Xavier et al. (2015). "A plant-wide aqueous phase chemistry module describing pH variations and ion speciation/pairing in wastewater treatment process models". In: *Water Res.* 85, pp. 255–265. ISSN: 18792448. DOI: `10.1016/j.watres.2015.07.014`. URL: `http://dx.doi.org/10.1016/j.watres.2015.07.014`.

Fumasoli, Alexandra, Eberhard Morgenroth, and Kai M Udert (2015). "Modeling the low pH limit of Nitrosomonas eutropha in high-strength nitrogen wastewaters". In: DOI: `10.1016/j.watres.2015.06.013`. URL: `http://creativecommons.org/licenses/by/4.0/`.

Fumasoli, Alexandra et al. (2016). "Operating a pilot-scale nitrification/distillation plant for complete nutrient recovery from urine". In: *Water Sci. Technol.* 73.1, pp. 215–222. ISSN: 0273-1223. DOI: `10.2166/wst.2015.485`. URL: `https://iwaponline.com/wst/article/73/1/215/18906/Operating-a-pilotscale-nitrificationdistillation`.

Fumasoli, Alexandra et al. (2017). "Growth of Nitrosococcus-Related Ammonia Oxidizing Bacteria Coincides with Extremely Low pH Values in Wastewater with High Ammonia Content". In: DOI: `10.1021/acs.est.7b00392`. URL: `https://www.ncbi.nlm.nih.gov/pmc/articles/PMC5538757/pdf/es7b00392.pdf`.

Fux, C. et al. (2004). "Difficulties in maintaining long-term partial nitritation of ammonium-rich sludge digester liquids in a moving-bed biofilm reactor (MBBR)". In: *Water Sci. Technol.* 49.11-12, pp. 53–60. ISSN: 02731223. DOI: `10.2166/wst.2004.0803`.

Fux, Christian et al. (2002). "Biological treatment of ammonium-rich wastewater by partial nitritation and subsequent anaerobic ammonium oxidation (anammox) in a pilot plant". In: *J. Biotechnol.* 99.3, pp. 295–306. ISSN: 01681656. DOI: `10.1016/S0168-1656(02)00220-1`.

Ganigué, R. et al. (2010). "Systematic model development for partial nitrification of landfill leachate in a SBR". In: *Water Sci. Technol.* 61.9, pp. 2199–2210. ISSN: 02731223. DOI: 10.2166/wst.2010.979.

Gernaey, A. Krist et al. (2001). "Activated sludge monitoring with combined respirometric–titrimetric measurements". In: *Water Res.* 35.5, pp. 1280–1294.

Gernaey, Krist V. et al. (2004). "Activated sludge wastewater treatment plant modelling and simulation: State of the art". In: *Environ. Model. Softw.* 19.9, pp. 763–783. ISSN: 13648152. DOI: 10.1016/j.envsoft.2003.03.005.

Ginestet, Philippe et al. (1998). "Estimation of nitrifying bacterial activities by measuring oxygen uptake in the presence of the metabolic inhibitors allylthiourea and azide". In: *Appl. Environ. Microbiol.* 64.6, pp. 2266–2268. ISSN: 00992240.

Gòdia, F. et al. (2002). "MELISSA: A loop of interconnected bioreactors to develop life support in Space". In: *J. Biotechnol.* 99.3, pp. 319–330. ISSN: 01681656. DOI: 10.1016/S0168-1656(02)00222-5.

Griffith, T David (2016). *Basic principles and calculations in process technology*. Prentice Hall.

Guisasola, Albert et al. (2005). "Respirometric estimation of the oxygen affinity constants for biological ammonium and nitrite oxidation". en. In: *J. Chem. Technol. Biotechnol.* 80.4, pp. 388–396. DOI: 10.1002/jctb.1202. URL: http://onlinelibrary.wiley.com.ezproxy.unilim.fr/doi/10.1002/jctb.1202/abstract.

Guisasola, Albert et al. (2007). "Inorganic carbon limitations on nitrification: Experimental assessment and modelling". In: *Water Res.* 41.2, pp. 277–286. ISSN: 00431354. DOI: 10.1016/j.watres.2006.10.030.

Gujer, Willi et al. (1999). "Activated Sludge Model No. 3". In: *Water Sci. Technol.* 39.1, pp. 183–193. ISSN: 02731223. DOI: 10.1016/S0273-1223(98)00785-9.

Haag, I. and B. Westrich (2002). "Processes governing river water quality identified by principal component analysis". In: *Hydrol. Process.* 16.16, pp. 3113–3130. ISSN: 08856087. DOI: 10.1002/hyp.1091.

Haag, Ingo (2006). "A basic water quality model for the River Neckar: Part 1 - Model development, parameter sensitivity and identifiability, calibration and validation". In: *Acta Hydrochim. Hydrobiol.* 34.6, pp. 533–548. ISSN: 03234320. DOI: 10.1002/aheh.200400652.

Haandel, A.C. van (2012). "Handbook of Biological Wastewater Treatment: Design and Optimisation of Activated Sludge Systems". In: *Water Intell. Online* 11. ISSN: 14761777. DOI: 10.2166/9781780400808. URL: https://iwaponline.com/ebooks/book/622/.

Habermacher, Jonathan et al. (2016). "Degradation of the unbiodegradable particulate fraction (XU) from different activated sludges during batch digestion tests at ambient temperature". en. In: *Water Res.* 98, pp. 206–214. DOI: 10.1016/j.watres.2016.04.005. URL: http://linkinghub.elsevier.com/retrieve/pii/S0043135416302020.

Hao, Xiaodi, Joseph J. Heijnen, and Mark C.M. Van Loosdrecht (2001). "Sensitivity analysis of a biofilm model describing a one-stage completely autotrophic nitrogen removal (CANON) process". In: *Biotechnol. Bioeng.* 77.3, pp. 266–277. ISSN: 00063592. DOI: 10.1002/bit.10105.

Harder, Robin et al. (2019). "Recycling nutrients contained in human excreta to agriculture: Pathways, processes, and products". In: *Crit. Rev. Environ. Sci. Technol.* 49.8, pp. 695–743. ISSN: 15476537. DOI: 10.1080/10643389.2018.1558889. URL: https://doi.org/10.1080/10643389.2018.1558889.

Harned, Herbert S and Raymond Davis (1943). "The Ionization Constant of Carbonic Acid in Water and the Solubility of Carbon Dioxide in Water and Aqueous

Salt Solutions from 0 to 50°". In: *J. Am. Chem. Soc.* 65.10, pp. 2030–2037. ISSN: 0002-7863. DOI: 10.1021/ja01250a059. URL: https://doi.org/10.1021/ja01250a059.

Hellinga, C, M C M Van Loosdrecht, and J J Heijnen (2010). "Mathematical and Computer Modelling of Dynamical Systems : Methods , Tools and Applications in Engineering and Related Sciences Model Based Design of a Novel Process for Nitrogen Removal from Concentrated Flows". In: April 2012, pp. 37–41.

Hellinga, C. et al. (1998). "The SHARON process: An innovative method for nitrogen removal from ammonium-rich waste water". In: *Water Sci. Technol.* 37.9, pp. 135–142. ISSN: 02731223. DOI: 10.1016/S0273-1223(98)00281-9. URL: http://dx.doi.org/10.1016/S0273-1223(98)00281-9.

Hellström, Daniel (1999). "Exergy Analysis: A Comparison of Source Separation Systems and Conventional Treatment Systems". In: *Water Environ. Res.* 71.7, pp. 1354–1363. ISSN: 1061-4303. DOI: 10.2175/106143096x122302.

Hellström, Daniel, Erica Johansson, and Kerstin Grennberg (1999). "Storage of human urine: Acidification as a method to inhibit decomposition of urea". In: *Ecol. Eng.* 12.3-4, pp. 253–269. ISSN: 09258574. DOI: 10.1016/S0925-8574(98)00074-3.

Henze, M et al. (1986). "Activated sludge model no. 1 by IAWPRC". In: 1.

Henze, Mogens (2007). *Activated sludge models ASM1, ASM2, ASM2d and ASM3*. eng. Reprinted. 9. London: IWA Publ, p. 121. ISBN: 978-1-900222-24-2.

Hindmarsh, Alan C. (1982). *Toward a Systematized Collection of Ode Solvers.*

Hinshelwood, C. N. (1945). *Physical chemistry*. Vol. 156. 3958, pp. 283–284. ISBN: 9780716787594. DOI: 10.1038/156283a0.

Holloway, B and G Lyberatos (1990). "Effect of temperature and ph on the effective maximum specific growth rate of nitrifying bacteria". In: 24.1, pp. 97–101. ISSN: 00431354. DOI: 10.1016/0043-1354(90)90070-M.

Hong, Junming et al. (2013). "Deciphering the effect of salinity on the performance of submerged membrane bioreactor for aquaculture of bacterial community". In: *Desalination* 316, pp. 23–30. ISSN: 00119164. DOI: 10.1016/j.desal.2013.01.015. URL: http://dx.doi.org/10.1016/j.desal.2013.01.015.

Hulle, Stijn Van, De Leenheer Decaan, and V a N Langenhove Promotor (2005). *Modelling , Simulation and Optimization of Autotrophic Nitrogen Removal Processes Modelleren , Simuleren En Optimaliseren Van*, p. 256. ISBN: 9059890507.

Hunik, J. H., H. J.G. Meijer, and J. Tramper (1992). "Kinetics of Nitrosomonas europaea at extreme substrate, product and salt concentrations". In: *Appl. Microbiol. Biotechnol.* 37.6, pp. 802–807. ISSN: 01757598. DOI: 10.1007/BF00174849.

Hunik, J. H., J. Tramper, and R. H. Wijffels (1994). "A strategy to scale up nitrification processes with immobilized cells of nitrosomonas europaea and nitrobacter agilis". In: *Bioprocess Eng.* 11.2, pp. 73–82. ISSN: 0178515X. DOI: 10.1007/BF00389563.

Hunik, J. H. et al. (1993). "Quantitative determination of the spatial distribution of Nitrosomonas europaea and Nitrobacter agilis cells immobilized in ??-carrageenan gel beads by a specific fluorescent-antibody labelling technique". In: *Appl. Environ. Microbiol.* 59.6, pp. 1951–1954. ISSN: 00992240.

Insel, Güçlü et al. (2006). "A calibration methodology and model-based systems analysis for SBRs removing nutrients under limited aeration conditions". In: *J. Chem. Technol. Biotechnol.* 81.4, pp. 679–687. ISSN: 02682575. DOI: 10.1002/jctb.1464.

Ishii, Stephanie K.L. and Treavor H. Boyer (2015). "Life cycle comparison of centralized wastewater treatment and urine source separation with struvite precipitation: Focus on urine nutrient management". In: *Water Res.* 79, pp. 88–103. ISSN:

18792448. DOI: 10.1016/j.watres.2015.04.010. URL: http://dx.doi.org/10.1016/j.watres.2015.04.010.

ISO, I S O (1984). "5663, Water Quality—Determination of Kjeldahl Nitrogen—Method after Mineralization with Selenium". In: *Int. Organ. Stand. Geneve*.

Jaatinen, Sanna et al. (2016). "Effect of source-separated urine storage on estrogenic activity detected using bioluminescent yeast Saccharomyces cerevisiae". In: *Environ. Technol. (United Kingdom)* 37.17, pp. 2172–2182. ISSN: 1479487X. DOI: 10.1080/09593330.2016.1144797.

Jacquin, Céline et al. (2018). "Link between dissolved organic matter transformation and process performance in a membrane bioreactor for urinary nitrogen stabilization". In: *Environ. Sci. Water Res. Technol.* 4.6, pp. 806–819. DOI: 10.1039/C8EW00029H. URL: http://dx.doi.org/10.1039/C8EW00029H.

Jagtap, Neha and Treavor H. Boyer (2020). "Integrated Decentralized Treatment for Improved N and K Recovery from Urine". In: *J. Sustain. Water Built Environ.* 6.2, pp. 1–9. ISSN: 23796111. DOI: 10.1061/JSWBAY.0000899.

Jang, Namjung et al. (2006). "Steady-state modeling of bio-fouling potentials with respect to the biological kinetics in the submerged membrane bioreactor (SMBR)". en. In: *J. Memb. Sci.* 284.1-2, pp. 352–360. DOI: 10.1016/j.memsci.2006.08.001. URL: http://linkinghub.elsevier.com/retrieve/pii/S0376738806005229.

Janus, T and B Ulanicki (2010). "Modelling SMP and EPS formation and degradation kinetics with an extended ASM3 model". In: *Desalination* 261.1–2, pp. 117–125. DOI: 10.1016/j.desal.2010.05.021. URL: http://www.sciencedirect.com/science/article/pii/S001191641000336X.

Jiang, T et al. (2008). "Modelling the production and degradation of soluble microbial products (SMP) in membrane bioreactors (MBR)". en. In: *Water Res.* 42.20, pp. 4955–4964. DOI: 10.1016/j.watres.2008.09.037. URL: http://linkinghub.elsevier.com/retrieve/pii/S0043135408004211.

Jiang, Tao et al. (2005). "Calibrating a side-stream membrane bioreactor using Activated Sludge Model No. 1". In: *Water Sci. Technol.* 52.10-11, pp. 359–367. URL: http://wst.iwaponline.com/content/52/10-11/359.abstract.

Jimenez, Julie et al. (2010). "Biological modelling of MBR and impact of primary sedimentation". en. In: *Desalination* 250.2, pp. 562–567. DOI: 10.1016/j.desal.2009.09.024. URL: http://linkinghub.elsevier.com/retrieve/pii/S0011916409009977.

Jones, R. et al. (2012a). "a Study of the Biodegradable Fraction of Sludges in Aerobic and Anaerobic Systems". In: *Proc. Water Environ. Fed.* 2007.3, pp. 20–35. ISSN: 1938-6478. DOI: 10.2175/193864707787975967.

Jones, R. M. et al. (2012b). "Simulation for Operation and Control of Reject Water Treatment Processes". In: *Proc. Water Environ. Fed.* 2007.14, pp. 4357–4372. ISSN: 1938-6478. DOI: 10.2175/193864707787974599.

Jubany, I, J a Baeza, and J Carrera (2007). "Operation, modeling and automatic control of complete and partial nitrification of highly concentrated ammonium wastewater". In: *Dep. d'Enginyeria Química* Ph.D.March, p. 286.

Jubany, Irene et al. (2005). "Respirometric calibration and validation of a biological nitrite oxidation model including biomass growth and substrate inhibition". en. In: *Water Res.* 39.18, pp. 4574–4584. DOI: 10.1016/j.watres.2005.08.019. URL: http://linkinghub.elsevier.com/retrieve/pii/S0043135405004719.

Jubany, Irene et al. (2008). "Start-up of a nitrification system with automatic control to treat highly concentrated ammonium wastewater: Experimental results and modeling". en. In: *Chem. Eng. J.* 144.3, pp. 407–419. DOI: 10.1016/j.cej.2008.02.010. URL: http://linkinghub.elsevier.com/retrieve/pii/S1385894708001095.

Judd, S J (2016). "The status of industrial and municipal effluent treatment with membrane bioreactor technology". en. In: *Chem. Eng. J.* 305, pp. 37–45. DOI: `10.1016/j.cej.2015.08.141`. URL: `http://linkinghub.elsevier.com/retrieve/pii/S1385894715012346`.

Judd, Simon (2008). "The status of membrane bioreactor technology". en. In: *Trends Biotechnol.* 26.2, pp. 109–116. DOI: `10.1016/j.tibtech.2007.11.005`. URL: `http://linkinghub.elsevier.com/retrieve/pii/S0167779907003216`.

Kaelin, David et al. (2009). "Extension of ASM3 for two-step nitrification and denitrification and its calibration and validation with batch tests and pilot scale data". In: *Water Res.* 43.6, pp. 1680–1692. ISSN: 00431354. DOI: `10.1016/j.watres.2008.12.039`. URL: `http://dx.doi.org/10.1016/j.watres.2008.12.039`.

Kampschreur, Marlies J. et al. (2007). "Unraveling the Source of Nitric Oxide Emission During Nitrification". In: *Water Environ. Res.* 79.13, pp. 2499–2509. ISSN: 1061-4303. DOI: `10.2175/106143007x220815`.

Kartal, B., J. G. Kuenen, and M. C.M. Van Loosdrecht (2010). "Sewage treatment with anammox". In: *Science (80-.).* 328.5979, pp. 702–703. ISSN: 00368075. DOI: `10.1126/science.1185941`.

Kim, Dong Jin, Dong Ig Lee, and Jürg Keller (2006). "Effect of temperature and free ammonia on nitrification and nitrite accumulation in landfill leachate and analysis of its nitrifying bacterial community by FISH". In: *Bioresour. Technol.* 97.3, pp. 459–468. ISSN: 09608524. DOI: `10.1016/j.biortech.2005.03.032`.

Kong, Z et al. (1996). *SIMULTANEOUS DETERMINATION OF INHIBITION KINETICS OF CARBON OXIDATION AND NITRIFICATION WITH A RESPIROMETER.* Tech. rep. 4, pp. 825–836. URL: `https://pdf.sciencedirectassets.com/271768/1-s2.0-S0043135400X00048/1-s2.0-0043135495002324/main.pdf?X-Amz-Security-Token=AgoJb3JpZ2luX2VjEKH{\%}2F{\%}2F{\%}2F{\%}2F{\%}2F{\%}2F{\%}2F{\%}2F{\%}2F{\%}2FwEaCXVzLWVhc3QtMSJGMEQCIAJ{\%}2Fgf{\%}2BBPwM8RJlQ7m5K4W1HdGczYxQ{\%}2BVm2zhbD5uN5iAiBR8Qypbou`.

Koops, Hans Peter and Andreas Pommerening-Röser (2001). "Distribution and ecophysiology of the nitrifying bacteria emphasizing cultured species". In: *FEMS Microbiol. Ecol.* 37.1, pp. 1–9. ISSN: 01686496. DOI: `10.1016/S0168-6496(01)00137-4`.

Koops, Hans-Peter et al. (2006). "The Lithoautotrophic Ammonia-Oxidizing Bacteria". In: *The Prokaryotes*. New York, NY: Springer New York, pp. 778–811. ISBN: 0387307451. DOI: `10.1007/0-387-30745-1_36`. URL: `http://link.springer.com/10.1007/0-387-30745-1{\_}36`.

Koper, Teresa E et al. (2004). "Urease-Encoding Genes in Ammonia-Oxidizing Bacteria". In: *Appl. Environ. Microbiol.* 70.4, pp. 2342–2348. ISSN: 0099-2240. DOI: `10.1128/AEM.70.4.2342-2348.2004`. URL: `http://aem.asm.org/cgi/doi/10.1128/AEM.70.4.2342-2348.2004`.

Kowalchuk, George A. and John R. Stephen (2001). "Ammonia-Oxidizing Bacteria: A Model for Molecular Microbial Ecology". In: *Annu. Rev. Microbiol.* 55.1, pp. 485–529. ISSN: 0066-4227. DOI: `10.1146/annurev.micro.55.1.485`.

Lackner, Susanne et al. (2014). "Full-scale partial nitritation/anammox experiences - An application survey". In: *Water Res.* 55.0, pp. 292–303. ISSN: 18792448. DOI: `10.1016/j.watres.2014.02.032`. URL: `http://dx.doi.org/10.1016/j.watres.2014.02.032`.

Larsen, Tove A. (2013). *Source Separation and Decentralization for Wastewater Management.* Vol. 12. ISBN: 9781843393481. DOI: `10.2166/9781780401072`.

Larsen, Tove A. and Willi Gujer (1996). "Separate management of anthropogenic nutrient solutions (human urine)". In: *Water Sci. Technol.* 34.3-4 -4 pt 2, pp. 87–94.

ISSN: 02731223. DOI: `10.1016/0273-1223(96)00560-4`. URL: `http://dx.doi.org/10.1016/0273-1223(96)00560-4`.

— (1997). "The concept of sustainable urban water management". In: *Water Sci. Technol.* 35.9, pp. 3–10. ISSN: 02731223. DOI: `10.1016/S0273-1223(97)00179-0`. URL: `http://dx.doi.org/10.1016/S0273-1223(97)00179-0`.

Larsen, Tove A. et al. (2009). "Source Separation: Will We See a Paradigm Shift in Wastewater Handling? 1". In: *Environ. Sci. Technol.* 43.16, pp. 6121–6125. ISSN: 0013-936X. DOI: `10.1021/es803001r`. URL: `https://doi.org/10.1021/es803001rhttps://pubs.acs.org/doi/10.1021/es803001r`.

Larsen, Tove A. et al. (2016). "Emerging solutions to the water challenges of an urbanizing world". In: *Science (80-.).* 352.6288, pp. 928–933. ISSN: 10959203. DOI: `10.1126/science.aad8641`.

Laspidou, Chrysi S and Bruce E Rittmann (2002a). "A unified theory for extracellular polymeric substances, soluble microbial products, and active and inert biomass". In: *Water Res.* 36.11, pp. 2711–2720. DOI: `10.1016/S0043-1354(01)00413-4`. URL: `http://www.sciencedirect.com/science/article/pii/S0043135401004134`.

— (2002b). "Non-steady state modeling of extracellular polymeric substances, soluble microbial products, and active and inert biomass". In: *Water Res.* 36.8, pp. 1983–1992. URL: `http://www.sciencedirect.com/science/article/pii/S0043135401004146`.

Le-Clech, Pierre, Vicki Chen, and Tony A G Fane (2006). "Fouling in membrane bioreactors used in wastewater treatment". en. In: *J. Memb. Sci.* 284.1-2, pp. 17–53. DOI: `10.1016/j.memsci.2006.08.019`. URL: `http://linkinghub.elsevier.com/retrieve/pii/S0376738806005679`.

Lee, Yonghun et al. (2002). "Modeling of submerged membrane bioreactor process for wastewater treatment". In: *Desalination* 146.1, pp. 451–457. DOI: `10.1016/S0011-9164(02)00543-X`. URL: `http://www.sciencedirect.com/science/article/pii/S001191640200543X`.

Lewis, E. L. and R. G. Perkin (1981). "The practical salinity scale 1978: conversion of existing data". In: *Deep Sea Res. Part A, Oceanogr. Res. Pap.* 28.4, pp. 307–328. ISSN: 01980149. DOI: `10.1016/0198-0149(81)90002-9`.

Libralato, Giovanni, Annamaria Volpi Ghirardini, and Francesco Avezzù (2011). "To centralise or to decentralise: An overview of the most recent trends in wastewater treatment management". In: DOI: `10.1016/j.jenvman.2011.07.010`. URL: `https://pdf.sciencedirectassets.com/272592/1-s2.0-S0301479711X00129/1-s2.0-S0301479711002751/main.pdf?X-Amz-Security-Token=AgoJb3JpZ2luX2VjEKP{\%}2F{\%}2F{\%}2F{\%}2F{\%}2F{\%}2F{\%}2F{\%}2F{\%}2FwEaCXVzLWVhc3QtMSJHMEUCIQDEKLIK}2Fm2CPuJH5PLI05hyuRXhmJtQIgEzn1UkEh24`.

Lim, Jun Wei et al. (2011). "Nitrogen removal in moving bed sequencing batch reactor using polyurethane foam cubes of various sizes as carrier materials". In: *Bioresour. Technol.* 102.21, pp. 9876–9883. ISSN: 09608524. DOI: `10.1016/j.biortech.2011.08.014`. URL: `http://dx.doi.org/10.1016/j.biortech.2011.08.014`.

Lin, Hongjun et al. (2014). "A critical review of extracellular polymeric substances (EPSs) in membrane bioreactors: Characteristics, roles in membrane fouling and control strategies". en. In: *J. Memb. Sci.* 460, pp. 110–125. DOI: `10.1016/j.memsci.2014.02.034`. URL: `http://linkinghub.elsevier.com/retrieve/pii/S0376738814001586`.

Liu, Qianliang et al. (2016). "Integrated forward osmosis-membrane distillation process for human urine treatment". In: *Water Res.* 91, pp. 45–54. ISSN: 18792448. DOI: `10.1016/j.watres.2015.12.045`. URL: `http://dx.doi.org/10.1016/j.watres.2015.12.045`.

Lobos, J, M Heran, and A Grasmick (2009). "Optimization of the operations conditions in membrane bioreactors through the use of ASM3 model simulations". en. In: *Desalin. Water Treat.* 9.1-3, pp. 126–130. DOI: `10.5004/dwt.2009.761`. URL: `http://www.tandfonline.com/doi/abs/10.5004/dwt.2009.761`.

Loosdrecht, Mark C M van et al. (2016). *Experimental methods in wastewater treatment*. IWA publishing.

Lu, S G et al. (2001). "A model for membrane bioreactor process based on the concept of formation and degradation of soluble microbial products". In: *Water Res.* 35.8, pp. 2038–2048. DOI: `10.1016/S0043-1354(00)00461-9`. URL: `http://www.sciencedirect.com/science/article/pii/S0043135400004619`.

Lu, Yong-sheng et al. (2010). "Hydrodynamics and oxygen transfer in a novel extra-loop fluidized bed bioreactor". en. In: *J. Shanghai Univ. (English Ed.* 14.4, pp. 266–274. ISSN: 1007-6417, 1863-236X. DOI: `10.1007/s11741-010-0642-1`. URL: `http://link.springer.com/10.1007/s11741-010-0642-1`.

Lubello, C et al. (2009). "A modified Activated Sludge Model to estimate solids production at low and high solids retention time". en. In: *Water Res.* 43.18, pp. 4539–4548. DOI: `10.1016/j.watres.2009.08.001`. URL: `http://linkinghub.elsevier.com/retrieve/pii/S0043135409005016`.

Luedeking, Robert and Edgar L. Piret (1959). "Kinetic study of the lactic acid fermentation. Batch process at controlled pH". In: *Biotechnol. Bioeng.* 67.6, pp. 636–644. ISSN: 00063592. DOI: `10.1002/(SICI)1097-0290(20000320)67:6<636::AID-BIT3>3.0.CO;2-U`.

Luo, Wenhai et al. (2015). "Effects of salinity build-up on biomass characteristics and trace organic chemical removal: Implications on the development of high retention membrane bioreactors". en. In: *Bioresour. Technol.* 177, pp. 274–281. DOI: `10.1016/j.biortech.2014.11.084`. URL: `http://linkinghub.elsevier.com/retrieve/pii/S0960852414016964`.

Luo, Wenhai et al. (2016). "Effects of salinity build-up on the performance and bacterial community structure of a membrane bioreactor". en. In: *Bioresour. Technol.* 200, pp. 305–310. DOI: `10.1016/j.biortech.2015.10.043`. URL: `http://linkinghub.elsevier.com/retrieve/pii/S0960852415014467`.

Machdar, Izarul et al. (2018). "Effects of sponge pore-size on the performance of a down-flow hanging sponge reactor in post-treatment of effluent from an anaerobic reactor treating domestic wastewater". In: *Sustain. Environ. Res.* 28.6, pp. 282–288. ISSN: 24682039. DOI: `10.1016/j.serj.2018.07.001`. URL: `https://doi.org/10.1016/j.serj.2018.07.001`.

Mackey, H. R. et al. (2014). "Combined seawater toilet flushing and urine separation for economic phosphorus recovery and nitrogen removal: A laboratory-scale trial". In: *Water Sci. Technol.* 70.6, pp. 1065–1073. ISSN: 02731223. DOI: `10.2166/wst.2014.335`.

Magri, A. et al. (2007). "A model for the simulation of the Sharon process: pH as a key factor". In: *Environ. Technol.* 28.3, pp. 255–265. ISSN: 09593330. DOI: `10.1080/09593332808618791`.

Manser, Reto, Willi Gujer, and Hansruedi Siegrist (2005). "Consequences of mass transfer effects on the kinetics of nitrifiers". en. In: *Water Res.* 39.19, pp. 4633–4642. DOI: `10.1016/j.watres.2005.09.020`. URL: `http://linkinghub.elsevier.com/retrieve/pii/S0043135405005130`.

Massé, Anthony, Mathieu Spérandio, and Corinne Cabassud (2006). "Comparison of sludge characteristics and performance of a submerged membrane bioreactor and an activated sludge process at high solids retention time". In: *Water Res.*

40.12, pp. 2405–2415. DOI: `10.1016/j.watres.2006.04.015`. URL: `http://www.sciencedirect.com/science/article/pii/S0043135406002375`.

Maurer, M., W. Pronk, and T. A. Larsen (2006). "Treatment processes for source-separated urine". In: *Water Res.* 40.17, pp. 3151–3166. ISSN: 00431354. DOI: `10.1016/j.watres.2006.07.012`.

McCleskey, Blaine B., Kirk K. Nordstrom, and Joseph N. Ryan (2012). "Comparison of electrical conductivity calculation methods for natural waters". In: *Limnol. Oceanogr. Methods* 10.NOVEMBER, pp. 952–967. ISSN: 15415856. DOI: `10.4319/lom.2012.10.952`.

McCleskey, R.B. (2018). *Calculated specific conductance using PHREEQCI*. DOI: `https://doi.org/10.5066/F7M907VD.`. URL: `sciencebase.gov/catalog/item/5a0e0d6ae4b09af898cf2c18`.

McConville, J. R. et al. (2017). "Source separation: Challenges & opportunities for transition in the swedish wastewater sector". In: *Resour. Conserv. Recycl.* 120, pp. 144–156. ISSN: 18790658. DOI: `10.1016/j.resconrec.2016.12.004`. URL: `http://dx.doi.org/10.1016/j.resconrec.2016.12.004`.

McDonough, W., andBraungart, M. (2010). "Cradle to Cradle: Remaking the Way we Make Things". In: *London:MacMillan.*

Meng, Fangang et al. (2009). "Recent advances in membrane bioreactors (MBRs): Membrane fouling and membrane material". en. In: *Water Res.* 43.6, pp. 1489–1512. DOI: `10.1016/j.watres.2008.12.044`. URL: `http://linkinghub.elsevier.com/retrieve/pii/S0043135408006581`.

Mobley, H. L T and R. P. Hausinger (1989). "Microbial ureases: Significance, regulation, and molecular characterization". In: *Microbiol. Rev.* 53.1, pp. 85–108. ISSN: 01460749.

Mook W (2000). "Chemistry of carbonic acid in water". In: *Environ. Isot. Hydrol. Cycle Princ. Appl.*, pp. 143–165. URL: `http://www-naweb.iaea.org/napc/ih/documents/global{\_}cycle/volI/cht{\_}i{\_}09.pdf`.

Morgenroth, E., R. Kommedal, and P. Harremoës (2002). "Processes and modeling of hydrolysis of particulate organic matter in aerobic wastewater treatment - A review". In: *Water Sci. Technol.* 45.6, pp. 25–40. ISSN: 02731223. DOI: `10.2166/wst.2002.0091`.

Moussa, M. S. et al. (2005). "Modelling nitrification, heterotrophic growth and predation in activated sludge". In: *Water Res.* 39.20, pp. 5080–5098. ISSN: 00431354. DOI: `10.1016/j.watres.2005.09.038`.

Moussa, M. S. et al. (2006). "Nitrification activities in full-scale treatment plants with varying salt loads". In: *Environ. Technol.* 27.6, pp. 635–643. ISSN: 09593330. DOI: `10.1080/09593332708618673`.

Muys, Maarten (2014). "Optimization of sustainable nitrification strategies for source separated urine". In: p. 106.

Naessens, W, T Maere, and I Nopens (2012a). "Critical review of membrane bioreactor models – Part 1: Biokinetic and filtration models". In: *Bioresour. Technol.* 122, pp. 95–106. DOI: `10.1016/j.biortech.2012.05.070`. URL: `http://www.sciencedirect.com/science/article/pii/S0960852412008231`.

Naessens, W., T. Maere, and I. Nopens (2012b). "Critical review of membrane bioreactor models – Part 1: Biokinetic and filtration models". en. In: *Bioresour. Technol.* 122, pp. 95–106. ISSN: 09608524. DOI: `10.1016/j.biortech.2012.05.070`. URL: `http://linkinghub.elsevier.com/retrieve/pii/S0960852412008231`.

Noguera, Daniel R, Nobuo Araki, and Bruce E Rittmann (1994). "Soluble microbial products (SMP) in anaerobic chemostats". In: *Biotechnol. Bioeng.* 44.9, pp. 1040–

1047. URL: http://onlinelibrary.wiley.com/doi/10.1002/bit.260440904/full.

Oldenburg, M. et al. (2007). "EU demonstration project for separate discharge and treatment of urine, faeces and greywater – Part II: Cost comparison of different sanitation systems". In: *Water Sci. Technol.* 56.5, pp. 251–257. ISSN: 0273-1223. DOI: 10.2166/wst.2007.578. URL: https://iwaponline.com/wst/article/56/5/251/14046/EU-demonstration-project-for-separate-discharge.

Oliveira-Esquerre, K P et al. (2006). "Incorporation of the concept of microbial product formation into ASM3 and the modeling of a membrane bioreactor for wastewater treatment". In: *Brazilian J. Chem. Eng.* 23.4, pp. 461–471. URL: http://www.scielo.br/scielo.php?pid=S0104-66322006000400004{\&}script=sci{_}arttext{\&}tlng=pt.

Olofsson, Marianne (2016). "Stabilization of urine by nitrification in a Moving Bed Biofilm Reactor". In:

Oren, Aharon (2011). "Thermodynamic limits to microbial life at high salt concentrations". In: *Environ. Microbiol.* 13.8, pp. 1908–1923. ISSN: 14622912. DOI: 10.1111/j.1462-2920.2010.02365.x.

Pambrun, V., E. Paul, and M. Spérandio (2006). "Modeling the partial nitrification in sequencing batch reactor for biomass adapted to high ammonia concentrations". In: *Biotechnol. Bioeng.* 95.1, pp. 120–131. ISSN: 0006-3592. DOI: 10.1002/bit.21008. arXiv: bit.20858 [10.1002]. URL: http://doi.wiley.com/10.1002/bit.21008.

Parco, Valentina, Mark Wentzel, and George Ekama (2006). "Kinetics of nitrogen removal in a MBR nutrient removal activated sludge system". en. In: *Desalination* 199.1-3, pp. 89–91. DOI: 10.1016/j.desal.2006.03.149. URL: http://linkinghub.elsevier.com/retrieve/pii/S001191640600511X.

Patsios, S I and A J Karabelas (2010). "A review of modeling bioprocesses in membrane bioreactors (MBR) with emphasis on membrane fouling predictions". en. In: *Desalin. Water Treat.* 21.1-3, pp. 189–201. DOI: 10.5004/dwt.2010.1383. URL: http://www.tandfonline.com/doi/abs/10.5004/dwt.2010.1383.

Pearce, D. W. (1995). "The economics of pollution". In: *Clean Technol. Environ.*, pp. 147–173. DOI: 10.1007/978-94-011-1312-0_5.

Petersen, Britta (2000). "Calibration, identifiability and optimal experimental design of activated sludge models". PhD thesis. Ghent University.

Philips, Sarah, Hendrikus J. Laanbroek, and Willy Verstraete (2002). "Origin, causes and effects of increased nitrite concentrations in aquatic environments". In: *Rev. Environ. Sci. Bio/Technology* 1.2, pp. 115–141. ISSN: 1569-1705. DOI: 10.1023/A:1020892826575. URL: http://link.springer.com/openurl.asp?id=doi:10.1023/A:1020892826575.

Prakasam, T. B.S. and R. C. Loehr (1972). "Microbial nitrification and denitrification in concentrated wastes". In: *Water Res.* 6.7, pp. 859–869. ISSN: 00431354. DOI: 10.1016/0043-1354(72)90038-3.

Puyol, Daniel et al. (2017). "Resource recovery from wastewater by biological technologies: Opportunities, challenges, and prospects". In: *Front. Microbiol.* 7.JAN, pp. 1–23. ISSN: 1664302X. DOI: 10.3389/fmicb.2016.02106.

Ramdani, Abdellah et al. (2012). "Biodegradation of the endogenous residue of activated sludge in a membrane bioreactor with continuous or on-off aeration". en. In: *Water Res.* 46.9, pp. 2837–2850. DOI: 10.1016/j.watres.2012.01.008. URL: http://linkinghub.elsevier.com/retrieve/pii/S0043135412000243.

Randall, Dyllon G. et al. (2016). "A novel approach for stabilizing fresh urine by calcium hydroxide addition". In: *Water Res.* 95, pp. 361–369. ISSN: 18792448. DOI: `10.1016/j.watres.2016.03.007`.

Reichert, P. et al. (2001). "River Water Quality Model no. 1 (RWQM1): II. Biochemical process equations". In: *Water Sci. Technol.* 43.5, pp. 11–30. ISSN: 02731223. DOI: `10.2166/wst.2001.0241`.

Reijken, Chris et al. (2018). "Incorporating the influent cellulose fraction in activated sludge modelling". In: *Water Res.* 144, pp. 104–111. ISSN: 18792448. DOI: `10.1016/j.watres.2018.07.013`.

Rieger, Leiv (2013). *Guidelines for using activated sludge models*. eng. 22. London [u.a]: IWA Publ, p. 281. ISBN: 978-1-84339-174-6 978-1-78040-116-4.

Rodier, J, B Legube, and N Merlet (2016). *L'analyse de l'eau - 10e éd.* Dunod. ISBN: 9782100756780. URL: `https://books.google.fr/books?id=ZevzDAAAQBAJ`.

Romero, Estela et al. (2016). "Long-term water quality in the lower Seine: Lessons learned over 4 decades of monitoring". In: *Environ. Sci. Policy* 58, pp. 141–154. ISSN: 18736416. DOI: `10.1016/j.envsci.2016.01.016`.

Roš, Milenko, Milan Dular, and Peter A. Farkas (1988). "Measurement of respiration of activated sludge". In: *Water Res.* 22.11, pp. 1405–1411. ISSN: 00431354. DOI: `10.1016/0043-1354(88)90097-8`.

Rose, C. et al. (2015). "The characterization of feces and urine: A review of the literature to inform advanced treatment technology". In: *Crit. Rev. Environ. Sci. Technol.* 45.17, pp. 1827–1879. ISSN: 15476537. DOI: `10.1080/10643389.2014.1000761`.

Rosenberg, Eugene et al. (2013). *The Prokaryotes*. Ed. by Eugene Rosenberg et al. Berlin, Heidelberg: Springer Berlin Heidelberg, pp. 1–662. ISBN: 978-3-642-30140-7. DOI: `10.1007/978-3-642-30141-4`. URL: `http://link.springer.com/10.1007/978-3-642-30141-4`.

ROUSE, JOSEPH D. et al. (2004). "Swim-bed Technology as an Innovative Attached-growth Process for High-rate Wastewater Treatment". In: *Japanese J. Water Treat. Biol.* 40.3, pp. 115–124. ISSN: 0910-6758. DOI: `10.2521/jswtb.40.115`. URL: `http://joi.jlc.jst.go.jp/JST.Journalarchive/jswtb1964/40.115?from=CrossRef`.

Ruano, M. Victoria et al. (2007). "Parameter subset selection for the dynamic calibration of activated sludge models (ASMs): Experience versus systems analysis". In: *Water Sci. Technol.* 56.8, pp. 107–115. ISSN: 02731223. DOI: `10.2166/wst.2007.605`.

Rusten, Bjorn et al. (2006). "Design and operations of the Kaldnes moving bed biofilm reactors". In: *Aquac. Eng.* 34.3, pp. 322–331. ISSN: 01448609. DOI: `10.1016/j.aquaeng.2005.04.002`.

S. Krause, M. Wagner, and P. Cornel (2003). "Comparison of different oxygen transfer testing procedures in full-scale membrane bioreactors". In: *Water Sci. Technol.* 47 (12), pp. 169–176. URL: `http://s3.amazonaws.com/academia.edu.documents/32235795/Comparison{\_}of{\_}different{\_}OTR{\_}testing{\_}procedur.pdf?AWSAccessKeyId=AKIAJ56TQJRTWSMTNPEA{\&}Expires=1480588211{\&}Signature=ory2tV8ldc867wCshfVFXFc5bAw{\%}3D{\&}response-content-disposition=attachment{\%}3Bfilename{\%}3D`.

Sancho, I. et al. (2019). "New concepts on carbon redirection in wastewater treatment plants: A review". In: *Sci. Total Environ.* 647, pp. 1373–1384. ISSN: 18791026. DOI: `10.1016/j.scitotenv.2018.08.070`. URL: `https://doi.org/10.1016/j.scitotenv.2018.08.070`.

Saroj, Devendra P et al. (2008). "Modeling and simulation of membrane bioreactors by incorporating simultaneous storage and growth concept: an especial attention to fouling while modeling the biological process". en. In: *Desalination* 221.1-3,

pp. 475–482. DOI: 10.1016/j.desal.2007.01.108. URL: http://linkinghub.elsevier.com/retrieve/pii/S001191640700731X.

Schielke-Jenni, Sarina et al. (2015). "Observability of anammox activity in single-stage nitritation/anammox reactors using mass balances". In: *Environ. Sci. Water Res. Technol.* 1.4, pp. 523–534. ISSN: 20531419. DOI: 10.1039/c5ew00045a. URL: http://dx.doi.org/10.1039/C5EW00045A.

Sharma, Keshab, Ramon Ganigue, and Zhiguo Yuan (2013). "PH dynamics in sewers and its modeling". In: *Water Res.* 47.16, pp. 6086–6096. ISSN: 00431354. DOI: 10.1016/j.watres.2013.07.027. URL: http://dx.doi.org/10.1016/j.watres.2013.07.027.

Sheng, Guo-Ping, Han-Qing Yu, and Xiao-Yan Li (2010). "Extracellular polymeric substances (EPS) of microbial aggregates in biological wastewater treatment systems: A review". en. In: *Biotechnol. Adv.* 28.6, pp. 882–894. DOI: 10.1016/j.biotechadv.2010.08.001. URL: http://linkinghub.elsevier.com/retrieve/pii/S0734975010001035.

Simha, Prithvi et al. (2020). "Alkaline dehydration of source-separated fresh human urine: Preliminary insights into using different dehydration temperature and media". In: *Sci. Total Environ.* 733, p. 139313. ISSN: 18791026. DOI: 10.1016/j.scitotenv.2020.139313. URL: https://doi.org/10.1016/j.scitotenv.2020.139313.

Sin, Gurkan and Peter A. Vanrolleghem (2006). "Evolution of an ASM2s-like model structure due to operational changes of an SBR process". In: *Water Sci. Technol.* 53.12, pp. 237–245. ISSN: 02731223. DOI: 10.2166/wst.2006.426.

Sin, Gürkan et al. (2008). "Modelling nitrite in wastewater treatment systems: A discussion of different modelling concepts". In: *Water Sci. Technol.* 58.6, pp. 1155–1171. ISSN: 02731223. DOI: 10.2166/wst.2008.485.

Soetaert, Karline and Thomas Petzoldt (2010). "Inverse modelling, sensitivity and monte carlo analysis in R using package FME". In: *J. Stat. Softw.* 33.3, pp. 1–28. ISSN: 15487660. DOI: 10.18637/jss.v033.i03.

Spanjers, Henri and Peter Vanrolleghem (1995a). "Respirometry as a tool for rapid characterization of wastewater and activated sludge". In: *Water Sci. Technol.* 31.2, pp. 105–114. URL: http://wst.iwaponline.com/content/31/2/105.abstract.

— (1995b). "Respirometry as a tool for rapid characterization of wastewater and activated sludge". In: *Water Sci. Technol.* 31.2, pp. 105–114. URL: http://wst.iwaponline.com/content/31/2/105.abstract.

Spérandio, M and M C Espinosa (2008). "Modelling an aerobic submerged membrane bioreactor with ASM models on a large range of sludge retention time". en. In: *Desalination* 231.1-3, pp. 82–90. DOI: 10.1016/j.desal.2007.11.040. URL: http://linkinghub.elsevier.com/retrieve/pii/S0011916408003482.

Spérandio, Mathieu, Marc Heran, and Sylvie Gillot (2007). "Modélisation dynamique des procédés biologiques de traitement des eaux". In: *Tech. l'Ingénieur* W6500 V1.0, pp. 1–18. URL: see{_}the{_}document{_}in{_}the{_}desktop{_}folder{_}Techniques{_}de{_}lingenieur.

Spérandio, Mathieu et al. (2013). "Modelling the degradation of endogenous residue and 'unbiodegradable' influent organic suspended solids to predict sludge production". en. In: *Water Sci. Technol.* 67.4, p. 789. DOI: 10.2166/wst.2012.629. URL: http://wst.iwaponline.com/cgi/doi/10.2166/wst.2012.629.

Stenstrom, M K et al. (1989). "Estimating Oxygen Transfer Capacity of a Full-Scale Pure Oxygen Activated Sludge Plant". In: *J. (Water Pollut. Control Fed.* 61.2, pp. 208–220. ISSN: 00431303. URL: http://www.jstor.org/stable/25046915.

Sun, F. Y. et al. (2012). "Stabilization of source-separated urine by biological nitrification process: Treatment performance and nitrite accumulation". In: *Water Sci. Technol.* 66.7, pp. 1491–1497. ISSN: 02731223. DOI: 10.2166/wst.2012.337.

Suzuki, I., U. Dular, and S. C. Kwok (1974). "Ammonia or ammonium ion as substrate for oxidation by Nitrosomonas europaea cells and extracts". In: *J. Bacteriol.* 120.1, pp. 556–558. ISSN: 00219193.

Svehla, Pavel et al. (2014). "Inhibition effect of free ammonia and free nitrous acid on nitrite-oxidising bacteria during sludge liquor treatment: influence of feeding strategy". In: *Chem. Pap.* 68.7, pp. 871–878. ISSN: 1336-9075. DOI: 10.2478/s11696-014-0538-6. URL: http://www.degruyter.com/view/j/chempap.2014.68.issue-7/s11696-014-0538-6/s11696-014-0538-6.xml.

Tan, Teck Wee, How Yong Ng, and Say Leong Ong (2008). "Effect of mean cell residence time on the performance and microbial diversity of pre-denitrification submerged membrane bioreactors". en. In: *Chemosphere* 70.3, pp. 387–396. DOI: 10.1016/j.chemosphere.2007.07.003. URL: http://linkinghub.elsevier.com/retrieve/pii/S0045653507008703.

Teichgräber, Burkhard and Andreas Stein (1994). "Nitrogen elimination from sludge treatment reject water – comparison of the steam-stripping and denitrification processes". In: *Water Sci. Technol.* 30.6, pp. 41–51. ISSN: 0273-1223. DOI: 10.2166/wst.1994.0251. URL: https://iwaponline.com/wst/article/30/6/41-51/3972.

Tun, Lat Lat et al. (2016). "Dewatering of source-separated human urine for nitrogen recovery by membrane distillation". In: *J. Memb. Sci.* 512, pp. 13–20. ISSN: 18733123. DOI: 10.1016/j.memsci.2016.04.004. URL: http://dx.doi.org/10.1016/j.memsci.2016.04.004.

Udert, K M et al. (2003a). *Nitrification and autotrophic denitrification of source-separated urine*. Tech. rep. URL: http://citeseerx.ist.psu.edu/viewdoc/download?doi=10.1.1.588.3931{\&}rep=rep1{\&}type=pdf.

Udert, Kai M., Tove A. Larsen, and Willi Gujer (2003). "Estimating the precipitation potential in urine-collecting systems". In: *Water Res.* 37.11, pp. 2667–2677. ISSN: 00431354. DOI: 10.1016/S0043-1354(03)00071-X.

— (2005). "Chemical Nitrite Oxidation in Acid Solutions as a Consequence of Microbial Ammonium Oxidation". In: *Environ. Sci. Technol.* 39.11, pp. 4066–4075. ISSN: 0013-936X. DOI: 10.1021/es048422m. URL: https://pubs.acs.org/sharingguidelineshttps://pubs.acs.org/doi/10.1021/es048422m.

Udert, Kai M. et al. (2003b). "Urea hydrolysis and precipitation dynamics in a urine-collecting system". In: *Water Res.* 37.11, pp. 2571–2582. ISSN: 00431354. DOI: 10.1016/S0043-1354(03)00065-4.

Udert, Kai M. et al. (2015). "Technologies for the treatment of source-separated urine in the eThekwini Municipality". In: *Water SA* 41.2, pp. 212–221. ISSN: 18167950. DOI: 10.4314/wsa.v41i2.06.

Udert, K.M., T.A. Larsen, and W Gujer (2006). "Fate of major compounds in source-separated urine". In: *Water Sci. Technol.* 54.11-12, pp. 413–420. ISSN: 0273-1223. DOI: 10.2166/wst.2006.921. URL: https://pdfs.semanticscholar.org/f555/47516985304354f905b1fcccb6b608a6c580.pdfhttps://iwaponline.com/wst/article/54/11-12/413-420/13916.

Udert, K.M. and M. Wächter (2012). "Complete nutrient recovery from source-separated urine by nitrification and distillation". In: *Water Res.* 46.2, pp. 453–464. ISSN: 00431354. DOI: 10.1016/j.watres.2011.11.020. URL: www.elsevier.com/locahttps://linkinghub.elsevier.com/retrieve/pii/S0043135411007044.

Uhlmann, Corine (2014). "Dynamics of complete and partial nitrification of source-separated urine". In: URL: https://www.research-collection.ethz.ch:443/handle/20.500.11850/108164.

Vadivelu, V. M., J. Keller, and Zhiguo Yuan (2007). "Free ammonia and free nitrous acid inhibition on the anabolic and catabolic processes of Nitrosomonas and Nitrobacter". In: *Water Sci. Technol.* 56.7, pp. 89–97. ISSN: 02731223. DOI: 10.2166/wst.2007.612.

Vadivelu, Vel M. et al. (2006). "The Inhibitory Effects of Free Nitrous Acid on the Energy Generation and Growth Processes of an Enriched Nitrobacter Culture". In: *Environ. Sci. Technol.* 40.14, pp. 4442–4448. ISSN: 0013-936X. DOI: 10.1021/es051694k. URL: https://pubs.acs.org/doi/10.1021/es051694k.

Van Hulle, S. W.H. et al. (2005). "Construction, start-up and operation of a continuously aerated laboratory-scale SHARON reactor in view of coupling with an Anammox reactor". In: *Water SA* 31.3, pp. 327–334. ISSN: 03784738. DOI: 10.4314/wsa.v31i3.5222.

Van Hulle, Stijn W.H. et al. (2010). "Engineering aspects and practical application of autotrophic nitrogen removal from nitrogen rich streams". In: *Chem. Eng. J.* 162.1, pp. 1–20. ISSN: 13858947. DOI: 10.1016/j.cej.2010.05.037. URL: http://dx.doi.org/10.1016/j.cej.2010.05.037.

Van Loosdrecht, Mark C.M. and Mogens Henze (1999). "Maintenance, endogeneous respiration, lysis, decay and predation". In: *Water Sci. Technol.* 39.1, pp. 107–117. ISSN: 02731223. DOI: 10.1016/S0273-1223(98)00780-X. URL: http://dx.doi.org/10.1016/S0273-1223(98)00780-X.

Vavilin, V. A. and S. V. Rytov (2015). "Nitrate denitrification with nitrite or nitrous oxide as intermediate products: Stoichiometry, kinetics and dynamics of stable isotope signatures". In: *Chemosphere* 134, pp. 417–426. ISSN: 18791298. DOI: 10.1016/j.chemosphere.2015.04.091. URL: http://dx.doi.org/10.1016/j.chemosphere.2015.04.091.

Verrecht, Bart et al. (2010). "Model-based energy optimisation of a small-scale decentralised membrane bioreactor for urban reuse". en. In: *Water Res.* 44.14, pp. 4047–4056. DOI: 10.1016/j.watres.2010.05.015. URL: http://linkinghub.elsevier.com/retrieve/pii/S0043135410003234.

Villain, Maud and Benoît Marrot (2013). "Influence of sludge retention time at constant food to microorganisms ratio on membrane bioreactor performances under stable and unstable state conditions". en. In: *Bioresour. Technol.* 128, pp. 134–144. DOI: 10.1016/j.biortech.2012.10.108. URL: http://linkinghub.elsevier.com/retrieve/pii/S0960852412016173.

Visek, W J (1972). "Effects of urea hydrolysis on cell life-span and metabolism." In: *Fed. Proc.* 31.3, pp. 1178–93. ISSN: 0014-9446. URL: http://www.ncbi.nlm.nih.gov/pubmed/4555778.

Volcke, E I P, P Vanrolleghem, and M C M van Loosdrecht (2006). *Modelling, analysis and control of partial nitration in a SHARON reactor*, p. 327. ISBN: 9059891082.

Volcke, Eveline I P et al. (2001). "Modelling the Sharon Process in View of COUPLING WITH ANAMMOX". In:

Warneck, Peter (1988). "Chemistry of the natural atmosphere". In: *Orlando FL Acad. Press Inc Int. Geophys. Ser.* 41.

WEF (2011). *Nutrient Removal - Manual of Practice*, p. 676. ISBN: 9780071737104.

Wett, Bernhard and Wolfgang Rauch (2003). "The role of inorganic carbon limitation in biological nitrogen removal of extremely ammonia concentrated wastewater". In: *Water Res.* 37.5, pp. 1100–1110. ISSN: 00431354. DOI: 10.1016/S0043-1354(02)00440-2.

Whang, L. M. et al. (2009). "Microbial ecology and performance of ammonia oxidizing bacteria (AOB) in biological processes treating petrochemical wastewater with high strength of ammonia: Effect of Na2CO3 addition". In: *Water Sci. Technol.* 59.2, pp. 223–231. ISSN: 02731223. DOI: 10.2166/wst.2009.848.

Wielemaker, Rosanne C., Jan Weijma, and Grietje Zeeman (2018). "Harvest to harvest: Recovering nutrients with New Sanitation systems for reuse in Urban Agriculture". In: *Resour. Conserv. Recycl.* 128, pp. 426–437. ISSN: 18790658. DOI: 10.1016/j.resconrec.2016.09.015. URL: https://doi.org/10.1016/j.resconrec.2016.09.015.

Wiesmann, Udo, In Su Choi, and Eva Maria Dombrowski (2006). *Fundamentals of Biological Wastewater Treatment*, pp. 1–362. ISBN: 9783527312191. DOI: 10.1002/9783527609604.

Wilsenach, J (2002). *Separate urine collection and treatment: options for sustainable wastewater systems and mineral recovery*, p. 121. ISBN: 9057731975.

Wilsenach, J. A. et al. (2003). "From waste treatment to integrated resource management". In: *Water Sci. Technol.* 48.1, pp. 1–9. ISSN: 02731223. DOI: 10.2166/wst.2003.0002.

Wilsenach, Jac A. and Mark C.M. van Loosdrecht (2006). "Integration of processes to treat wastewater and source-separated urine". In: *J. Environ. Eng.* 132.3, pp. 331–341. ISSN: 07339372. DOI: 10.1061/(ASCE)0733-9372(2006)132:3(331).

Wilsenach, Jacobus Albertus (2006). *Treatment of source separated urine and its effects on wastewater systems*. ISBN: 9789064640162. DOI: urn:NBN:nl:ui:24-uuid:7bb02cc8-5be3-41fc-99ab-1f916a98700b. URL: http://repository.tudelft.nl/view/ir/uuid:7bb02cc8-5be3-41fc-99ab-1f916a98700b/.

Wilt, Arnoud de et al. (2016). "Micropollutant removal in an algal treatment system fed with source separated wastewater streams". In: *J. Hazard. Mater.* 304, pp. 84–92. ISSN: 18733336. DOI: 10.1016/j.jhazmat.2015.10.033.

Wolfe, Alan J. et al. (2012). "Evidence of uncultivated bacteria in the adult female bladder". In: *J. Clin. Microbiol.* 50.4, pp. 1376–1383. ISSN: 00951137. DOI: 10.1128/JCM.05852-11.

Yogalakshmi, K. N. and Kurian Joseph (2010). "Effect of transient sodium chloride shock loads on the performance of submerged membrane bioreactor". In: *Bioresour. Technol.* 101.18, pp. 7054–7061. ISSN: 09608524. DOI: 10.1016/j.biortech.2010.03.135. URL: http://dx.doi.org/10.1016/j.biortech.2010.03.135.

Young, Bradley et al. (2017). "Low temperature MBBR nitrification: Microbiome analysis". In: *Water Res.* 111, pp. 224–233. ISSN: 18792448. DOI: 10.1016/j.watres.2016.12.050.

Zhang, Haifeng et al. (2014). "Performance enhancement and fouling mitigation by organic flocculant addition in membrane bioreactor at high salt shock". In: *Bioresour. Technol.* 164, pp. 34–40. ISSN: 09608524. DOI: 10.1016/j.biortech.2014.04.053. URL: http://dx.doi.org/10.1016/j.biortech.2014.04.053https://linkinghub.elsevier.com/retrieve/pii/S0960852414005586.

Zhao, Linting et al. (2016). "Characteristics of extracellular polymeric substances from sludge and biofilm in a simultaneous nitrification and denitrification system under high salinity stress". en. In: *Bioprocess Biosyst. Eng.* 39.9, pp. 1375–1389. DOI: 10.1007/s00449-016-1613-x. URL: http://link.springer.com/10.1007/s00449-016-1613-x.

Zhou, S. Q. (2001). "Theoretical stoichiometry of biological denitrifications". In: *Environ. Technol. (United Kingdom)* 22.8, pp. 869–880. ISSN: 1479487X. DOI: 10.1080/09593332208618223.

Zhou, Shaoqi (2007). "Stoichiometry of biological nitrogen transformations in wetlands and other ecosystems". In: *Biotechnol. J.* 2.4, pp. 497–507. ISSN: 18606768. DOI: 10.1002/biot.200600078. URL: http://doi.wiley.com/10.1002/biot.200600078.

Zhu, Songming and Shulin Chen (2001). "Effects of organic carbon on nitrification rate in fixed film biofilters". In: *Aquac. Eng.* 25.1, pp. 1–11. ISSN: 01448609. DOI: 10.1016/S0144-8609(01)00071-1.

Juan David ARCE VELASQUEZ

Modélisation de la stabilisation de l'urine par nitrification au sein d'un bioréacteur à membrane

Résumé

Dans cette thèse, la conceptualisation d'un modèle biocinétique ainsi qu'une analyse expérimentale d'un système de bioréacteur à membrane traitant des eaux usées jaunes (urine) sont présentées. Le système est un bioréacteur à membrane conçu pour traiter l'urine séparée à la source. L'objectif principal est de traiter la charge azotée dans l'urine par nitrification biologique et d'en produire un effluent stable.

Cette thèse développe et valide un modèle intégré qui représentera le comportement du bioréacteur en échelle réelle. Ce modèle permettra de simuler différentes conditions de fonctionnement, ainsi que l'intégration de processus physico-chimiques et biologiques, en comprenant les différents mécanismes d'assimilation/inhibition influençant les bactéries nitrifiantes.

Le calage et la validation du modèle exigent un pilote de laboratoire pour acclimater les boues activées classiques à traiter fortes charges en azote. Une stratégie d'acclimatation basée sur le contrôle du pH a permis de démarrer et piloter le système de façon autonome. Ce protocole d'acclimatation a été optimisé pour utiliser de l'urine hautement concentré. Les paramètres du modèle ont été calés par mesures respirométriques dans ces conditions de haute teneur en azote.

Mots-clés: Urine, Séparation à la source, traitement des eaux jaunes, nitrification, bactéries nitrifiantes, boues activées, acclimatation, inhibition, modélisation, modèles intégrés, respirométrie, contrôle du procédé.

Summary

In this thesis, the conceptualization of an integrated physico-biological model, as well as an experimental analysis of a biological system treating yellow wastewater are presented. The system is a membrane bioreactor designed to treat source separated urine. The main objective is to treat the nitrogen load in the urine by biological nitrification and produce a stable effluent.

This thesis develops and validates an integrated model that will represent the bioreactor's behavior on a real scale. This model will simulate different operating conditions, as well as the integration of physico-chemical and biological processes, by understanding the different assimilation/inhibition mechanisms influencing nitrifying bacteria.

The calibration and validation of the model requires a laboratory pilot to acclimatize conventional activated sludge to high nitrogen loads. A pH control driven strategy was developed for the acclimation phase, allowed the system to be started and controlled automatically. This acclimation protocol was optimized to use highly concentrated urine. The model parameters were calibrated by respirometric measurements under these high nitrogen conditions.

Keywords: Urine, source separation, yellow wastewater treatment, nitrification, nitrifying bacteria, activated sludge, acclimation, inhibition, modelling, integrated models, respirometry, process control.